

Northumbria Research Link

Citation: Scalacci, Nicolò (2017) Tackling the antibiotic resistance in tuberculosis: Synthesis and biological evaluation of novel antitubercular agents and development of novel methodologies for the synthesis of heterocycles. Doctoral thesis, Northumbria University.

This version was downloaded from Northumbria Research Link:
<https://nrl.northumbria.ac.uk/id/eprint/36135/>

Northumbria University has developed Northumbria Research Link (NRL) to enable users to access the University's research output. Copyright © and moral rights for items on NRL are retained by the individual author(s) and/or other copyright owners. Single copies of full items can be reproduced, displayed or performed, and given to third parties in any format or medium for personal research or study, educational, or not-for-profit purposes without prior permission or charge, provided the authors, title and full bibliographic details are given, as well as a hyperlink and/or URL to the original metadata page. The content must not be changed in any way. Full items must not be sold commercially in any format or medium without formal permission of the copyright holder. The full policy is available online: <http://nrl.northumbria.ac.uk/policies.html>



**Northumbria
University**
NEWCASTLE



UniversityLibrary

Northumbria Research Link

Citation: Scalacci, Nicolò (2017) Tackling the antibiotic resistance in tuberculosis: Synthesis and biological evaluation of novel antitubercular agents and development of novel methodologies for the synthesis of heterocycles. Doctoral thesis, Northumbria University.

This version was downloaded from Northumbria Research Link:
<http://nrl.northumbria.ac.uk/id/eprint/36135/>

Northumbria University has developed Northumbria Research Link (NRL) to enable users to access the University's research output. Copyright © and moral rights for items on NRL are retained by the individual author(s) and/or other copyright owners. Single copies of full items can be reproduced, displayed or performed, and given to third parties in any format or medium for personal research or study, educational, or not-for-profit purposes without prior permission or charge, provided the authors, title and full bibliographic details are given, as well as a hyperlink and/or URL to the original metadata page. The content must not be changed in any way. Full items must not be sold commercially in any format or medium without formal permission of the copyright holder. The full policy is available online: <http://nrl.northumbria.ac.uk/policies.html>



**Northumbria
University**
NEWCASTLE



University**Library**

**Tackling the Antibiotic Resistance in
Tuberculosis: Synthesis and Biological
Evaluation of Novel Antitubercular
Agents and Development of Novel
Methodologies for the Synthesis of
Heterocycles**

Nicolò Scalacci

PhD

2017

Tackling the Antibiotic Resistance in
Tuberculosis: Synthesis and Biological
Evaluation of Novel Antitubercular Agents
and Development of Novel Methodologies
for the Synthesis of Heterocycles

Nicolò Scalacci

A thesis submitted in fulfilment of the
requirements of the University of
Northumbria at Newcastle for the degree of
Doctor of Philosophy

Research undertaken in Department of
Applied Sciences at Northumbria University
and at the Institute of Pharmaceutical
Science, King's College London.

July 2017

ABSTRACT: *Mycobacterium tuberculosis* (Mtb), the etiological agent of Tuberculosis (TB) is developing new multi drug-resistant (MDR) and extensively drug-resistant (XDR) strains to the current drugs used in therapy. Of particular concern the wide spreading of tuberculosis, the high rate of development of resistance, and the high mortality of the patients due to the lack of effective therapy against TB infections. In order to face this problem, two series of novel compounds were designed, synthesised and evaluated against a panel of mycobacterial strains. The first series of compounds includes analogues of the third line drug thioridazine (TZ). TZ is a known antipsychotic drug belonging to the phenothiazine drug group, which showed good activity against MDR-TB infections but causes severe side effects which limit its use in therapy. Among the first series of compounds, five new compounds showed anti-tubercular activity similar or higher than TZ. Moreover, two derivatives showed potent inhibition towards the whole-cell drug efflux pump activity of mycobacteria comparable to that of verapamil, and turning to be promising multi-drug resistance reversal agents. A second series of compounds consist of small molecules which have originally been designed as hybrids of the anti-tubercular drugs BM212 and SQ109. Computational studies revealed a perfect superposition of the structures of SQ109 and BM212 and showed that the two drugs share common features. Five of the resulting compounds showed micromolar anti-tubercular activity on pathogenic TB. Two of them proved to be highly active also against multi-drug resistant clinical isolates and one of these also showed minimal eukaryotic cell toxicity, and therefore would be an excellent lead candidate for preclinical trials. In parallel to the identification of novel compounds active against mycobacteria, new synthetic methodologies for the synthesis of antitubercular heterocyclic scaffolds have been developed. In particular two approaches for the synthesis of pyrrole compounds were developed. Both procedures involve an olefin or enyne metathesis reaction as a key step. The first approach involves the synthesis of 1,2,3-substituted pyrroles, through a tandem enyne cross metathesis-cyclization reaction of propargylamines with ethyl-vinyl ether. The reaction is rapid, procedurally simple and represents a facile entry to the synthetically challenging 4,5-unsubstituted pyrroles. The second methodology allows the synthesis of substituted pyrroles from diallyl-amines via a chemo-enzymatic cascade based on the combination of olefin metathesis together with monoamine oxidase (MAO) biocatalysts. These reactions were carried out in aqueous media and mild temperature leading to the formation of substituted pyrroles in a single step and in high yields.

List of contents

1. Introduction.....	1
1.1. Statement of the Problem.....	1
1.2. <i>Mycobacterium tuberculosis</i>	2
1.3. Pathogenesis.....	4
1.3.1. Primary infection.....	4
1.3.2. Active infection.....	5
1.4. Tuberculosis and HIV.....	6
1.5. Treatment of TB.....	7
1.5.1. First line drugs.....	7
1.5.2. Second and third line drugs.	10
1.5.3. MDR-TB reversal agents.....	13
1.5.4. Vaccination.....	14
1.6. MDR-TB, XDR-TB and causes of development of resistance.....	14
1.7. Correlation between new advances in synthetic methodologies and drug discovery and optimization.....	16
1.8. Statement of research objectives.....	17
1.8.1. Structure of the thesis.....	17
2. Design and synthesis of potent antitubercular agents effective against multidrug-resistant mycobacteria.	20
2.1. Introduction.	20
2.1.1. Approaches for the drug discovery of novel molecules active against Mtb.....	20
2.2. Repurposing and molecular simplification of thioridazine as strategy for the development of novel antitubercular agents effective against multidrug-resistant mycobacteria.....	21
2.2.1. Results and discussion.....	24
2.2.1.1. Synthesis of thioridazine derivatives.....	24
2.2.1.2. Evaluation against a panel of mycobacteria.....	28
2.2.1.3. Evaluation as efflux pump inhibitors.....	31
2.2.2. Conclusions.....	32
2.3. Synthesis of novel antitubercular agents effective against multidrug-resistant mycobacteria via molecular hybridization approach.....	33

2.3.1. Results and discussion.....	35
2.3.1.1. Computational design and hypothesis on the common chemical features shared by BM212 and SQ109.....	35
2.3.1.2. Synthesis of BM212-SQ109 hybrid derivatives.....	37
2.3.1.3. Evaluation of hybrid derivatives of I and II against a panel of Mycobacteria.....	41
2.3.1.4. SAR considerations and development of a new pharmacophoric model.....	48
2.3.1.5. Evaluation of the hybrid derivatives of I and II as efflux pump inhibitors.....	49
2.3.2. Conclusions.....	50
3. Development of novel methodologies for the synthesis of heterocyclic drug-like compounds.....	51
3.1 Introduction.....	51
3.1.1. New approaches for the synthesis of pyrroles: Metathesis reaction.....	51
3.1.2. Novel insight for the sustainable synthesis of pyrroles.....	56
3.2. Synthesis of 1,2,3-substituted pyrroles from propargylamines via a one-pot tandem enyne cross metathesis–cyclization reaction.....	57
3.2.1. Results and discussion.....	59
3.2.1.1. Optimization of the reaction conditions.....	59
3.2.1.2. Synthesis of pyrroles from propargylamines via one-pot tandem enyne CM-cyclization reaction.....	65
3.2.1.3. Functionalization of pyrroles on C5 and derivatization on the methyl group on C3.	66
3.2.2. Conclusions.....	68
3.3. Novel applications of mono-amino oxidase (MAO-N & 6-HDNO) biocatalysts toward the synthesis of pyrroles.....	69
3.3.1. Results and discussion.....	74
3.3.1.1. Preliminary investigation of the MAO-N & 6-HDNO biocatalyst aromatization property.....	74
3.3.1.2. Synthesis of additional substrates for biocatalysis.....	75
3.3.1.3. MAO-N and 6-HDNO catalysed aromatization of 1-aryl-3-pyrrolines into 1-aryl-pyrroles.....	81

3.3.1.4. MAO-N and 6-HDNO catalysed aromatization of 1-alkyl-3-pyrrolines in 1-alkyl-pyrroles.....	84
3.3.1.5. Development and Optimization of chemo-enzymatic cascade.....	87
3.3.1.6. Expanding the scope of the RCM-MAO cascade reaction.....	90
3.3.1.7. Application of MAO oxidation/aromatization reaction toward the synthesis of antitubercular pyrrole derivative.....	95
3.3.2. Conclusions.....	96
4. Thesis conclusions.....	97
5. Materials and Methods.....	104
5.1. Materials.....	104
5.1.1. Physical measurements.....	104
5.1.2 Microwave Irradiation Experiments.....	105
5.2 Methods.....	105
5.2.1. Repurposing and molecular simplification of thioridazine as strategy for the development of novel antitubercular agents effective against multidrug-resistant mycobacteria	105
5.2.1.1. Biology.....	105
5.2.1.2. Chemistry.....	108
5.2.2. Virtual molecular hybridization approach for the synthesis of novel antitubercular agents effective against Multidrug-Resistant Mycobacteria.....	128
5.2.2.1. Biology.....	128
5.2.2.2. Computational details.....	130
5.2.2.3. Chemistry.....	131
5.2.3. Synthesis of 1,2,3-substituted pyrroles from propargylamines via a one-pot tandem enyne cross metathesis–cyclization reaction.....	147
5.2.3.1. Chemistry.....	147
5.2.4. Application of MAO oxidation/aromatization reaction toward the synthesis of a putative antitubercular pyrrole derivative.....	168
5.2.4.1. Preparation of Biocatalysts.....	168
5.2.4.2. Computational Details.....	168
5.2.4.3. Chemistry.....	169
6. References.....	195

List of abbreviations

Abbreviation	Term
6-HDNO	6-hydroxy-D-nicotine oxidase
AcOH	acetic acid
ADC	albumin-dextrose-catalase
ADMET	acyclic diene metathesis polymerization
AG	arabinogalactan
AMK	Amikacin
Ap	Ampicillin
ARVs	antiretroviral therapy
Boc	<i>tert</i> -butoxyl
BCG	Bacille Calmette-Guerin
CBr ₄	tetrabromomethane
CAP	capreomycin
CM	cross metathesis
Cmpd	Compound
CNS	central nervous system
CS	cycloserine
DCE	dichloroethane
DCM	dichloromethane
DIPEA	<i>N,N</i> -diisopropylethylamine
DMAP	4-dimethylaminopyridine
DMF	<i>N,N</i> -dimethylformamide
DME	1,2-dimethoxyethane
DMEM	Dulbecco's Modified Eagle's Medium
DMSO	dimethyl sulfoxide
DR-TB	resistant mutated <i>Mycobacterium tuberculosis</i> strains
EDTA	trypsin/ethylenediamine tetracetic acid
EMB	ethambutol
EPI	efflux pump inhibitory
Et ₂ O	diethylether
EtOAc	ethylacetate

ETH	ethionamide
EVE	ethyl vinyl ether
FAD/FADH2	flavin adenine dinucleotide redox cofactor
FAD	flavin adenine dinucleotide
FADH2	reduced form of the flavin adenine dinucleotide
FAS II	fatty acid synthesis complex
FBS	fetal bovine serum
FQs	fluoroquinolones
GII	Grubbs' Catalyst II generation
GIC ₅₀	50% growth inhibitory concentration
H	hydrophobic region
HAA	hydrogen atom acceptor
HGII	Hoveida Grubbs' catalyst
HIV-1	human immunodeficiency virus
IAR	isonicotinic acyl radical
INH	Isoniazid
InhA	enol-acyl carrier protein reductase
h	Hour
KAN	kanamycin
KatG	mycobacteria catalase peroxidase
LB broth	Luria-Bertani
LP	lipoarabinoamannan
MA	mycolic acids
MABA	microplate alamar blue assay
MAO	monoamine oxidase
MAO-N	monoamine oxidase variants from <i>Aspergillus niger</i>
MeOH	Methanol
MHC	major histocompatibility complex
MIC ₉₀	minimum inhibitory concentration
MDR	multi drug-resistant
MDR-TB	multidrug-resistant <i>Mycobacterium tuberculosis</i>
MmpL	mycobacterial membrane protein large

mol%	Mole percent
Mtb	<i>Mycobacterium tuberculosis</i>
Mw	microwave irradiation
NaBH(AcO) ₃	sodium triacetoxyborohydride
NAD ⁺	nicotinamide adenine dinucleotide
NBS	<i>N</i> -bromosuccinimide
NDH-2	type-2 NADH dehydrogenase
NLRs	nucleotide binding oligomerization domain-like receptors
OADC	oleic acid-albumin-dextrose-catalase
os	oral administration
P	positively ionisable group
PAS	<i>p</i> -amino salicylic acid
PG	peptidoglycan
PIP3	phosphatidylinositol 3-phosphate
PknG	serine/threonine kinase
PPh ₃	triphenylphosphine
PTH	prothionamide
PZA	pyrazinamide
RCM	ring-closing metathesis
REMA	resazurin microtiter assay
RIF	Rifampin
RND	resistance-nodulation-cell division
ROCM	ring-opening cross metathesis
ROMP	ring-opening metathesis polymerization
r.t.	room temperature
SAR	structure activity relationship
SI	selective index
SM	streptomycin
ss	saturated solution in water
T	temperature
TACO	coronin 1/tryptophan aspartate coat protein
TB	tuberculosis

TBAF	tetra- <i>N</i> -butylammonium fluoride
TDR-TB	total drug resistant <i>Mycobacterium tuberculosis</i> strain
TEA	triethylamine
TEMPO	(2,2,6,6-Tetramethylpiperidin-1-yl)oxyl
TFA	trifluoroacetic acid
THF	tetrahydrofuran
THP-1	human monocyte-derived
TIPS	triisopropylsilyl
TLRs	toll like receptors
TZ	thioridazine
UNESP	Universidade Estadual Paulista "Júlio de Mesquita Filho"
WHO	World Health Organisation
WT	wild type
XDR	extensively drug-resistant
XDR-TB	extensively drug resistant <i>Mycobacterium tuberculosis</i>

List of accompanying material

The present PhD thesis is based on the following papers:

- Scalacci, N.; Brown, A. K.; Pavan, F. R.; Ribeiro, C. M.; Manetti, F.; Bhakta, S.; Maitra, A.; Smith, D. L.; Petricci, E.; Castagnolo, D. *Eur. J. Med. Chem.* **2017**, *127*, 147–158.
- Bhakta, S.; Scalacci, N.; Maitra, A.; Brown, A. K.; Dasugari, S.; Evangelopoulos, D.; McHugh, T. D.; Mortazavi, P. N.; Twist, A.; Petricci, E.; Manetti, F.; Castagnolo, D. *J. Med. Chem.* **2016**, *59* (6), 2780–2793.
- Chachignon, H.; Scalacci, N.; Petricci, E.; Castagnolo, D. *J. Org. Chem.* **2015**, *80* (10), 5287–5295.
- Scalacci, N.; Black, G. W.; Mattedi, G.; Brown, N. L.; Turner, N. J.; Castagnolo, D. *ACS Catal.* **2017**, *7*, 1295.

Acknowledgements

During my PhD course, I have been accompanied and supported by many people. I am glad that within this thesis I could have the opportunity to express my gratitude to all of them.

First of all, I would like to express my deep and sincere gratitude to my team of supervisors, Dr. Daniele Castagnolo, Prof. Stephen P. Stanforth and Dr. Justin Perry, who gave me the opportunity to study at Northumbria University and then at King's College London as a visitor student. I am deeply grateful especially to Daniele for his endless guidance, support, motivation and patience. His immense knowledge and contagious enthusiastic view on research have helped me throughout the whole PhD program. I could not have imagined having a better mentor for this study.

I would like to thank Northumbria University for generously founding this project.

Special thanks are due to all the research and technical staff at Northumbria for their generous and continuous help, not only in the research but even in private arena, especially Costas, Michael, Stefania, Hanna, Alex, Jon, and Fraser.

I am also very grateful to Kate, Vincenzo, Simona, Tommaso, Giulio, Umberto, Sonia and to all the PhD student and Post-Docs of the Institute of Pharmaceutical science at King's College London for their guidance and invaluable friendship during the last year of my PhD.

During these years, I have met a lot of good friends in Newcastle and in London. I thank all of them, especially Paolo, for standing beside me whenever I needed a rest.

A special mention is due also to Chiara who followed me in the biggest adventure of my life, adding her magic to all my days.

Last, but not least, I would like to give special thanks to my family, and especially my parents and my brother, who were always there for me, throughout the good and bad times.

Declaration

I declare that the work contained in this thesis has not been submitted for any other award and that it is all my own work. I also confirm that this work fully acknowledges opinions, ideas and contributions from the work of others.

Any ethical clearance for the research presented in this thesis has been approved. Approval has been sought and granted by the Faculty Ethics Committee on 02/10/2013.

I declare that the Word Count of this Thesis is 38,852 words

Name: Nicolò Scalacci

Signature:

Date: 28/07/2017

1. Introduction.

1.1. Statement of the Problem.

In 1882, Robert Koch discovered and demonstrated that *Mycobacterium tuberculosis*, (Mtb), is the etiological agent of Tuberculosis (TB),¹ an airborne, chronic, progressive infection which, nowadays, causes almost 1.5 million deaths per year.² The WHO (World Health Organisation) report 2016 shows that one third of worldwide population has got a latent, asymptomatic infection of Mtb and that one patient with latent infection in ten will develop the active form at some point during their life.² Active infections are symptomatic and contagious causing death of tissue in the infected organs, possibly resulting in death. Mtb most often affects the lungs, causing pulmonary TB, however, in immunocompromised individuals, a primary lung infection can spread through blood vessels to any part of the body causing an extra-pulmonary infection. Typical locis for extra-pulmonary infection are the upper portion of the lungs, followed by kidneys, meninges, corpus vertebrae and epiphyses of the long bones. The most common symptoms are intense cough, fever, weight loss caused by lack of appetite and general malaise. The diagnosis is difficult for the asymptomatic latent infection cases, but easy and day by day more reliable for the active infections. Diagnosis usually occurs by the culture and analysis of the sputum and, recently, by rapid molecular-based diagnostic assay.² According to the last WHO report, the new TB cases were estimated at 9.6 million worldwide (Figure 1).

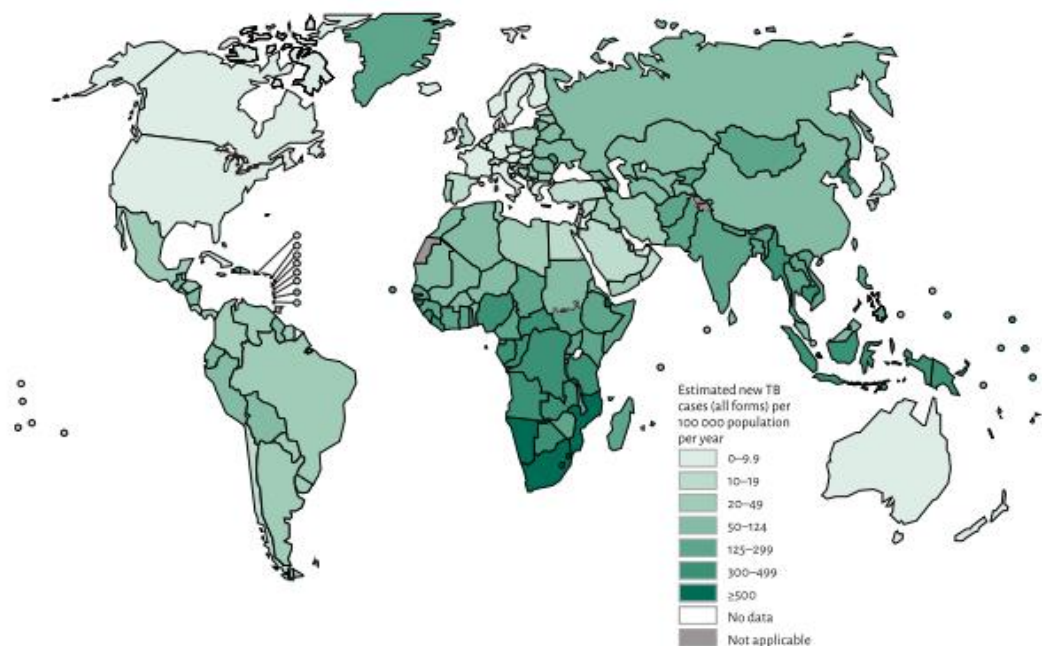


Figure 1. Estimated incidence TB rates (WHO 2015)²

The global incidence is 122 cases per 100,000 population, however it is noteworthy that, the disease is not homogeneously widespread. In fact, 58% of the population affected by *Mtb* infection is in Asia while the 28% and the 8% are respectively in Africa and the Eastern Mediterranean region. The smallest incidence values are pointed out in the American continent (3%) and in the European region (3%).² Despite the grim epidemic scenario, nowadays, the majority of TB cases are treatable with a 6-12 months multidrug therapy. However the breakdown in health services, the development of multidrug-resistant *Mycobacterium tuberculosis* strains (MDR-TB) and extensively resistant *Mycobacterium tuberculosis* strains (XDR-TB), combined with the wide spreading of HIV-1 infections³ (the most common and widespread human immunodeficiency virus strain) and diabetes⁴ are compromising the chemotherapy used for the treatment of TB. In 1993, WHO declared TB a global emergency and stipulated a plan that aimed to end the global TB, MDR and XDR-TB threat. One of the key points for the success of this plan is to speed up the discovery and the development of new anti-TB agents. During the last 20 years, huge progress in the treatment of *Mtb* infections was achieved thanks to the WHO, several investors, and the development of an increased awareness of the TB threat by the governments. Relevant improvements have been the optimization of the multidrug therapy and the study conducted on its potential interaction with the antiretroviral therapy (ARVs) for the treatment of HIV-1 positive TB patients. However, nowadays, no new class of drugs active against *Mtb* and MDR/XDR-TB have been put in the market yet. Therefore, it is of remarkable relevance to speed up the discovery of novel anti-tubercular agents in order to have new therapeutic strategies to stem the epidemic TB threat. Moreover, it is noteworthy to point out that the traditional way to develop new drugs is a long, slow and expensive process. Thus, it is evident both the necessity to discover new drugs as well as new technologies and methodologies, which would streamline and expedite the drug-discovery process. Therefore, the intention of this work is to design and synthesise molecules endowed with activity against TB and MDR-TB and to develop new, more sustainable and faster synthetic methodologies for the production of drug-like compounds.

1.2. *Mycobacterium tuberculosis*.

Mycobacterium is the single genus within the family of Mycobacteriaceae, in the order Actinomycetales.⁵ They are rod shaped organisms, which are characterised by slow growth speed under aerobic conditions as well as by a staining property called acid-fastness (i.e., resistant to de-colorization by acid after staining with carbol-fuchsin).⁶ Furthermore,

mycobacteria are classified into two major groups, slow growers and fast growers depending on their generation time. *Mycobacterium tuberculosis* is a typical slow grower with a generation time of 15-20 hours. It is possible to observe visible colonies only after days to weeks of incubation from the dilute inoculum in a cell culture. Such a slow generation time, compared to other bacterial species, is one of its main peculiar physiological features and contributes to its virulence. Mtb is an obligate aerobe, rod-shaped, non-spore forming and featured by a cell wall. Human lungs are natural hosts for this pathogen, where it causes pulmonary tuberculosis, although it can affect every part of the human body causing the so-called “extra-pulmonary infection”. One of the distinctive feature of Mtb is its mycobacterial cell wall (Figure 2).

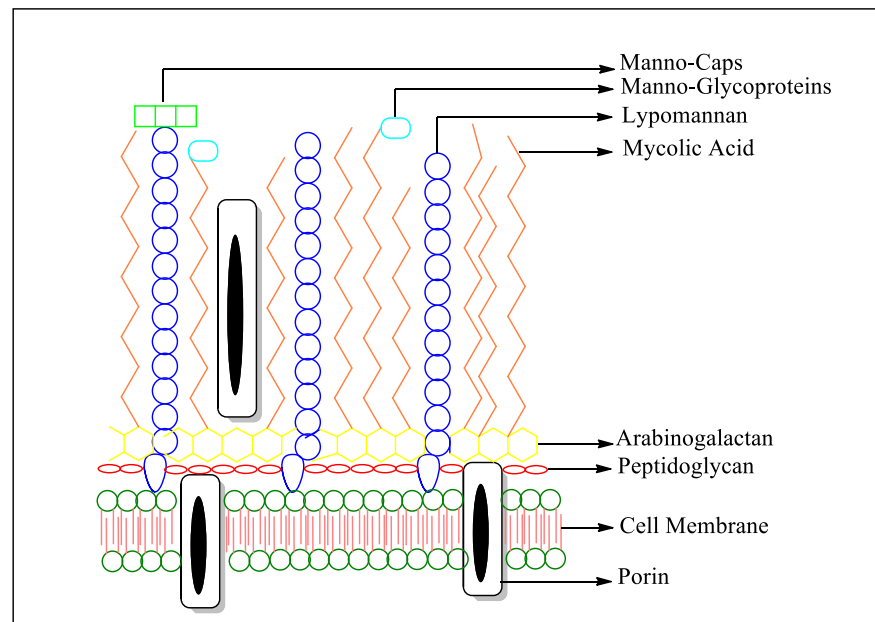


Figure 2. Structure of Mycobacterium cell wall.

It consists of an inner and an outer layer which envelope the plasma membrane. This structure is unique among prokaryotes, and it plays a paramount role for the virulence of the bacterium. The outer layer is composed mainly of lipids and proteins while the inner one has a more complex structure. The inner compartment consists of a frame of peptidoglycan (PG) and arabinogalactan (AG). This structure links covalently to an impermeable layer of extremely long chain α -branched β -hydroxylated fatty acids (C60-C90) called mycolic acids (MA).⁷ Across this frame, there are several glycolipids, such as lipoarabinomannan (LP), which is a major determinant on the inactivation of macrophages. PG is the major cause of

bacteria shape maintaining and protecting the bacteria from osmotic changes of the environment. AG links the PG and the important mycolic acids (MA). The mycolic acids are critical as well for the growth of the mycobacterium as for its survival in the infected host. MA affect the permeability of the cell wall forming an impermeable layer which shields the organism from environmental stress.⁸

1.3. Pathogenesis.

TB is an airborne disease, which is transmitted by individuals with Mtb active infection through droplet nuclei containing bacilli expelled by sneezing, coughing or even talking. Infection requires the inhalation of such small droplets. Then, once inhaled, Mtb have to overcome the upper respiratory defences reaching the terminal alveoli in the lungs. Usually, long and repeated exposure is necessary to an infected individual in order to start a primary infection.

1.3.1. Primary infection.

The first step of the infection is the recognition of *Mycobacteria* as non-self-pathogen by the innate immune system. Mtb is recognised by macrophages and dendritic cells through Toll like receptors (TLRs), nucleotide binding oligomerization domain-like receptors (NLRs), and C-type lectins.⁹ The alveolar macrophage ingests the *Mycobacteria*, enveloping it in a phagosome.¹⁰ Phagosomes are a class of endosome which are small vesicles utilized by the cell to internalize external material from the extracellular environment.¹¹ Once formed, the endosome is then distributed to other parts of the cell depending on the cellular needs. The natural route for a phagosome is the lysosome, where the cargo material is finally degraded and digested. However, Mtb, once inside the phagosome, activates a series of defensive methods which allows its survival. As mentioned before the mycobacteria existence inside the phagosome is mainly dependant on its cell wall. LP interferes with the generation of phosphatidylinositol 3-phosphate (PIP3) which is a host membrane component that plays a paramount role in the phagosome-lysosome fusion.¹² Moreover, LP blocks the macrophage activation interfering with MAPK, interferon- γ -mediated gene expression, TLR activation and phagosome lysosome fusion.^{13,14} However, if the phagosome-lysosome fusion occurs, forming a structure called phagolysosome, Mtb is able to resist the digestion process caused by reactive oxygen species and acid environment by its thick, mycolic acid cell wall layer. Furthermore, Mtb secretes a series of proteins such as coronin 1/tryptophan aspartate coat protein (TACO),¹⁵ the phosphate SapM¹⁶ and the serine/threonine kinase PknG in order to enhance its chances of surviving in the host organism. All the proteins secreted from Mtb,

aim to prevent the formation of the phagolysosome and so the consequent attempt to digest the content of the vesicle.¹⁷ However, once Mtb has been ingested, the immune system isolates the macrophages containing phagosomes surrounding them with other macrophages and T cells, forming a granuloma.¹⁸ The granuloma is a classic structure cluster of the cell-mediated immune response, which aims to stop the bacterial proliferation and isolate the infection site. In the early weeks of infection, it is possible that infected macrophages could travel to regional lymph nodes, where they gain access to the circulatory system and therefore, to any part of the body, developing potential extra-pulmonary infections. On the other hand, the classic scenario of primary infections ends with the macrophagic digestion of the *Mycobacteria*. When it happens the macrophage combines the antigenic fragments of Mtb to the major histocompatibility complex (MHC) class II molecules exposing it on its plasma membrane.¹⁹ There, antigen-MHC class II complex activates T cells which secrete cytokines and chemokines activating the other granuloma macrophages and ensuring the recruitment of other immune cells to the site of infection.²⁰ The activation of the granuloma's cells induce consequently the activation of the adaptive immune system which leads, in brief time, to the suppression of bacillary replication. Anyway, even in this scenario, the complete eradication of the infection is rare.²¹ The *Mycobacteria* could survive inside the granulomas for long time, even up to the lifetime of the host. However, in 95% of cases the primary infection is arrested and as long as the host immune system is effective Mtb do not cause any adverse effect on the host health.^{22,23} This stage of the infection is completely asymptomatic and it is called "latent infection".

1.3.2. Active infection.

People with Mtb latent infection have circa 10% lifetime risk of developing the active infection.² In the majority of the cases, TB primary infection reactivates within the first couple of years, but it can also occur decades later. The active infection occurs when the granuloma is no more capable to keep at bay the replication of the *Mycobacteria* inside the immune system cells. Any deterioration of the host immune system such as immunosuppressive medication, co-infection with HIV-1 or other diseases, and even malnutrition or ageing, could transform a latent infection to an active infection, which is symptomatic and contagious.²⁴ The active infection causes tissue lesions, which often mature in granulomatous lesions characterized by mononuclear cells surrounding a core of caseous necrosis tissue rich with Mtb bacilli. Such clusters are characteristic of lung tissue Mtb infections and they are called tubercles. The erosion of the tubercles into an adjacent airway

leads to the formation of a cavity in the lung tissue, the infection of another alveolar space, and the release of a huge load of bacilli into the sputum. The course of infection varies greatly, depending on the state of host defenses and the virulence of the Mtb strain. Without an effective treatment the mortality caused by TB is estimated to be 50%.²⁵

1.4. Tuberculosis and HIV.

TB infections are the second leading cause of death from an infectious disease worldwide.² TB mortality is second only to HIV-1 ones but it is demonstrated that the chances of developing an active TB infection is definitely higher among people infected with HIV-1 than healthy individuals.² In 2014, among the 9.6 million people with active Mtb infection 1.2 million were HIV-1 co-infected; and the majority of them (75%) were from the African region (Figure 3).²

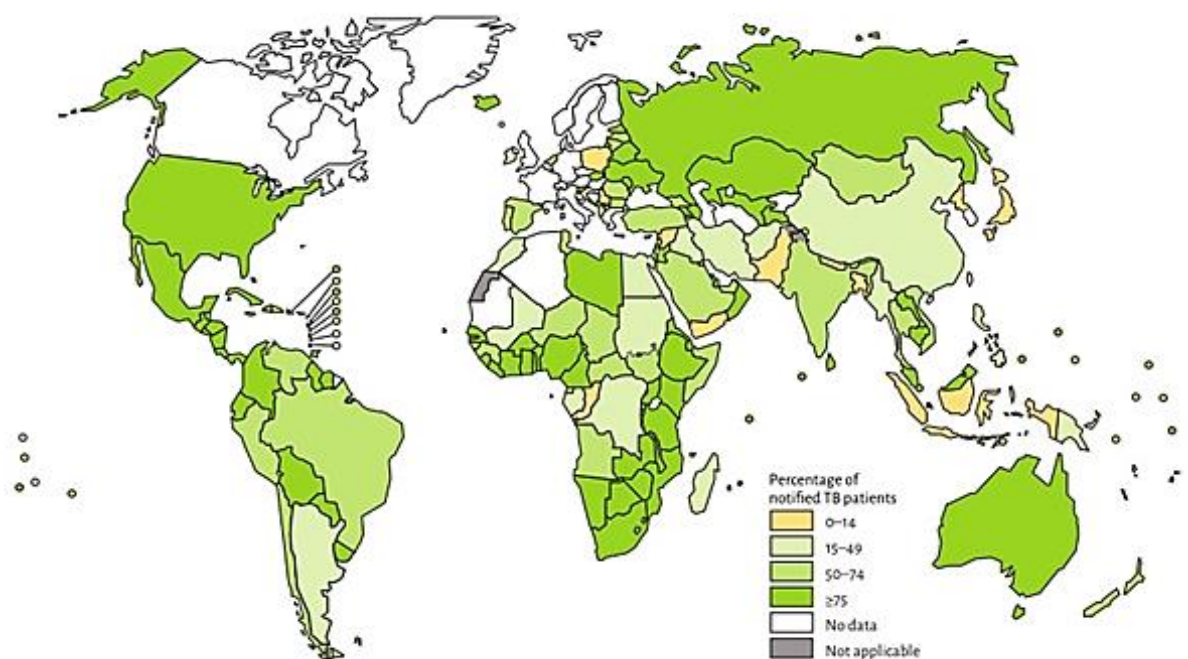


Figure 3. Estimated HIV-1 prevalence in new TB cases 2014.²

The risk of contracting TB mainly depends by the average degree of immunodeficiency of the community, followed by the predominant socioeconomic conditions and the incidence of TB infections among the population. In fact, following HIV-1 infection the risk of contracting TB increase from 10% in a lifetime to 10% every year.²⁶ HIV-1 causes a

depletion of CD₄⁺ T₄ helper cell which rules the recognition of the antigens in the adaptive immune system response.²⁷ When the CD₄⁺ T₄ helper cells counts start to decrease because of HIV-1 infection, the immune system is no more capable to fight *Mtb* latent infections or to protect the body from a first contact with the *Mycobacterium*.²⁸ Furthermore, the treatment of HIV-1 and *Mtb* co-infected patients is extraordinarily challenging and expensive. The combination of HIV-1 treatment with the multidrug treatment often lead to severe side effects exacerbating the bad compliance of the patient with the therapy.

1.5. Treatment of TB

Hospitalised individuals affected by *Mtb* infection are treated with a 6 months ambulatory therapy with so-called first line anti-mycobacterial drugs, such as isoniazid, rifampin, pyrazinamide and ethambutol (paragraph 1.5.1). The therapy begins with an “intensive” treatment phase of two months followed by a four months “continuation” phase. During the intensive treatment, the patient takes all the first line drugs, while during the continuation phase the treatment is reduced at just isoniazid and rifampin. The therapy is so structured in order to prevent the development of drug resistant strains and it is considered concluded when there is disappearance of viable tubercle bacilli from sputum, rendering the patient non-infectious. If TB condition persists over the first six months, it means that the infection has developed resistant strains to the first line drugs.¹¹ In case of resistant infections, the first period of treatment is followed by at least other six months with second line drugs (paragraph 1.5.2.). In the most extreme cases of resistance, the treatment is prolonged by another six months with third line drugs and MDR-TB reversal agent drugs. The drugs used for TB treatment are classified on the base of their activity, toxicity levels, availability and price in first line, second line, third line drugs and MDR-TB reversal agent drugs.

1.5.1. First line drugs

The first line drugs are the drugs endowed with higher activity for the treatment of TB and they are all available for oral administration (per os).

- **Isoniazid**

Isoniazid (INH) (Figure 4) is a synthetic bactericidal agent with a MIC of ~0.24 µg/mL against *Mtb* characterized by high tissue penetration.

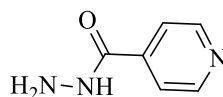


Figure 4. Chemical structure of isoniazid.

It is considered the single cheapest and most useful antitubercular agent among the first line drugs. INH is a prodrug which is converted in situ to its bactericidal active forms by *Mycobacteria* catalase peroxidase KatG.^{29,30} KatG converts INH in reactive species such as the isonicotinic hydrazyl radical and the isonicotinic acyl radical (IAR) which form adducts with the coenzyme nicotinamide adenine dinucleotide (NAD⁺). The adduct IAR-NAD blocks the biosynthesis of long chain mycolic acids through the inhibition of enol-acyl carrier protein reductase (InhA), which is a key component of the fatty acid synthesis complex (FAS II).³¹ It is used for the prevention and the treatment of both latent and active TB³². However, decades of wrong use in many developing countries, often as monotherapy, have greatly increased the percentage of INH resistant strains.³³ Studies on the identification of mutations that could lead to INH resistant strains proved to be not exhaustive. In fact, the 50-60% of INH resistant strains show mutations, insertions or small deletions that are not present on INH sensitive control strains. Mutations leading to INH resistance have been identified in different genes involved in the bio-synthesis of INH cellular targets such as *KatG* (36.8%), *InhA* (31.6%), *ahpC* (13.2%) and other genes which function remain to be established.³⁴

- **Rifampin**

Rifampin (RIF) together with INH is one of the key component of the initial anti-TB treatment. It is a bactericidal semi-synthetic agent derived from a metabolite of *Amycolatopsis rifamycinica* and it shows good tissue and cell penetration, acting rapidly. Furthermore it affects extra and intra-macrophagical mycobacteria and is dramatically effective for the treatment of latent infections.

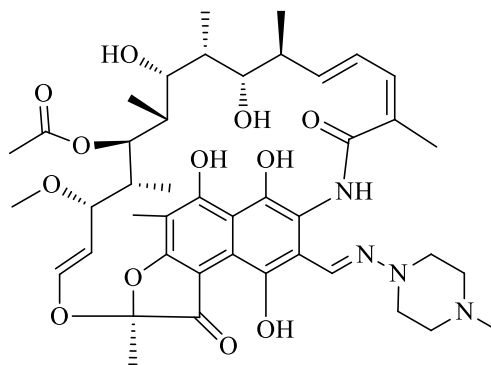


Figure 5. Chemical structure of rifampin.

RIF carries out its action on the DNA-dependent RNA polymerase β subunit.³⁵ However, *Mtb* generates easily rifampin resistant strains. In the 96% of the RIF resistant *Mtb* strains there is a mutations in the 81-bp core region of *rpoB* gene, which encodes the β subunit of RNA polymerase. It is noteworthy that 90% of rifampin resistant isolates are also resistant to isoniazid, making RIF resistance a useful surrogate marker for the identification of MDR-TB strains.³⁶

- **Ethambutol**

Ethambutol (EMB) possess the safest profile among the first-line drugs (Figure 6).

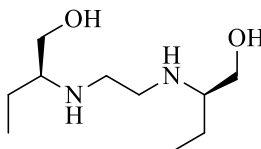


Figure 6. Chemical structure of ethambutol.

Despite the fact that its mechanism of action has not been completely elucidated, there is evidence that EMB exerts its bacteriostatic activity blocking the biosynthesis of the mycobacterial cell wall constituent AG, inhibiting the activity of the arabinosyl transferase.³⁵ The lack of a clear mechanism of action limits also the investigation on the causes of development of EMB resistant strains. Mutation in the gene *EmbB* is the cause of EMB resistance in roughly 70% of *Mtb* clinical isolates. However, EMB resistance has been observed in many organisms lacking mutations in *EmbB*, suggesting that mutation in other genes could encode for resistant strains.³⁷

- **Pyrazinamide**

Pyrazinamide (PZA) is a bactericidal prodrug converted inside the granuloma to the active pyrazinoic acid by a nicotinamidase-peroxydase enzyme known as pyrazinamidase mycolic acids. It acts synergistically with RIF, it kills the semi-dormant tubercle bacilli, and its activation seems to be directly correlated to the acidic environment of the phagolysosome (pH 5.5) in the presence of pyrazinamidase. In fact, PZA shows its high sterilizing activity *in vitro* only if in acidic cultures. Its mechanism of action has not yet been elucidated but there is evidence that it binds to the ribosomal protein S1 affecting the trans-translation.³⁸ In order to understand how Mtb develops PZA resistant strains, mutations on the *pncA* gene encoding pyrazinamidase have been widely studied. A remarkably large array of *pncA* mutations (70%) lead to tertiary structure modification of pyrazinamidase. Such modifications are often followed by a detrimentally change to the enzyme function, avoiding the conversion of pyrazinamide in the active pyrazinoic acid.³⁹ Furthermore, some PZA-resistant strains show mutations in the genes *panD* and *RpsA* which encode respectively for aspartate decarboxylase and the ribosomal protein S1.⁴⁰

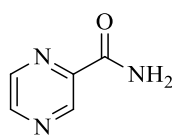


Figure 7. Chemical structure of pyrazinamide.

1.5.2. Second and third line drugs.

The second and third line drugs were not specifically designed as antitubercular drugs but, they found a relevant application in the TB treatment since they possess activity against Mtb and its resistant strains. They are generally less active, more toxic and more expensive than the first line drugs. Their application is limited to treat MDR/XDR-TB cases or when the patient, after the first six months treatment, still shows the presence of Mtb spores in the sputum.

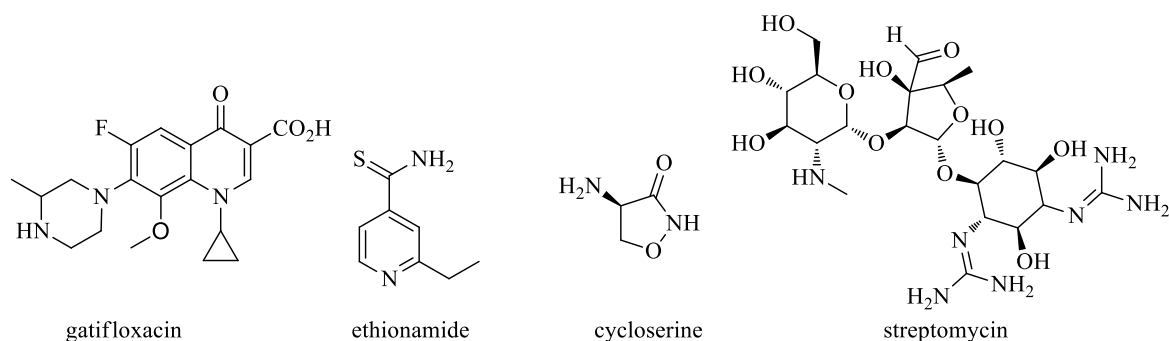


Figure 8. Some examples of second line drugs.

- **Streptomycin**

Streptomycin (SM) is an antibiotic of the class of the aminoglycosides, and it was the first drug to be used in the treatment of TB in 1948.⁴¹ Nowadays, the SM is considered a second line drug because its administration is only intramuscular and because it causes severe ototoxicity and nephrotoxicity after prolonged treatment. Furthermore, SM bactericidal effect is limited to actively growing tubercle bacilli (MICs between 2–4 $\mu\text{g/mL}$), but it is completely ineffective against non-growing or intracellular bacilli. SM mechanism of action consists of the inhibition of protein synthesis by its binding with the subunit 16S ribosomal RNA.⁴² Direct mutations on its cellular target associated with genes *rrs* and *rpsL* are the main cause of SM resistance strains (75% of the cases). However, failure to identify resistance-associated mutations in these genes on the 25% of organisms indicates that other molecular mechanisms of SM resistance take place.⁴³

- **Fluoroquinolones (ciprofloxacin, ofloxacin, levofloxacin, gatifloxacin and moxifloxacin)**

The Fluoroquinolones (FQs) are a class of broad-spectrum antibiotics which are commonly used for the treatment of gastrointestinal, respiratory, and urinary tract bacterial infections as well as sexually transmitted diseases.⁴⁴ FQs show good activity against Mtb and their cellular targets are the bacterial DNA gyrase and topoisomerase IV.⁴⁵ They are the safest and most active antitubercular drugs after INH and RIF, however they are not considered first-line drugs because their high rate of development of FQs resistant Mtb strains.^{45,46}

- **Aminoglycosides (kanamycin, amikacin and capreomycin)**

The aminoglycosides amikacin (AMK), kanamycin (KAN) and the cyclic polypeptide capreomycin (CAP) are important injectable drugs for the MDR-TB treatment. All of them interfere with protein synthesis at the level of protein translation. AMK/KAN and CAP based

therapy easily develop nephrotoxicity and their use is limited by the high rate of development of cross resistant Mtb strains.^{47,48} However, KAN is the most commonly used injectable for MDR-TB.

- **Ethionamide/Prothionamide**

Ethionamide (ETH) and prothionamide (PTH) are derivatives of isonicotinic acid and have been used as anti-tubercular agents since 1956. They both act as prodrugs, and they share the same mechanism of action of INH blocking the mycolic acid synthesis pathway.^{49,50} However, ETH and PTH active metabolite forms have not been identified yet. Studies have demonstrated that Mtb resistant strains to ETH show cross-resistant to PTH and INH.⁵¹ Their use is limited to the MDR-TB treatment because they both causes severe gastrointestinal side effects. They cannot be associated in the treatment with *p*-amino salicylic acid because the co-administration causes hypothyroidism, further shortening their therapeutic window as second line drugs.

- ***p*-Amino salicylic acid**

p-Amino salicylic acid (PAS) is one of the oldest known antitubercular agents and it has been used in co-administration with INH and SM till the discovery of more effective and safer alternatives such as RIF.⁵² Despite the fact PAS is one of the oldest molecules to be used as antitubercular agent, its mechanism of action is still not clear. Furthermore, PAS use is limited only to the treatment of XDR-TB cases because of its extreme gastrointestinal toxicity.²

- **Cycloserine**

Cycloserine (CS) is an antibiotic, for which the exact mechanism of action is still unknown. However, there is evidence showing its effect on the biosynthesis of the peptidoglycan which is a paramount constituent of the mycobacterial cell wall. CS possesses high gastric tolerance, and lacks cross-resistance to other compounds, but it causes severe adverse psychiatric effects;⁵³ which relegates it as second line drug. However, CS shows good application in the treatment for MDR-TB and XDR-TB.⁵⁴

- **Phenothiazine (thioridazine, chlorpromazine)**

Phenothiazine derivatives, especially thioridazine (TZ), have been recently used in therapy as third line drugs (Figure 9).⁵⁵

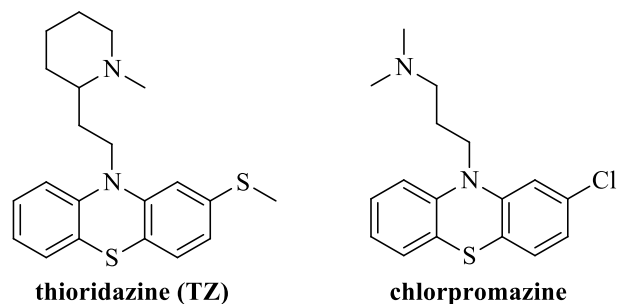


Figure 9. Chemical structures of thioridazine and chlorpromazine.

These compounds are normally employed for the management of psychosis⁵⁶ but, activity assessment against mycobacteria demonstrated that phenothiazines inhibit the growth *in vitro* of Mtb, affecting also MDR-TB and XDR-TB.⁵⁷ The mechanism of action is still unclear but there are evidence that they affect Mtb at several biological targets.⁵⁵ Furthermore, they interfere with the synthesis of efflux pumps which is correlated to the development of resistant strains turning out to be good anti-TB reversal agent. However, their use is limited to the treatment of XDR-TB infections because their severe cardiac side effects and their potent activity on the CNS.⁵⁸

1.5.3. MDR-TB reversal agents

Against some MDR-TB and XDR-TB cases, the application of first line drugs and second line drugs alone have no efficacy. The more relevant and the most frequent tool for the development of resistance adopted by the bacteria is the expression of efflux pumps. This special mechanism of active efflux allows the bacteria to extrude unwanted toxic substances through specific protein channels deployed on the cell wall.^{59,60} Some efflux systems are drug-specific, whereas others may accommodate multiple drugs, and thus contribute to bacterial multidrug resistance (MDR). MDR-TB reversal agents are compounds, which inhibit directly, or reduce the expression of efflux pumps in the mycobacteria. Once the efflux pump system is inhibited, drugs, which previously were extruded by such mechanisms, are again free to reach their site of action and have effect on the bacteria. The cornerstone of the reversal agents is Verapamil (a Ca^{2+} antagonist) that has high efficacy in blocking the efflux pump proteins such as P-glycoproteins.⁶¹ An other example of an MDR-TB reversal agent is thioridazine, which has been used successfully in co-administration with INH for the treatment of XDR-TB cases.^{58,62}

1.5.4. Vaccination.

During the last century, several disease which have afflicted humanity have been annihilated with the development of vaccines. The slow decline in TB incidence globally and the growing problem of MDR-TB have been the driving force for the development of a vaccine for Mtb infections. The older vaccine available is the Bacille Calmette-Guerin (BCG) which is obtained by an avirulent strain of *Mycobacterium bovis*.⁶³ BCG however is almost a century old, and while the vaccine is effective against severe forms of TB in children, its efficacy in preventing pulmonary TB in adults is highly variable. BCG is also not recommended for patients infected with HIV-1 due to the risk of disseminated BCG disease.⁶⁴ The development of novel genetic manipulation techniques combined with the completion of the *M. tuberculosis* genome sequence in the 1990s, provide in the past two decades, the chance to approach the development of novel vaccines with two different strategies. The first involves the research of vaccines that would have a higher efficacy than BCG. That includes the study of an improved version of BCG or a new attenuated Mtb strain vaccine.⁶⁵ The second strategy instead is based on the development of a second vaccine to be used as a “booster” for the BCG dose given to neonates which would aim to increase the efficacy and extend the duration of protection.⁶⁶ TB vaccine candidates in clinical trials in August 2015 are shown in Figure 10.

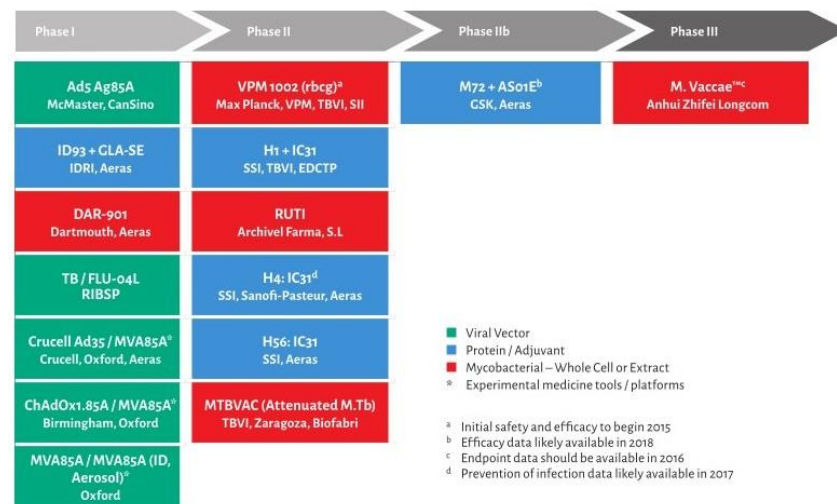


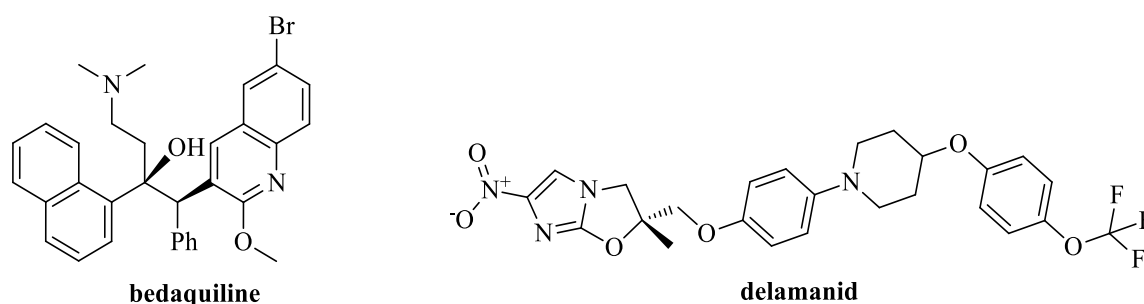
Figure 10. TB vaccine candidates in clinical trials in August 2015²

1.6. MDR-TB, XDR-TB and causes of development of resistance.

Bacteria become resistant to drugs used in therapy through several mechanisms. First of all the organism may produce enzymes or metabolites capable to modify, inactivate or degrade

the antibacterial agent before it can conduct its effect. Next in order, the bacteria could change the permeability of the cell wall, limiting the contact with the antimicrobial agent. In fact, one of the most common causes of drug resistance in bacteria is the development and expression on the cell wall of efflux pumps capable of expelling unwanted molecules out of the cell.⁶⁷ All these mechanisms involve spontaneous mutations or the acquisition of genetic information that encodes resistance from other bacteria.⁵⁹ The new strains, which evolved in such ways, may be no more affected by the class of drugs, which were previously sensitive. Paradoxically, studies have demonstrated that the major cause of development of mutated strains is erroneous antimicrobial drugs use. Incomplete, erratic, or single-drug therapy for the treatment of TB selected over the last five decades, Mtb resistant mutated strains (DR-TB). Moreover, this phenomenon, combined with 40 years of no active research for novel antitubercular agents endowed with novel mechanism of actions against Mtb, has played a paramount role in the formation of DR-TB.^{25,68} Once DR-TB has developed and proliferated, it potentially can gain resistance to additional drugs through the same process, developing multidrug-resistant strains. The development of MDR-TB and XDR-TB has complicated enormously the treatment of hospitalized patients. MDR-TB infections are hardly treatable, because they are Mtb strains resistant to at least two of the four first line drugs. They require a longer hospitalization time and the use of alternative treatment course with more toxic, less effective, and more expensive drugs.² As reported in the WHO annual reports the incidence of MDR-TB cases is increasing year by year. In 2011 the estimated MDR-TB cases worldwide were between 220,000 to 440,000 while in the last report the estimated worldwide cases were 480,000.^{2,69} On the other hand, XDR-TB are MDR-TB strains which have developed resistance to fluoroquinolones and at least one injectable drug (e.g., streptomycin, amikacin, kanamycin, capreomycin).² The treatment of XDR-TB infections is complicated and in some cases completely ineffective. The drugs used against XDR-TB infections consist of the co-administration of the remaining active drugs available, which usually cause severe side effects and have high costs. The outcome of resistant strain infections depends strictly on the number of effective drugs still available as well as the compliance of the patients for the entire length of the enhanced treatment. However, for XDR-TB infection the mortality is higher than all the other TB cases.⁶⁸ In 2013 the “Centers for Diseases Control and Preventions” of South Africa reported the first cases of infection caused by total drug resistant Mtb strain (TDR-TB) which was unaffected *in vitro* by all the known antitubercular agents.⁷⁰ Nowadays, in order to stem the development of new DR-TB, several new anti-TB drugs are in preclinical or clinical development. The diamine SQ109,⁷¹ the fluoroquinolone gatifloxacin⁷² and linezolid⁷³ are just some of a large pipeline of compounds. However, the

validation process for a new drug candidate is so long and so severely selective that the majority of the molecules presented in the pipeline probably will never be available or they will be after several years of intense study and optimization. For example, TBA-354, a nitroimidazole derivative such as delamanid and pretomanid, is the first lead candidate endowed with antitubercular activity in the last 6 years to enter a Phase I clinical trial.^{74,75} Only recently, two new molecules endowed with activity against TB and MDR-TB gained partial access to the market: bedaquiline and delamanid (Figure 11). In December 2012, bedaquiline was approved by the US Food and Drug Administration (FDA) for treatment of adults with pulmonary MDR-TB as part of combination therapy when other available therapeutic strategies have failed. However, safety and efficacy parameters of bedaquiline, in combination with first or second line drugs for short duration treatment, are currently being investigated as part of the Phase III trial.⁷⁶ In November 2013, the European Medicines Agency (EMA) granted a conditional marketing authorization for delamanid which is now used as part of a multi-drug therapy for pulmonary MDR-TB in adult patients. However its application as antitubercular agent is limited only “when an effective treatment regimen cannot otherwise be composed for reasons of resistance or tolerability”.⁷⁷ Despite these two molecules represent a huge step onward for the treatment of MRD-TB and XDR-TB, their limited application does not satisfy the need of novel alternatives for tackling the TB threat. In fact, nowadays, no new class of molecules active against MDR/XDR-TB have been approved worldwide. Finally, until treatment programs are consolidated (eg., by full supervision of each dose, and improved access to culture and susceptibility testing), stepwise resistance to the new drugs discovered is still likely.⁷⁸



desired and specific pharmaceutical activity. The synthesis of a putative drug has to be as cheap, fast and simple as possible, in order to reduce costs and research time. At an early stage of the drug discovery, traditional synthetic protocols are usually applied, however, the use of novel reactions which increase the repertory of the available bond forming strategies have often a remarkable impact in reducing the costs of the drug optimization programs.⁷⁹ Furthermore, the detection of new reactions often unlock and made highly desirable synthetic pathways considered previously impractical to follow in a drug discovery program.⁸⁰ Therefore, the development of novel methodologies is a field of research at high impact for the discovery of the bioactive compounds of the future. Every new reaction is important and has the potential to increase the chances of success of a drug discovery program. However, the transformations which have major appeal on both academia and industry, are reactions with application toward the synthesis of heterocycles.⁸¹ Heterocycles are recurrent structures in several natural products and thus relevant building blocks to be used for the production of compounds of pharmaceutical interests.⁸² Therefore, the discovery of new methodology toward the synthesis of such privileged scaffold could be the key turning point to solve challenging synthetic problems which affects nowadays the drug discovery and optimization process making more efficient and faster the development of novel medicines.

1.8. Statement of research objectives.

The TB treatment scenario urgently require acceleration of the development of novel alternatives to the drugs available in the market. Therefore, the research presented hereafter is intended to show the rational design, synthesis and effective antimicrobial screening of novel molecules endowed with activity against Mtb following two validated strategies of the phenotypic drug discovery approach.² Furthermore, as mentioned in paragraph 1.7, it is well documented that every drug discovery program and drug optimization process heavily relies on the synthetic methodologies available for the synthesis of heterocycles.⁸⁰ Therefore, the pharmaceutical work presented in this thesis is enriched with the development of new and sustainable synthetic methodologies for the production of highly valuable building blocks to be used in the synthesis of antitubercular drugs.

1.8.1. Structure of the thesis.

This thesis consists of two main sections. Each section has two self-contained chapters, including their introduction, results and discussion, experimental part, and conclusion.

The first section focuses on the discovery, synthesis and biological evaluation of novel anti-tubercular drugs through two distinct strategies. The first strategy adopted is the molecular simplification approach applied to the synthesis of derivatives of a drug recently repurposed against TB. The drug chosen for this approach is thioridazine (TZ), which is a well-known neuroleptic drug, endowed with good anti-tubercular activity. TZ has been recently used for the treatment of MDR and XDR-TB cases where alternative treatment resulted ineffective.⁸³ The second strategy used for the design of novel TB agents, is the virtual molecular hybridization approach. The molecular hybridization approach is one of the strategies included within the rational design protocol for identification of new biologically relevant small molecules. This approach is based on the recognition of structurally comparable or similar molecular portions of two or more bioactive compounds. The approach was applied to two molecules endowed with anti-tubercular activity (BM212 and SQ109) (Figure 12).

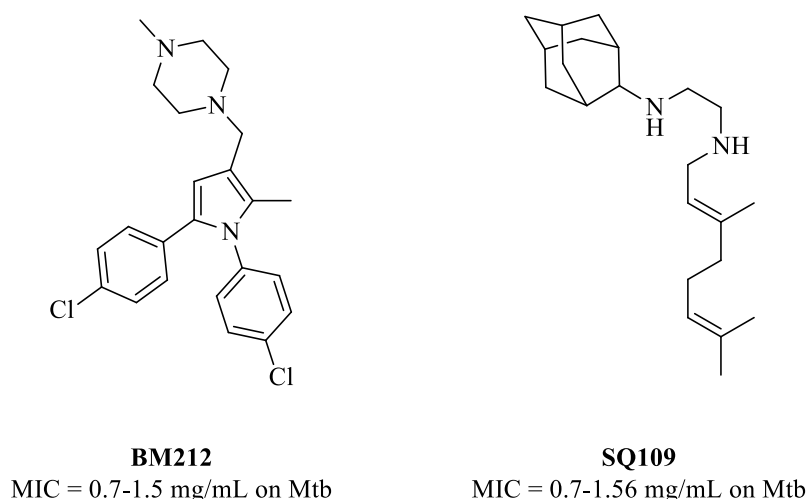


Figure 12. Chemical structures of BM212 and SQ109.

The activity against a panel of mycobacteria of all the compounds synthesised have been finally reported. The most promising molecules were also assessed against a panel of MDR-TB clinical isolates. Moreover, the most active compounds were evaluated as whole-cell efflux pump inhibitors.

In the second section, two novel cascade processes for the synthesis of drug-like compounds, namely pyrroles, were fully explored and developed. The development of novel synthetic methodologies has always been the driving force for the synthesis of more and more complex molecules in a faster, easier, cheaper, greener and competitive fashion. The two cascade

processes described in these chapters involve metathesis reactions applied for the synthesis of heterocycles, especially pyrroles, which are the scaffold of many drugs including the antitubercular compounds developed in this work. The first methodology allows the synthesis of 1,2,3-substituted pyrroles through a one-pot tandem enyne cross metathesis (CM)-cyclization reaction starting from appropriate propargylamines.⁸⁴ A large variety of synthetically challenging pyrroles bearing aryl, hetero-aryl and alkyl substituents were obtained in medium-good yields through this process, which involves microwave irradiation and a weak Lewis acid as CuSO₄ to promote the cyclization step. The reaction is rapid, procedurally simple and represents a facile entry to the synthetically challenging 4,5-unsubstituted pyrroles. In the second part of this section, a novel and sustainable chemo-enzymatic process for the synthesis of pyrroles is described. Pyrroles were obtained exploiting the oxidative and previously undisclosed aromatizing properties of monoamine oxidase (MAO) biocatalysts combined efficiently in the same reaction medium with a ring closing metathesis (RCM) reaction.⁸⁵ The main charm of this technique is represented by the successful combination of chemo- and enzymatic catalysis in a concurrent fashion. Mimicking the compartmentalization of cellular processes by appropriate choice of solvents and reaction conditions, it has been possible to overcome the compatibility issues of the catalysts and the difference of the reaction conditions in which these generally operate. The novel methodology can be exploited for the sustainable production of highly valuable putative antitubercular drugs.

2. Design and synthesis of potent antitubercular agents effective against multidrug-resistant mycobacteria.

2.1. Introduction.

2.1.1. Approaches for the drug discovery of novel molecules active against Mtb.

The drug discovery process is a slow, expensive process with high risk of failure but it is in continual evolution and optimization. Nowadays, new biologically relevant small molecules active against bacteria are identified by the means of a rational design protocol, which may involve two distinct approaches, the target based approach and the phenotypic approach.⁸⁶ The target-based approach consists of the identification of a key biological target and in the design and development of a molecular entity capable to have a selective and potent activity on it. The phenotypic approach instead selects a drug candidate on the base of its overall effect on intact biological systems (cells, tissues, or animals). The target-based approach is often simpler and faster to execute than a phenotypic approach, and provides detailed data on the interaction of a molecule with the specific target. However, this approach does not take into account several variables, which characterize the “druggability” of a molecule (bioavailability, metabolic pathways etc.), and it has never been applied successfully to the design of antibacterial compounds.⁸⁷ Furthermore, the reliability of this approach is directly related to the precision of the available information on the selected cellular site of action, limiting its application to drug discovery processes where there is available a clearly validated target. On the other hand, the phenotypic approach generally takes more effort and resources, but usually the *in-vitro* results are more directly related to the *in-vivo* activity. In contrast with target based approach, the phenotypic systems often do not take into account the mechanism of action and the biological target of assessed molecules. Therefore, the identification of the structure activity relationship (SAR) and the further optimization is slower and perilous. However, this approach finds a huge application in the drug discovery process whenever there is a lack of information about a validated cellular target (new or neglected diseases) or in the development of new treatments for diseases which develop quickly drug resistance.⁸⁷ One of these diseases is TB, which has been considered for over 40 years a neglected disease until the MDR-TB and XDR-TB cases, raised all around the world, forced the WHO to declare TB treatment a health emergency. In order to identify molecules endowed with potent activity against Mtb and MDR-TB two different approaches have been adopted: the virtual molecular hybridization approach and the molecular simplification approach starting from a recently repurposed drug. The virtual molecular hybridization approach is based on the recognition of structurally comparable or similar

molecular portions of two or more bioactive compounds. By means of merging of these molecular portions, new hybrid chemical entities that maintain structural elements of the parent compounds could be designed. On the other hand, the molecular simplification approach applied to the structure of a recently repurposed molecule aims to identify structurally simpler derivatives of a well-known biologically active structure, allowing a pioneering study of a potential novel class of bio-active compounds. The synthesis and the activity assessment of the drug derivatives could elucidate unexpected novel biological targets, which can lead to the discovery of putative innovative lead compounds.

2.2. Repurposing and molecular simplification of thioridazine as a strategy for the development of novel antitubercular agents effective against multidrug-resistant mycobacteria.

In 2012, bedaquiline (Figure 11),^{88,89} the first MDR-TB drug to be developed in 40 years, was launched in the market and as of now there is a blooming pipeline of putative new molecules endowed with antitubercular activity in clinical trials. However, the conventional overall therapeutic approach, and the slowness of the drug discovery process make probable that further new MDR-TB strains will relentlessly evolve also for these novel drugs.⁹⁰ The practical solution, adopted nowadays for avoiding development of resistant strains after point mutations, is the administration of several antitubercular drugs simultaneously.^{91,92} However, this is not a perfect solution, especially for TB treatment. The nature of Mtb forces the application of a multidrug therapy for months decreasing even further the already bad compliance of the patients with the actual TB treatment.^{93,94} Hence, the ideal approach to defeat TB, is to discover a drug capable of inhibiting multiple Mtb targets simultaneously while also retaining activity against MDR and latent TB. Studies aimed to the elucidation of the mechanism of action of the third line antitubercular drug TZ (Figure 12),^{55,83} showed that the mechanism of action of this drug involves several mycobacterial targets and it affects a large variety of bacterial pathways at the same time.. . It induces an increase in the wall-cell permeability,⁹⁵ and reduces the expression of genes related to the over-expression of efflux pumps in Mtb,^{60,96} which is one of the most common causes of multidrug resistance.^{33,97} By the inhibition of efflux pump genes such as *mmpL7*, *p55*, *efpA*, *mmr*, *Rv1258c* and *Rv2459* TZ makes MDR-TB strains susceptible again to the attach of first line drugs.^{98,99} Moreover, Dutta *et al.* demonstrated that TZ is active against many genes which code for essential proteins on the mycobacteria.^{100,101} One of them is the *ndh* gene that encodes the type-2 NADH dehydrogenase (NDH-2) which is a key enzyme on the

mycobacterial aerobic respiratory pathway.¹⁰² Furthermore, thioridazine kills dormant Mtb^{103,104} by the mean of an effect on the macrophage which could represent a novel way for the treatment of pulmonary TB. By targeting both the macrophage and the mycobacteria, TZ has the chance to bypass any developed drug resistance of the bacteria. It is noteworthy that, thioridazine is accumulated inside the alveolar macrophages reaching concentrations ten times higher than its concentration in plasma which justifies its scarce activity *in vitro*. In order to explain this host target mechanism Amaral and coworkers demonstrated that high intracellular concentration of TZ in macrophages inhibits the transport of calcium and potassium ions, causing a reduction of the pH in the phagolysosomal vacuole.¹⁰⁵ The acidification of this latter promotes the hydrolysis of the mycobacterium entrapped in the phagolysosome.^{106–108} This mechanism of action enhances the killing activity of the macrophages which become then capable to degrade even the most XDR-TB strain within the latent stage of the infection.¹⁰⁹ Moreover, it has been reported by Amaral and coworkers that several drugs of the phenothiazine class have similar mechanism of action against Mtb. However, among them just chlorpromazine, trifluoroperazine and thioridazine showed enough potency to have a practical application in TB therapy and only this latter is possible to be used at the dose required as third line antitubercular agent (Figure 13).¹⁰¹

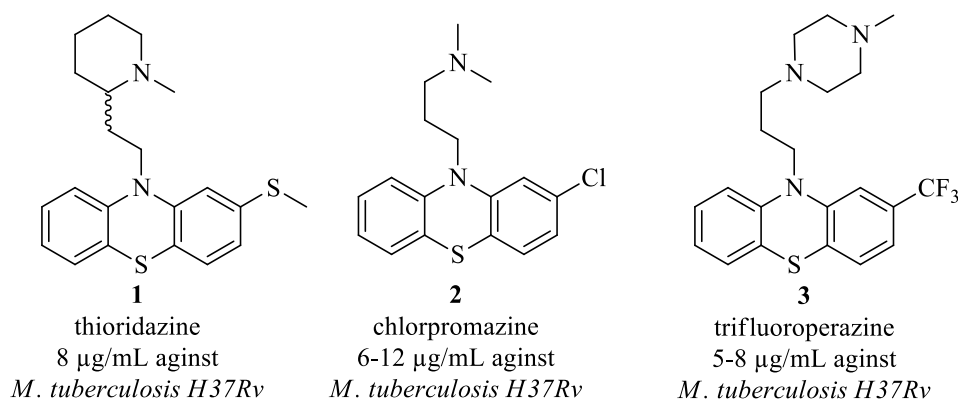


Figure 13. Thioridazine, chlorpromazine and trifluoroperazine.

Despite the huge variety of potential targets that TZ has against Mtb and its resistant strains only few derivatives have been synthesised so far and no drug derivatization and optimization studies have been carried out on TZ analogues as inhibitors of MDR-TB.^{110–112} Thus, a new library of TZ derivatives has been designed, synthesised and evaluated for their antitubercular activity against a panel of mycobacteria including MDR-TB clinical isolates.

The role of the aliphatic side chain of **1** and its importance for the antitubercular activity was firstly explored as shown in Figure 14.¹¹³

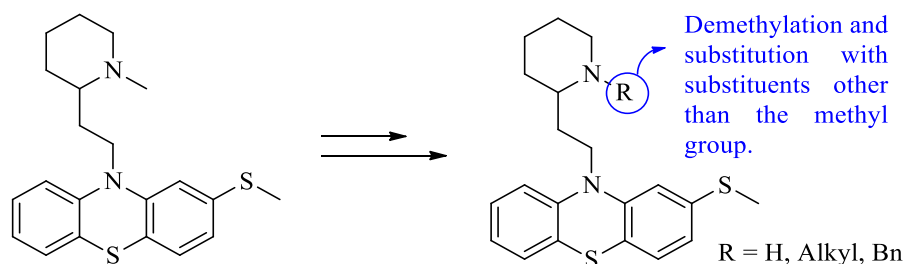


Figure 14. First set of **1** analogues. Replacement of the methyl group.

The *N*-methyl substituent on the piperidine ring of **1** has been removed and then decorated with groups other than the methyl one. Furthermore, the impact on the antitubercular activity of a basic side chain was investigated through the synthesis and the biological evaluation of derivatives with the amine nitrogen protected as carbamate. Then a second series of derivatives was synthesised where the piperidine ring of **1** was replaced with different aliphatic heterocycles, keeping fixed the distance between the piperidine nitrogen and the phenothiazine ring (Figure 15).

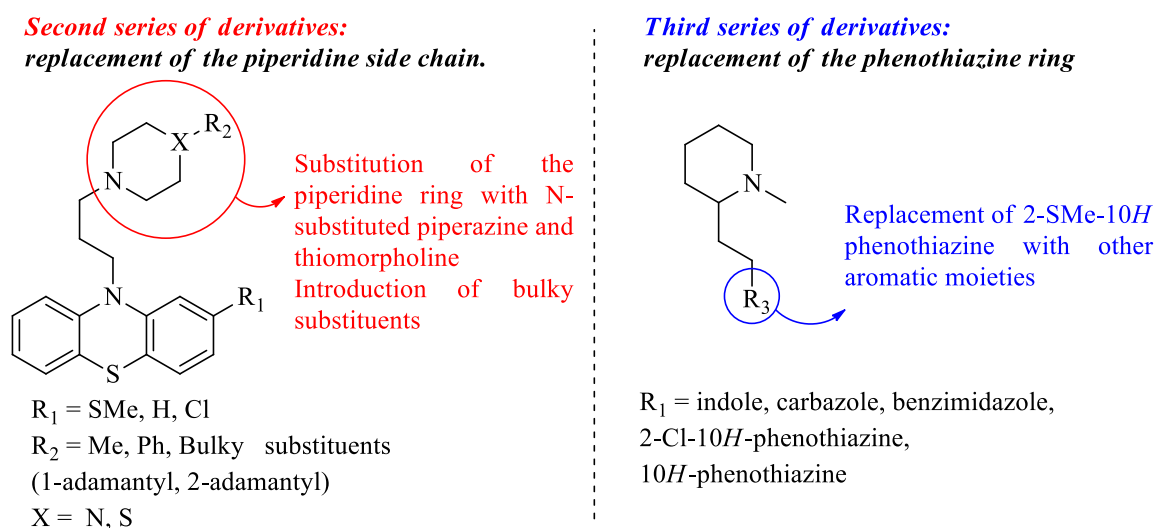


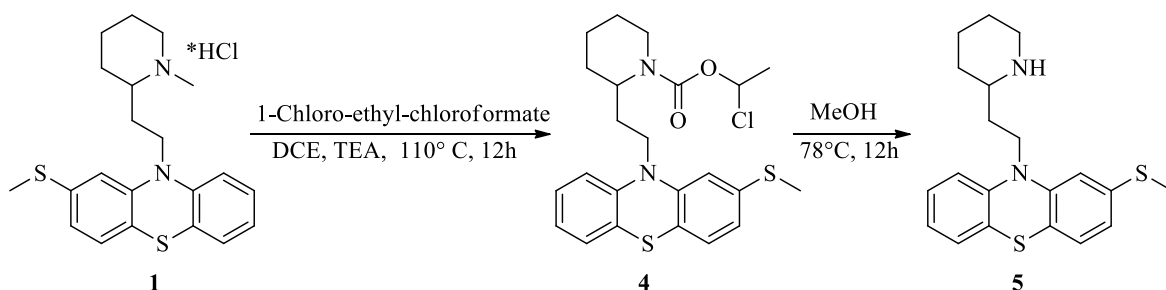
Figure 15. Second and third series of TZ derivatives.

Finally, the 2-thiomethyl-phenothiazine core, which is responsible for the main side effects on the central nervous system, was replaced with different hetero-aromatic rings, with the aim to reduce the toxicity of the molecule.

2.2.1. Results and discussion.

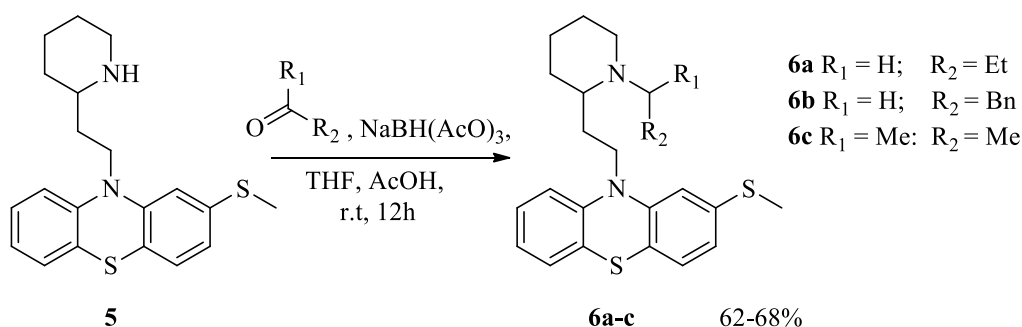
2.2.1.1. Synthesis of thioridazine derivatives.

The *N*-substituted derivatives **6a-c** have been synthesised in order to investigate the role of the methyl substituent on the piperidine nitrogen. **1** has been successfully de-methylated following the procedure described by Hopfner and coworkers.¹¹⁴ yielding compound **5** in 85% yield (Scheme 1). Compound **4** has been isolated in order to investigate the impact of a basic side chain on the antitubercular activity of **1** derivatives.



Scheme 1. Synthesis of *nor*-thioridazine.

Then, compound **5** was reacted with the appropriate ketone/aldehyde (namely propanone, propionaldehyde, and benzaldehyde) in the presence of the reducing agent sodium triacetoxyborohydride ($\text{NaBH}(\text{AcO})_3$) affording the corresponding alkyl-piperidine **6a-c** with good yields (Scheme 2).

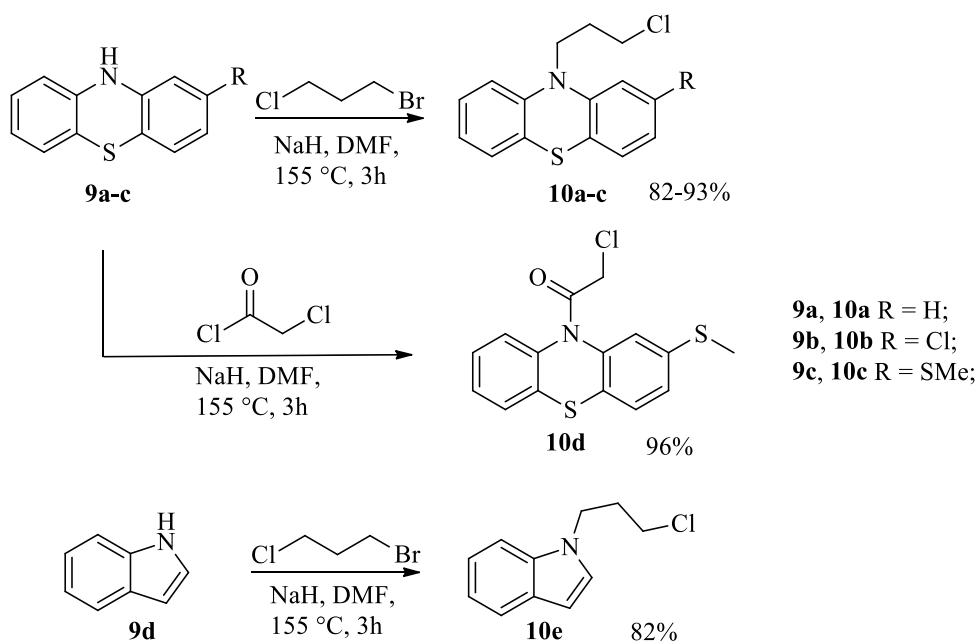


Scheme 2. Reductive amination reaction conditions for the synthesis of **6a-c**.

A second series of derivatives where the piperidine ring was replaced with commercially available *N*-substituted piperazine and thiomorpholine was then synthesised. In this second

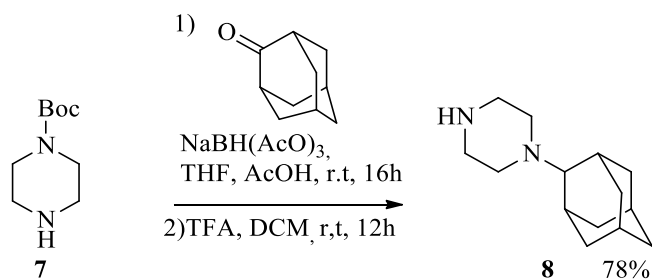
series, the 2-thiomethyl substituent on the phenothiazine ring was removed or replaced with chlorine, to evaluate its importance for the antitubercular activity. (Scheme 3, Table 1). In particular, the chlorine substituent was chosen because of structural similarity with chlorpromazine **2**, a phenothiazine derivative closely related to TZ.

Firstly, commercially available aromatic compounds **9a-d** (namely **9a** 10*H*-phenothiazine, **9b** 2-Cl-10*H*-phenothiazine, **9c** 2-SMe-10*H*-phenothiazine, **9d** indole) were alkylated to 1-bromo-3-chloropropane obtaining compounds **10a-c** and **10e**. Furthermore, **9c** was also reacted with 2-chloroacetyl chloride leading to **10d** (Scheme 3).



Scheme 3. Synthesis of compounds **10a-e**.

Then, 2-Adamantyl-piperazine **8** was obtained through a two step synthesis as described in Scheme 4.



Scheme 4. Synthesis of 2-Adamantyl-piperazine **8**.

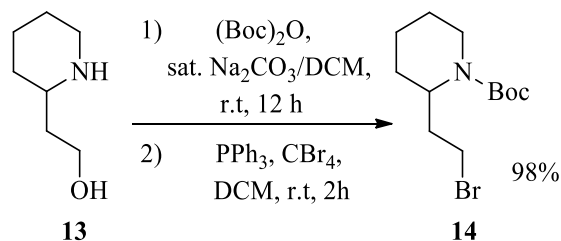
Finally, compounds **11a-j** and **12** were finally obtained through alkylation of compounds **10a-e** with thiomorpholine and other *N*-substituted piperazines (Table 1).

Table 1. Synthesis of **11a-j** and **12**.

Cmpd	R	R ₁	Yields% ^a
11a	H	1-methyl-piperazine	99%
11b	H	1-phenyl-piperazine	62%
11c	SMe	1-methyl-piperazine	99%
11d	SMe	1-phenyl-piperazine	77%
11e	SMe	thiomorpholine	99%
11f	SMe	1-adamantanyl-piperazine	71%
11g	SMe	2-adamantanyl-piperazine (8)	72%
11h	Cl	1-phenyl-piperazine	57%
11i	Cl	thiomorpholine	90%
11j	-	1-methyl-piperazine	96%
12	-	1-methyl-piperazine	63%

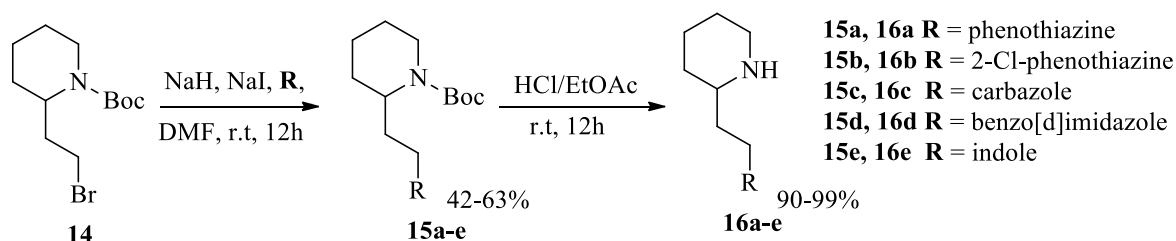
^a Isolated yields.

Finally, a library of TZ derivatives bearing different aromatic cores was synthesized according to classical synthetic procedures. 2-(Piperidin-2-yl)ethanol **13** was Boc-protected on the piperidine via Schotten-Baumann reaction. The resulting carbamate then undergoes Appel reaction with triphenylphosphine (PPh₃) and tetrabromomethane (CBr₄) in dichloromethane (DCM) giving the bromide **14** in good yield (98%) (Scheme 5).



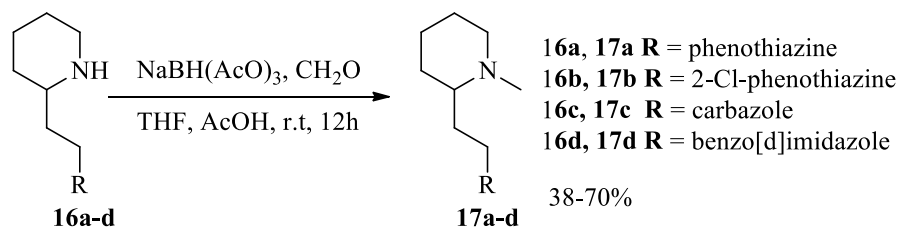
Scheme 5. Synthesis of bromide **14**.

Then, several commercially available heteroaromatic compounds were alkylated with **14** (namely **9a** phenothiazine, **9b** 2-Cl-phenothiazine, **9d** indole, **9e** carbazole and **9f** benzo[d]imidazole) in the presence of NaH in *N,N*-dimethylformamide (DMF) obtaining Boc-protected compounds **15a-e** which led to the desired amines **16a-e** after HCl-mediated Boc-cleavage.



Scheme 6. Synthesis of piperidine **16a-e**.

Finally, compounds **16a-e** and formaldehyde were reacted in the presence of the reducing agent $\text{NaBH}(\text{AcO})_3$ in THF to yield the corresponding methylated compounds **17a-d** with medium to good yields (38-70%).



Scheme 7. Synthesis of TZ derivatives **17a-d**.

The methylation of the indole **16e** has not been attempted because according to a recent paper by Pieroni and coworkers the methylated indole have poor activity against *M. tuberculosis* mc²7000.¹¹²

2.2.1.2. Evaluation against a panel of mycobacteria.

All the compounds were initially evaluated for their biological activity by determining the minimum inhibitory concentrations (MIC₉₀) against a panel of mycobacteria including the fast-growing nonpathogenic strains of *Mycobacterium smegmatis*¹¹⁵ followed by the vaccine strain *Mycobacterium bovis* BCG and the non pathogenic Mtb mc²7000 (Table 2). The first activity assessment and all the tests were performed by Dr Alistair Brown at Northumbria University. A preliminary SAR analysis from the compounds synthesised showed that removal of the methyl group of TZ did not affect the activity as reported for **5**. On the other hand, from compounds **6a-c** it is possible to observe that bulky aromatic substituents on the nitrogen of piperidine (**6b**) are favourable for the activity while aliphatic substituents, bulkier than methyl, (**6a**, and **6c**) are not. Noteworthy is that, the replacement of the piperidine-ethyl moiety with alkyl chains bearing piperazine or thiomorpholine rings as in **11** lead to a dramatic decrease of antimycobacterial activity, with the only exception of the bulky derivative **11g** which showed a MIC = 4 µg/mL on *M. smegmatis*. The data collected from the biological evaluation of the Boc protected derivatives **15a-e** show that none of them are active against the tested panel of mycobacteria. These data suggest that a hydrogen atom acceptor (HAA) in the side chain is paramount for the antibacterial activity. However, it is noteworthy that the carbamate **4** shows activity values similar to **5**. This data is possible to be explained by the fast hydrolysis which the labile chloroethyl carbamate **4** could undergo in the buffer used for the activity assessment affording directly *in vitro* the compound **5**. Furthermore, as shown in Table 2, removal of the methyl-thio substituent of **1** and **5** (as in **17a** and **16a**), as well as the replacement of the phenothiazine scaffold with different heterocyclic moieties (as in **17c-d** and **16c-d**) led to a significant loss in activity. On the contrary, replacement of the same SMe group with a chloride group (as in **16b** and **17b**) resulted in compounds with an antimycobacterial activity comparable to or better than that of **1** and **5**. In particular, the chloro-phenothiazine derivative **16b** showed a good activity against BGC and Mtb mc²700 strains with MIC = 5.3 µg/mL and 4 µg/mL, respectively. Similarly, the methylated analogue **17b** retained 8 µg/mL MIC value against *M. tuberculosis*

mc²7000. Interestingly, the indole derivative **16e** proved to be highly active against *M. smegmatis* with MIC = 1.6 µg/mL.

Table 2. Antitubercular activity (MIC₉₀) on *M. smegmatis* strains, *M. bovis* BCG and Mtb mc²7000.

Compound	<i>M. smeg</i> WT (MIC ₉₀) µg/mL	<i>M. smeg mmpL3</i> (MIC ₉₀) µg/mL	<i>M. bovis</i> BCG (MIC ₉₀) µg/mL	Mtb mc ² 7000 (MIC ₉₀) µg/mL
TZ	16	12	16	8-5(6.5)
4	16	8	8	8
5	16	8	8	8
6a	>64	64	>64	64
6b	16	8	8	8
6c	>64	>64	64	>64
11a	64	32	64	26.7
11b	>64	>64	>64	>64
11c	32	16	8	26.7
11d	>64	>64	>64	>64
11e	>64	>64	>64	>64
11f	64	64	64	64
11g	4	8	>64	>64
11h	>64	>64	>64	>64
11i	>64	>64	>64	>64
11j	>64	>64	>64	>64
12	>64	>64	>64	>64
15a	>64	>64	>64	>64
15b	>64	>64	>64	>64
15c	>64	>64	>64	>64
15d	>64	>64	>64	>64
15e	>64	>64	>64	>64
16a	>64	64	>64	>64
16b	16	16	5.3	4
16c	>64	>64	>64	>64
16d	>64	>64	>64	>64
16e	1.6	1.6	64	64
17a	32	32	64	16
17b	16	16	8	8
17c	>64	64	>64	64
17d	>64	>64	>64	>64
INH	N.D ^a	4	0.063	0.125

^aN.D not determined. The experiments were performed in triplicate.

Then, the most promising compounds have been assessed against the pathogenic *M. tuberculosis* H37Rv, susceptible *M. tuberculosis* strain CF73, and two MDR-TB clinical isolates (CF104 and CF81). All the tests and the activity assessment were performed by Prof.

Fernando R. Pavan at Universidade Estadual Paulista "Júlio de Mesquita Filho" (UNESP) (Table 3). Compound **5** and **6b** which are active against Mtb mc²7000 showed weak activity against *Mycobacterium tuberculosis* H37Rv. The same trend was observed for compounds **11a** and **11c** bearing an *N*-Me-piperazine moiety on the side chain. On the other hand, compounds **16b**, **16e**, and **17b**, bearing the piperidine side chain, showed the best results. In particular, the chloro-derivatives **16b** and **17b** showed an activity toward CF73 and the MDR strains similar to that of **1** in the same range of concentration (8-16 µg/mL). On the other hand, the indole derivative **16e** proved to be the best compound of the series, with an increased activity against both Mtb H37Rv and CF73 strains (2.9 and 1.0 µg/mL, respectively, in comparison to 10.0 and 8.0 µg/mL found for **1**). Moreover, **16e** also showed a similar profile of **1** against MDR-CF104 (10 vs 11 µg/mL) and a slightly improved activity against MDR-CF81 (4 vs 10 µg/mL). These data suggested that the presence of a secondary amine on the scaffold of the side chain could be beneficial for the antitubercular activity, as also observed in the work exposed in paragraph 2.3.1.¹¹⁶

Table 3. Antitubercular activity on a panel of photogenic *M. tuberculosis* strains.

Cmpd	Mtb H37Rv MIC ₉₀ (µg/mL)	Susceptible (CF73) MIC ₉₀ (µg/mL)	MDR-TB (CF104) MIC ₉₀ (µg/mL)	MDR-TB (CF81) MIC ₉₀ (µg/mL)
TZ	10	8	11	10
5	100	>100	>100	>100
6b	>100	37	32	44
11a	100	>100	>100	>100
11c	69	27	23	33
11g	43	98	20	48
16b	26	11	19	11
16e	2.9	1	10	4
17a	>64	47	>64	58
17b	19	16	16	12
INH	0.03	0.03	>25	>25
RIF	0.3	8	>25	>25

The experiments were performed in triplicate.

Finally, to prove the effectiveness of the most active compounds, their cytotoxicity was evaluated by Prof. Fernando R. Pavan at Universidade Estadual Paulista "Júlio de Mesquita Filho" (UNESP) on human lung fibroblast MRC-5 cells and murine macrophage J774A.1

cells (ATCC TIB-67). Mouse models are routinely used for testing the efficacy of both antitubercular drugs and vaccines and are considered a highly appropriate model. Mouse models such as J774A.1 cells and the murine macrophage RAW264.7 cells are key players in the stimulation of specific immune reactions capable of eliciting a whole host of inflammatory responses and have been studied and characterized in great detail over many decades.¹¹⁷ The ratio of the MIC₉₀ observed against *M. tuberculosis* Susc. (CF73) and the GIC₅₀ values provided the selectivity index (SI), or the therapeutic window, offered by these molecules. As a result, **16e** showed a selectivity index 15 fold higher than that of TZ (Table 4).

Table 4. Cytotoxicity of compounds **TZ**, **16b**, **16e** and **17b**.

Cmpds	GIC ₅₀ (μg/mL)		SI ^a	
	MRC-5	J774A.1	MRC-5	J774A.1
TZ	8.2	4.1	1	0.5
16b	10	10.7	1.1	1
16e	15	7.3	15	7.3
17b	13	8.3	1.2	1.9

^aSelectivity index are calculated as the ratio between the *M. tuberculosis* Susc. (CF73) MIC₉₀ and the GIC₅₀. The experiments were performed in triplicate.

2.2.1.3. Evaluation as efflux pump inhibitors.

The efflux pump inhibitory (EPI) activity of TZ derivatives on the model *M. smegmatis* was tested in order to investigate their effect as potential MDR-TB reversal agents. Dr. Bhakta group at Birbeck College London carried out an efflux pump activity whole-cell-based assay and as a consequence, the results account for the total activity of the whole population of efflux pumps present in the cells. Verapamil (VP) was chosen as positive control for the test. The numbers 1–4 shows low to very high EPI (as a representation of an increased level of ethidium bromide accumulation above the cell control). In detail, EPI value of 0 indicates no inhibition, 1 indicates low inhibition (efflux substrate accumulation above cell control to 20000 relative fluorescence units), 2 indicates moderate inhibition (between 20000 and 30000 units), 3 indicates high inhibition (between 30000 and 40000 units), and 4 indicates very high inhibition (between 40000 and 50000 units). The experiments were performed in triplicate, and the Table 5 reports the average values obtained.

Table 5. Efflux pump inhibitory (EPI) activity.

Cmpd	EPI <i>M. smegmatis</i>	Cmpd	EPI <i>M. smegmatis</i>
4	2	16b	2
5	2	16e	1
6b	2	17a	2
11a	3	17b	2
11c	3	2	3
11g	1	VP	4

The efflux pump assay showed that some TZ derivatives are endowed with a good EPI activity. However, a weak correlation between inhibition of bacterial growth and efflux pump mechanism is observed. The compounds **16b** and **16e**, which showed the most promising antimycobacterial activities, proved to be poor efflux pump inhibitors (Table 3 – Scheme 6). On the other hand, the piperazine derivatives **11a** and **11c** which showed a MIC of 26.7 µg/ml on *Mtb* mc²7000, inhibit efflux pumps similarly to the reference chlorpromazine **2**, thus looking as promising candidates in a multidrug therapy owing to synergistic combinations.

2.2.2. Conclusions.

Within this chapter the synthesis and the development of novel anti-tubercular drugs was described following the drug simplification approach on the structure of the third line drug thioridazine.^{55,83} A small library of TZ derivatives bearing structural changes in three key different positions of the original scaffold, has been synthesised. Antimycobacterial activity of the resulting compounds showed that the piperidine-ethyl side chain of TZ is required to inhibit non-pathogenic, pathogenic and MDR mycobacterial strains. Moreover, the SMe-phenothiazine scaffold of **1** could be only replaced with the Cl-phenothiazine analogue or simplified into an indole moiety. The most active compound **16e**, bearing a demethylated piperidine ring in addition to an indole heterocycle, showed an activity profile better than that of **1** and a cytotoxicity about 15-fold lower toward MRC-5 and J774A.1 cells. Furthermore, the most promising compounds were evaluated for their ability to inhibit the efflux pump activity in mycobacteria. Compounds **11a** and **11c** showed similar EPI activity than the reference **2** proving to be potential MDR-TB reversal agents.

2.3. Synthesis of novel antitubercular agents effective against multidrug-resistant mycobacteria via molecular hybridization approach.

The virtual molecular hybridization approach is one of the strategies included in the rational design protocol for the identification of new biologically relevant small molecules. It consists on the recognition of structurally comparable or similar molecular portions of two or more bioactive compounds. Then, through merging these molecular portions, it is possible to design new hybrid chemical entities that maintain structural elements of the parent compounds. The two bioactive compounds chosen for the virtual molecular hybridization are BM212 (**I**) and SQ109 (**II**) (Figure 12). About fifteen years ago, the pyrrole compound **I** was discovered to be a potent antimycobacterial agent.¹¹⁸ In an effort to identify new pyrrole analogues with improved solubility and ability to kill multidrug-resistant and extensively drug-resistant mycobacteria, many **I** derivatives were designed and synthesized.¹¹⁹ **I** congeners showed a submicromolar activity toward *M. tuberculosis* H37Rv. However, the first series of **I** analogues (including **I** itself) suffered from poor pharmacokinetic parameters (in terms of clearance and microsomal stability) and significant cytotoxicity.¹¹⁸ Although the most recent derivatives showed an improved pharmacokinetic and cytotoxic profile, their physicochemical parameters (such as lipophilicity and aromaticity) need further optimization. On the other hand, adamantane-diamine compound, SQ109 **II** was described as an antitubercular drug that is active against susceptible and drug resistant *M. tuberculosis* strains.⁷¹ SQ109 exhibited promising activity in drug combination during animal preclinical studies and it is currently undergoing phase 2 clinical trials for further development.¹²⁰ The cellular target of both these molecules is the trehalose monomycolate exporter, MmpL3 protein (Rv0206c), and member of the MmpL (mycobacterial membrane protein large) family.^{116,121} MmpL3 is a validated drug target in *M. tuberculosis*.¹²¹ This family has primary structure homology to the resistance-nodulation-cell division (RND) protein family, mainly involved in drug resistance in Gram-negative bacteria.¹¹⁹ Although the *M. tuberculosis* genome encodes 13 members of the MmpL family, their function has not been clearly elucidated. Despite their annotation as multidrug transporters, they do not contribute to antimycobacterial drug resistance.¹²² MmpL3 has also been implicated in heme acquisition by *M. tuberculosis*, although it might not be its primary role in an endogenous environment.¹²¹ By means of an *in silico* molecular modelling approach conducted by Prof Fabrizio Manetti at the University of Siena (see paragraph 2.3.1.1) the three-dimensional structure of both compounds **I** and **II** was studied (Figure 16).

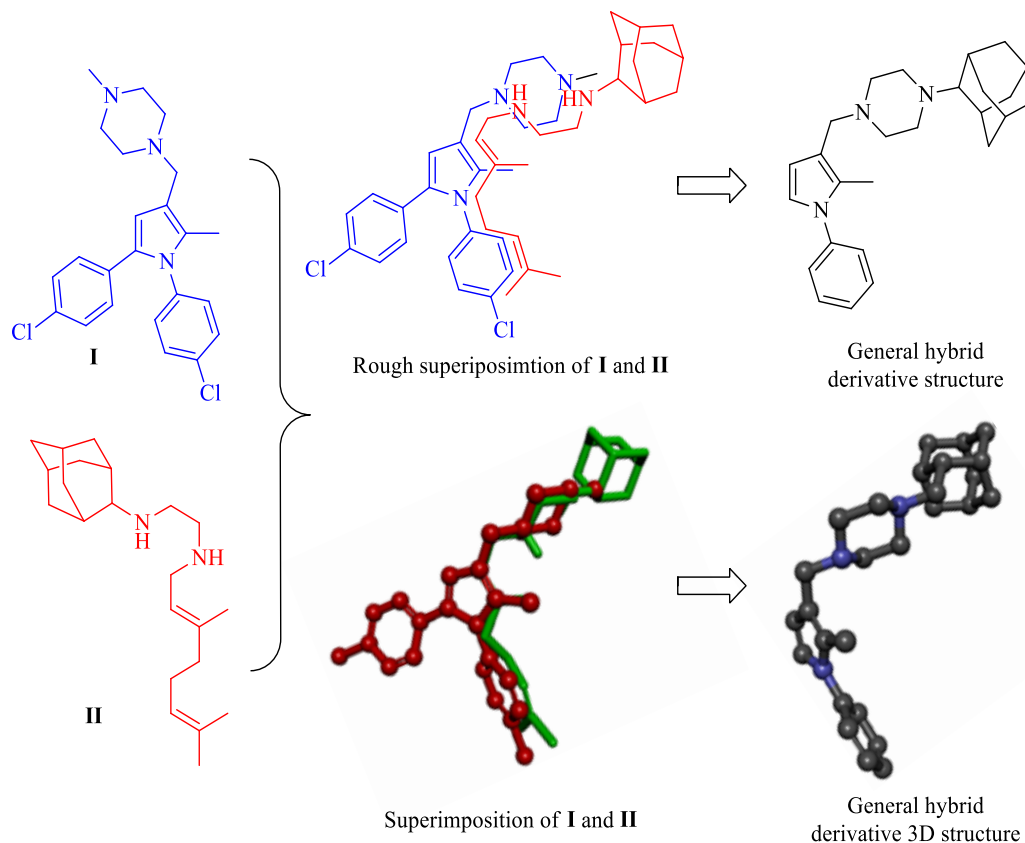


Figure 16. Graphical representation of **I** and **II** (left panel), a rough superimposition of the topological distribution of their chemical features and superimposition of their three dimensional conformers (central upper panel) and superimposition of their three-dimensional conformers as generated by the common feature hypothesis generation routine (central lower panel), general hybrid derivative structure (right upper panel) and its three dimension conformation (right lower panel).

Although the apparent structural dissimilarity between the two compounds, a rough superposition of specific conformers of **I** and **II** showed an unexpected high similarity between them (Figure 16). In fact, except from the terminal adamantyl moiety of SQ109 and the *p*-Cl phenyl ring at the C5 position of **I**, the remaining part of the SQ109 structure was superimposable to that of **I**. Because of this similarity, a molecular hybridization approach has been applied to design new putative antimycobacterial compounds. The more rigid scaffold of **I** was chosen as the template for the new hybrid derivatives and adjusted upon comparison with the flexible structure of **II**. As a result, the *N*-(substituted-phenyl)pyrrole core of **I** with a piperazinylmethyl side chain at position C3 was maintained, while the second phenyl substituent at position C5 of **I** was deleted from the new hybrid compounds. In addition, the adamantyl moiety present in **II** was inserted as the terminal group bound to N4

of the piperazine ring, leading to the design of a general hybrid derivative structure as shown in Figure 16. Hence, a set of novel pyrrole derivatives inspired to the general hybrid structure obtained by the superimposition of the antitubercular agents **I** and **II**, have been designed, synthesized, and biologically evaluated. To explore the chemical space around the C3 piperazino-methyl moiety of the new compounds, the distal piperazine nitrogen was substituted with different bulky moieties, such as adamantyl, norbornyl, cyclohexyl, or aryl groups. Moreover, the role of the substituent on C5 and its importance for the antitubercular activity were explored. According to the superposition hypothesis, the aryl moiety at C5 of **I** was replaced by a methyl substituent, thus leading to design the first series of pyrroles derivatives described in Figure 17.

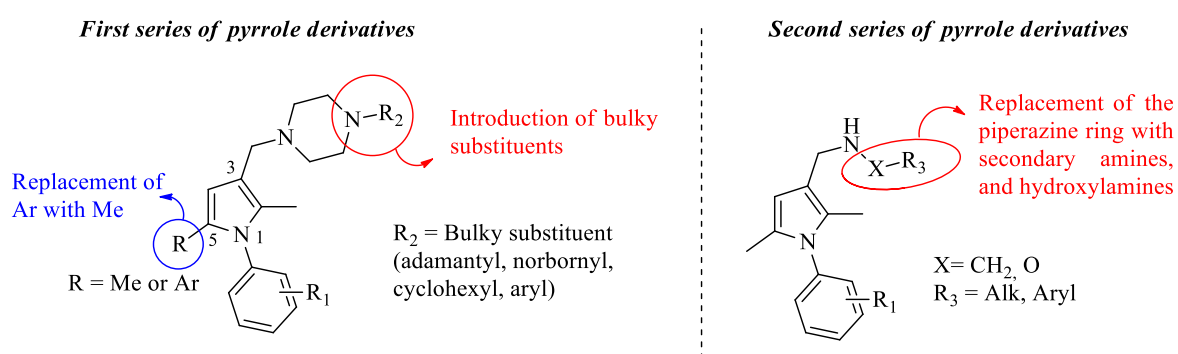


Figure 17. Synthetic plan for the synthesis of the first and second series of pyrroles derivatives.

In addition, a second series of hybrid derivatives was also designed through molecular simplification of the general hybrid structure described in Figure 16 in order to evaluate the influence of the piperazine ring on the antitubercular activity. Within this series, also according to previous works,¹²³ the piperazine ring was removed from the structure and replaced with a secondary amine (or hydroxylamine) at C3. In both cases, the methyl substituent at C2 and C5, as well as the N1 aryl groups, were left unchanged as shown in Figure 17.

2.3.1. Results and discussion

2.3.1.1. Computational design and hypothesis on the common chemical features shared by BM212 and SQ109.

In order to confirm the superposition pattern above-described for **I** and **II**, and in collaboration with Prof. Manetti at the University of Siena, the Phase software (Phase,

version 3.3, Schrodinger LLC, New York, 2011.) was used to find the three-dimensional arrangements of the common chemical portions shared by **I** and **II** (thereafter referred to as common feature models or superposition models). As a result, a four-feature representation was obtained, comprised of two hydrophobic groups and two protonatable atoms (Figure 18).

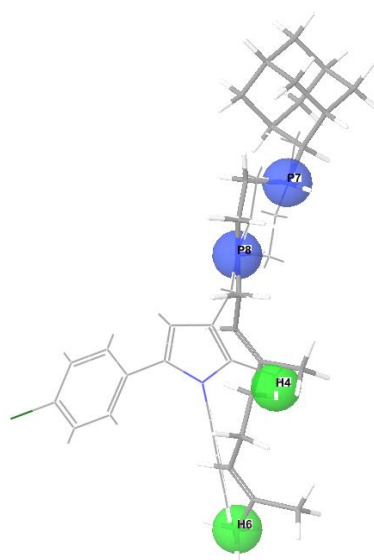


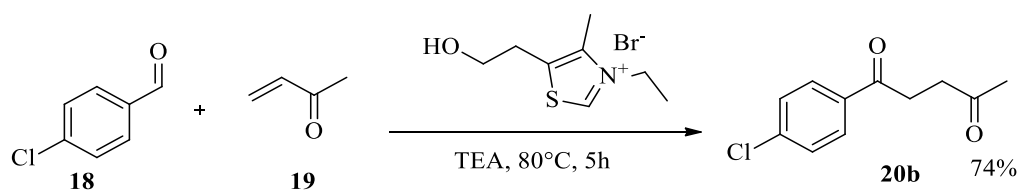
Figure 18 Graphical representation of the four-feature superposition model common to **I** (thin lines) and **II** (thick lines). The two protonatable chemical features (P7 and P8) are in blue, while the two hydrophobic regions (H4 and H6) are in green. The conformer of **I** represented in the picture is 0.013 kJ/mol from the lowest energy conformation, while the energy difference between the lowest energy conformation of **II** and the conformer reported in the picture is 4.660 kJ/mol.

In detail, the *p*-Cl group at the phenyl in N1 position of the pyrrole ring of **I** and one of the terminal methyl groups of **II** matched one of the common hydrophobic regions (H6). The central methyl group of **II** and the 2-methyl group of **I** corresponded to the second hydrophobic portion (H4). On the other hand, the two positively ionizable features (P7 and P8) accommodated the two basic nitrogen atoms of both compounds. It is important to point out that this representation of the common chemical features of **I** and **II** showed two protonatable sites that are chemically unrealistic at neutral pH. However, this qualitative model only accounts for the presence of the two piperazine nitrogens of **I** and for the two amine nitrogens of **II**, while it does not take into consideration the mutual influence of the

two amines during the protonation steps. Analysis of the superposition pattern of **I** and **II** suggested to omit the aromatic portion at position 5 of **I**. In fact, a visual inspection of the superimposed structures of **I** and **II** showed that this moiety does not match an analogous group on **II** (Figure 18) and consequently, it does not represent a common feature of both compounds. Moreover, since the three aromatic rings forced the structure of these compounds toward planarity, the removal of one or more of them could be in principle profitable for better solubility and bioavailability. In addition, given the well-established relationship between late-stage drug development problems (i.e., the high attrition rate of compounds entering the clinical phase) and the lipophilicity of compounds,¹²⁴ modulation of lipophilicity should be taken into account when new putative anti-mycobacterial compounds are designed. In addition, since the terminal methyl group of **I** is partially superimposed on the adamantyl moiety of **II**, a hydrophobic group at this position was maintained. Following these suggestions and taking into account the similarity between **I** and **II**, a new class of pyrrole derivatives was designed on the basis of the molecular hybridization routine with the aim of obtaining new putative antimycobacterial compounds. The more rigid scaffold of **I** was chosen as the template for the design of novel antitubercular compounds while the adamantyl group (already found in **II**) and other bulky alkyl substituents were introduced on the piperazine ring, while the 5-phenyl ring of **1** was removed.

2.3.1.2. Synthesis of BM212-SQ109 hybrid derivatives.

A library of pyrrole derivatives bearing an *N*-substituted piperazinomethyl chain at C3 was first synthesised according to classical synthetic procedures. Pyrroles **22a–f** were synthesized through a microwave-assisted Paal–Knorr reaction starting from diones **20a** and **20b** and different anilines (Table 6).^{123,125} 1-(4-Chlorophenyl)pentane-1,4-dione **20b** was obtained from *p*-chloro-benzaldehyde via a Stetter reaction catalysed by thiazolium salt (Scheme 8).¹²⁶



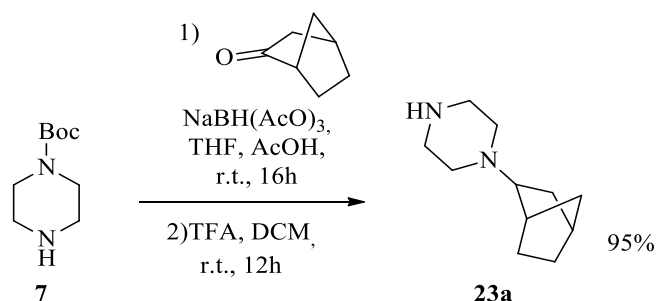
Scheme 8. Synthesis of **20b**.

Computational studies suggested that the *p*-Cl-Ph moiety in position N1 of **I** should be kept in the hybrid derivatives, however, a small number of different substituents were also introduced in the phenyl ring to evaluate their steric and electronic effects on the anti-mycobacterial activity confronting their impact on the activity with the BM212 derivatives already reported in the literature.¹¹⁸ (Table 6).

Table 6. Synthesis of pyrroles **22a-f**.

Aniline	R	R ₁	Pyrrole	Yield%
21a	Me	4-Cl	22a	93%
21b	Me	4-F	22b	98%
21a	4-Cl-C ₆ H ₄	4-Cl	22c	90%
21c	Me	2-F	22d	92%
21d	Me	4- <i>i</i> -Pr	22e	95%
21e	Me	3-Me	22f	97%

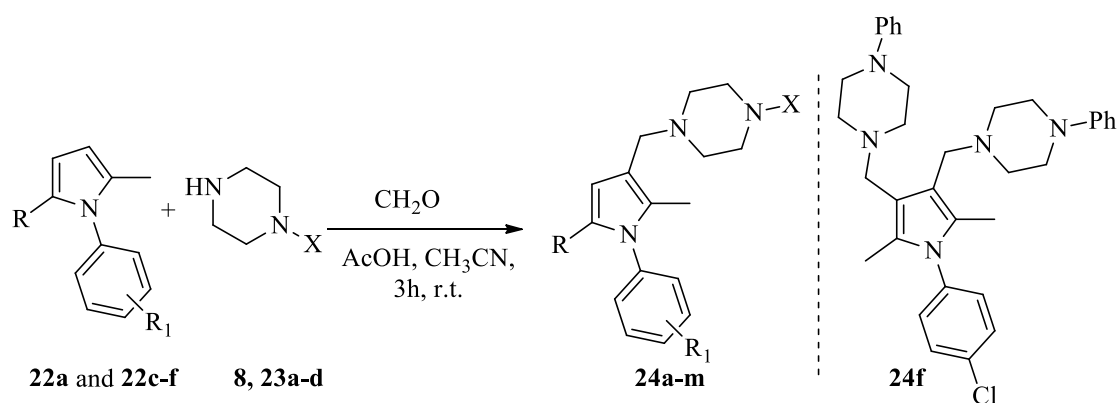
Moreover, different bulky substituents were introduced on the piperazine ring to explore the chemical space around the pyrrole nucleus. 2-Norbornyl-piperazine **23a** was synthesised through a two step synthesis as shown in Scheme 9 and then reacted with pyrroles **22a** and **22c-f**.



Scheme 9. Synthesis of piperazine **23a**.

The Boc-piperazine **7** and 2-norbornanone were reacted in the presence of the reducing agent $\text{NaBH}(\text{OAc})_3$ to yield the corresponding alkylpiperazine intermediate as a mixture of exo/endo isomers, which was immediately converted into the desired piperazines **23a** by TFA-mediated Boc cleavage. Finally, the piperazines **8**, (synthesised following Scheme 4) **23a–d** (*N*-cyclohexylpiperazine **23b**, *N*-phenylpiperazine **23c**, 1-adamantylpiperazine **23d** are commercially available) were coupled via Mannich reaction with the pyrroles **22a** and **22c–f** affording pyrroles **24a–m**. The yields of the reactions are reported in Table 7.

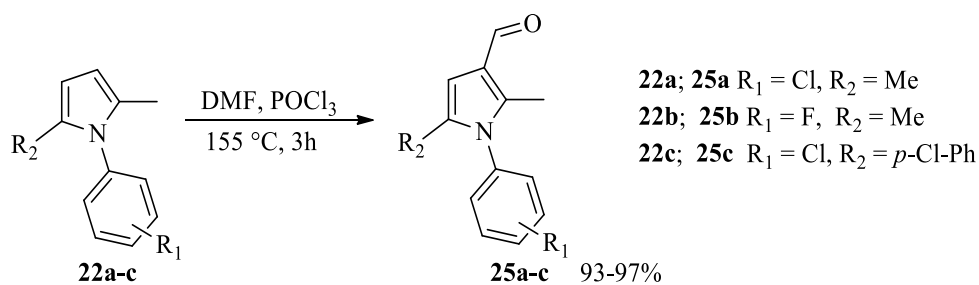
Table 7. First series of pyrrole derivatives **24a–m**.



Cmpd	R	R ₁	X	Yield% ^a
24a	Me	4-Cl	2-Adamantyl	56
24b	Me	2-F	2-Adamantyl	45
24c	Me	4- <i>i</i> Pr	2-Adamantyl	51
24d	Me	3-Me	2-Adamantyl	48
24e	Me	4-Cl	Phenyl	65
24g	Me	4-Cl	2-Norbornyl ^b	55
24h	Me	4-Cl	Cyclohexyl	52
24i	Me	4-Cl	1-Adamantyl	54
24j	4-Cl-C ₆ H ₄	4-Cl	Phenyl	64
24k	4-Cl-C ₆ H ₄	4-Cl	2-Adamantyl	65
24l	4-Cl-C ₆ H ₄	4-Cl	1-Adamantyl	60
24m	4-Cl-C ₆ H ₄	4-Cl	2- Norbornyl ^b	56

^aIsolated yields are reported. ^bMixture of exo/endo isomers. Compound **24f** was isolated as a side product, 35% yield.

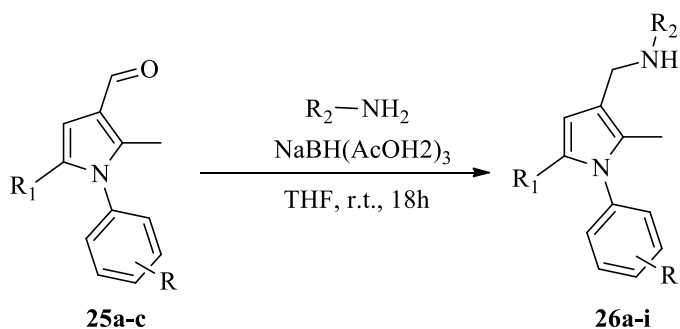
Then, a second series of pyrrole derivatives was synthesised according to the strategy described on chapter 2.3. Pyrroles **22a–c** were formylated through the Vilsmeier–Haack reaction, affording the aldehydes **25a–c** with good yields (Scheme 10).



Scheme 10. Synthesis of aldehydes **25a-c**.

The aldehydes **25a-c** were then reacted with different primary amines in the presence of $\text{NaBH}(\text{AcO})_3$ to yield pyrroles **26a-i**, as shown in Table 8.

Table 8. Synthesis of second series of hybrids **26a-i**

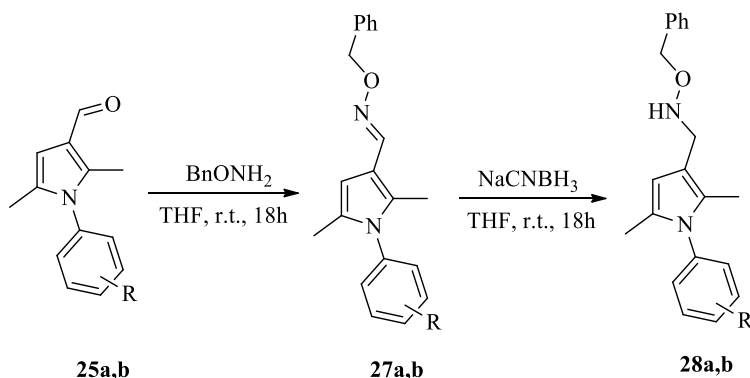


Cmpd	R	R ₁	R ₂	Yields% ^a
26a	4-Cl	Me	PhCH ₂ CH ₂	75
26b	4-Cl	Me	PhCH ₂	79
26c	4-Cl	Me	Cyclohexyl	77
26d	4-Cl	Me	2-Adamantyl	60
26e	4-Cl	Me	4-Me-Bn	82
26f	4-Cl	Me	4-Cl-Bn	78
26g	4-Cl	Me	4-F-Bn	80
26h	4-F	Me	PhCH ₂	82
26i	4-Cl	4-Cl-C ₆ H ₄	PhCH ₂	78

^aIsolated yields

Furthermore, aldehydes **25a** and **25b** were reacted with benzylhydroxylamine to afford oximes **27a** and **27b**,¹²³ which, after treatment with NaBH₃CN, led to the corresponding hydroxylamines **28a** and **28b** in excellent yields. (Table 9).

Table 9. Synthesis of pyrroles **27a**, **27b**, **28a** and **28b**.



Cmpd	R	Yields% ^a
27a	4-Cl	75
27b	4-F	78
28a	4-Cl	80
28b	4-F	82

^aIsolated yields

2.3.1.3. Evaluation of hybrid derivatives of I and II against a panel of mycobacteria.

Compounds **24-28** were assessed for their biological activity by determining the minimum inhibitory concentrations (MIC₉₀) against a panel of fast-growing and slow-growing mycobacterial species and clinical isolates by collaborators at Birkbeck College and UCL London.

A preliminary screening has been conducted by Dr. Bhakta group at Birbeck college London on the fast-growing non-pathogenic strains of *Mycobacterium smegmatis*, the vaccine strain *M. bovis* BCG, and relatively fast-growing intra-cellular surviving *Mycobacterium aurum*,¹¹⁵ (Tables 10).

Table 10. Antitubercular activity on *M. smegmatis*, *M. bovis* BCG, and *M. aurum* mycobacterial strains of compound **24-28**.

Cmpd	<i>M. smegmatis</i> mc ² 155	<i>M. bovis</i> BCG	<i>M. aurum</i>
	MIC ₉₀ (µg/mL)	MIC ₉₀ (µg/mL)	MIC ₉₀ (µg/mL)
24a	8.0	3.3	7.8
24b	13	1.3	250
24c	21	4.0	500
24d	64	62	500
24e	32	32	31
24f	>64	>64	250
24g	27	32	16
24h	27	21	31
24i	8.0	16	16
24j	>64	2.0	>125
24k	>64	64	>125
24l	3.3	2.0	62
24m	64	64	250
26a	32	16	16
26b	4.0	0.5	1.9
26c	8.0	0.4	7.8
26d	16	2.0	62
26e	8.0	4.0	1.9
26f	4.0	8.0	1.9
26g	2.0	0.5	1.9
26h	16	13	7.8
26i	8.0	8.0	1.0
27a	>64	>64	>125
27b	>125	>125	>125
28a	>64	>64	>125
28b	>64	>64	>125
I	25	0.78	16
II	4.0	2.0	7.8
INH	N.D ^a	N.D ^a	N.D ^a

^a not determined. The experiments were performed in triplicate.

Then all the compounds have been assessed by Dr. Bhakta group at Birbeck college London for their activity against the non-pathogenic *M. tuberculosis* mc²7000, the pathogenic *M.*

tuberculosis H37Rv, and finally against a panel of MDR-TB clinical isolates obtained from Royal Free Hospital NHS Trust, London, UK. (Table 11).

Table 11. Biological evaluation of compounds against a panel of *M. tuberculosis* strains.

Cmpd	<i>M. tuberculosis</i>			
	mc ² 7000	H37Rv	MDR1MIC ₉₀	MDR2
	MIC ₉₀ (µg/mL)	MIC ₉₀ (µg/mL)	(µg/mL)	MIC ₉₀ (µg/mL)
24a	3.3	7.8	7.8	16
24b	1.0	3.9	7.8	16
24c	3.3	16	62	125
24d	32	16	31	125
24e	32	7.8	31	>125
24f	>64	31	62	>125
24g	2.0	1.9	3.9	31
24h	8.0	3.9	7.8	62
24i	8.0	16	125	125
24j	1.0	1.9	3.9	>125
24k	>64	62	125	125
24l	0.5	7.8	16	62
24m	64	ND	N.D	N.D
26a	4.0	1.0	1.9	7.8
26b	0.5	0.5	1.0	3.9
26c	0.5	0.2	0.5	16
26d	1.0	1.9	3.9	125
26e	2.0	1.0	3.9	7.8
26f	2.0	16	31	>125
26g	0.7	>125	>125	16
26h	4.0	1.0	7.8	62
26i	16	N.D	N.D	N.D
27a	>64	>125	>125	>125
27b	>125	25	N.D	N.D
28a	>64	>125	125	>125
28b	>64	>125	62	>125
I	8.0	1.0	3.9	16
II	2.0	0.51	N.D	N.D
INH	N.D	0.24	10	25

The experiments were performed in triplicate. N.D not determined.

The data arising from the screening of non-pathogenic *M. tuberculosis* mc²7000 (Table 11) have been analysed for first. In agreement with initial hypothesis (paragraph 2.3.1.1), the insertion of a 1- and a 2- adamantylpiperazine group in place of the *N*-methylpiperazine of **I** led to compounds **24l** and **24k** which are endowed with significantly contrasting activity. In fact, **24k**, bearing the same 2-adamantyl group found in **II**, was inactive (MIC value >64 µg/mL). On the contrary, the corresponding 1-adamantyl analogue **24l** showed a strong activity against Mtb mc²7000, with a MIC value of about 0.5 µg/mL. Compound **24l** was then chosen as the most representative compound to be further studied for deducing SAR considerations of the new class of hybrid compounds on Mtb mc²7000. In particular, according to the suggestions derived from the superposition pattern between **I** and **II**, the *p*-Cl phenyl moiety at C5 of **24l** was simplified to a methyl group, leading to **24i**, with a significant 16-fold drop in activity (8.0 µg/ mL). The corresponding 2-adamantyl analogue **24a** showed a slight increase in activity (3.3 µg/mL). Moreover, small changes in substituents and substitution pattern at its 1-phenyl ring clearly showed that small substituents (*i*-Pr and F) at para and *o*-positions (such as in **24c** and **24b**) guaranteed activity retention or enhancement (3.3 and 1.0 µg/mL, respectively). On the other hand, a *m*-methyl group as in **24d** caused a significant drop in activity (32 µg/mL), in agreement with that previously found for derivatives of **I**.^{118,127} Decreasing the bulkiness of the hydrophobic moiety on the piperazine ring from an adamantyl (such as in **24i** or **24a**) to a norbornane group led to a slight improvement of activity (MIC of **24g** was 2.0 µg/mL). On the contrary, a further simplification to a cyclohexyl ring (**24h**) and its aromatization to a phenyl ring (**24e**) further reduced activity to 8.0 and 32 µg/mL, respectively. Introduction of a second *p*-Cl phenyl moiety at C5 of **24e** restored a 1.0 µg/mL activity in **24j**. SAR considerations obtained from data collected in Table 11 for both **24j** and **24e** (1.0 and 32 µg/mL, respectively) suggested that in several cases the presence of the *p*-Cl phenyl moiety at C5 could improve antimycobacterial activity. On the other hand, a comparison between the activity of **24e** and its adamantyl analogues **24a** and **24i** (3.3 and 8.0 µg/mL, respectively) clearly showed that the *p*-Cl phenyl moiety at C5 was not mandatory for obtaining active compounds, as suggested by the common feature model described in paragraph 2.3.2.1. Also, the comparison of the biological profiles of **24g** and **24m** bearing norbornyl groups at N4 clearly shows that the *p*-Cl phenyl moiety at C5 in **24m** could be detrimental for the antitubercular activity (2.0 and 64 µg/mL, respectively). Moreover, after the observation of the comparable antimycobacterial activities of **24j** and **24l** (1.0 and 0.5 µg/mL, respectively) it is possible to hypothesize that the distal nitrogen atom of the piperazine ring (which is protonatable in **24l** but has anilino character in **24j**) could be inconsequential for activity.

This result was in agreement with previous pharmacophoric-based calculations and the *in vitro* activity of piperidine analogues of **I**.¹¹⁹ In order to validate this hypothesis, the second series of hybrid derivatives **26**, **27**, and **28** bearing a linear amino spacer instead of the piperazine ring were synthesised. Among them, **26a** had an overall size comparable to that of **24e** and lacked the distal nitrogen atom of the parent piperazine ring. Its activity was 8-fold better than that of the piperazine analogue **24e** (4.0 and 32 µg/mL, respectively). Attempts to modify the phenylethylamino side chain of **26a** by introduction of an oxygen atom (as in **28a** and **28b**) or by partial rigidification into an aryl oxime (as in **27a**) led to inactive compounds (>64 µg/mL). Alternatively, shortening the phenylethylamino spacer led to very active compounds. As an example, the benzylamino analogue **26b** showed a 0.5 µg/mL MIC value. Decoration of the para position of the terminal phenyl ring with small substituents (such as F, Cl, and Me) led to **26g**, **26f**, and **26e** which are endowed with comparable or slightly lower activity (0.7, 2.0, and 2.0 µg/mL, respectively). These data further confirm that the distal nitrogen atom of the piperazine ring was not necessarily required for the antimycobacterial activity of the new hybrid compounds. On the contrary, replacement of the *p*-Cl of **26b** with a *p*-F group as in **26h** caused an 8-fold drop in activity (from 0.5 to 4.0 µg/mL). A further reduction of the amino side chain length to a cyclohexylamino and to the bulky 2-adamantylamino moiety as in **26c** and **26d**, respectively, also maintained a 0.5 and 1.0 µg/mL activity. Interestingly, when the methyl group at C5 of compounds **26b** was replaced with a *p*-Cl phenyl moiety leading to derivative **26i**, a significant drop in activity was observed (16 µg/mL). Compounds **26b** and **26c** proved to be much more active than **I** against Mtb mc²7000. These latter data confirm the initial hypothesis that an aryl substituent at C5, such in **I**, is not mandatory to obtain derivatives active against *M. tuberculosis*. Furthermore, compounds bearing a secondary amine show a better activity profile than **II**, thus pointing out that a diamine backbone could be unessential for antitubercular activity. All the compounds were also assayed on additional mycobacterial strains. Activity against the pathogenic Mtb H37Rv (Table 11.) followed the same trend already shown for the Mtb mc²7000 strain. Compounds **26f** and **26g** were the only exceptions. They resulted both inactive or weakly active toward Mtb H37Rv (16 and >125 µg/mL, respectively), while their congener compounds **26e** and **26b** showed a 1.0 and 0.5 µg/mL activity. The hybrid compounds **24a**, **24b**, **24e**, and **24h** showed a good profile with MIC = 7.8, 3.9, 7.8, and 3.9 µg/mL, respectively. The derivative **24j** bearing a *p*-Cl-phenyl substituent at C5 showed an improved biological profile (1.9 µg/mL). As a general trend, the simplified compounds **26** showed higher activity against Mtb H37Rv than derivatives **24**. In particular, compounds **26b** and **26c** proved to be the most active, with MIC values of 0.5 and

0.2 µg/mL, respectively resulting more active than **I** and **II**. Furthermore, it is noteworthy that the hybrid compounds showed weak activity toward *M. smegmatis* mc²155 (MIC values ranging from 4.0 to >64 µg/mL), with the only exception of compounds **24i** and **26g** which showed MIC values of 3.3 and 2.0 µg/mL, respectively (Table 10). Similarly, *M. aurum* was scarcely sensitive to the test compounds: only four compounds (namely, **26b**, **26e**, **26f**, and **26g**) showed a MIC value of about 2.0 µg/mL (Table 10). As the whole genome sequence of *M. aurum* has been published recently, comparative genomic analyses of these transporter proteins should elucidate why the difference in their drug susceptibilities is observed.¹¹⁵ On the contrary, a better antimycobacterial activity profile was found toward *M. bovis* BCG (Table 10). Ten hybrid derivatives showed MIC values in the range below 4.0 µg/mL and three of them (namely, **26b**, **26c**, and **26g**) with a MIC value of 0.5 µg/mL. The data arising from the screening of MDR-TB strains (Table 11) showed that the test compounds were poorly active against MDR2 strain with **26a** and **26b** as the only exceptions, which showed a good activity of 7.8 and 3.9 µg/mL. Differently, MDR1 growth was inhibited by seven compounds with MIC values lower than 4.0 µg/mL. Exceptional results were observed for compounds **26b** and **26c**, which showed MIC values of about 1.0 and 0.5 µg/mL, respectively. **26b** and **26c** proved to have a better activity profile than those of the parent compound **I** and INH. From an analysis of the data reported on Table 10 and 11, compounds **26a-c** show the best activity profile whilst they are characterized by structural features significantly different from those of the parent compound **I**. In detail, they lacked both the distal nitrogen atom of the original piperazine ring and the *p*-Cl-Ph group at position C5 of the pyrrole nucleus. Furthermore, it is noteworthy that the overall activity underwent an improvement when the basic linear side chain was shortened from the phenylethylamino of **26a**, to the benzylamino of **26b**, to the cyclohexylamino of **26c**. The aryl moiety at position C5 was not a mandatory substituent for the synthesis of active compounds, and data suggested that small modifications on N1-phenyl ring are allowed. A bulky terminal group, such as an adamantyl or norbornanyl, improve the activity of piperazine analogues, while antimycobacterial activity highly benefits from the replacement of the piperazine moiety with shorter, linear aryl and alkylamino side chains. Finally, cytotoxicity analysis of compounds **24-28** was carried out by collaborators at Birkbeck College (Table 12.). The eukaryotic cell toxicity of each compound was tested against murine macrophage RAW264.7 cells and human monocyte-derived THP-1 cell line to ascertain the 50% growth inhibitory concentration (GIC₅₀). The ratio of the MIC₉₀ observed against *Mtb* H37Rv and the GIC₅₀ values provided the selectivity index offered by these molecules. It must brought to note that there are differences in the assay methods to determine the inhibitory

concentrations of the compounds against the bacterial pathogen and the eukaryotic cells. However, these methods have been extensively standardized so as to reduce ambiguity in inferring the selectivity index from these assays.¹²⁸

Table 12. Biological evaluation of compounds **24-28** against a panel of Eukaryotic cells.

Cmpd	GIC ₅₀ (μg/mL)		SI ^b	
	RAW264.7	THP-1	RAW264.7	THP-1
24a	5.7	32 ± 1	0.7	4.1
24b	11	26 ± 1	2.8	6.7
24c	92	72 ± 1	5.7	4.5
24d	22	37 ± 1	1.4	2.3
24e	33	25 ± 1	4.2	3.2
24f	500	113 ± 1	16	3.6
24g	5.6	16 ± 1	2.9	8.4
24h	5.5	16 ± 1	1.4	4.1
24i	0.1	16 ± 1	0.006	1.0
24j	175	294 ± 5	92	155
24k	95	500 ± 10	1.5	8.1
24l	23	35 ± 18	2.9	4.5
24m	N.D	429	N.D	6.7
26a	9.9	7.3 ± 2.7	10	7.3
26b	5.5	7.2 ± 3.7	11	14
26c	10	7.4 ± 1.4	50	37
26d	19	15 ± 10	10	7.8
26e	0.1	6.1 ± 2.1	0.1	6.1
26f	0.1	18 ± 1	0.006	1.1
26g	26	8.4 ± 1.7	-	-
26h	5.6	28 ± 1	5.6	28
26i	N.D	99 ± 1	N.D	6.1
27a	128	500 ± 22	≅1	< 4.0
27b	- ^a	- ^a	N.D	N.D
28a	133	67 ± 1	-	-
28b	123	292 ± 41	≅1	< 2.3
I	19	3.23	19	3.23
II	N.D	- ^a	N.D	N.D
INH	N.D	- ^a	N.D	-

^a no inhibition was seen ^b Selectivity index (SI) is calculated as the ratio between *M. tuberculosis* H37Rv and GIC₅₀. The experiments have been performed in triplicate. N.D not determined.

Among the most active compounds **24j**, **26b** and **26c**, showed an excellent cytotoxicity profile, with a SI of 92, 11, and 50 against RAW264.7 cells and 155, 14 and 37 against THP-

1 cells, respectively. Both **24j** and **26c** have a higher SI than the parent compound **I** against both the murine and human cells.

2.3.1.4. SAR considerations and development of a new pharmacophoric model.

The high antimycobacterial activity maintained even after a significant structural simplification of 1,5-diarylpyrroles derivatives of **I** into the corresponding 1-aryl hybrid analogues (Table 10 – Table 11) could be accounted for by a comparison of the original pharmacophoric model for antimycobacterial compounds belonging to the pyrrole class of **I**¹²⁷ with the simplified common feature model described in paragraph 2.3.1.1. In fact, the original pharmacophoric model¹²⁷ was able to accommodate **I** and its derivatives in two different orientations, rotated by about 180° around the pyrrole plane. Following this, the aryl moieties at positions N1 and C5 of **I** could reciprocally change their spatial location and, consequently, match with the pharmacophore. These results suggested that the pharmacophoric portions able to accommodate the substituents at positions N1 and C5 are redundant and could be simplified, as also suggested by the superposition between **I** and **II**. In a further attempt to codify the structural features of the new hybrid pyrroles, a second-generation common feature model was built at the University of Siena starting from a larger set of compounds, comprised of **I**, **II**, and the most active pyrroles (with MIC values ≤ 1.0 $\mu\text{g/mL}$) (Figure 19).

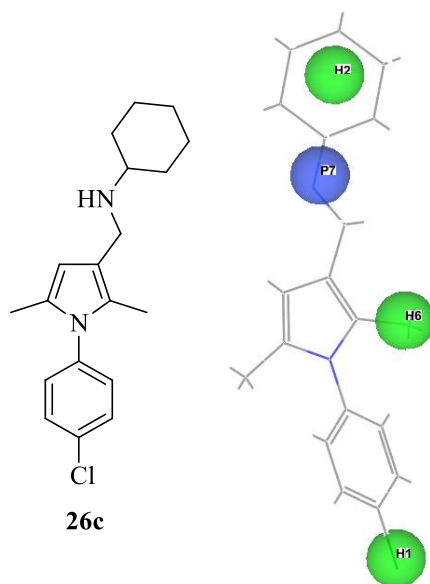


Figure 19. Graphical representation of the four-feature improved model matched by the most active hybrid pyrrole **26c**.

The improved model showed that the distal nitrogen of the piperazine ring of **I** (corresponding to P8 in the previous common feature model) was omitted, while an additional hydrophobic region (H2), adjacent to the P7 feature (a positively ionizable feature), accommodated the terminal hydrophobic groups of the C3 side chain.

2.3.1.5. Evaluation of the hybrid derivatives of **I** and **II** as efflux pump inhibitors.

Finally, the effect of pyrroles on the efflux pump inhibitory (EPI) activity of the model surrogate organism *M. aurum* was tested by Dr. Bhakta group at Birbeck College London in order to identify compounds able to reverse multidrug resistance in TB. An efflux pump activity whole-cell-based assay has been carried out, and therefore, the results account for the total activity of the whole population of efflux pumps present in the cells. Verapamil (VP) was chosen as positive control for the test. The numbers 1–4 shows low to very EPI activity (as a representation of an increased level of ethidium bromide accumulation above the cell control). In detail, EPI value of 0 indicates no inhibition, 1 indicates low inhibition (efflux substrate accumulation above cell control to 20000 relative fluorescence units), 2 indicates moderate inhibition (between 20000 and 30000 units), 3 indicates high inhibition (between 30000 and 40000 units), and 4 indicates very high inhibition (between 40000 and 50000 units). The experiments were performed in triplicate, and the Table 13 reports the average values obtained.

Table 13. Efflux pump inhibitory (EPI) activity of **24**, **26**, **27** and **28**.

Cmpd	EPI <i>M. aurum</i>	Cmpd	EPI <i>M. aurum</i>	Cmpd	EPI <i>M. aurum</i>
24a	1	24l	3	27a	1
24b	1	24m	N.D	27b	N.D
24c	3	26a	2	28a	2
24d	2	26b	2	28b	4
24e	1	26c	2	I	2
24f	2	26d	1	II	2
24g	1	26e	2	INH	N.D
24h	4	26f	2	VP	4
24i	4	26g	1		
24j	2	26h	1		
24k	0	26i	1		

ND: not determined.

The efflux pump assay revealed that most of the pyrrole compounds, except **24k**, possess at least low or moderate inhibitory property. However, a weak correlation between inhibition of bacterial growth and efflux pump mechanism is observed. For example, **26a–c** are very efficient in killing mycobacterial cells but only display moderate modulatory effect on the pumps. Differently, the inactive compound **28b** inhibits efflux inhibition on a par with the control inhibitor Verapamil. Interestingly, **24c**, **24h**, **24i**, and **24l**, bearing a bulky alkyl substituent on the piperazine ring, showed good/ excellent inhibitory activity. These findings suggest that specific endogenous targets for these compounds are still elusive; however, the results indicate that they may have pleiotropic modes of action and thus, potential to reverse antimicrobial resistance. As TB treatment involves a combination of complementary drugs, this off-target effect of the compounds could enhance the effectiveness of drug treatment regimens. Within this context, it is noteworthy that five compounds (namely, **28b**, **24c**, **24h**, **24i**, **24l**) show a much higher EPI activity than **I** and **II** (Table 13) which are known inhibitors exclusively of the pump transporter MmpL3. In fact, the less potent mycobacterial growth inhibitors but, endowed with higher whole-cell efflux inhibitory features, may also prove to be prospective leads in a multidrug therapy owing to synergistic combinations, should that arise. Thus, unlike **I** and **II**, which show poor EPI activity, **28b** and **24b** could be used in combination with standard antitubercular drugs such as INH or RIF to reverse multidrug resistance in tuberculosis.

2.3.2. Conclusions.

Within this chapter the synthesis and development of novel anti-tubercular drugs through the application of a molecular hybridization approach was described. A library of hybrid pyrrole derivatives was designed, synthesised, and then evaluated for its antitubercular activity against Mtb and MDR-TB clinical isolates. Five compounds showed antitubercular activity against Mtb at ≤ 1.0 $\mu\text{g/mL}$, and two of them (**26b** and **26c**) proved to be highly active also against MDR-TB strains. SAR studies have been conducted and they revealed the key features essential for the antimycobacterial activity for this new class of antitubercular compounds. Finally, compound **26c** showed a better drug profile than **I** in terms of activity, cytotoxicity, and potency toward MDR-TB clinical isolates turning out to be an excellent lead candidate for preclinical trials.

3. Development of novel methodologies for the synthesis of heterocyclic drug-like compounds.

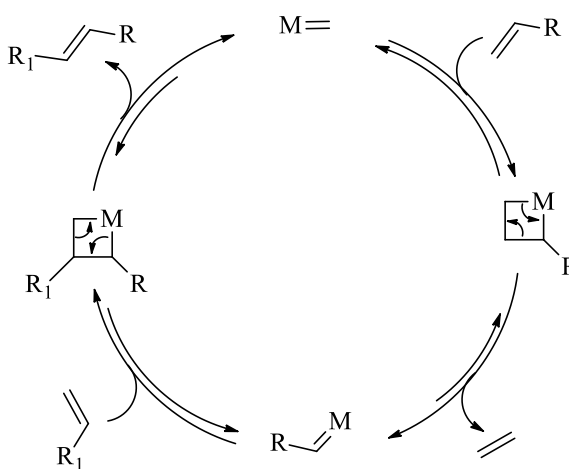
3.1 Introduction

Heterocycles are recurring structural moieties in Nature and they have remarkable relevance in organic chemistry, particularly finding outstanding applications in medicinal chemistry.¹²⁹ The development of new drugs in the last century has largely taken into account the use of natural products as source of structures endowed with biological activity. Often, such molecules are decorated with, or even made of, heterocycles making these structures interesting building blocks for the design of medicines. Applications of heterocycles in medicinal chemistry range from their ability to modify key characteristics of a drug scaffold (such as its lipophilicity, polarity and its solubility), to their application as bioisosteres for a large variety of functional groups. Therefore, they are great tools for the drug optimization processes in modulating potency and efficacy of a drug.¹³⁰ It is noteworthy that the occurrence of aromatic nitrogen heterocycles in many natural and synthetic biologically active compounds is high. This represents an incentive toward the development of new synthetic methodologies towards these important chemicals.¹²⁹ Moreover, it has been estimated that more of 50% of the bestselling drugs contain a nitrogen heterocyclic nucleus, thus fuelling a demand for broadly applicable synthetic methods that deliver aromatic heterocycles in high yield. In chapter 2.3 the discovery of a class of pyrroles endowed with potent activity against drug-resistant tuberculosis was described. In the following chapters two novel and sustainable approaches for the production of this extremely important class of heterocycles are described.¹¹⁶

3.1.1. New approaches for the synthesis of pyrroles: Metathesis reaction.

Typical approaches for the synthesis of pyrroles include the Paal–Knorr¹³¹ and Clauson–Kass reactions,¹³² the aza-Wittig reaction¹³³ or other multicomponent approaches.¹³⁴ More recently, metathesis emerged as a powerful and effective reaction for the synthesis of many functionalized pyrroles from acyclic precursors. Metathesis is a Greek word (μετάθεσις) which means transposition and it is used in organic chemistry to define a class of bimolecular processes involving the exchange of one or more bonds between similar interacting chemical species affording products with similar or identical bonding affiliations to those in the reactants. The most widely used metathesis reactions are catalysed by metal

carbene complexes which allow the formation of a carbon-carbon bond through exchange of groups on two alkenes (olefin metathesis) or between an alkene and an alkyne (enyne metathesis). From the first discovery of metathesis reactions by Karl Ziegler, over 60 years ago, metathesis reactions have become very important tools for organic chemists both in research and industry.¹³⁵ The widely accepted mechanism for olefin metathesis reactions was proposed by Yves Chauvin in 1971.¹³⁶ The Chauvin mechanism involves the formation of a metallocyclobutane intermediate between a metal carbene complex (also called carbenoid) and an alkene double bond. The instable intermediate, thus could lead to either the original species or a new alkene and alkylidene (Scheme 11).



Scheme 11. Chauvin mechanism.

The applications of this molecular process developed as quickly as the development of new, more and more stable, selective and powerful carbenoids. In 1988, Schrock and coworkers introduced a variety of stable and easy to prepare Mo and W catalysts. These complexes provided the first controlled catalysts in metathesis and enabled the reaction to occur under milder conditions than ever before. Furthermore, they are powerful enough to allow the conversion of sterically demanding substrates in the desired products. However, their applications are limited by their poor tolerance towards functional groups.¹³⁷

Grubbs and coworkers expanded the studies conducted by Schrock and developed two generations of Ru alkylidene catalysts endowed with high specificity for olefinic groups and increased stability to oxygen and moisture which make them easier to handle than the more powerful but unstable Schrock catalysts.¹³⁸ During the last decade, many groups dedicated their effort to the development of novel ruthenium carbene complexes bearing various ligands which enhance the stability of the carbenoid, the functional group tolerance and the potency of the catalysts toward structurally complex substrates (Figure 20).^{139–143}

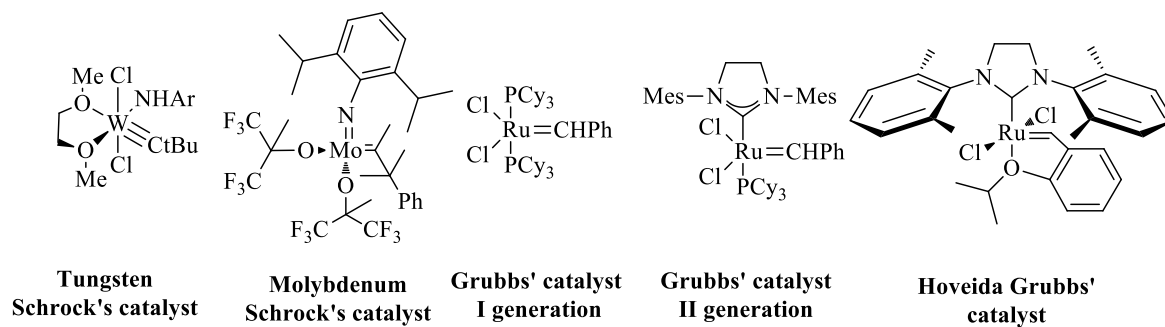


Figure 20. Schrock and Grubbs' catalysts.

Olefin metathesis was the first metathesis reaction to be widely used for the synthesis of a large variety of chemicals of interest. This class of reaction found several applications such as ring-closing metathesis (RCM), cross metathesis (CM), ring-opening cross metathesis (ROCM), ring-opening metathesis polymerization (ROMP) and acyclic diene metathesis polymerization (ADMET) as shown in Figure 21.

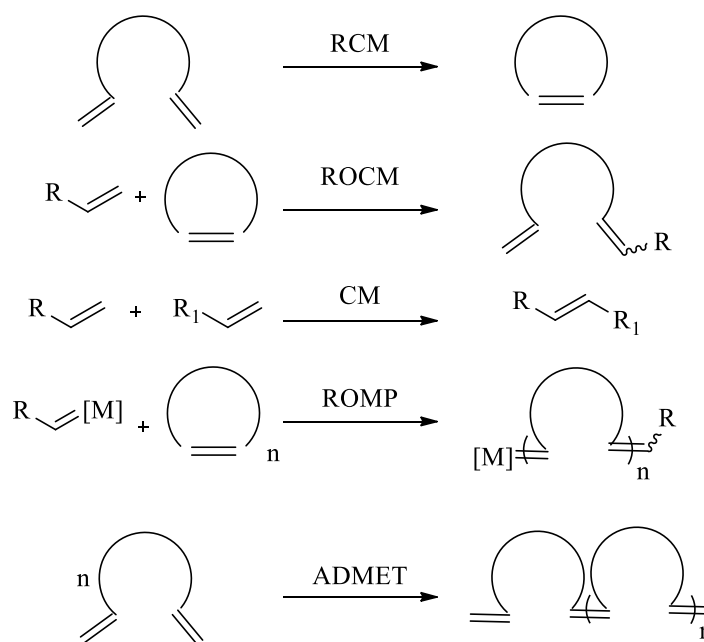
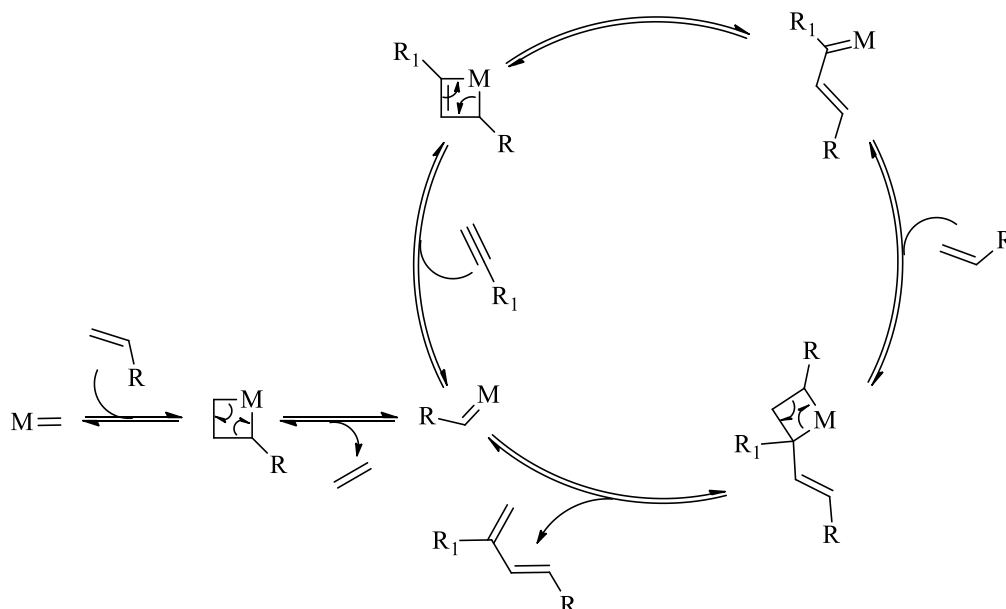


Figure 21. Classification of Olefin Metathesis.

Enyne metathesis (EYM) consists in a bond reorganization between an alkene and an alkyne to produce a 1,3-diene. EYM could be intramolecular (enyne RCM) and intermolecular (enyne CM, enyne ROMP) depending on the nature of the starting materials.¹⁴⁴ The general mechanism for EYM is showed in Scheme 12.



Scheme 12. Enyne metathesis reaction mechanism.

The EYM mechanism of reaction involves an activation step followed by the proper catalytic cycle. In the activation step, the olefin group reacts with the catalyst affording a metallocyclobutane intermediate, which then undergoes cycloelimination forming a metallo-carbene complex and ethylene as a side product. The metallo-carbene complex so formed enters the catalytic cycle reacting with an alkyne, leading to a vinylcarbene intermediate via a metallocyclobutene transition state. Finally, the vinyl carbene reacts with another olefin group yielding the 1,3-diene and restoring the metallo-carbene complex, which enters again into a new catalytic cycle. Both olefin and enyne metathesis reactions generally occur with low catalyst loading (1-10%) and afford products in high yields and short reaction times. Furthermore, the catalyst high affinity for olefin and olefin moiety combined with its large tolerance for other functional groups, makes the reaction highly chemo-specific, and therefore, minimal substrate protection is necessary. The large amount of advantages which metathesis reactions offer over other metal catalysed carbon-carbon bond formation processes has inspired several groups to use this reaction for the synthesis of high requested substrates such as functionalised pyrroles. Donohoe^{145,146} and Rutjies¹⁴⁷ first developed a two step sequence to pyrroles from diallylamines **III** via olefin ring-closing metathesis followed by aromatization mediated by RuCl_3 , Pd/C , FeCl_3 or $t\text{-BuOOH}$ (Figure 22).^{148–151} This latter step is supposed to occur through the oxidation of the amine **IV** into the corresponding iminium intermediate **V** leading in turn to pyrrole **VI** by tautomerization.

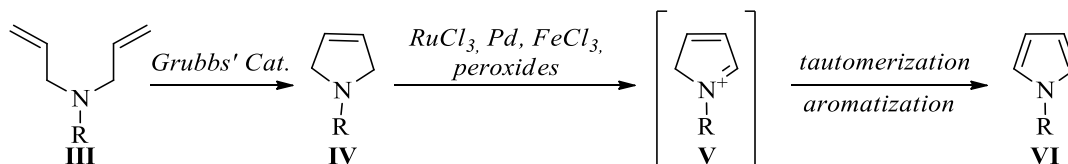


Figure 22. Olefin metathesis approaches to pyrroles.

More recently, Donohoe¹⁵² and Grela¹⁵³ described an olefin cross-metathesis approach for the synthesis of pyrroles. Both approaches are based on the CM of appropriately substituted allylamines and enones followed by acid catalysed cyclization (Figure 23).

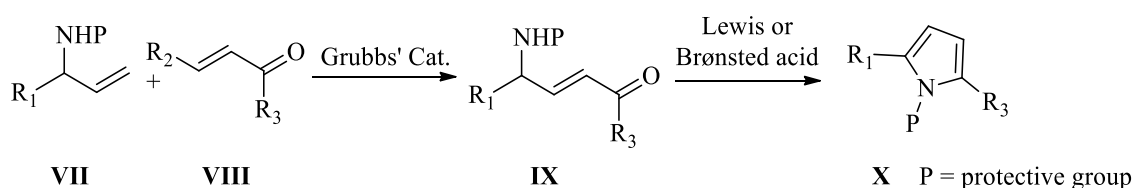


Figure 23. Two steps olefin CM-cyclization approach.^{152,153}

Also the alkyne-alkene (enyne) metathesis has been successfully applied toward the synthesis of heterocyclic compounds.^{144,154} Both RCM-enyne and CM-enyne approaches have found large application for the synthesis of indoles, pyrrolines, dihydrofurans and dihydropyranes.¹⁵⁵ However, only Stevens and coworkers¹⁵⁶ described a synthesis of pyrroles via a RCM-enyne metathesis-aromatization sequence whilst there are no examples in the literature describing the synthesis of pyrroles via a CM-enyne approach (Figure 24).

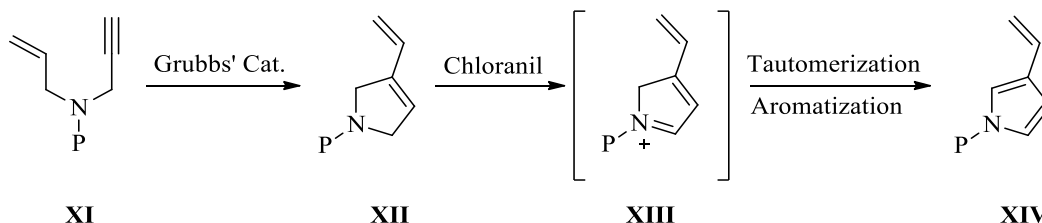


Figure 24. Stevens's RCM enyne approach.

Therefore, the development of a methodology involving enyne CM toward the synthesis of this important class of heterocycles could have the double potential to enhance the

application field of enyne CM class of reaction and to make accessible versatile building blocks such as functionalised pyrroles for application in medicinal chemistry. In paragraph 3.2 a novel methodology for the synthesis of 1,2,3 substituted pyrroles from inexpensive starting materials such as propargylamines via a tandem enyne CM-cyclization reaction is described.

3.1.2. Novel insight for the sustainable synthesis of pyrroles.

It is noteworthy that the majority of the approaches for the synthesis of pyrroles described in this chapter relies on the oxidation of a cyclic amine like a pyrroline to an iminium ion, which then leads via tautomerization and aromatization to the formation of the desired pyrrole. The direct oxidation of amines into imines or iminium ions still represents a challenge in organic synthesis and only few approaches have been described so far. These methods rely on the use of metal catalysts such Fe, Pd, Ru in the presence of oxygen or TEMPO and often require harsh reaction conditions.¹⁴⁸ However, in Nature, the oxidation of an amine group into the corresponding imine is a common biochemical transformation catalysed by a class of oxidoreductases enzymes called amino oxidases.^{157–159} Among this class of enzymes, monoamine oxidase (MAO), in particular MAO variants from *Aspergillus niger* (MAO-N) and 6-hydroxy-D-nicotine oxidase (6-HDNO) found a broad application as biocatalysts for asymmetric synthesis of pharmaceuticals and natural products. Furthermore both MAO-N and 6-HDNO have been widely studied as biocatalysts for the production of enantiomerically pure amines through the selective oxidation and deracemization of a range of chiral aliphatic substrates such as chiral pyrrolidines (Figure 25).^{160–162}

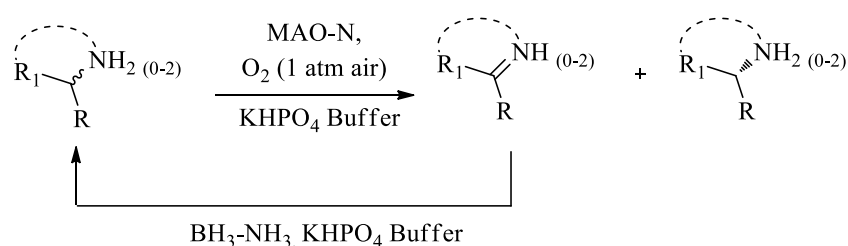


Figure 25. General mechanism for the dynamic deracemization of chiral aliphatic substrates.

The structural similarity between the pyrrolidine ring and the pyrroline inspired the development of a sustainable approach for the synthesis of pyrroles from 3-pyrrolines

exploiting the oxidizing property of MAO-N biocatalysts described in paragraphs 3.3.1.3. and 3.3.1.4. Furthermore, oxidizing/aromatizing properties of MAO-N biocatalysts have been coupled with the RCM approach generally used for the synthesis of 3-pyrrolines thus leading to the development of a chemo-enzymatic cascade for the synthesis of pyrroles as described in paragraph 3.3.1.6.

3.2. Synthesis of 1,2,3-substituted pyrroles from propargylamines via a one-pot tandem enyne cross metathesis – cyclization reaction.

Pyrroles are a class of compounds widely present in Nature, (Figure 26) and they are interesting heterocyclic scaffolds to be used for the synthesis of compounds of pharmaceutical interest.

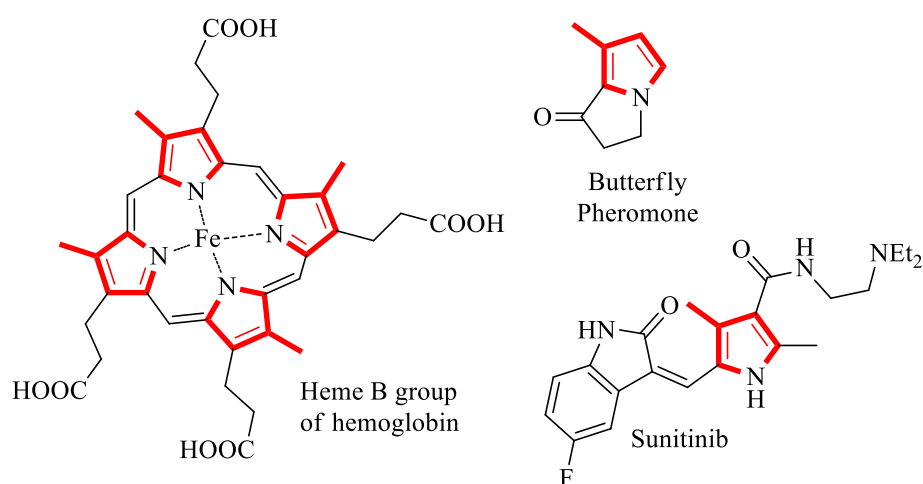
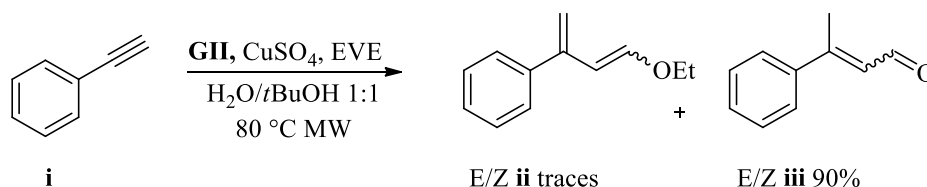


Figure 26. Some example of pyrroles in Nature and in pharmaceutical industry.

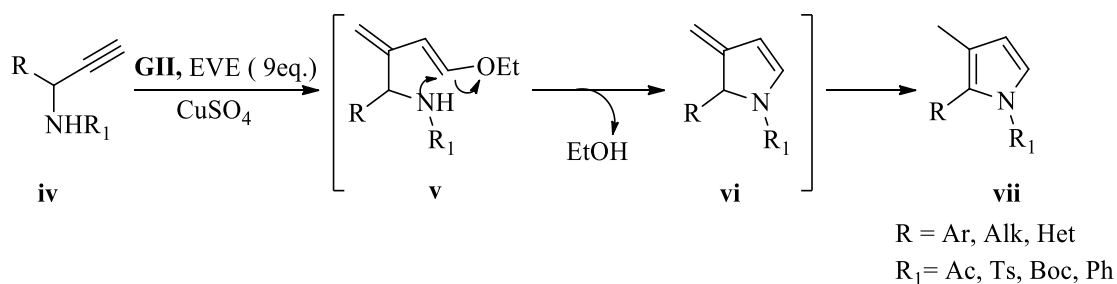
Only a few examples for the synthesis of 4,5-unsubstituted pyrroles have been reported so far and most of them rely on multistep synthetic sequences.^{163,164} As described in paragraph 3.1.1, there are no examples reported in the literature about the synthesis of pyrroles via enyne cross-metathesis reaction. The development of the first synthetic approach to pyrroles involving such reaction is described. Enyne-CM reaction is an useful version of catalytic olefin metathesis, and it involves the formation of a diene from an alkene and an alkyne. The synthetic appeal of enyne cross-metathesis is that it offers a catalytic, direct, and regiocontrolled access to conjugated dienes, which have broad application in synthesis.

Castagnolo *et al.* recently demonstrated that ethyl vinyl ether (EVE) can be used as the olefin synthetic equivalent of the acetaldehyde in enyne CM reactions, leading to the formation of crotonaldehydes when reacted with terminal alkynes in the presence of the weak Lewis acid CuSO₄ as shown in Scheme 13.¹⁶⁵



Scheme 13. EVE used as olefin equivalent of acetaldehyde in an enyne CM.

This reaction allows the formation of diene **ii** that, in presence of CuSO₄ in aqueous medium is hydrolysed, affording the corresponding enol. The latter finally tautomerizes into crotonaldehyde **iii**. It was hypothesized that an analogous strategy could be a short and elegant approach for the synthesis of 4,5-unsubstituted pyrroles when propargylamines are used as starting materials as shown in Scheme 14.



Scheme 14. Proposed one-step enyne CM-cyclization approach for the synthesis of pyrroles.

In the proposed method the propargylamines **iv** and EVE undergo enyne CM reaction under microwave irradiation conditions affording the corresponding diene **v**. The weak Lewis acid CuSO₄ catalyses both the cleavage of the ethoxy group and the electrophilic activation of the diene **v** which undergoes a cyclization reaction affording the five membered ring intermediate **vi**. Such intermediates quickly tautomerize into the desired pyrrole **vii**. In the

next pages is therefore described the exploration, the development and the application of a one-pot tandem enyne cross metathesis-cyclization reaction for the production of the synthetically challenging 1,2,3-substituted pyrroles from opportunely substituted propargylamines.⁸⁴

3.2.1. Results and discussion.

3.2.1.1. Optimization of the reaction conditions.

Bearing in mind the work present in literature, the research of the best reaction conditions for the one pot synthesis of pyrrole **41a** from the simple *N*-Boc propargylamine **29a** was investigated as described in Table 14.

Table 14. Optimization of the reaction conditions.

<p>Reaction scheme: 29a (N-Boc propargylamine) + EVE (9eq.) $\xrightarrow[\text{Time, Temp, MW, Solvent}]{\text{GII, Additive}}$ 30 (diene intermediate) \rightarrow 41a (pyrrole).</p>					
Entry	Solvent	GII mol%	CuSO ₄	T °C/ Time	Yield % ^a
1	H ₂ O/ <i>t</i> BuOH	5	2 eq.	80°C/20min	29%
2	H ₂ O/ <i>t</i> BuOH	10	2 eq.	80°C/20min	25%
3	Toluene	5	2 eq.	80°C/30min	36%
4	Toluene	5	2 eq.	120°C/30min	56%
5	Toluene	5	-	120°C/30min	0% ^b
6	Toluene	5	1 eq.	120°C/30min	18%
7	Toluene	10	2 eq.	120°C/30min	55%
8	Toluene	5	- ^c	120°C/30min	56%

^a Isolated yields. ^b 41% diene **30** isolated. ^c 2 eq. of Cu(OTf)₂ were used.

The Boc-protected propargyl amine **29a** was first reacted with EVE, in the presence of **GII** and CuSO₄ at 80 °C under microwave irradiation in 1:1 *tert*-butanol/water leading to the formation of the desired pyrrole **41a** with 25-29% yield (*entries 1-2*). The use of a higher **GII** loading (*entry 2*) did not lead to any improvement of the yield, while a slightly higher amount of pyrrole **41a** was isolated when the reaction was run in degassed toluene (36%, *entry 3*). In *entry 4*, it is shown that increasing the temperature to 120°C and the time at 30 minutes, was beneficial for the reaction outcome, enhancing the yield to 56%. When the reaction was run with the same reaction condition of *entry 4* but without CuSO₄ the pyrrole **41a** is not formed and the reaction led to the formation of the corresponding diene **30** in 41% yield (*entry 5*). Moreover, the use of a stoichiometric amount of CuSO₄ led to **41a** in only 18% yield (*entry 6*). It is noteworthy that when the reaction was performed with 5 mol% or 10 mol% catalyst loading there were no significant differences in the yield (*entries 4-7*). Finally, the use of a different copper source, such as the stronger Lewis acid Cu(OTf)₂, did not lead to any improvement in the yield of the reaction (*entry 8*). These data suggest that CuSO₄ plays a relevant role for the outcome of the reaction thus, further experiments were carried out in order to understand better the influence of the Lewis acid as additive for the cyclization step which led to **41a** from **30** (Table 15).

Table 15. Investigation of the role of CuSO₄.

Reaction scheme: Diene **30** (with NHBoc and OEt groups) reacts with an Additive in toluene at a specific temperature and time to form Pyrrole **41a** (with a methyl group and N-Boc group).

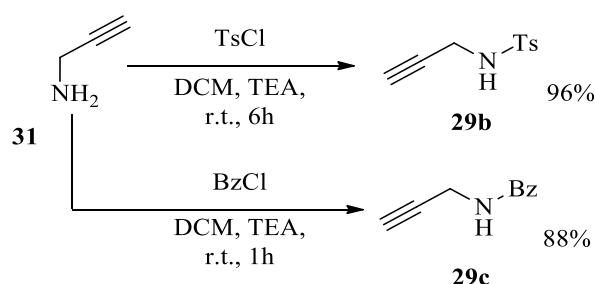
Entry	GII mol %	Additive	Time	T. °C	Conv. % ^a
1	-	-	24h	110 °C	70%
2	-	2 eq. CuSO ₄	6h	110 °C	100%
3	-	2 eq. CuSO ₄	20 minutes	120 °C Mw	30%
4	10 mol %	2 eq. CuSO ₄	10 minutes	120 °C Mw	100%

^a Conversion values were measured by ¹H-NMR spectroscopy.

It is noteworthy that without CuSO₄ the formation of pyrrole **41a** from propargylamine **29a** and EVE did not occur leading only to the formation of the diene **30** (Table 14, *entry 5*). When, the diene intermediate **30** was reacted in refluxing toluene for 24 h (*entry 1, table*

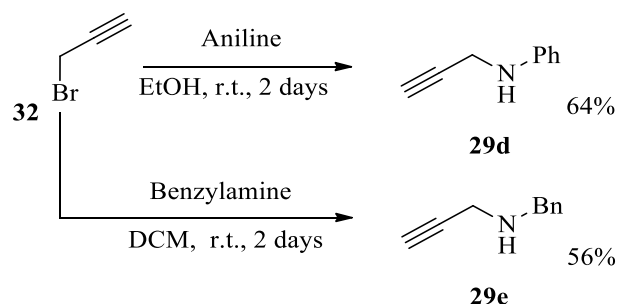
15) **41a** was obtained only with 70% yield, while in the presence of CuSO₄ (2 eq.) the reaction reached completion after 6 h (*entry 2*). These data suggests that Cu²⁺ could help the cyclization step coordinating the ethoxy group and facilitating its cleavage. Surprisingly, when **30** was heated at 120 °C under microwave irradiation and in the presence of CuSO₄ (2 eq.) for 20 min, only 30% of conversion was observed (*entry 3*). Moreover,, if the same reaction was run in the presence of 10 mol % of **GII**, the full conversion of **30** into **41a** was observed after 10 min. Thus, the data gathered suggest that both the Cu²⁺ and [Ru] (from the **GII**) contribute to the cyclization of **30** and to the formation of **41a**.

In order to assess the flexibility of the methodology toward different amine group substituents a set of *N*-substituted propargylamines **29b-e** was synthesised according to the literature.^{166–169} *N*-Tosyl-propargylamine **29b** and *N*-benzoyl-propargylamine **29c** were obtained from propargylamine **31** reacted respectively with tosyl chloride and benzoyl chloride in DCM and TEA (Scheme 15).



Scheme 15. Synthesis of propargylamines **29b** and **29c**.

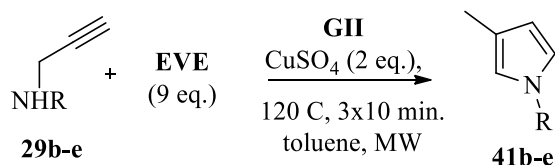
Subsequently, *N*-phenyl-propargylamine **29d** was obtained reacting propargylbromide **32** with aniline in EtOH, while the treatment of propargylbromide with benzylamine in DCM afforded *N*-benzyl-propargylamine **29e** in good yields as shown in Scheme 16.



Scheme 16. Synthesis of propargylamines **29d** and **29e**.

The propargylamines **29b-e** were then reacted with EVE, in the presence of **GII** and 2 equivalent of CuSO₄ at 120 °C under microwave irradiation in degassed toluene as described in Table 16

Table 16. Synthesis of pyrroles **41b-e**.

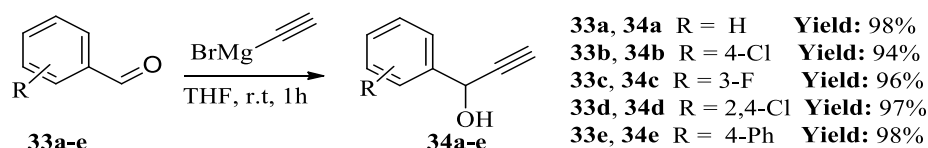


Entry	Cmpd	R	GII mol%	Additive	Pyrrole	Yield % ^a
1	29b	Ts	5	-	41b	25%
2	29b	Ts	10	-	41b	53%
3	29c	Bz	10	-	41c	39%
4	29d	Ph	10	-	41d	54%
5	29e	Bn	10	-	41e	N.O ^b
6	29e	Bn	10	TsOH*H ₂ O (1.2 eq.)	41e	N.O ^b

^aIsolated yields were reported. ^b Product **41e** was not observed

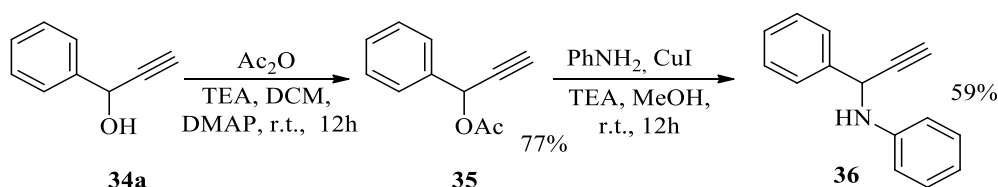
The treatment of the tosyl derivative **29b** with 5 mol% of **GII** led to desired **41b** in 25% yield, while a higher amount of **41b** (53%) was recovered when 10 mol% of catalyst was used (*entry 1-2*). The pyrrole **41c** was obtained in moderate yield from the benzoyl compound **29c** (*entry 3*) while propargylaniline **29d** afforded the phenyl-pyrrole **41d** in good yield (*entry 4*). On the contrary, the benzyl-derivative **29e** was recovered unreacted from the reaction mixture and no pyrrole **41e** was observed (*entry 5*). It is reported in literature that, contrary to the electron poorer anilines and tertiary hindered amines, the aliphatic primary and secondary amines poison the Ru-catalysts thus preventing the metathesis reactions.^{170,171} In order to overcome such issue, in *entry 6*, a Brønsted acid was added to the reaction mixture in order to coordinate the nitrogen lone pair of the amine **29e** making it unable to poison the ruthenium.¹⁷² Unfortunately, when the amine **29e** was treated with a stoichiometric amount of *p*-toluenesulfonic acid (PTSA) and then reacted with an excess of EVE under standard reaction conditions no pyrrole **41e** was formed and a mixture of side products was observed from the crude reaction mixture by ¹H-NMR spectroscopy.

In order to expand the scope of this tandem metathesis-cyclization protocol to the synthetically challenging 1,2,3-substituted pyrroles, propargylamines **37a-h**, **36** and **40a-d** were synthesised. Three different synthetic approaches for the synthesis of highly substituted propargylamines were employed. In order to synthesise the propargylamines **37a-h** and **36** a first batch of aryl-propargylalcohols **34a-e** was synthesised in high yields from the appropriately substituted benzyl aldehydes **33a-e** (Scheme 17)^{173–175}



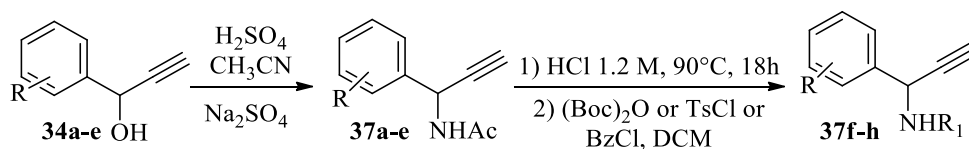
Scheme 17. Synthesis of aryl-propargyl-alcohols **34a-e**.

Compounds **33a-e** were reacted with ethynyl magnesium bromide in dry tetrahydrofuran (THF) affording the aryl-propargyl alcohols **34a-e** in excellent yield (96-99%). As shown in Scheme 18, propargyl alcohol **34a** was acetylated to give the alkyne **35** which was in turn converted into the phenyl substrate **36** through a copper mediated amination reaction (59%).¹⁷⁶



Scheme 18. Synthesis of aniline **36**.

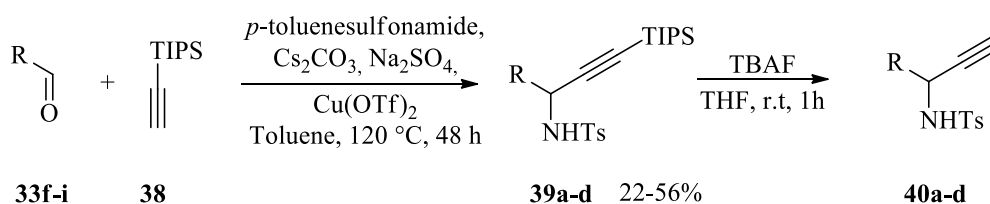
Moreover, propargyl-alcohols **34a-e** were treated with H_2SO_4 in CH_3CN and Na_2SO_4 affording aryl-propargylacetamides **37a-e** in good yields. Then, the hydrolysis of **37a-b** followed by Boc-, Bz and Ts-protections led to substrates **37f-h** with good yields as shown in Table 17.

Table 17. Synthesis of compounds **37a-h**.

Cmpd	R	R ₁	Yield % ^a
37a	H	Ac	78%
37b	4-Cl	Ac	77%
37c	3-F	Ac	73%
37d	2,4-Cl	Ac	76%
37e	4-C ₆ H ₅	Ac	75%
37f	H	Ts	62%
37g	4-Cl	Boc	60%
37h	4-Cl	Bz	65%

^aIsolated yields.

A second batch of aliphatic and heteroaryl substituted propargylamines **40a-d** was obtained by a multicomponent strategy.¹⁷⁷ The appropriate aldehydes **33f-i** were refluxed in toluene in the presence of *p*-toluenesulfonamide and (triisopropylsilyl)acetylene (TIPS) **38** and $\text{Cu}(\text{OTf})_2$ affording tosyl propargylamines **39a-d**, which afforded the terminal alkynes **40a-d** after silyl-deprotection with tetra-*N*-butylammonium fluoride (TBAF). (Table 18).

Table 18. Synthesis of aliphatic and heteroaryl derivatives **40a-d**.

Aldehyde	R	Product	Yield % ^a
33f	2-Furyl	40a	82
33g	Cyclohexyl	40b	99
33h	<i>i</i> -Propyl	40c	95
33i	<i>i</i> -Butyl	40d	93

^aIsolated yields.

3.2.1.2. Synthesis of pyrroles from propargylamines via one-pot tandem enyne CM-cyclization reaction.

The alkynes **34a-h**, **36** and **40a-d** were then reacted with EVE in the presence of **GII** and CuSO₄ under microwave irradiation in toluene at 120 °C for 20 minutes obtaining pyrroles **41f-r** (Table 19.).

Table 19. Synthesis of 1,2,3-substituted pyrroles **41f-r**. Scope of the reaction.

$$\text{R}-\text{C}\equiv\text{C}-\text{CH}_2-\text{NHR}_1 + \text{CH}_2=\text{CH}-\text{OEt} \xrightarrow[\text{Toluene, MW } 120^\circ\text{C, } 2 \times 10 \text{ min}]{\text{GII (10 mol\%), CuSO}_4 \text{ (2 eq.)}} \text{Pyrrole } \mathbf{41f-r}$$

34a-h, 36, 40a-d

Alkyne	R	R ₁	Pyrrole	Yield ^a
34a	Ph	Ac	41f	70%
34b	4-Cl-C ₆ H ₄	Ac	41g	72%
34c	3-F-C ₆ H ₄	Ac	41h	76%
34d	2,4-Cl-C ₆ H ₃	Ac	41i	38%
34e	4-Ph-C ₆ H ₄	Ac	41j	59%
34f	Ph	Ts	41k	38%
34g	4-Cl-C ₆ H ₄	Boc	41l	50%
34h	4-Cl-C ₆ H ₄	Bz	41m	64%
36	Ph	Ph	41n	Traces ^b
40a	2-Furyl	Ts	41o	76%
40b	Cyclohexyl	Ts	41p	43%
40c	<i>i</i> -Pr	Ts	41q	71%
40d	<i>i</i> -Bu	Ts	41r	69%

^aIsolated yields were reported. ^bObserved by GC-MS

Acetamides **34a-e** were first reacted with EVE and **GII** leading to desired pyrroles **41f-j** in high yields (59-76%). Only pyrrole **41i** bearing a 2,4-Cl-phenyl group was obtained in lower yield (38%) probably due to a combination of steric and electronic factors. The pyrroles **41l** and **41m**, bearing the bulky groups Boc and Bz respectively, were obtained in lower yields than the acetyl analogue **41g**. Similarly, the tosyl-pyrrole **41k** was isolated in lower yield than **41f**. On the other hand, the aliphatic and the furyl *N*-tosyl-propargylamides **40a-d** were converted into pyrroles **41o-r** in excellent yields with the only exception of the bulky

cyclohexyl derivative **41p**. Finally, the treatment of the substrate **36** with EVE and **GII** did not lead to the desired pyrrole **41n** in significant amount. Traces of **41n** were detected only by GC-MS analysis of the crude reaction mixture.

In order to expand the flexibility of the cascade reaction to the synthesis of 1,2,4-substituted pyrroles, propargylamine **29a** was reacted with 2-methoxypropene, a substituted of EVE, in order to obtain **41s**. However all the attempts to obtain the desired pyrrole proved to be unsuccessful (Table 20).

Table 20. Attempts for the synthesis of 1,2,4 substituted pyrrole **41s**

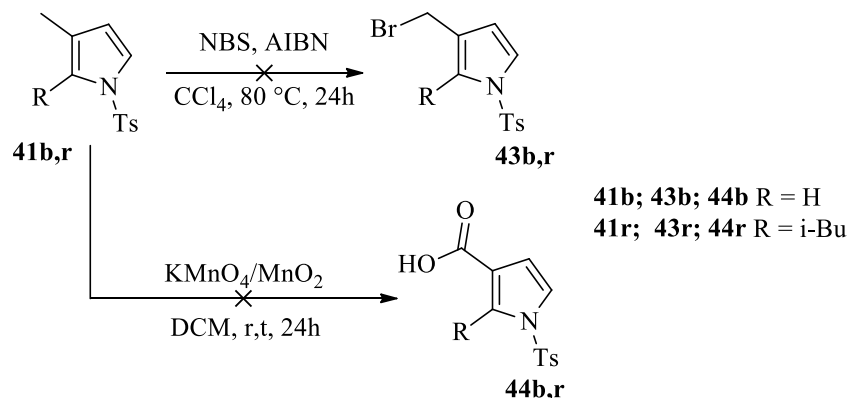
Entry	GII mol%	Time	Temp. °C	Yield %
1	5%	10 min.	120 °C Mw	-
2	10%	10 min.	120 °C Mw	-
3	5%	20 min.	120 °C Mw	-
4	10%	20 min.	120 °C Mw	-
5	5%	6h	110 °C	-
6	10%	6h	110 °C	-

Methoxypropene proved to be unreactive toward enyne-CM due to its steric hindrance and propargylamine **29a** was recovered unreacted from the reaction mixtures in all the reaction conditions tested.

3.2.1.3. Functionalization of pyrroles on C5 and derivatization on the methyl on C3.

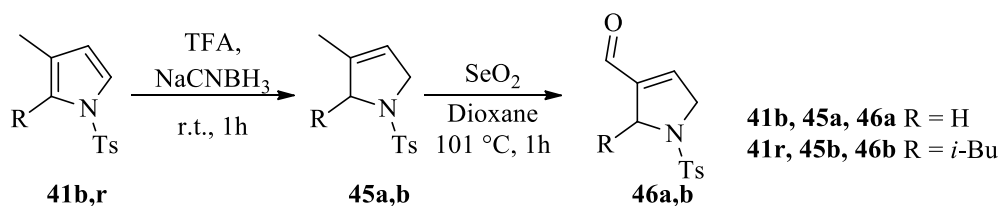
The enyne cross metathesis-cyclization reaction described in paragraph 3.2.1.2. allows the synthesis in one synthetic step of pyrroles unsubstituted on C4-C5 from appropriately substituted propargylamines, EVE and a weak Lewis acid. In order to expand the library of compounds synthesised, the possibility to further functionalise the 1,2,3-substituted pyrroles

in the methyl at C3 and C5 was explored. All the pyrroles **41** have a methyl group at C3 deriving from the diene intermediate **30** of the enyne metathesis reaction. Attempts to decorate the methyl group through *N*-bromosuccinimide-mediated (NBS) bromination¹⁷⁸ or KMnO₄ oxidation¹⁷⁹ of **41b,r** were unsuccessful due to the presence of the reactive CH at positions C4 and C5, leading to a complex mixture of polymeric derivatives (Scheme 19).



Scheme 19. Attempts of derivatization on the methyl at C3 of **41b** and **41r**.

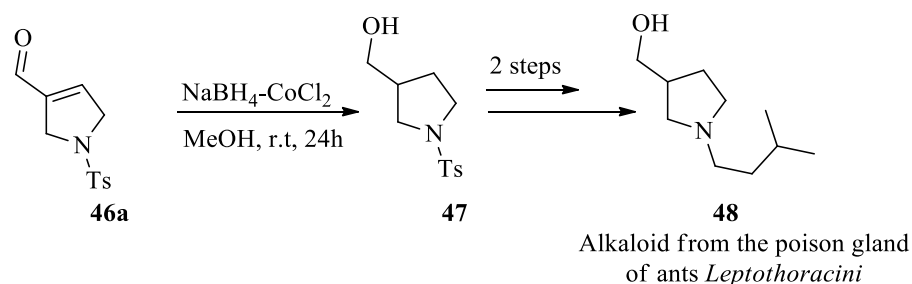
Derivatization of the methyl at position C3 was accomplished after reduction with NaCNBH₃ in TFA of the pyrroles **41b** and **41r** to the corresponding pyrrolines **45a,b**.¹⁸⁰ The pyrrolines so obtained were in turn oxidized at the methyl group on C3 with SeO₂ affording the aldehydes **46a,b** in 65-56% yield (over two-steps) respectively (Scheme 20).



Scheme 20. Functionalization of methyl group in C3.

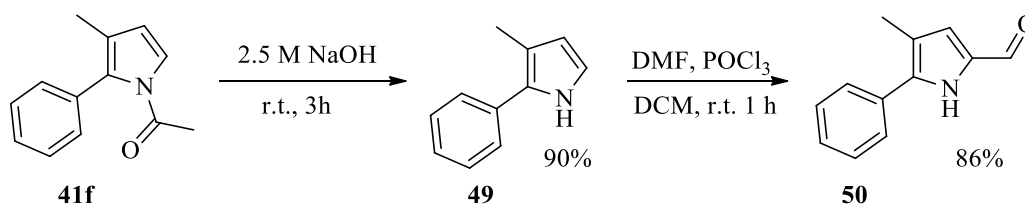
The aldehyde **46a** proved to be an interesting building block for the production of the racemic form of the alkaloid from the poison gland of ants *Leptothoracini* **48**.¹⁸¹ **46a** was converted into the corresponding pyrrolidine **47** through reduction with NaBH₄-CoCl₂ following the procedure described by Aramini *et al.*^{182,183} The alkaloid **48** could be obtained

in its racemic form, in two steps from precursor **47** as described by Aramini's work (Scheme 21).



Scheme 21. Synthesis of alkaloid **48**.

Finally, modification in C5 was easily obtained in two steps. De-protection of compound **41f** with 2.5 M NaOH affords pyrrole **49** with good yields which was then formylated at C5 via the Vilsmeier-Haack reaction obtaining the aldehyde **50** with 86% yield.



Scheme 22. Derivatization at C5 of pyrrole **50**.

3.2.2. Conclusions

In conclusion, the first approach for the synthesis of pyrrole scaffolds from propargylamines and EVE has been planned, fully developed and described within this chapter. This methodology is the first example of one-pot synthesis of pyrroles via enyne CM reaction and it constitutes a facile approach to the synthetically challenging 1,2,3-substituted pyrroles. It is noteworthy that the substituent at C3 of the pyrroles obtained with this methodology is always a methyl group deriving from the diene intermediate of the enyne metathesis reaction. However, the value of the methodology is corroborated by the conversion of pyrroles into 3-pyrrolines and consequent derivatization of the methyl substituent in C3. Furthermore, the pyrroles obtained with this methodology could be further decorated by formylation in position C5 obtaining reactive functionalised scaffolds to be used for the synthesis of compounds of pharmaceutical interest. Finally, the methodology has been applied toward

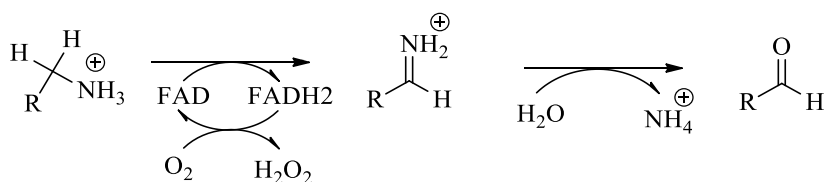
the production of compound **47**, which proved to be an important building block for the synthesis of the alkaloid **48**.

3.3. Novel applications of mono-amino oxidase (MAO-N & 6-HDNO) biocatalysts toward the synthesis of pyrroles.

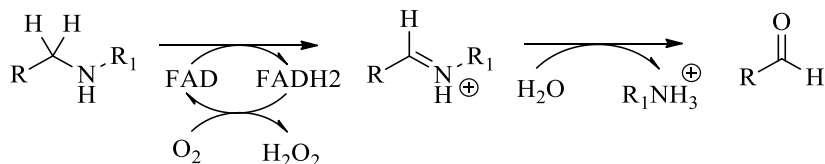
Nature has always fascinated and inspired scientists all around the world in developing new molecular transformations, which allow the conversion of one molecule into one other. However, only recently the interest of the organic chemists began to strive for matching the ability of Nature to synthesise molecules of interest under the greenest possible conditions. The classic synthetic procedures developed during the past two centuries allow the conversion of one compound into one other exploiting the large array of reagents, solvents and catalysts available in the market. With a series of transformations, in which the starting material of one is the product of the previous reaction, organic chemists could plan the synthesis of molecules of interest with controlled, multi-step protocols. This systematic, precise and laborious approach often needs drastic reaction conditions such as high temperature or special atmosphere. Furthermore, almost all the synthetic steps require the isolation and the purification of a product producing large amounts of waste and high manufacturing costs. However, the large number of reactions available, the possibility to combine them, and the versatility of their applications make them the easiest way available to synthesise molecules. On the other hand, Nature, in billions of years of evolution, evolved a vast array of tools (enzymes) which allow the synthesis of small molecules at ambient temperature, in one vessel (the cell), and in an aqueous environment. Every enzyme catalyses a few or even a single reaction, usually, with high substrate specificity which leads to products with an unmatched chemo-control, regio-control, and stereo-control of the reaction. The application of enzymes to the production of molecules of interests have always attired investors due to the unique catalytic characteristics of biocatalysts combined to the lower costs and waste production. Nowadays, some enzymes and even entire living cells are used for the production of small molecules of interests.¹⁸⁴ Moreover, advances in DNA sequencing and gene synthesis have allowed a huge progress in tailoring enzymes with protein engineering. Metabolic engineers use the most modern molecular biology techniques for the modification of biocatalysts leading to enzymes with enhanced ability to process non-natural substrates or to work in non-physiological conditions.^{185–187} However, despite these advances in the field of biocatalysis, organic chemistry has a wider repertoire of reactions compared to the ones offered by enzymatic catalysts. Moreover, despite the fact that in a near future advances in enzymatic engineering will broaden even more the application of

modified enzymes, it seems unlikely that biocatalysis will be able to equal the versatility of classic organic chemistry techniques. Therefore, probably, the future of the organic chemistry is to absorb biocatalysis.¹⁸⁸ Organic chemists will eventually collaborate with the molecular engineers for the discovery of novel synthetic procedures, which incorporate the unparalleled selectivity of the enzymes with the versatility of organic chemistry reactions. The discovery of novel reactions catalysed by enzymes and the development of chemo-enzymatic cascade protocols is the future of the organic chemistry as well the topic of this chapter. Within this chapter novel applications of mono-amino-oxidase (MAO) enzymes toward the synthesis of pyrroles are described. In Nature, the flavoproteins MAO catalyse the oxygen-dependent oxidation of primary, secondary and tertiary amines, respectively, into imines or iminium ions by means of the flavin adenine dinucleotide (FAD/FADH₂) redox cofactor. As described in Scheme 23, the Schiff's base so formed is then hydrolysed under the physiological environment forming aldehydes and ammonium from primary amines, or the cleavage of the secondary or tertiary amine.^{157–159}

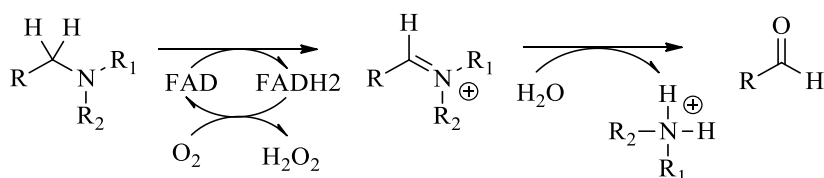
Primary amines



Secondary amines



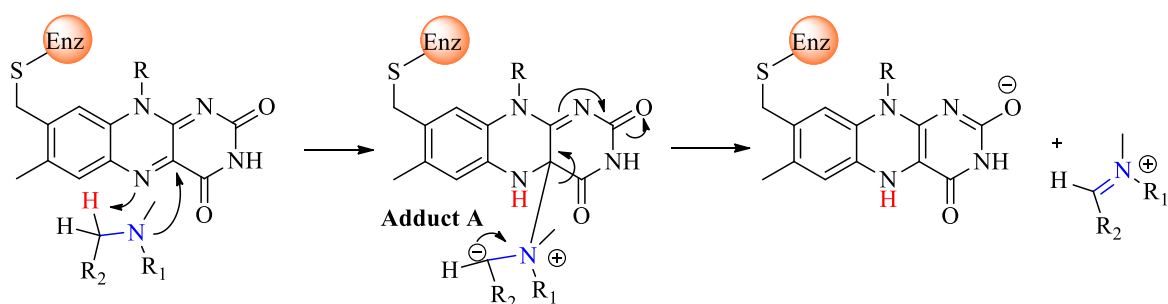
Tertiary amines



Scheme 23. Oxidation of amines catalyzed by flavoproteins MAO.

The exact mechanism of reaction of MAO has not been fully elucidated, and several models have been suggested based on the observation of the interaction of the substrates with the enzymes. The models suggested are: 1) single electron transfer (SET) mechanism, 2) hydrogen atom transfer mechanism, 3) nucleophilic mechanism, 4) hydride transfer

mechanism.¹⁸⁹ The most accredited model among them is the nucleophilic mechanism which is showed in Scheme 24.



Scheme 24. Plausible mode of action of MAO-N. Nucleophilic mechanism.

Following the nucleophilic mechanism the amine attacks the redox cofactor flavin adenine dinucleotide (FAD) leading to the adduct A. Consequent transfer of proton from amine to FAD leads to the formation of the reduced form of the flavin (FADH₂) and the corresponding iminium ion as shown in Scheme 24. The catalytic cycle is then closed by the oxidation of FADH₂ to FAD by O₂ with the formation of H₂O₂. During the last decade, Turner and coworkers designed and developed the directed evolution of a set of different MAO variants from *Aspergillus niger* (MAO-N).^{190–193}

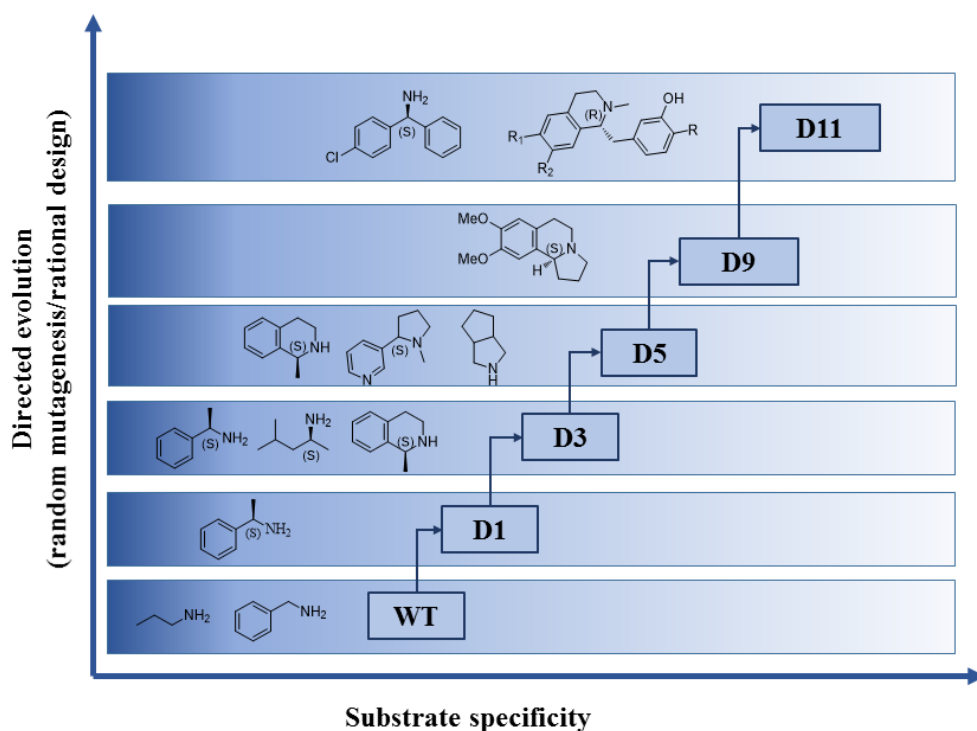
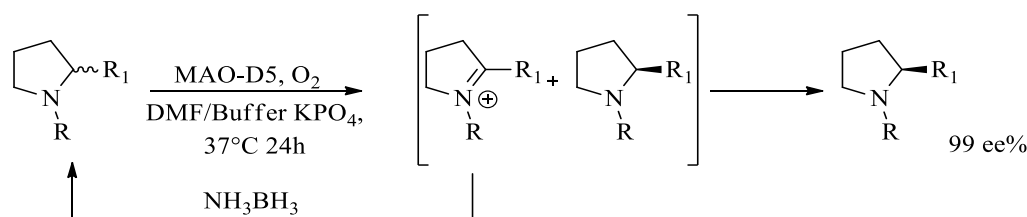


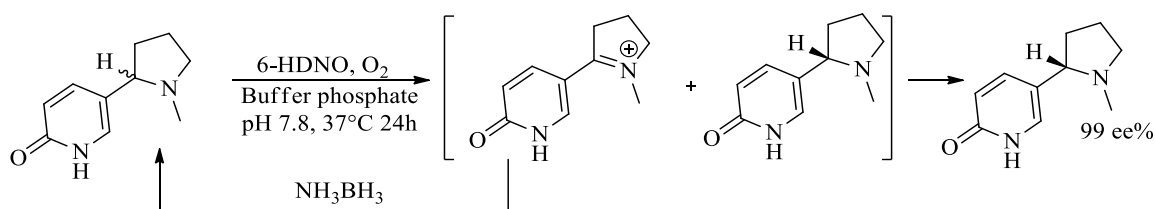
Figure 27. Directed evolution of MAO variants from *Aspergillus niger*.¹⁹³

The original MAO-WT (wild type) oxidises only simple primary amines to imines while the new variants D3-D11 found broad application as biocatalysts for asymmetric synthesis of pharmaceuticals and natural products. Furthermore, MAO-N have been widely studied as biocatalysts for the production of enantiomerically pure amines through the selective oxidation and deracemization of tertiary, secondary and primary racemic amines with broad structural variability.^{157,160–162} For instance, the variant MAO-D5 catalyses the dynamic deracemization of racemic pyrrolidines in the presence of a chemical reducing agent such as NH_3BH_3 as shown in Scheme 25.



Scheme 25. Dynamic deracemization of racemic 1,2 substituted pyrrolidine.

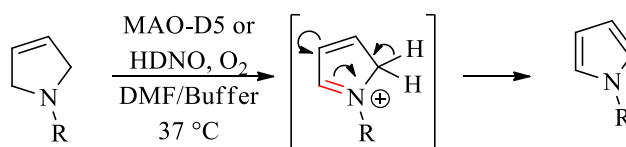
The oxygen dependant oxidation to iminium ion catalysed by MAO-N enzyme is faster for the (*S*) enantiomer of the racemic mixture. The reaction affords the iminium ion which is reduced *in situ* by a chemical reducing agent obtaining again the pyrrolidine as a racemic mixture. After every catalytic oxidation/reduction cycle the racemic mixture became more and more enriched with the (*R*) enantiomer. Recently, a similar but (*R*) selective biotransformation was obtained with the monoamine oxidase 6-HDNO as well.



Scheme 26. Dynamic deracemization of racemic 6-hydroxy nicotine catalyzed by 6-HDNO.

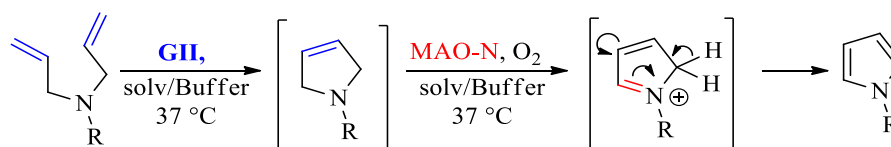
Furthermore, Turner and coworkers developed a variant of 6-HDNO (E350L/E352D) with a wider substrate scope compared to the wild-type enzyme, which is active only with (*S*)-6-

hydroxy nicotine.¹⁶² A large variety of enantiomerically pure cyclic amines, including functionalized pyrrolidines, have been synthesised by combining the oxidizing properties of 6-HDNO variants with an *in situ* reduction as shown in Scheme 26. Due to the structural similarity between the pyrrolidine ring and the pyrroline structure, it is possible to hypothesise that the oxidation of the carbon-nitrogen bond on a pyrroline ring, is feasible with MAO-N and 6-HDNO biocatalysts leading to the formation of pyrroles (Scheme 27).



Scheme 27. Hypothetical approach for the MAO-N & 6-HDNO catalysed aromatization of 3-pyrrolines into pyrroles.

The remaining part of this doctoral thesis is dedicated to the description of MAO catalysed highly sustainable approach for the synthesis of pyrroles from opportunely substituted 3-pyrrolines. Furthermore, as shown extensively on paragraph 3.1.1, 3-pyrrolines are easily prepared from the corresponding appropriately substituted diallylamines via RCM reaction.^{145–148,156} It is thus reasonable to think that the development of a one pot chemo-enzymatic reaction, which streamlines the conversion of diallylamines or anilines directly in pyrroles, would be an high requested protocol for the synthesis of this important class of heterocycles. Accordingly to the potential high impact which such procedure would have in all the branches of chemistry, the last part of this chapter is dedicated to the discovery, development and full exploration of a novel methodology which involves the in-situ combination of RCM reaction with MAO-N catalysed oxidation for the production of pyrroles from appropriately substituted diallylamines and anilines (Scheme 28).⁸⁵

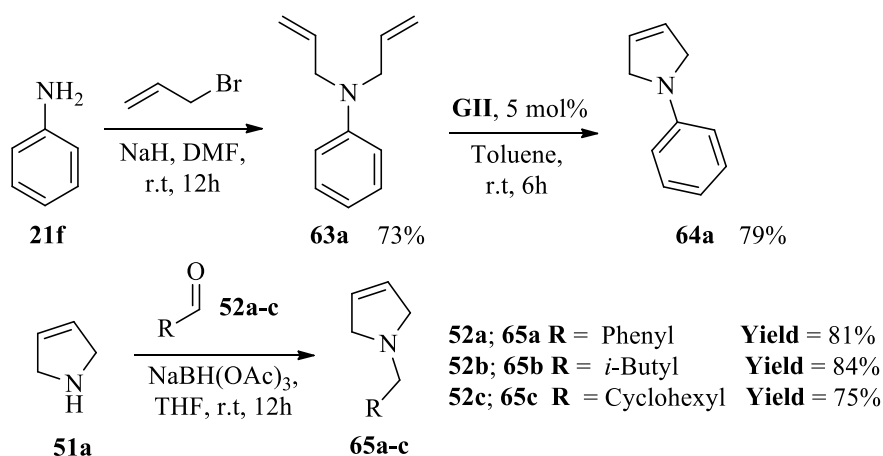


Scheme 28. Hypothesised RCM-MAO-N approach for the synthesis of pyrroles from diallylamines and anilines.

3.3.1. Results and discussion.

3.3.1.1. Preliminary investigation of the MAO-N & 6-HDNO biocatalyst aromatization property.

A preliminary investigation was carried out in order to test the hypothesis that 3-pyrrolines are good substrates for MAO-N and 6-HDNO biocatalysts. A library of *N*-substituted pyrroline derivatives was first synthesised according to classical synthetic procedures as reported in Scheme 29.



Scheme 29. Synthesis of 1-substituted pyrrolines **64a** and **65a-c**.

Aniline **21f** was *N*-alkylated with allyl-bromide affording diallylaniline **63a** which was treated with **GII** in toluene obtaining *N*-phenyl-pyrroline **64a** with 79% yield. Alkyl pyrrolines **65a-c** were synthesised through reductive amination reaction of 3-pyrroline **51a** and appropriately substituted aldehydes **52a-c** (namely, **52a** benzaldehyde, **52b**, isovalerylaldehyde, **52c** cyclohexylaldehyde) in presence of the reductive agent $\text{NaBH}(\text{OAc})_3$. Then, the MAO aromatization properties on the 3-pyrroline substrates **64a** and **65a-c**, were investigated (Table 21). MAO-N freeze-dried whole cell variants D5 and D9 were selected on the basis of their known activity and selectivity towards structurally related pyrrolidines.^{160,193,194} In addition, the oxidising/aromatizing properties of the recently developed nicotine oxidase biocatalyst 6-HDNO E350L/E352D13 were also explored. All the enzymatic biotransformations were initially carried out at 37 °C in a phosphate buffer solution (1 M pH = 7.8) using DMF as co-solvent where appropriate, according to the protocols.¹⁹³

Table 21. Conversion of *N*-substituted 3-pyrroline in pyrroles **66a**, **67a-c**.

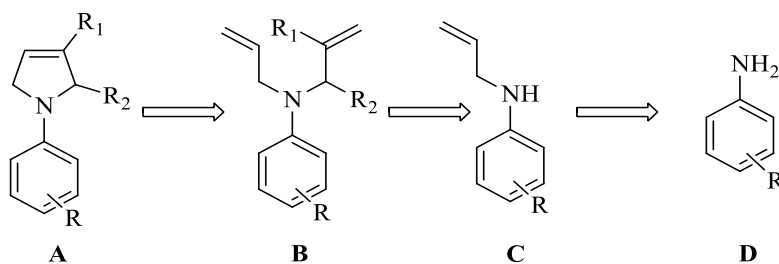
Entry	Cmpd	R	Biocatalyst ^a	Pyrrole	Conversion % ^b
1	64a	Phenyl	MAO-D5	66a	61%
2			MAO-D9		32%
3			6-HDNO		60%
4	65a	Benzyl	MAO-D5	67a	99%
5			MAO-D9		61%
6			6-HDNO		95%
7	65b	Isovaleryl	MAO-D5	67b	99%
8			MAO-D9		54%
9			6-HDNO		96%
10	65c		MAO-D5	67c	99%
11			MAO-D9		57%
12			6-HDNO		94%

^aFreeze-dried *E.coli* whole cells were used. ^bConversion values were measured by GC-MS.

The phenyl-pyrroline **64a** was converted into pyrrole **66a** by MAO-D5 and 6-HDNO (*entry 1* and *entry 3*) in good amount (61%), whilst the variant D9 led to **66a** in only 32% conversion (*entry 2*). Full conversion of *N*-benzylpyrroline **65a**, *N*-isovaleryl pyrroline **65b** and *N*-methylcyclohexyl-pyrroline **65c** in the corresponding pyrroles **67a-c** were observed with MAO D5 (99%) (*entry 4-7-10*), while 6-HDNO converted the substrates for the 94-96% in the corresponding pyrroles (*entry 6-9-12*). On the other hand, MAO-D9 proved to be the less active enzyme toward the substrates affording pyrroles in medium conversions (32%-61%).

3.3.1.2. Synthesis of additional substrates for biocatalysis.

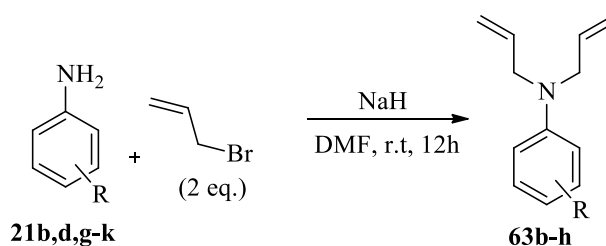
In order to assess the versatility of the MAO-N catalysed aromatization reaction of 3-pyrrolines in pyrroles a small set of substrates was synthesised. First, a small library of aryl 3-pyrrolines bearing various substituents in the phenyl ring was obtained starting from appropriately substituted anilines, following the retrosynthetic approach shown in Scheme 30.



Scheme 30. Retrosynthetic approach for the synthesis of pyrrolines **A**.

The retrosynthetic plan shows how 3-pyrrolines **A** can be obtained from a RCM reaction on appropriately substituted diallylanilines **B**. Aryl and alkyl substituents were inserted as R_1 and R_2 in the scaffold of **B** by alkylation of *N*-allyl-anilines **C** with appropriately substituted allyl halides. Finally, allylanilines **C** were obtained from appropriately decorated anilines **D** by alkylation with allyl-bromide. Accordingly to the retrosynthetic approach proposed in Scheme 30, a set of *N*-diallylanilines **63b-h** bearing various substituents on the phenyl ring, was synthesised from allyl-bromide and commercially available anilines **21b**, **21d** and **21g-k** (namely, 4-F-aniline **21b**, 4-*i*-Br-aniline **21d**, 4-Pr-aniline **21g**, 4-OMe-aniline **21h**, 2-5-Me-aniline **21i**, 4-NO₂-aniline **21j**, 4-CN-aniline **21k**). *N*-diallylanilines **63b-h** were isolated with excellent to good yields as reported in Table 22.

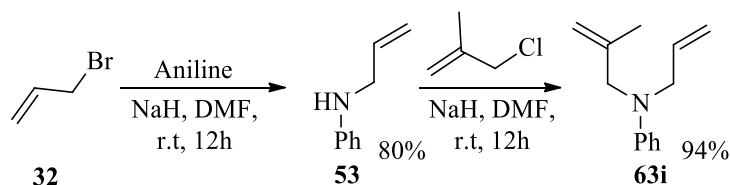
Table 22. Synthesis of *N*-allylanilines **63b-h**.



Aniline	R	Diallylaniline	Yield% ^a
21b	4-F	63b	93%
21d	4-Br	63c	86%
21g	4- <i>i</i> Pr	63d	94%
21h	4-OMe	63e	79%
21i	2-5-Me	63f	92%
21j	4-NO ₂	63g	92%
21k	4-CN	63h	92%

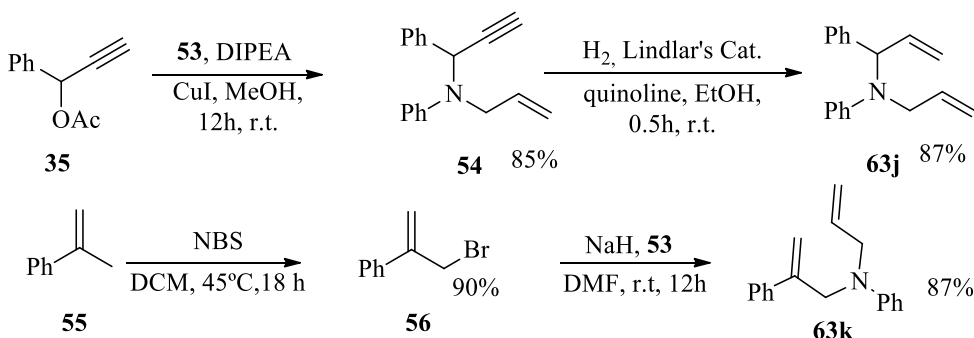
^aIsolated yields were reported.

A second set of *N*-diallylanilines **63i-k** was synthesised in order to obtain, according to the retrosynthetic approach proposed previously, a set of di-substituted pyrrolines. This set aim is to explore the affinity of MAO biocatalysts toward 3-pyrrolines bearing groups on various position of the five-member ring. Compound **63i** was obtained according to Scheme 31.



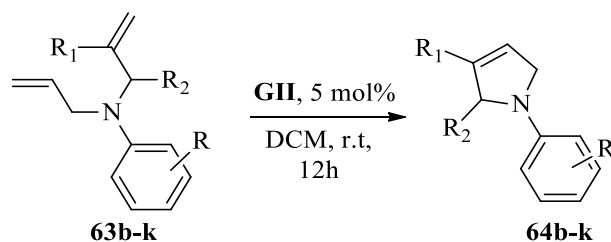
Scheme 31. Synthesis of compound **63i**.

In detail, aniline was mono alkylated affording *N*-allylaniline **53** which was then reacted with 3-chloro-2-methylprop-1-ene and NaH obtaining compound **63i** with 94% yield. Moreover, the synthesis of *N*-diallylanilines **63j** and **63k** was accomplished as described in Scheme 32.



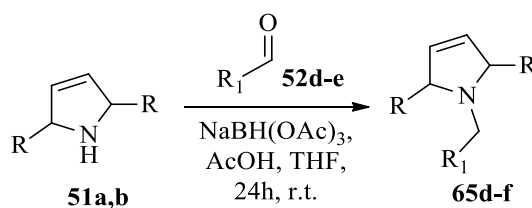
Scheme 32. Synthesis of compounds **63j** and **63k**.

1-Phenylprop-2-yn-1-yl acetate **35** (obtained as previously described in Scheme 18) was converted into the propargyl aniline **54** through a copper mediated amination reaction with *N*-allylaniline **53** (90%).¹⁷⁶ Then, compound **54** was reduced to the desired compound **63j** through hydrogenation reaction catalysed with Lindlar's catalyst and quinoline in order to prevent over reduction of the allyl groups to alkane. On the other hand, compound **63k** was synthesised by alkylation of *N*-allylaniline **53** with the bromide **56**. Compound **56** was obtained, according to the procedure reported in literature, by NBS promoted bromination reaction on α -methylstyrene **55**.¹⁹⁵ Finally the diallylanilines **63b-k** were converted into the corresponding 3-pyrrolines **64b-k** via RCM reaction catalysed by **GII** in DCM. (Table 23).

Table 23. Synthesis of aryl 3-pyrroline **64b-k**.

Cmpd	R	R ₁	R ₂	Pyrroline	Yield%
63b	4-F	H	H	64b	75%
63c	4-Br	H	H	64c	75%
63d	4- <i>i</i> Pr	H	H	64d	79%
63e	4-OMe	H	H	64e	79%
63f	2-5-Me	H	H	64f	79%
63g	4-NO ₂	H	H	64g	80%
63h	4-CN	H	H	64h	79%
63i	H	Me	H	64i	79%
63j	H	H	Ph	64j	65%
63k	H	Ph	H	64k	70%

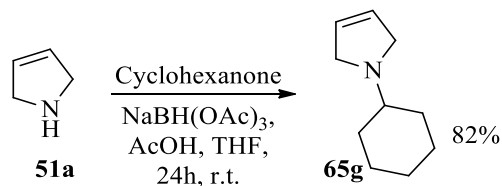
Then, a set of *N*-alkyl 3-pyrrolines **65d-m** were synthesised in order to study how different substituents on the pyrroline nitrogen and steric factors could influence the reactivity toward the MAO biocatalysts. A first set of *N*-alkyl 3-pyrrolines **65d-f** was obtained from commercially available 3-pyrroline **51a** or 2,5-methyl-3-pyrroline **51b** via reductive amination reaction as described in Table 24.

Table 24. Synthesis of pyrrolines **65d-f**.

Cmpd	R	R ₁	Pyrroline	Yield% ^a
51a	H	4-Cl-C ₆ H ₄	65d	76%
51b	Me	Cyclohexyl	65e^b	52%
51b	Me	4-Cl-C ₆ H ₄	65f^b	46% ^b

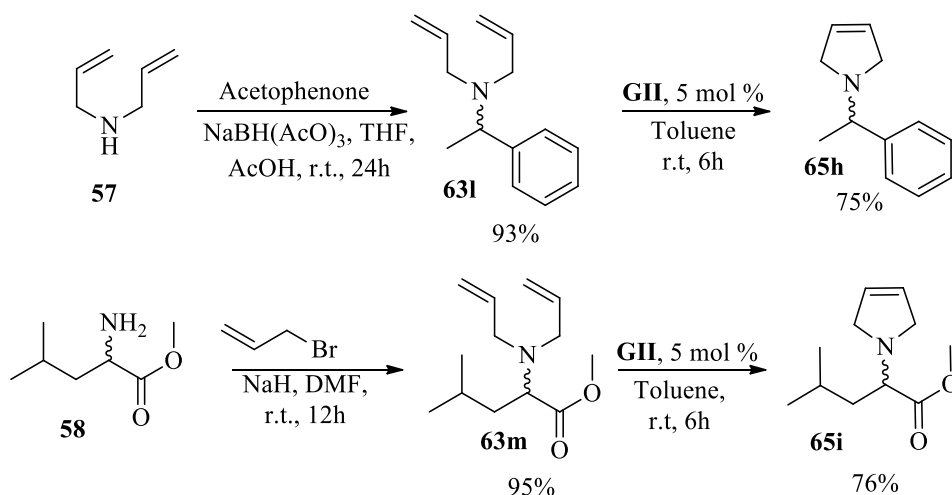
^aIsolated yields, ^bmixture of *cis* and *trans*.

Moreover, pyrroline **65g** was obtained from 3-pyrroline **51a** and cyclohexanone under reductive amination conditions affording the desired compound with 82% yield (Scheme 33).



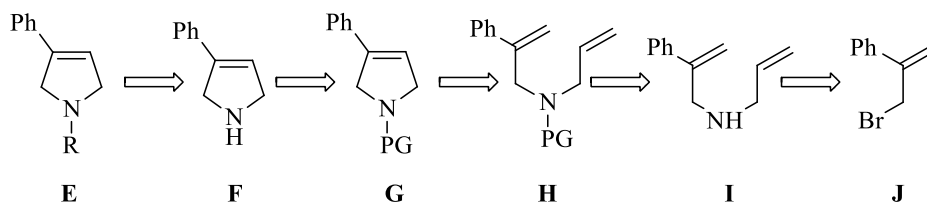
Scheme 33. Synthesis of pyrroline **65g**.

Furthermore, *N*-alkyl 3-pyrroline **65h,i** were synthesised, as reported in Scheme 33, in order to understand if the MAO-N biocatalyst aromatization reaction could occur in pyrrolines bearing branched or bulky alkyl substituents. In detail, *N*-diallylamine **57** was converted into **63l** through reductive amination reaction with acetophenone and the weak reducing agent NaBH(AcO)₃. Then, compound **63l** afforded pyrroline **65h** with 75% yield via RCM reaction. In addition, racemic mixture of leucine methyl ester **58** was reacted with allylbromide and NaH in DMF affording *N*-diallylamine **63m** in excellent yield. Then **65i** was obtained from compound **63m** via RCM reaction.



Scheme 34. Synthesis of pyrrolines **65h** and **65i**.

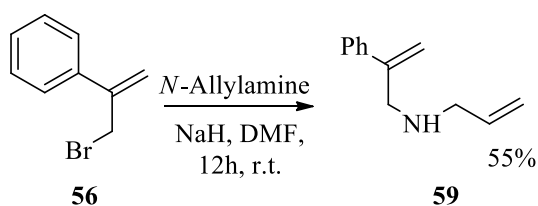
Finally, a retrosynthetic approach for the synthesis of 3-phenyl-1-alkyl-3 pyrrolines **65j-k** was planned (Scheme 35).



Scheme 35. Retrosynthetic approach for 3-pyrroline **65j-k**.

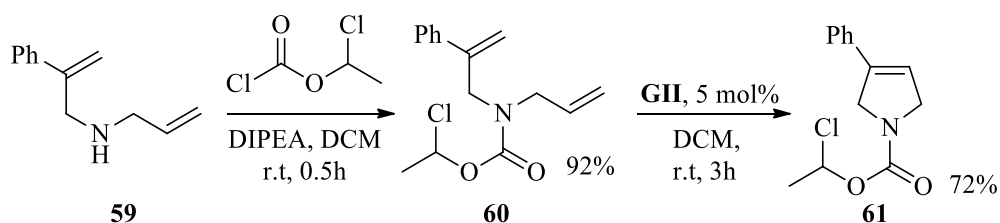
Target pyrrolines **65** (**E**) could be obtained from the *N*-unsubstituted pyrroline **F** via reductive amination reaction with appropriate carbonyl compounds. **F** is the result of protective group de-protection of the pyrroline **G** which can be achieved by RCM reaction on the *N*-protected diallylamine **H**. This latter is obtained after protection of the aminic nitrogen of **I** which is the result of alkylation reaction between **J** (compound **56**) and *N*-allylamine.

Following the retrosynthetic approach proposed, compound **56** was reacted with an excess of *N*-allylamine and NaH in order to obtain *N*-diallylamine **59** (Scheme 36).



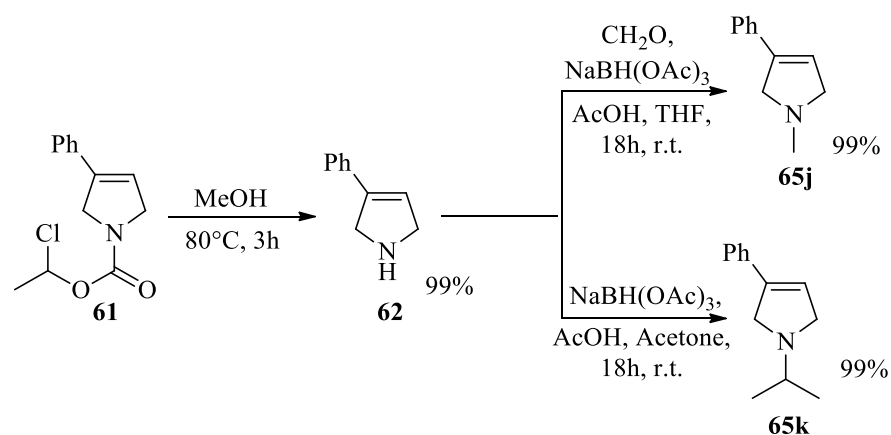
Scheme 36. Synthesis of *N*-diallylamine **59**.

Compound **59**, was then *N*-protected with 1-chloroethyl chloroformate and *N,N*-diisopropylethylamine (DIPEA) in DCM affording the carbamate **60** in excellent yield (92%). Then the carbamate **60** underwent RCM reaction yielding **61** with 72% yield. (Scheme 37).



Scheme 37. Synthesis of compound **61**.

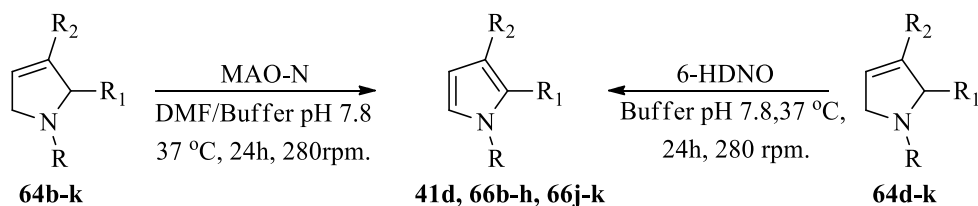
The amine **59** is protected as a chloroethyl carbamate for a dual reason. Firstly, protection of the nitrogen is necessary to overcome the well-known poor reactivity of secondary unprotected amines toward RCM reactions.¹⁹⁶ This is due to the inactivation of **GII** which forms stable complexes with the amine and thus prevents the RCM reaction to occur.¹⁷¹ The second reason is that chloroethyl carbamate **61** quickly hydrolyses when dissolved in a protic solvent, such as MeOH, affording 3-pyrroline **62** in quantitative yield and short reaction times. Finally, *N*-substituted pyrrolines **65j** and **65k** were obtained by reductive amination reaction of **62** with formaldehyde and acetone, respectively, as described in Scheme 38.



Scheme 38. Synthesis of pyrrolines **62**, **65j** and **65k**.

3.3.1.3. MAO-N and 6-HDNO catalysed aromatization of 1-aryl-3-pyrrolines into 1-aryl-pyrroles.

The 1-aryl-3-pyrrolines **64b-k** were converted into pyrroles **41d**, **66b-h** and **66j-k** with very poor to excellent yields depending on the substituents on the pyrroline ring and on the substituents on the *N*-aryl group (Table 25).

Table 25. MAO-N and 6-HDNO aromatization of pyrrolines **64b-k**.

3-pyrroline	R	R ₁	R ₂	Biocat. ^a	pyrrole	Conv (%) ^b
64b	4-F-C ₆ H ₄	H	H	MAO-D5	66b	60
64c	4-Br-C ₆ H ₄	H	H	MAO-D5	66c	40
64d	4- <i>i</i> Pr-C ₆ H ₄	H	H	MAO-D5	66d	>99
		H	H	MAO-D9		50
		H	H	6-HDNO		27
64e	4-MeO-C ₆ H ₄	H	H	MAO-D5	66e	82
				MAO-D9		54
				6-HDNO		21
64f	2,5-Me-C ₆ H ₃	H	H	MAO-D5	66f	45
				MAO-D9		34
				6-HDNO		30
64g	4-NO ₂ -C ₆ H ₄	H	H	MAO-D5	66g	2
				MAO-D9		2
				6-HDNO		1
64h	4-CN-C ₆ H ₄	H	H	MAO-D5	66h	2
				MAO-D9		2
				6-HDNO		1
64i	Ph	H	Me	MAO-D5	41d	>99
				MAO-D9		51
				6-HDNO		55
64j	Ph	Ph	H	MAO-D5	66j	0
				MAO-D9		0
				6-HDNO		0
64k	Ph	H	Ph	MAO-D5	66k	0
				MAO-D9		0
				6-HDNO		0

^aFreeze-dried *E.coli* whole cells were used. ^bConversion values were measure by ¹H-NMR spectroscopy.

As described previously in Table 21, pyrroline **64a** was partially converted into the pyrrole **66a** by MAO-D5 (61%). In Table 25 is shown that pyrrolines **64b** and **64c**, bearing an halogen atom in *para* position of the phenyl ring, when reacted with MAO-D5, afforded respectively pyrrole **66b** and **66c** with medium conversion values (60%, 40%). On the other hand, full conversion (>99%) of pyrrolines **64d** and the 3-methyl-substituted **64i** was observed with MAO-D5, while D9 and 6-HDNO converted only moderately the substrates in the corresponding pyrroles. A similar trend was observed also for pyrrolines **64e** and **64f**, which were converted respectively in pyrrole **66e** and **66f** in 82% and 45%, while the variant D9 and 6-HDNO led to the corresponding pyrroles in less amount. On the contrary, substrates **64g** and **64h** bearing an electron withdrawing group on the aromatic ring (-NO₂ and -CN, respectively) were not converted into corresponding pyrroles. Despite the exact mechanism of action of MAO has not fully elucidated, as mentioned in paragraph 3.3, one of the proposed models suggests that the oxidation of amines proceeds through a nucleophilic mechanism where the amine attacks the FAD by nucleophilic addition and it is in turn oxidised to imine leading to the formation of the reduced FADH₂.^{197,198} Thus, it is likely that the electron withdrawing substituents on the phenyl ring of **64g** and **64h** reduce the electronic density and consequently the nucleophilicity of the pyrroline nitrogen, thus preventing the attack of **64g,h** to FAD and their following oxidation into pyrroles. Furthermore, no conversion of the pyrrolines **64j-k** into the corresponding pyrroles **66j-k** bearing a phenyl substituent at C2 and C3 respectively was observed for all the set of enzymes. As shown by docking simulations carried out by collaborators at King's College London, steric factors prevented **64j-k** to enter into the catalytic site of MAO-D5 (Figure 28). The docking simulations purpose was to show the interaction of 1-phenyl-3-pyrrolines **64a** and **64k** within the catalytic site of MAO-D5 and explain the experimental data observed. The substrates **64a** and **64k** were docked into MAO-N-D5 (PDB: 2VVM)¹⁹⁹ with the PLANTS 1.2 software²⁰⁰ using the ChemPLP²⁰¹ scoring function. In the docking pose both **64a** and **64k** orient their pyrroline group over the tricyclic system of FAD, while the *N*-phenyl ring interacts with the highly lipophilic region below. The pocket is formed by the residues W94, F210, C214, W230, L231, L245, M246, F382, W430, S465 and F466. The approximate shape is that of an inverted cone with a base of about 6Å in diameter departing from the polycyclic portion of FAD and terminating with F210 with a height of about 10Å. Docking simulations predict a close contact between the pyrroline ring and FAD for molecules such as **64a** that bear on the heterocycle an hydrophobic substituent of the size of a phenyl ring and have no or only small additional substituents. However, docking simulations were able to suggest that the size of the active site strongly influences the

reactivity of certain, bigger, molecules such as **64k**. Whilst **64a** fits within the catalytic site of MAO-D5, the phenyl substituent (in yellow, Figure 28) of the bulkier **64k** lays in a region of the catalytic site where an aminoacidic residue is located, thus preventing **64k** from entering the enzyme's active site and being aromatized. Thus, it is plausible to hypothesise that the nonconversion of **64k** and **64j** is due to steric factors that prevent entering of the compound into the active site

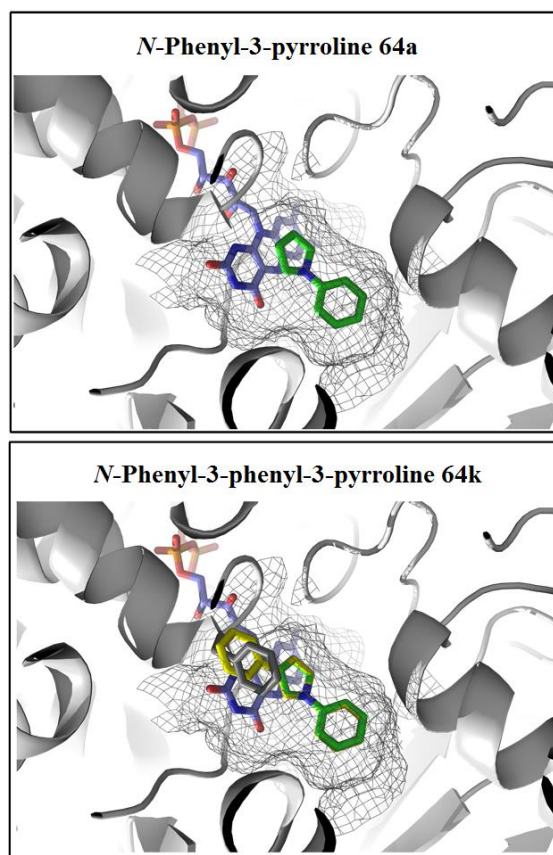
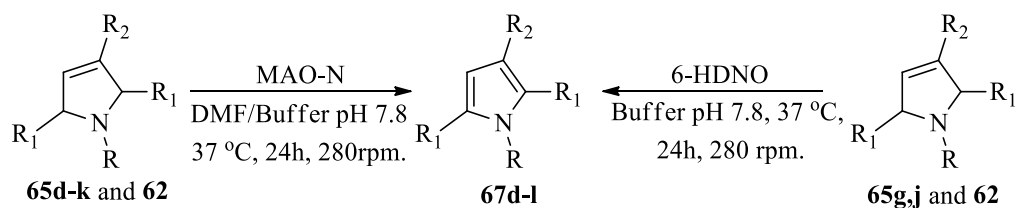


Figure 28. Docking of pyrroline **64a** into the MAO-D5 catalytic site and superposition of **64k** on the predicted conformation of **64a**.

3.3.1.4. MAO-N and 6-HDNO catalysed aromatization of 1-alkyl-3-pyrrolines in 1-alkyl-pyrroles.

1-Alkyl-3-pyrrolines **65d-k**, and 3-pyrroline **62** were treated with MAO-N and 6-HDNO biocatalyst as shown in Table 26. After a practical analysis of the conversion values obtained by the biotransformations shown in paragraph 3.3.1.1., MAO-D5 biocatalyst was chosen as the key enzyme for the next set of biotransformations.

Table 26. MAO-N and 6-HDNO catalyse aromatization of pyrrolines **65d-k** and **62** into pyrroles **67d-l**.



3-Pyr.	R	R ₁	R ₂	Biocat. ^a	Pyrrole	Conv (%) ^b
65d	4-Cl-Bn	H	H	MAO-D5	67d	88
65e		Me	H	MAO-D5 MAO-D9	67e	48 32
65f	4-Cl-Bn	Me	H	MAO-D5 MAO-D9	67f	51 33
65g		H	H	MAO-D5 MAO-D9 6-HDNO	67g	>99 51 65
65h		H	H	MAO-D5	67h	>99
65i		H	H	MAO-D5	67i	56
65j	Me	H	Ph	MAO-D5 MAO-D9 6-HDNO	67j	92 78 87
65k	<i>i</i> Pr	H	Ph	MAO-D5 MAO-D9	67k	31 0
62	H	H	Ph	MAO-D5 MAO-D9 6-HDNO	67l	33 57 10

^aFreeze-dried *E.coli* whole cells were used. ^cConversion values were measured by ¹H-NMR spectroscopy.

As further confirmation that the oxidation of amines with MAO-D5 proceeds through a nucleophilic mechanism, the more nucleophilic alkyl pyrrolines **65d**, **65g**, **65h** were fully converted (88%, >99% and >99%, respectively) by MAO-D5. **65g** undergoes partial oxidation when treated with MAO-D9 and 6-HDNO (51% and 65%, respectively). Furthermore, the nicotine oxidase 6-HDNO was able to oxidise pyrroline **65j** (87%) while lower conversion (10%) was observed for the secondary amine **62**. Pyrroline **65i** bearing a bulky substituent on the nitrogen was oxidised in low yields as well as the pyrrolines **65e-f** bearing two methyl substituents on the heterocyclic nucleus (48-51%). Finally, when the biotransformation was carried out with MAO-D5 and MAO-D9 both the amine **65k** and the secondary pyrroline **62** were poorly converted respectively into the pyrroles **67k** and **67l**. On the contrary, excellent conversion values were observed for the tertiary pyrroline **65j** (Figure 29).

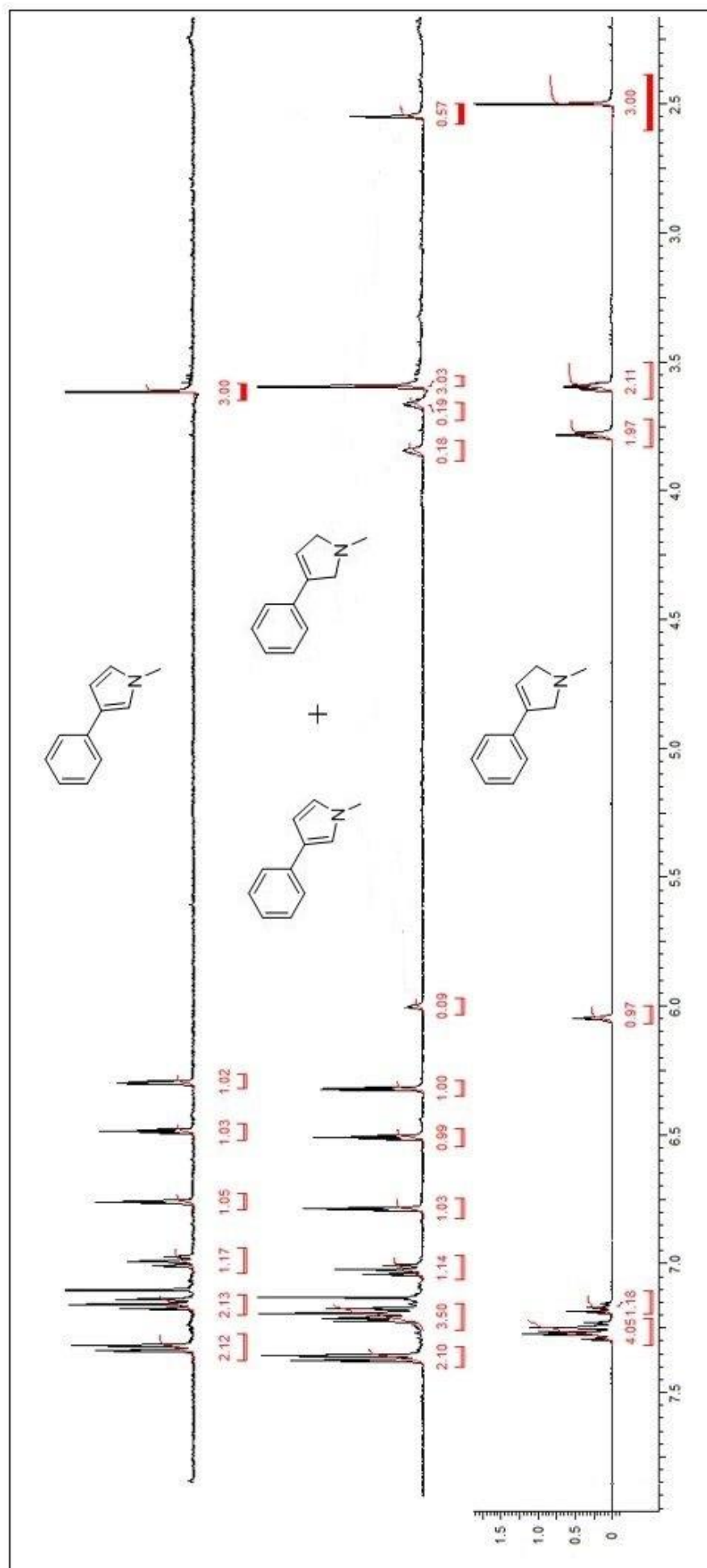
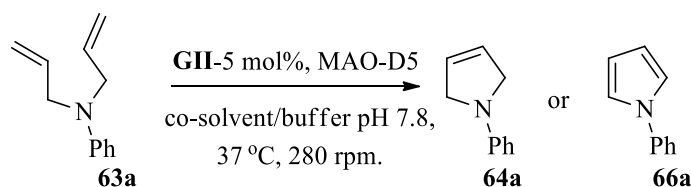


Figure 29. Conversion of pyrroline **65j** in pyrrole **67j** monitored by ^1H -NMR analysis of the crude of reaction.

3.3.1.5. Development and Optimization of chemo-enzymatic cascade.

The combination of RCM reactions with MAO biocatalysts in the same reaction medium was then investigated with the aim to develop a chemo-enzymatic cascade synthesis of pyrroles from allyl-amines/anilines as shown in Table 27. MAO-D5 was selected for the detection of the best reaction conditions because it was the enzyme that showed the best ability to oxidize aryl and alkyl 3-pyrrolines (paragraph 3.3.1.3., paragraph 3.3.1.4). Furthermore, the diallylamine **63a** was chosen as reference for the development of the chemo-enzymatic cascade because it undergoes easily RCM under standard conditions, and showed good conversion with MAO-D5 as shown in Table 21. **Table 27.** Study of the best reaction conditions.



Entry	Co-Solvent	Buffer/Cosolvent	Ratio 63a/64a/66a (%) ^a
1	DMF	60:1	90/10/0
2	Acetone	60:1	10/90/0
3	-	100:0	5/95/0
4	DMF	4:1	77/23/0
5	DMSO	4:1	73/27/0
6	THF	4:1	92/8/0
7	DCM	4:1	75/25/0
8	Toluene	4:1	53/47/0
9	Hexane	4:1	100/0/0
10	EtOAc	4:1	100/0/0
11	Et ₂ O	4:1	100/0/0
12	<i>Iso</i> -octane	4:1	0/12/88

^aConversion values were measured by ¹H-NMR.

The diallylaniline **63a** was first dissolved in a 1:60 DMF/ phosphate buffer pH=7.8 1 M solution and treated simultaneously with 5 mol% **GII** and MAO-D5 at 37 °C. Unfortunately aniline **63a** was recovered from the reaction mixture after 24h and only 10% of 3-pyrroline

64a was obtained, whilst no traces of the pyrrole **66a** were detected by ¹H-NMR analysis of the crude of reaction (*entry 1*). A set of experiments were carried out in order to evaluate the influence of the co-solvent toward the reaction outcome with the aim to make the RCM reaction possible in the same medium of the MAO catalysed oxidation reaction. Acetone was selected in *entry 2*, because it is reported that it is a more suitable solvent for RCM reactions than DMF.²⁰² In fact, when the same biotransformation was performed in 1:60 acetone/buffer mixture, 90% of **64a** was recovered. However, no traces of **66a** were observed in the reaction mixture. It is noteworthy that, when the reaction was carried out (*entry 3*), in absence of co-solvent pyrroline **64a** was obtained in 95% but no oxidation to **66a** occurred. Increasing the co-solvent/buffer ratio to 1:4 (*entry 4*) and using different water-miscible co-solvents (THF and DMSO) (*entries 5 and 6*) did not affect the outcome of the biotransformation. In all cases, variable amounts of the RCM product **64a** were detected but no traces of the desired pyrrole **66a** were obtained. Previous work of Turner and coworkers showed that MAO biocatalysts generally suffer the co-presence of chemo-catalysts in the same reaction medium.¹⁶⁰ In order to avoid the interaction between the Ru catalyst and the enzyme, the possibility to perform the reaction in a biphasic system was investigated. When the reaction was carried out with not-water-miscible-solvents (*entry 7-11*) no RCM reaction occurred, except when toluene or DCM or *iso*-octane were used as co-solvent. However, even in these cases (*entry 7-8*), only variable amount of **64a** and no traces of pyrrole **66a** were detected from the reaction mixture. Recently Zhao *et al.*, showed that *iso*-octane can work as an excellent co-solvent in chemo-enzymatic biotransformations, due to its ability to form a biphasic system with low mass transfer together with the buffer solution.^{203–205} When the chemo-enzymatic reaction was carried out in an *iso*-octane/buffer 1:4 mixture (*entry 12*), the pyrrole **64a** was highly converted (88%) in the corresponding pyrrole **66a** (Figure 30). The use of the non-water miscible co-solvent *iso*-octane proved to be crucial to prevent the interaction between the Ru-catalyst and the MAO-D5 and avoid the deactivation of the enzyme due to the Ru binding. In fact, in an immiscible *iso*-octane-buffer mixture, the homogeneous Ru-catalyst is portioned in the organic phase, while the biocatalyst is suspended in water. The diene **63a** undergoes RCM reaction affording the 3-pyrroline **64a** in the *iso*-octane phase, and then, **64a** is oxidised by MAO-D5 leading to the desired pyrrole **66a**. The biphasic reaction medium acts mimicking the compartmentalization of cellular processes allowing thus the cascade reactions to take place in an efficient manner.

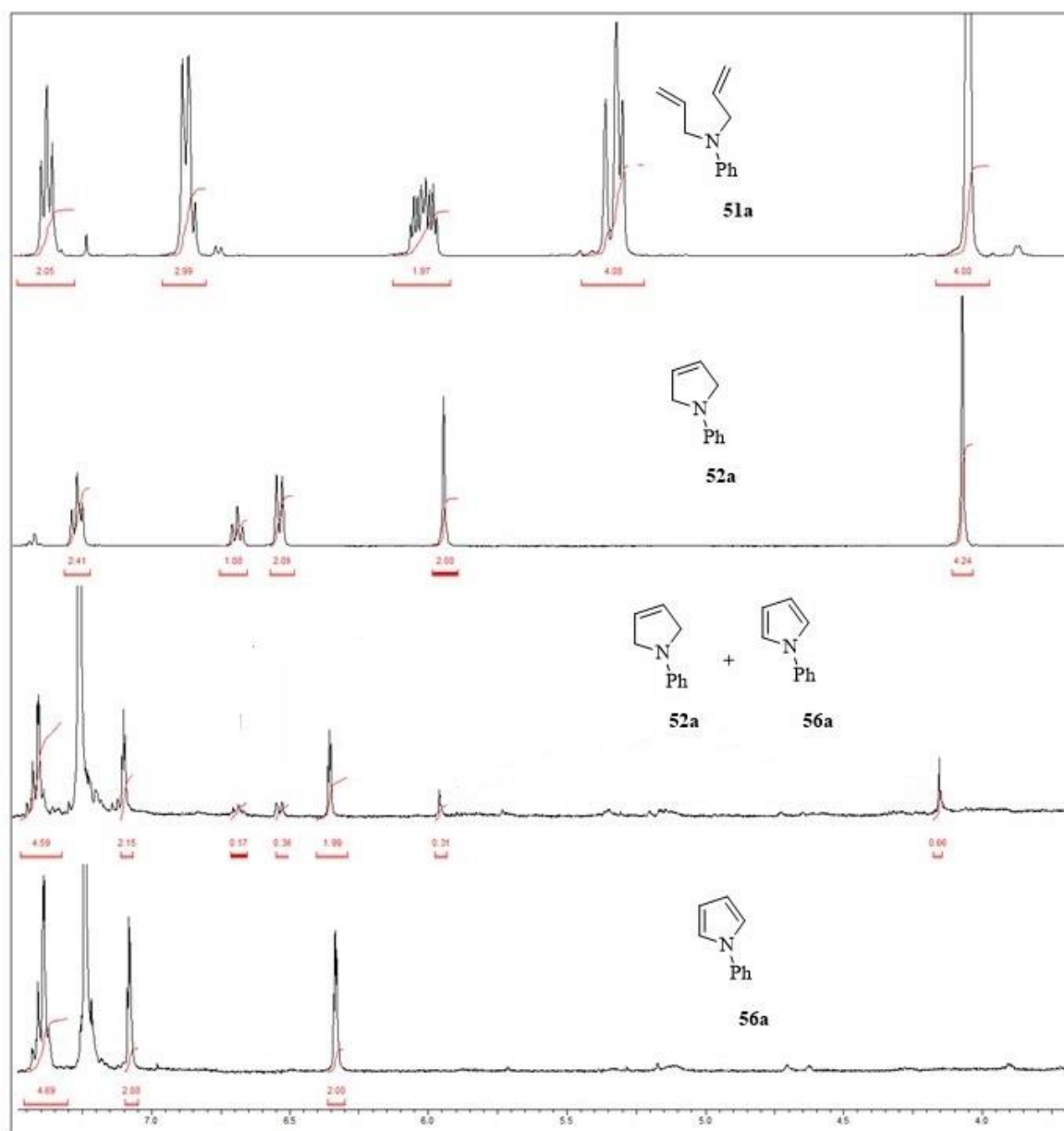


Figure 30. Analysis of the chemo-enzymatic reaction of **63a** with MAO-D5 affording **66a**. ¹H-NMR analysis of diallylaniline **63a**, 3-pyrroline **64a**, crude of reaction with MAO-D5 and *N*-phenyl pyrrole **66a**.

3.3.1.6. Expanding the scope of the RCM-MAO cascade reaction.

In order to enhance the structural diversity of the small library of substrates obtained so far, a second set of *N*-diallylanilines/amines **63n-r** were synthesised as shown in Table 28.

Table 28. Synthesis of *N*-diallylanilines/amines **63n-r**

21a and 21l-n	63n-q	57
diallylaniline/amine	R	Yield %^a
63n	4-Cl-C ₆ H ₄	74%
63o	4-Me-C ₆ H ₄	88%
63p	2-MeO-C ₆ H ₄	88%
63q	3,4-(OCH ₂ O)-C ₆ H ₃	92%
63r	-	97%

^aIsolated yield.

In detail, allylbromide was reacted with opportunely substituted anilines (namely **21a** 4-Cl-aniline, **21l** 4-Me-aniline, **21m**, 2-MeO-aniline and **21n** benzo[d][1,3]dioxol-5-amine,) affording *N*-diallylanilines **63n-q** with good to excellent yields (74%-92%). Differently, compound **63r** was obtained through the reductive amination reaction from *N,N*-diallylamine **57** and benzaldehyde with the presence of the mild reducing agent NaBH(AcO)₃.

Then the scope of the chemo-enzymatic reaction has been explored as shown in Table 29. *N,N*-diallylamines/anilines **63a-f**, **63i**, and **63l-o** and **63r** were reacted in a 1:4 *iso*-octane/Buffer pH=7.8 mixture and treated simultaneously with 5 mol% **GII** and MAO-D5 at 37 °C (method A). Furthermore, a two steps method was also set up, (method B) with the aim to improve the conversion in pyrroles of the substrates. In method B, the substrates were reacted with **GII** and MAO-D5 and stirred at 37 °C for 6 h, after which time an additional amount of MAO-D5 was added.

Table 29. Chemo-enzymatic cascade of *N*-diallylanilines- substrate scope.

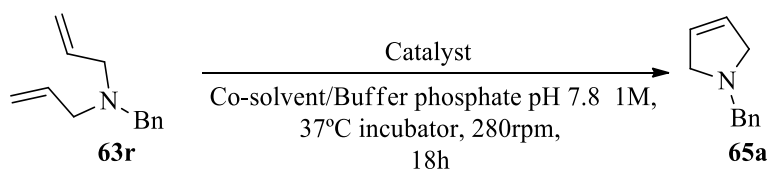
Method A				Method B		
<p>63a-f, 63i, 63l-o and 63r</p> <p>41d, 66a-f, 66l-o and 67a</p>				<p>63a-f, 63i, 63l-o and 63r</p> <p>41d, 66a-f, 66l-o and 67a</p>		
Entry	R	R ₁	Pyrrole	Conv. (%) ^a	Yield (%) ^b	Method
1	Ph	H	66a	88	78	A
2	Ph	H	66a	95	65	B
3	4-F-C ₆ H ₄	H	66b	86	63	A
4	4-F-C ₆ H ₄	H	66b	99	59	B
5	4-Br-C ₆ H ₄	H	66c	13	10	A
6	4-Br-C ₆ H ₄	H	66c	15	10	B
7	4- <i>i</i> Pr-C ₆ H ₄	H	66d	35	22	A
8	4- <i>i</i> Pr-C ₆ H ₄	H	66d	75	70	B
9	4-MeO-C ₆ H ₄	H	66e	45	35	A
10	4-MeO-C ₆ H ₄	H	66e	50	42	B
11	2,5-Me-C ₆ H ₄	H	66f	24	19	A
12	2,5-Me-C ₆ H ₄	H	66f	25	20	B
13	Ph	Me	41d	82	45	A
14	Ph	Me	41d	87	64	B
15	4-Cl-C ₆ H ₄	H	66l	73	65	A
16	4-Cl-C ₆ H ₄	H	66l	90	56	B
17	4-Me-C ₆ H ₄	H	66m	99	50	A
18	4-Me-C ₆ H ₄	H	66m	90	45	B
19	2-MeO-C ₆ H ₄	H	66n	94	84	A
20	2-MeO-C ₆ H ₄	H	66n	81	72	B
21	3,4-(OCH ₂ O)-C ₆ H ₃	H	66o	75	51	A
22	3,4-(OCH ₂ O)-C ₆ H ₃ Ph	H	66o	84	57	B
23	Bn	H	67a	9	5	A & B

^aConversion values were measured by ¹H-NMR spectroscopy. ^bIsolated yields

Pyrrole **66a** was obtained in 88% conversion and 78% isolated yield following method A while, higher conversion (95%), but poorer yield (65%) was observed with the one-pot two

steps protocol (*entry 1 and 2*). It is noteworthy that the treatment of **64a** with MAO-D5 led to **66a** with 61% conversion, while the chemo-enzymatic cascade led to **66a** from diallylaniline **63a** in 95% conversion. It is plausible that in the chemo-enzymatic cascade the aniline **63a** is converted into the pyrroline **64a** slowly. As soon as **64a** is formed, it is immediately oxidised by MAO-D5 affording **66a**. In this way only a low amount of **64a** is oxidised by MAO-D5 time by time allowing a more rapid enzyme turnover. Similarly, pyrroles **66b** and **66l** (*entries 3-4, 15-16*) were isolated in high yields when the one-pot one-step method A was used, whilst higher conversion values were observed with the two steps one-pot protocol B. As general trend, excellent conversion and high yields were observed for pyrroles bearing chloro- (**66l**), methyl- (**66m**) and alkoxy-substituents (**66n**, **66o**) (*entries 15-22*). Medium to good conversions (50-75%) were observed for *N*-aryl-pyrroles **66d-e** (*entries 8-10*). One possible explanation of this trend could be found in the lower reactivity of electron-rich *N,N*-diallylanilines toward the RCM reaction. Furthermore, several other factors must be taken into account in the chemo-enzymatic cascade, such as the reactivity of anilines in the metathesis reaction, where electron donating substituents on the phenyl ring disfavour the ring closure, as well as the biocatalytic oxidation, where electron withdrawing substituents prevent the pyrroline oxidation. Not surprisingly, the benzylpyrrole **67a** was obtained in low yield (*entry 23*) due to the poor reactivity of alkyl-diallylamines toward RCM reactions.²⁰⁶

An elegant way to overcome Ru inactivation with tertiary amines is to convert them into the corresponding salts in order to make impossible the attachment of the nucleophilic nitrogen to the Ru catalyst. However, this strategy cannot be chosen with the purpose of this biotransformation because the ammonium salt would be added to the aqueous mixture needed for the biotransformation. The presence of the buffer in the reaction mixture dissolves the ammonium salt affording the corresponding tertiary amine which will be partitioned between the organic phase and the aqueous phase. Thus the dissolution of the ammonium salt in the buffer restores the ability of the lone pair of the amine to poison the metal catalyst. Therefore, a series of experiments were carried out in order to obtain the ring-closing metathesis of *N*-benzyl-diallylamine **63r** in an aqueous environment. A variety of co-solvents and different catalyst loadings were employed in these experiments in order to find an alternative route toward the synthesis of benzylpyrroline **65a**. Furthermore, Hoveyda Grubbs' catalyst (**HGII**) which has been used successfully for metathesis reaction conducted in water was tested as an alternative catalyst of the versatile **GII** (Table 30).^{207,208}

Table 30. Studies on RCM of *N*-benzyl-diene **63r** in aqueous medium.

Entry	Solvent	Catalyst	Catalyst mol%	Buffer/solvent	Conversion %
1	DME	GII	30%	62:1	32%
2	DME	GII	30%	1:1	4%
3	DME	GII	20%	62:1	28%
4	DME	GII	10%	62:1	25%
5	DME	GII	5%	62:1	27%
6	Acetone	GII	30%	62:1	55%
7	Acetone	GII	30%	1:1	56%
8	Acetone	GII	20%	62:1	42%
9	Acetone	GII	10%	62:1	27%
10	Acetone	GII	5%	62:1	22%
11	Acetone	GII	5%	10:1	0%
12	<i>t</i> -BuOH	GII	5%	10:1	1%
13	Toluene	GII	5%	10:1	8%
14	Toluene	GII	30%	62:1	14%
15	Toluene	GII	30%	1:1	11%
16	-	GII	5%	62:1	0%
17	Acetone	HGII	20%	62:1	0%
18	Acetone	HGII	10%	62:1	0 %
19	Acetone	HGII	5%	62:1	0%
20	DME	HGII	20%	62:1	3%
21	DME	HGII	10%	62:1	1%
22	DME	HGII	5%	62:1	1%
23	DME	HGII	5%	4:1	0%
24	Toluene	HGII	5%	4:1	0%

^aConversion values were measured both by GC-MS as well as ¹H-NMR spectroscopy.

When acetone was used as co-solvent the pyrroline **65a** was obtained with 52% yield, however, as described before with *N*-phenyl-*N*-diallylaniline. **63a**, acetone does not prevent the inactivation of the enzyme from the Ru catalyst. On the other hand, the use of Hoveyda-Grubbs catalyst did not lead to any improvement of the reaction and the pyrroline **65a** was obtained only in poor yields. Also the use of different co-solvents like DME (1,2-dimethoxyethane) or toluene in combination with different catalyst loading did not lead to the desired pyrrole **65a**. These results confirmed that tertiary benzyl-amines cannot be used as substrates for the chemo-enzymatic reaction proposed. However, in order to expand the scope of the chemo-enzymatic reaction, conversion of the hindered substrates **63l-m** and the

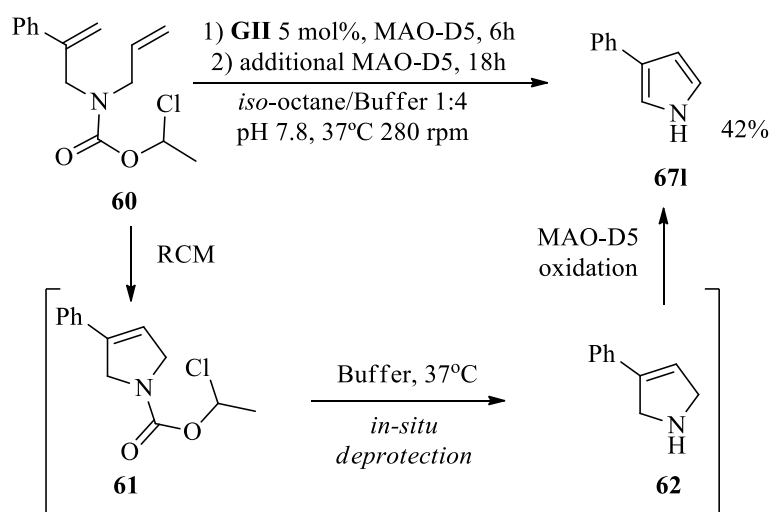
secondary amine **59** was attempted following the one pot-two step procedure (method B) as described in Table 31.

Table 31. Synthesis of pyrroles **67h**, **67i** and **67l**.

Entry	R	R ₁	Pyrrole	Conv.% ^a	Yield% ^b
1		H	67h	63	41
2		H	67i	37	21
3	H	Ph	67l	0	0

^aConversion values were measured by ¹H-NMR spectroscopy. ^bIsolated yields

Diallylamines **63l**, **63m** and the secondary amine **59** were reacted with **GII** and MAO-D5 and stirred at 37 °C for 6 h, after which time an additional amount of MAO-D5 was added. Branched pyrroles **67h** and **67i** were obtained from the corresponding allylamines **63l** and **63m** respectively with 63% and 37% conversion values (*entries 1-2*). These data suggest that branched 1-alkyldiallylamines could be included in the scope of the chemo-enzymatic reaction because the steric hindrance of the *N*-substitution prevent the nitrogen of the amine to poison the catalyst. On the other hand, as expected from previous results obtained with compound **63r**, the attempt to obtain the pyrrole **67l** via chemo-enzymatic cascade from the corresponding secondary amine **59** was unsuccessful (*entry 3*). An alternative route was thus developed as described in Scheme 39 leading to **67l** in one-pot from the carbamate **60**.

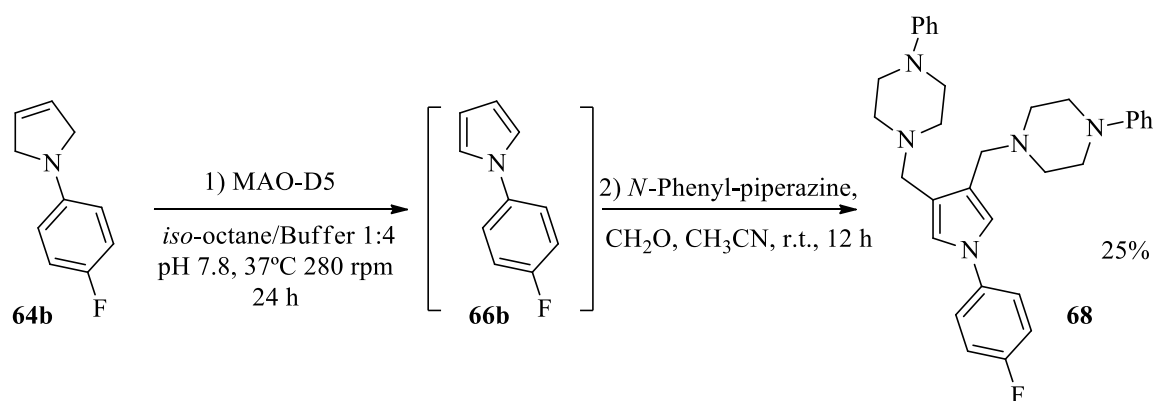


Scheme 39. Chemo-enzymatic synthesis of pyrrole **67l**.

The carbamate protecting group allows the RCM reaction of **60** to take place almost instantaneously (around 20 minutes) affording the intermediate **61**. The chloroethyl carbamate protecting group is labile under the reaction conditions and it is slowly cleaved leading to pyrroline **62** which is in turn oxidised by MAO-D5 affording the desired pyrrole **67I** in 42% overall yield.

3.3.1.7. Application of MAO oxidation/aromatization reaction toward the synthesis of a putative antitubercular pyrrole derivative.

Finally the present methodology has been applied to the synthesis of a pyrrole derivative of the novel class of antitubercular agents described in chapter 2 (Scheme 40).¹¹⁶



Scheme 40. MAO-Mannich cascade for the synthesis of the putative antitubercular agent **68**.

Pyrroline **64b** was converted in a single step into pyrrole **68** by treatment with MAO-D5 followed by in situ Mannich reaction with *N*-phenylpiperazine and formaldehyde. It is noteworthy that compound **68** has not been assessed yet for its antitubercular activity and it shows only moderate structural similarity with the antitubercular agents described in chapter 2. The pyrrole ring is not substituted at C2 and C5 with a methyl group, however the *N*-aryl substitution of the pyrrole and the presence of a substituted piperazine at C3 are common features to all the antitubercular compounds **24**. Therefore, if the antitubercular activity of this compound is confirmed this MAO-Mannich cascade approach would be a faster and greener procedure for the production of pyrroles endowed with antitubercular activity than the methodology used in chapter 2 for the production of BM212/SQ109 hybrid derivatives **24a-m**.

3.3.2. Conclusions

In conclusion, the aromatizing properties of MAO-N and 6-HDNO biocatalysts have been described and explored for the first time. MAO biocatalysts, and in particular the variant MAO-D5, catalyse the aromatization of a wide range of *N*-aryl- and *N*-alkyl-3-pyrrolines into the corresponding pyrroles. The ability of MAO-N biocatalysts to work in a concurrent way together with Grubbs' catalyst was also investigated leading to the development of a chemo-enzymatic cascade reaction for the one pot synthesis of pyrroles from *N,N*-diallylanilines and *N,N*-diallylamines. This work represents the first example of a chemo-enzymatic cascade combining in the same reaction medium MAO-N with a metal-catalyst, other than boron reducing agents. Finally, the aromatizing properties of MAO-D5 have been exploited for the synthesis of pyrrole **68**, which has structural similarity to the novel class of antitubercular compounds described within chapter 2, via a MAO-N-Mannich cascade reaction.

4. Thesis conclusions.

The aim of this doctoral thesis was to discover and synthesise molecules endowed with activity against TB and MDR-TB and to develop novel sustainable and faster synthetic methodologies for the synthesis of heterocycles for the production of drug-like compounds. To address these objectives, in the first section of this work was described the discovery of two novel classes of antitubercular agents, while in the second section, the development of two procedurally simple and fast methodologies for the synthesis of pyrroles were described. Within the first part of this work, two distinct strategies have been applied respectively to the research of two novel classes of antitubercular agents. The first strategy adopted was the molecular simplification approach on the structure of the third line drug thioridazine. Following the modification on the TZ scaffold described in paragraph 2.2, two series of derivatives were synthesised and assessed against a panel of Mycobacteria including clinical isolates. The analysis of the activity data of the set of thioridazine derivatives synthesised allowed the identification of the SAR summarized in Figure 31.

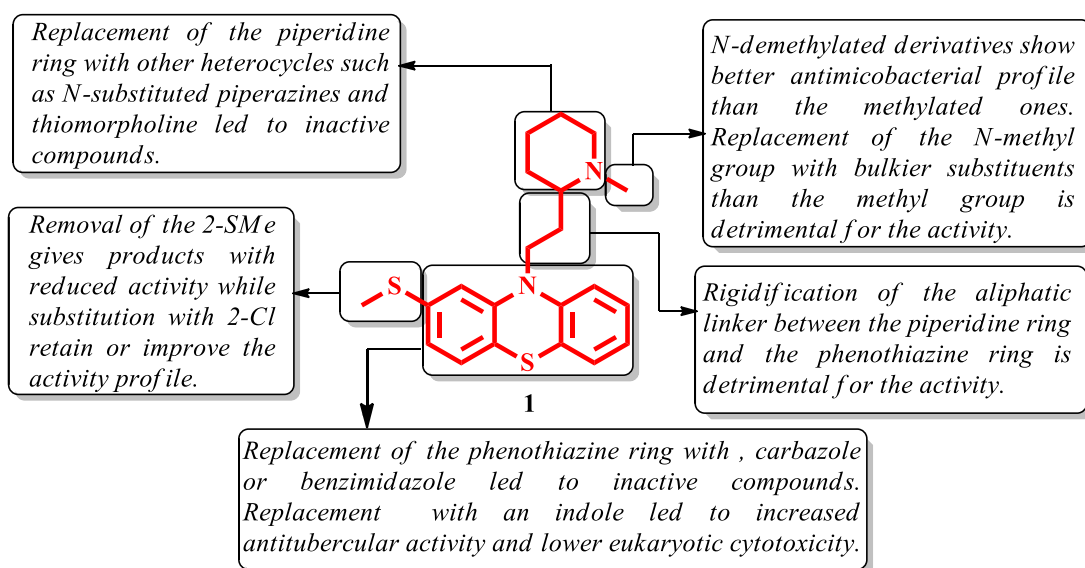


Figure 31. Diagrammatic summary of structure activity relationship of **1** derivatives.

The screening of TZ derivatives led to the identification of compound **16e**: a thioridazine derivative obtained by the demethylation of the piperidine ring in addition to the replacement of the phenothiazine core with an indole heterocycle (Figure 32). **16e** showed an activity profile better than that of TZ and a cytotoxicity about 15-fold lower toward both the cells lines MRC-5 and J774A.1. Despite the molecular target of this new class of molecules being still elusive, and the construction of a pharmacophoric model is still challenging to be formulated, the identification of **16e** opened a new field of research indeed. The future

synthesis of putative **16e** derivatives have the potential to lead to the identification of a novel class of potent antitubercular compounds and to increase the understanding on the mechanism of action of this new class of molecules.

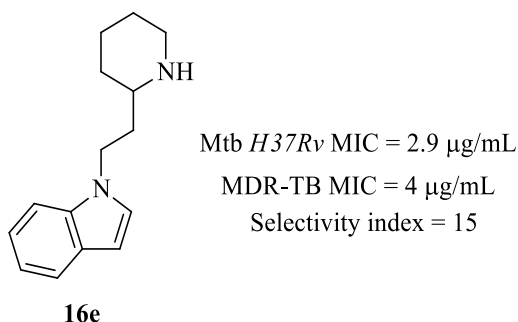


Figure 32. Thioridazine derivative **16e** and its activity profile.

In the second part of the first section of this work, a novel class of molecules, active against Mtb and MDR-TB, has been designed by the application of a molecular hybridization approach on the structures of the antitubercular agents BM212 (**I**) and SQ109 (**II**). The molecules synthesised have been evaluated for their activity against Mtb and MDR-TB clinical isolates leading to the identification of exhaustive SAR, which suggested the key features paramount for the antitubercular activity of this new class of pyrroles (Figure 33).

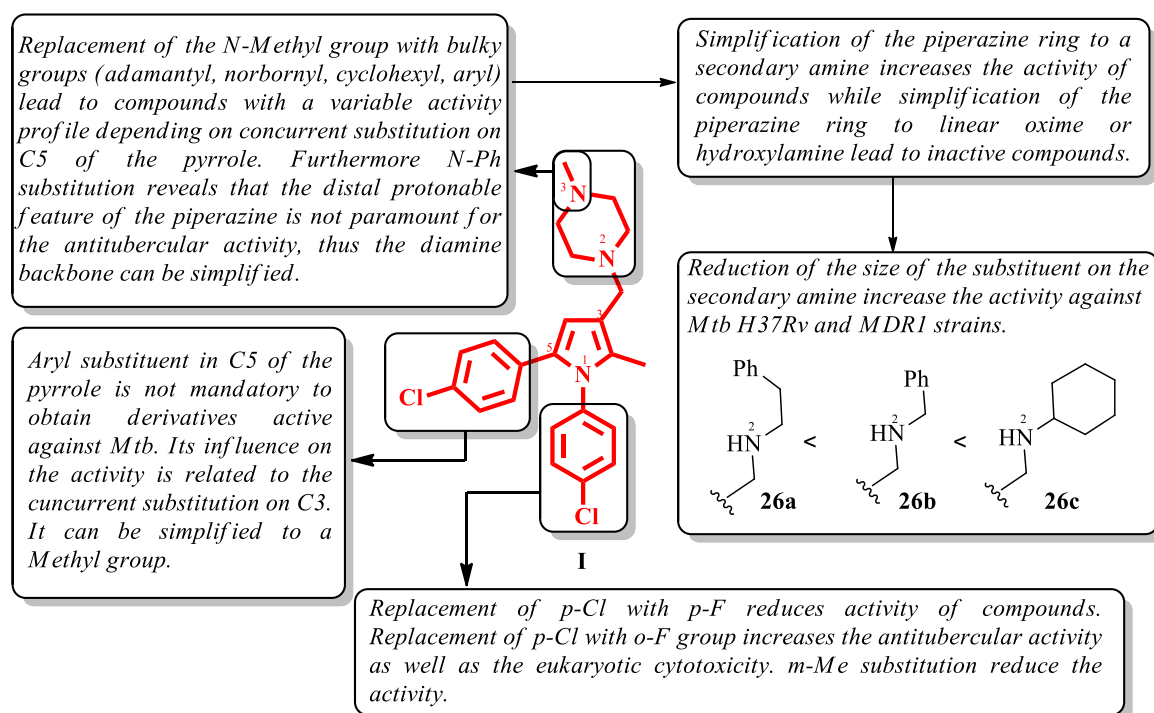


Figure 33. Diagrammatic summary of structure activity relationship of the hybrid derivatives of BM212 (**I**) and SQ109 (**II**).

Five compounds showed MIC values on Mtb *H37Rv* at ≤ 1.0 $\mu\text{g/mL}$, and two of them (**26b** and **26c**) proved to be highly active also against MDR-TB strains (Figure 34).

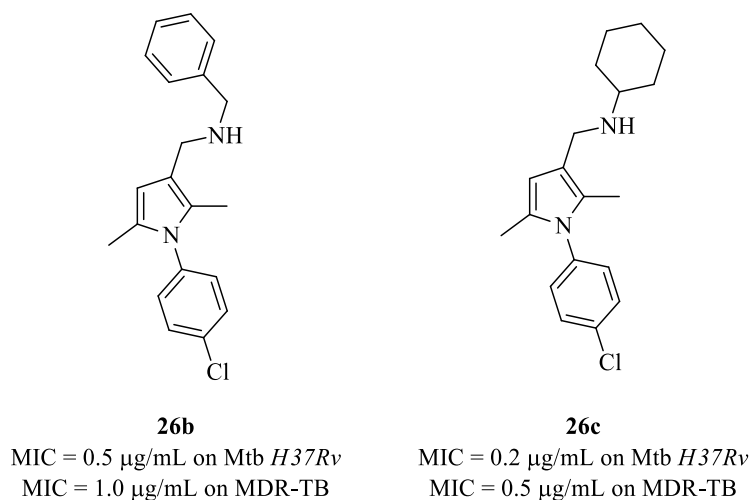
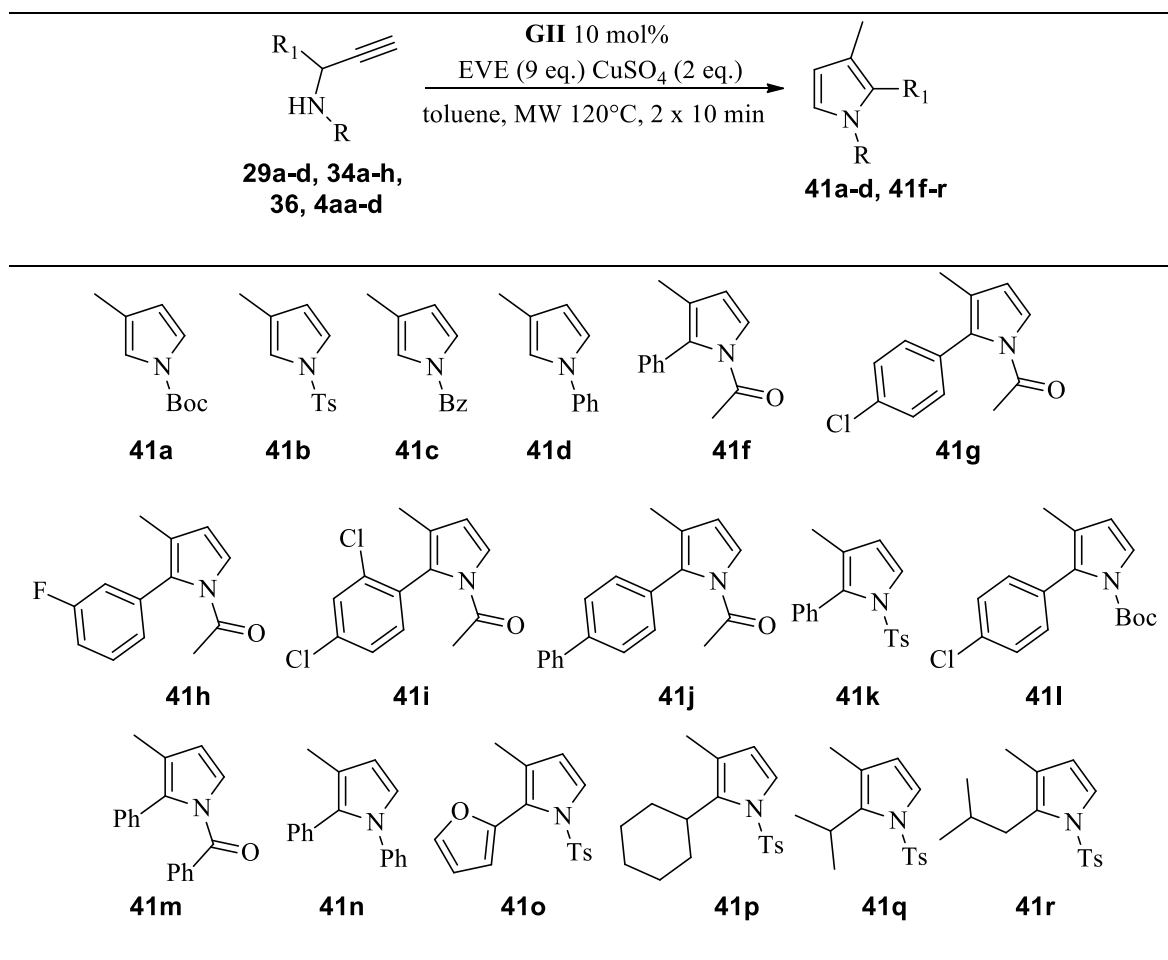


Figure 34. Superimposition of BM212 and SQ109 led to the discovery of hybrid derivatives **26b** and **26c**.

Among the compounds which had the better antitubercular profile, **26c** showed the best drug profile proving to be superior to BM212 in terms of activity, cytotoxicity, and potency toward MDR-TB clinical isolates, thus turning out to be an excellent lead candidate for preclinical trials. Moreover, compounds **24c**, **24h**, **24i**, and **24l**, bearing a bulky alkyl substituent on the piperazine ring, showed potent EPI activity, comparable to that of verapamil, turning out to be promising multi-drug resistance reversal agents.

Furthermore, the second section of this work was dedicated to the research of novel methodologies toward the synthesis of relevant building blocks for the production of drug-like compounds, in detail pyrroles. Therefore, two novel cascade processes involving the metathesis reaction for the production of functionalised pyrroles have been described. The first methodology allowed the synthesis of 1,2,3-substituted pyrroles through a one-pot tandem enyne cross metathesis (CM)-cyclization reaction starting from appropriate propargylamines and the inexpensive ethyl vinyl ether. The scope of the reaction was demonstrated by the synthesis with medium-good yields of a large variety of pyrroles bearing aryl, hetero-aryl and alkyl substituents (Table 32).

Table 32. Synthesis of 1,2,3-substituted pyrroles from propargylamines vis one pot enyne CM-cyclization reaction.

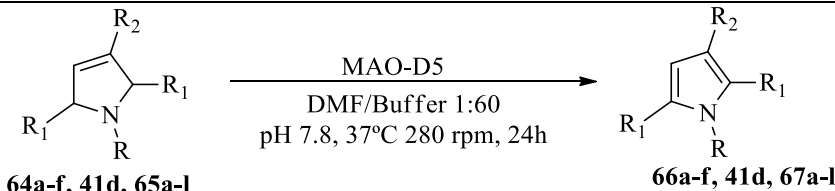
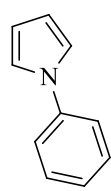
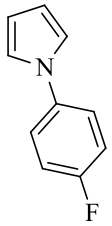
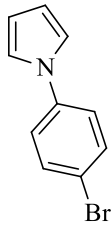
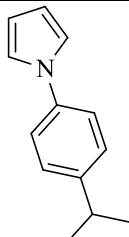
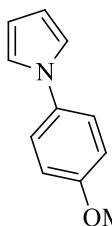
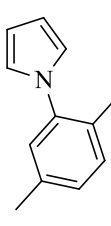
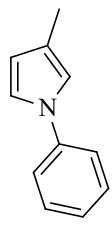
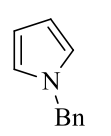
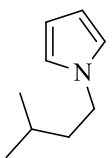
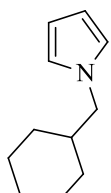
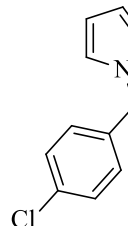
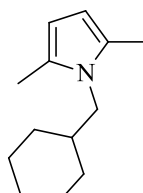
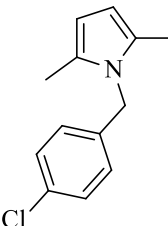
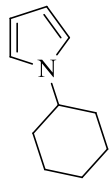
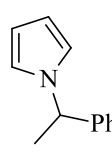
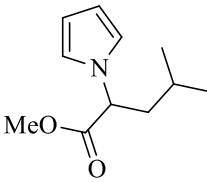
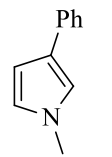
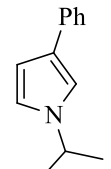
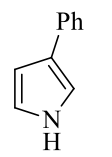


The reaction is rapid, procedurally simple and represents a facile entry to the synthetically challenging 4,5-unsubstituted pyrroles. All the pyrroles obtained with this methodology have a methyl group at C3 deriving from the diene intermediate of the enyne metathesis reaction. Attempts to decorate directly the methyl group were unsuccessful due to the presence of the reactive CH at positions C4 and C5. However, the value of the methodology is corroborated by the conversion of pyrroles into 3-pyrrolines and the consequent derivatization of the methyl substituent in C3 (Scheme 20). Moreover, the reaction was used for the synthesis of compound **47** that is an important building block for the synthesis of an alkaloid from the poison gland of ants *Leptothoracini* **48** (Scheme 21). This application highlights the versatility and usefulness of this reaction toward the production of important pharmaceuticals of interest.

The second part of chapter 3 was dedicated to the discovery and exploration of a novel chemo-enzymatic process for the synthesis of pyrroles. Firstly, the precedent undisclosed aromatization property of monoamine oxidase (MAO-N & 6-HDNO) biocatalysts has been

unveiled for the first time within this work, converting a library of 3-pyrrolines in the corresponding pyrroles through whole cell MAO catalysed oxidation-aromatization reaction. This biotransformation represents the first application of MAO biocatalysts as aromatizing agents and a series of pyrroles bearing alkyl and aryl substituents were synthesised with high conversion factors and good yield.

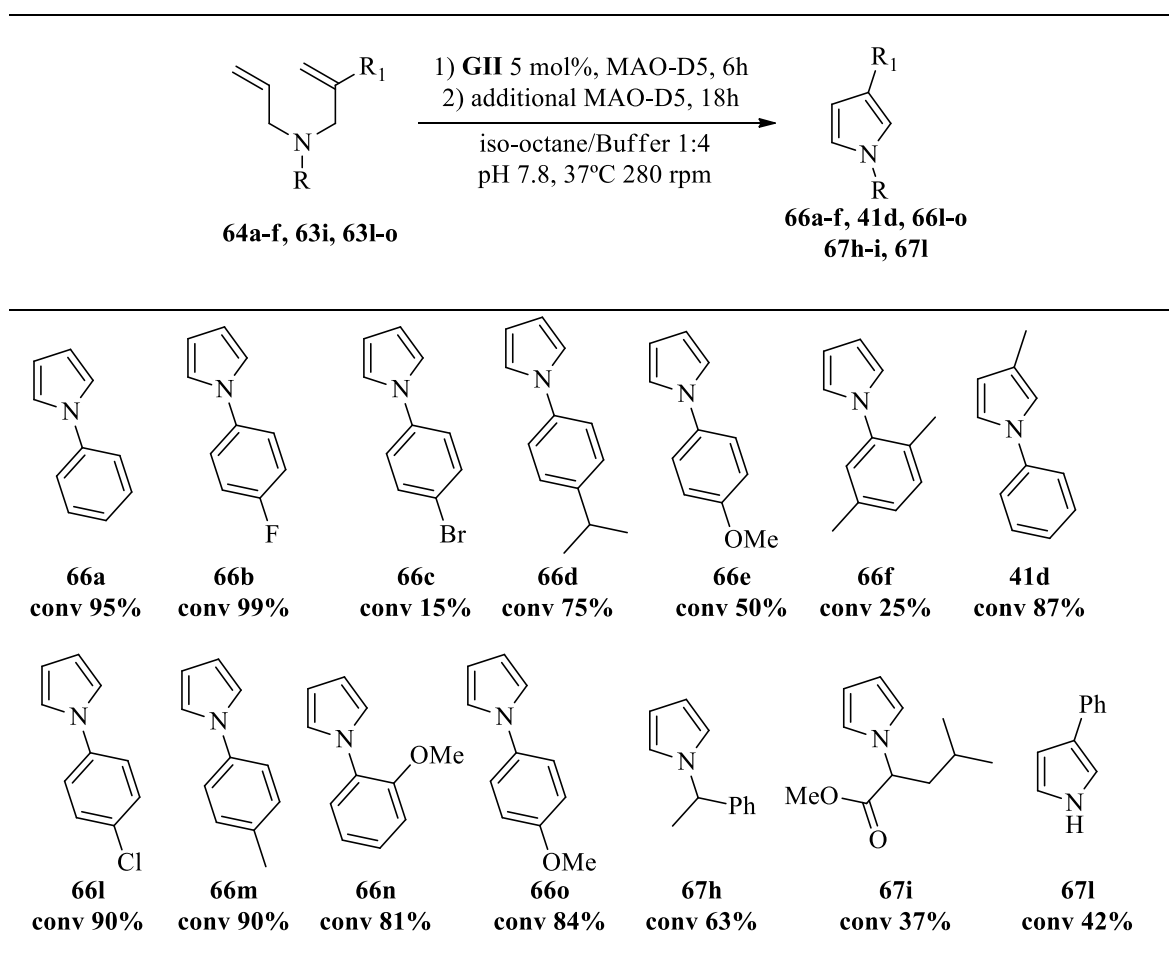
Table 33. MAO-D5 aromatization of 3-pyrroline in pyrroles.

	
 66a conv 61%	 66b conv 60%
 66c conv 40%	 66d conv 99%
 66e conv 82%	 66f conv 45%
 41d conv 99%	
 67a conv 99%	 67b conv 99%
 67c conv 99%	 67d conv 88%
 67e conv 48%	 67f conv 51%
 67g conv 99%	 67h conv 99%
 67i conv 56%	 67j conv 92%
 67k conv 31%	 67l conv 33%

From an analysis of the biotransformation conversion factors is highlighted that the success of the oxidation of 3-pyrrolines in pyrroles by MAO biocatalyst heavily depends on steric factors and on electronic effects that the pyrroline ring substituents could have on the nitrogen. As a general trend, *N*-alkyl-substituted pyrrolines afford the corresponding pyrroles with higher conversion factors than the *N*-aryl pyrrolines. Furthermore, *N*-aryl pyrrolines bearing electron withdrawing groups on the aromatic ring are not processed by

MAO biocatalyst. This is mainly due to the reduced nucleophilicity of the pyrroline nitrogen of these substrates, as described in paragraph 3.3.1.3. Moreover, in the same paragraph it is described that steric factors prevent *N*-aryl pyrrolines decorated with a phenyl group on C2 or C3 to be converted in the corresponding pyrroles. Despite these limitations, the discovery of the aromatizing property of MAO biocatalysts make them a valid and sustainable alternative to the chemical or metal agents used for the oxidation of C-N bonds for the synthesis of pyrroles. Moreover, further directed evolution of this class of enzyme could lead to the discovery of a monoamine oxidase with a larger substrate scope expanding even more the application field for such biocatalysts. Additionally, in the last part of this work is described the first attempt to combine efficiently MAO oxidation reaction in the same reaction medium with RCM reaction in order to produce pyrroles by convenient starting materials such as opportunistically substituted *N,N*-diallyl amines and anilines (Table 34).

Table 34. Novel one-pot chemoenzymatic methodology toward the synthesis of pyrroles.



The main charm of this technique is the successful combination of chemo- and enzymatic catalysis in a concurrent fashion. Mimicking the compartmentalization of cellular processes

by appropriate choice of solvents and reaction conditions, it is possible to overcome the compatibility issues of the catalysts and the difference on the reaction conditions in which these generally operate. This work is the first example of a chemo-enzymatic cascade which combines in the same reaction medium MAO-N with a metal-catalyst, other than boron reducing agents. Finally, the aromatizing properties of MAO-D5 has been exploited for the synthesis of pyrrole **68** which has structural similarity to the novel class of antitubercular compounds described within chapter 2. Further investigation on the aromatizing property of MAOs biocatalysts toward other unsaturated heterocyclic rings (e.g. 3-pyrazoline, 1,4-dihydropyridine, 1,2-dihydropyridine) is highly recommended. Success in these biotransformations could be an important turning point for the development of more sustainable and competitive synthesis of building blocks for compounds of pharmaceutical interest.

5. Materials and Methods.

5.1. Materials.

All solvents and reagents were purchased from Sigma-Aldrich, and Alfa-Aesar and used without further purification unless otherwise specified. Reactions were followed by commercially available precoated TLC plates using silica gel with UV light at 254 nm fluorescent indicator; KMnO_4 or ninhydrin solutions were used to reveal the products. Flash column chromatography was carried out using Fluorochem Davisil 40–63 μm , 60 Å. THF was distilled under nitrogen atmosphere from sodium using a benzophenone indicator. Dichloromethane was purchased from Aldrich. Petroleum ether refers to the fraction of light petroleum ether boiling between 40 and 65 °C. All reactions were conducted under a nitrogen atmosphere in oven-dried glassware unless stated otherwise.

5.1.1. Physical measurements.

^1H NMR and ^{13}C NMR spectra were recorded on an AVANCE 400 spectrometer Bruker, Germany or JEOL ECS-400 spectrometers operating at r.t. at the frequencies indicated. Chemical shifts (δ) are in ppm, referenced to tetramethylsilane. Coupling constants (J) are reported in hertz and rounded to 0.5 Hz. Splitting patterns are abbreviated as follows: singlet (s), doublet (d), triplet (t), quartet (q), quintet (quint), multiplet (m), broad (br) or some combination of them. Mass spectra (HRMS) were recorded at the EPSRC National Mass Spectrometry Service Centre on a Thermo Scientific LTQ Orbitrap XL mass spectrometer using low-resolution ESI or high-resolution nanoESI techniques. The purity of the compounds which have been evaluated for their antitubercular activity was assessed by reverse-phase liquid chromatography coupled with a mass spectrometer (Agilent series 1100 LC/MSD) with a UV detector at $\lambda = 254$ nm and an electrospray ionization source (ESI). HPLC analyses were performed at 0.4 mL/min flow rate and using a binary solvent system of 95:5 methanol/water. All the solvents were of HPLC grade. Mass spectra were acquired in positive mode scanning over the mass range of 50–1500. The following ion source parameters were used: drying gas flow, 9 mL/min; nebulize pressure, 40 psig; and drying gas temperature, 350 °C. All target compounds possessed a purity of $\geq 95\%$, as verified by HPLC analyses. GC-MS analyses were performed on a Thermo Electron Co. Focus GC coupled to a Thermo DSQ1 mass spectrometer and an AI3000 Auto Injector. Aliquots of the compound were dissolved in DCM (5 μL) and injected onto a DB-5MS (30 mm \times 0.25 mm i.d. \times 0.15 μm film thickness) column at 250 °C. The oven temperature was set at 40 °C for 4 min and raised at 15 °C/min to 135 °C, then at 5 °C/min to 250 °C and held at 250 °C for

5 min. The carrier gas flow was 1.0 mL/min. The mass spectrometer was operated in the full scan mode. The transfer line and ion source temperatures were 250 and 200 °C, respectively.

5.1.2. Microwave Irradiation Experiments.

Microwave irradiations were conducted using a CEM Discover Synthesis Unit. The machine consists of a continuous focused microwave power delivery system with operator, selectable power output from 0 to 300 W. The temperature of the contents of the vessels was monitored using a calibrated infrared temperature control mounted under the reaction vessel. All the experiments were performed using a stirring option whereby the contents of the vessel are stirred by means of rotating magnetic plate located below the floor of the microwave cavity and a Teflon coated magnetic stirring bar in the vessel.

5.2. Methods.

5.2.1. Repurposing and molecular simplification of thioridazine for the synthesis of novel antitubercular agents effective against multidrug-resistant mycobacteria

5.2.1.1. Biology.

Bacterial strains and growth conditions: The bacterial species used in this study were *Mycobacterium smegmatis* mc²155 (ATCC 700084), *Mycobacterium bovis* BCG Pasteur (ATCC 35734), *Mycobacterium tuberculosis* mc²7000, *Mycobacterium tuberculosis* H₃₇Rv (ATTC27294), *Mycobacterium tuberculosis* CF73 and two MDR-TB clinical isolates (CF104 and CF81) obtained from Clemente Ferreira Hospital, São Paulo, Brazil.²⁰⁹ Mycobacterial species were cultured in either Middlebrook 7H9 broth or Middlebrook 7H10 agar media supplemented with albumin-dextrose-catalase (ADC) or oleic acid-albumin-dextrose-catalase (OADC) enrichments, respectively, purchased from BD Biosciences. All reagents were purchased from Sigma-Aldrich unless stated otherwise. *Mycobacterium smegmatis* mc²155 (ATCC 700084), *Mycobacterium bovis* BCG Pasteur (ATCC 35734), *Mycobacterium tuberculosis* mc²7000, growth was carried out by Dr. Alistair Brown at Northumbria University. Prof. Fernando R. Pavan at Universidade Estadual Paulista "Júlio de Mesquita Filho" (UNESP) performed the growth of *Mycobacterium tuberculosis* H₃₇Rv (ATTC27294), *Mycobacterium tuberculosis* CF73 and of the two MDR-TB clinical isolates (CF104 and CF81),

Bacterial growth inhibition assays: This assay was carried out by Dr. Alistair Brown at Northumbria University. The MIC₉₀ of the compounds against *Mycobacterium smegmatis* mc²155, *Mycobacterium bovis* BCG, and *Mycobacterium tuberculosis* mc²7000 were

calculated by standard MABA (Microplate Alamar Blue assay) as previously described.¹¹⁶ Briefly, 200 μ L of sterile deionized water was added to all outer-perimeter wells of a sterile 96-well plate (Corning Incorporated, Corning, NY) to minimize evaporation of the medium in the test wells during incubation. The wells in rows B to G in columns 3 to 11 received 100 μ L of 7H9 medium containing 0.2% casamino acids, 24 μ g/mL pantothenate and 10% OADC (Beckton Dickinson, Sparks, MD). Compounds were added to rows B–G followed by 1:2 serial dilutions across the plate to column 10, and 100 μ L of excess medium was discarded from the wells in column 10. The bacterial culture at 0.5 McFarland standard diluted 1:50 (100 μ L) was added to the wells in rows B to G in columns 2 to 11, where the wells in column 11 served as drug-free controls. The plates were sealed with parafilm TM and were incubated at 37 °C. A freshly prepared 1:1 mixture of Alamar Blue (Celltiter-Blue™, Promega Corp, Madison, WI) reagent and 10% Tween® 80 (50 μ L) and re-incubated at 37 °C for 24 h.

Determination of Minimal Inhibitory Concentration (MIC₉₀): This assay was performed by Prof. Fernando R. Pavan at Universidade Estadual Paulista "Júlio de Mesquita Filho" (UNESP). The anti-*M. tuberculosis* activity of the compounds against *Mycobacterium tuberculosis* H₃₇Rv (ATTC27294), *Mycobacterium tuberculosis* CF73 and two MDR-TB clinical isolates (CF104 and CF81) was determined using the Resazurin Microtiter Assay (REMA) method according to Palomino *et al.*²¹⁰ Stock solutions of the tested compounds were prepared in dimethyl sulfoxide (DMSO), then diluted in Middlebrook 7H9 broth (Difco, Detroit, MI, USA) supplemented with oleic acid, albumin, dextrose and catalase (OADC enrichment) to obtain a final drug concentration range of 0.09–100 μ g/mL. A suspension of the *Mycobacterium tuberculosis* H₃₇Rv ATCC 27294 and clinical isolates were cultured in Middlebrook 7H9 broth supplemented with OADC and 0.05% Tween 80 for one week at 37 °C in an atmosphere of 5% CO₂. The concentration was adjusted at McFarland 1 and diluted to 2.4×10^5 CFU/mL. 100 μ L of the inoculum was added to each well of a 96-well microplate together with 100 μ L of the compounds. The plate was incubated for 7 days at 37 °C in an atmosphere of 5% CO₂. After 24 h, 30 μ L 0.01% resazurin (solubilized in water) was added. The fluorescence of the wells was read after 24 h using a Cytation 3 (BioTek®, Winooski, VT, USA). The MIC₉₀ was defined as the lowest concentration resulting in 90% inhibition of growth of *Mycobacterium tuberculosis*. Samples were set up in three independent assays.

Cytotoxic Analysis (GIC₅₀) of MRC-5 cell line: This analysis was performed by Prof. Fernando R. Pavan at Universidade Estadual Paulista "Júlio de Mesquita Filho" (UNESP). In these experiment, cells were collected in a solution of trypsin/ethylenediamine tetracetic acid (EDTA) (Vitrocell[®]) and centrifuged (252× g for 5 min). The number of cells was counted using a Neubauer chamber (Celeromics, Valencia, Spain) after staining non-viable cells with 0.4% trypan blue solution (Sigma-Aldrich[®]) via the cell exclusion assay. Then, the cell concentration was adjusted to 7.5×10^4 cells/mL in Dulbecco's Modified Eagle's Medium (DMEM) and MRC-5 cells (ATCC CCL-171). Next, a 200 µL suspension was deposited into each well of a 96-well microplate to a cell density of 1.5×10^4 cells/well. The cells were incubated at 37 °C in an atmosphere of 5% CO₂ for 24 h to allow the cells to attach to the plate.²¹¹ The compounds were solubilized in DMSO to an initial concentration of 10,000 µg/mL. Test solutions of the compounds were prepared to obtain concentrations from 500 to 1.95 µg/mL. The diluted solutions were added to the cells after changing the medium to remove any non-adherent cells, and the cultures were incubated for an additional 24 h. The cytotoxicity of the compounds was determined after incubating the cells in 30 µL of resazurin for approximately 2 h. The measurement was performed using a Synergy H1 microplate reader (BioTek[®], Winooski, VT, USA) with excitation and emission filters at wavelengths of 530 and 590 nm, respectively. The assays were performed in three independent experiments.

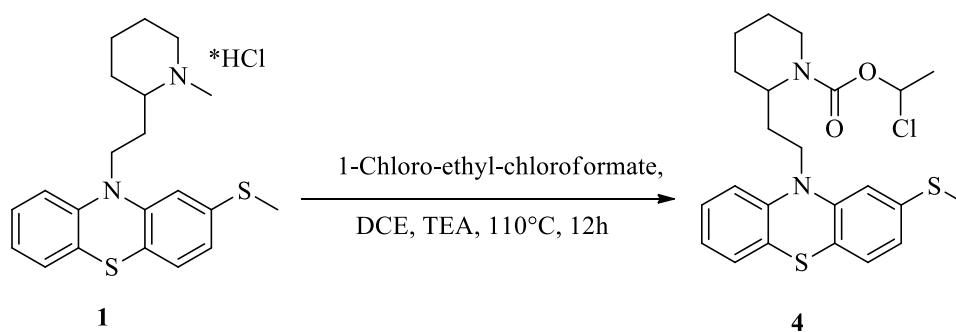
Cytotoxicity assay (GIC₅₀) of J774 cell line: This experiment was carried out by Prof. Fernando R. Pavan at Universidade Estadual Paulista "Júlio de Mesquita Filho" (UNESP). *In vitro* cytotoxicity assays (GIC₅₀) were performed on the J774 cell line, as previously reported.²¹² The cells were routinely maintained in Complete Medium (RPMI-1640 supplemented with 10% heat-inactivated fetal bovine serum (FBS); 100 U/mL penicillin and 100 µg/mL streptomycin), at 37 °C, in a humidified 5% CO₂ atmosphere. After reaching confluence, the cells were detached and counted. For the cytotoxicity assay, 1×10^5 cells/mL were seeded in 200 µL of Complete Medium in 96-well plates (NUNC). The plates were incubated at 37 °C under a 5% CO₂ atmosphere for 24 h, to allow cell adhesion prior to drug testing. The compounds were dissolved in DMSO and subjected to two-fold serial dilution from 1250 to 3.9 µg/mL. Cells were exposed to the compounds at various concentrations for a 24 h-period. Resazurin solution was then added to the cell cultures and incubated for 6 hours. Cell respiration, as an indicator of cell viability, was detected by reduction of resazurin to resorufin, whose pink colour and fluorescence indicates cell viability. A persistent blue colour of resazurin is a sign of cell death. The fluorescence

measurements (530 nm excitation filter and 590 nm emission filter) were performed in a SPECTRAfluor Plus (Tecan) microfluorimeter. The IC₅₀ value was defined as the highest drug concentration at which 50% of the cells are viable relative to the control.

Efflux pump inhibition assays: This assay was performed by Dr. Bhakta group at Birbeck College London. The assay was performed based on previously published protocols.¹¹² In brief, early log phase cells of *Mycobacterium smegmatis* were taken and the OD₆₀₀ was adjusted to 0.4 in 1× PBS. The test samples contained (4–6) × 10⁷ bacteria/mL in PBS, 0.4% glucose (as a source of energy for efflux pumps activity), 0.5 mg/L ethidium bromide (as a substrate for efflux pumps), and the compounds being tested at 1/4× MIC concentrations. Blank samples contained all of the components mentioned above, except the bacterial suspension, which was replaced with 1× PBS. Verapamil and chlorpromazine, known efflux pump inhibitors, were used as positive controls at concentrations of 125 µg/mL and 10 µg/mL respectively. The experiment was performed in a 96-well plates that was read in a fluorimeter (FLUOstar OPTIMA, BMG Labtech) with the following parameters: wavelengths of 544 and 590 nm for excitation and detection of fluorescence, gain 2200, a temperature of 37 °C, and a cycle of measurement every minute for a total period of 60 min. The accumulation or efflux of ethidium bromide was monitored in real-time for the mentioned period.

5.2.1.2. Chemistry.

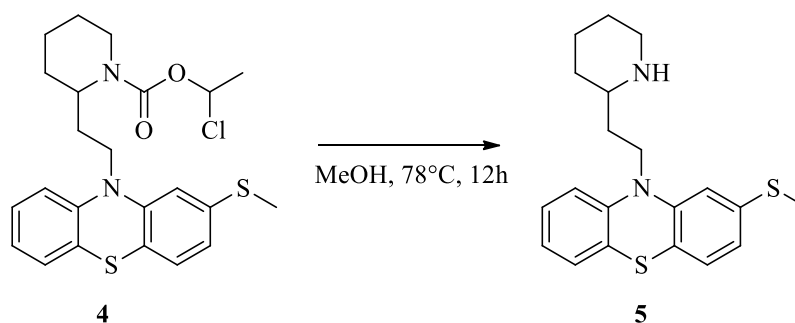
Synthesis of 1-chloroethyl 2-(2-(2-(methylthio)-10H-phenothiazin-10-yl)ethyl)piperidine-1-carboxylate (4).



Thioridazine hydrochloride **1** (1575 mg, 3.87 mmol, 1 eq.) was dissolved in a round bottom flask containing dry DCE (20 mL) and TEA (1.07 mL, 7.74 mmol, 2 eq.). The mixture was stirred at r.t for 20 minutes, then, 1-chloroethyl chloroformate (1099.1 mg, 7.74 mmol, 2 eq.)

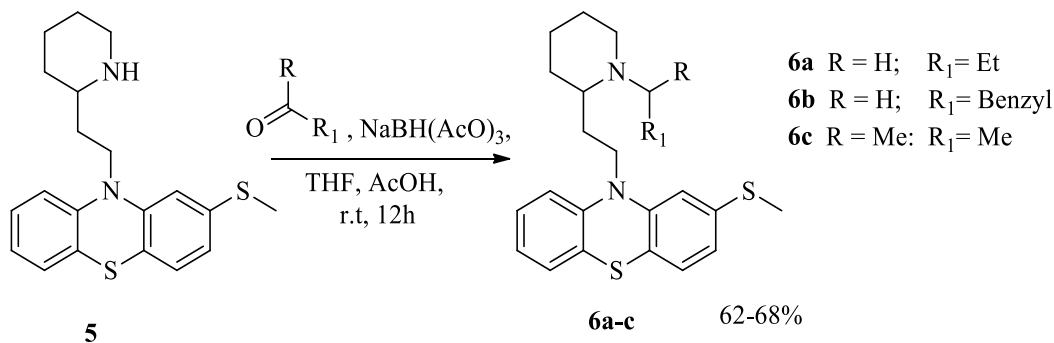
was added to the solution. The mixture was left under N₂ atmosphere at 110 °C for 12 h. Then, the reaction mixture was quenched with 10 mL of water and extracted twice with 20 mL of EtOAc. The combined organic layers were washed with brine, dried over Na₂SO₄ and concentrated under reduced pressure giving a yellow-brown crude oil. The crude product was purified by chromatography on silica gel, using hexane/EtOAc (4:1) as eluent, affording the pure product as a yellow solid **Yield**: 84% (1505 mg.). **¹H NMR** (400 MHz CDCl₃) δ 7.13-7.01 (m, 2H), 7.01-6.90 (m, 1H), 6.89-6.60 (m, 4H), 6.59-6.29 (m, 1H), 4.20-3.90 (m, 1H), 3.90-3.60 (m, 2H), 2.90-2.74 (m, 1H), 2.74-2.57 (m, 1H), 2.36 (s, 3H), 2.25-2.04 (m, 1H), 1.77-1.60 (m, 3H), 1.58-1.16 (m, 7H) ppm. **¹³C NMR** (100 MHz CDCl₃) δ 152.9, 145.1, 145.0, 137.9, 127.8, 127.7, 127.4, 122.8, 122.6, 121.2, 121.0, 115.2, 114.5, 83.4, 49.9, 44.5, 39.8, 29.1, 27.8, 25.4, 19.1, 16.5, 14.3 ppm. **LRMS** (ESI⁺): m/z = 463 [M + H]⁺.

Synthesis of 2-(methylthio)-10-(2-(piperidin-2-yl)ethyl)-10H-phenothiazine (**5**).



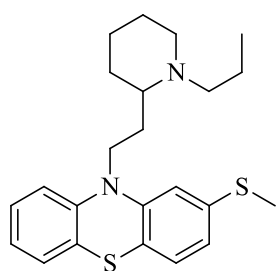
1-chloroethyl 2-(2-(2-(methylthio)-10H-phenothiazin-10-yl)ethyl)piperidine-1-carboxylate **4** (1505 mg, 3.25 mmol, 1 eq.) was dissolved in MeOH (20 mL). The reaction was allowed to stir at 78°C for 12 h then the reaction mixture was concentrated by reduced pressure evaporation. Then, the reaction mixture was quenched with 20 mL of water and extracted twice with 20 mL of EtOAc. The combined organic layers were washed with brine, dried over Na₂SO₄ and concentrated under reduced pressure giving a yellow-brown crude oil. The obtained product **5** was purified by chromatography on silica gel, using EtOAc/MeOH/TEA (3.9:1:0.1) as eluent. The pure product **5** was obtained as a yellow-brown oil. **Yield**: 85% (1021.7 mg). **¹H NMR** (400 MHz CDCl₃) δ 9.25 (br s., 1H), 7.20-7.08 (m, 2H), 7.03 (d, *J* = 7.0 Hz, 1H), 6.90 (d, *J* = 7.0 Hz, 2H), 6.82 (m, 2H), 4.13-3.93 (m, 2H), 3.29 (d, *J* = 13.0 Hz, 1H), 3.02 (m, 1H), 2.68 (t, *J* = 12.0 Hz, 1H), 2.46 (s, 3H), 2.18-2.05 (m, 1H), 1.90-1.75 (m, 3H), 1.75-1.53 (m, 3H), 1.44-1.28 (m, 1H) ppm. **¹³C NMR** (100 MHz CDCl₃) δ 145.9, 144.4, 138.3, 127.8, 127.7, 127.7, 125.9, 123.2, 122.5, 121.2, 116.3, 114.5, 55.7, 44.7, 43.7, 30.7, 28.8, 22.5, 22.2, 16.4 ppm. **LRMS** (ESI⁺): m/z = 357 [M + H]⁺.

General procedure for the synthesis of thioridazine derivatives (6a-c).



2-(methylthio)-10-(2-(piperidin-2-yl)ethyl)-10H-phenothiazine **5** (49.8 mg, 0.14 mmol, 1 eq.) was added to a round bottom flask containing a solution of the appropriate aldehyde/ketone (0.21 mmol, 1.5 eq.) and AcOH (0.024 mL, 0.28 mmol, 1 eq.) in THF (5 mL). The solution was then allowed to stir at room temperature for 30 minutes. Then, NaBH(AcO)₃ (59.3 mg, 0.28 mmol, 2.0 eq.) was added and the reaction was allowed to react for 12 h at r.t. Then the reaction was quenched with (20mL) NaOH 1N solution and the mixture was allowed to stir for 20 minutes. Then the organic solvent was removed through reduced pressure evaporation. The residue was diluted with EtOAc, extracted with EtOAc (3 X 10 mL) and dried over anhydrous MgSO₄. The obtained product **6a-c** was purified by chromatography on silica gel, using EtOAc/MeOH/TEA (3.9:1:0.1) as eluent. Pure products **6a-c** were obtained as yellow-brown oils.

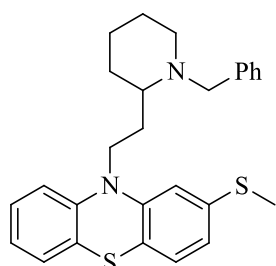
Synthesis of 2-(methylthio)-10-(2-(1-propylpiperidin-2-yl)ethyl)-10H-phenothiazine (6a).



Yield: 62% (34.5 mg). **¹H NMR** (400 MHz CDCl₃) δ 7.15-7.11 (m, 2H), 7.03 (d, *J* = 4.0 Hz, 1H), 6.92-6.88 (m, 2H), 6.80 (d, *J* = 4.0 Hz, 2H), 3.94-3.99 (m, 1H), 3.83-3.79 (m, 1H), 2.82-2.77 (m, 1H), 2.51-2.48 (m, 2H), 2.45 (s, 3H), 2.33-2.22 (m, 2H), 2.16-2.06 (m, 1H), 1.85-1.56 (m, 4H), 1.43-1.29 (m, 5H), 0.75 (t, *J* = 8.0 Hz, 3H) ppm.

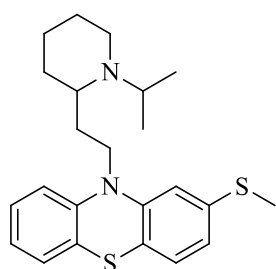
¹³C NMR (100 MHz CDCl₃) δ 145.8, 145.0, 137.6, 127.6, 127.5, 127.3, 125.4, 122.6, 122.3, 120.9, 115.8, 114.7, 57.9, 55.7, 51.4, 44.4, 30.2, 27.9, 25.2, 23.3, 18.9, 16.6, 12.0 ppm. **LRMS** (ESI⁺): *m/z* = 399 [M + H]⁺. **HRMS** (ESI) *m/z* calcd. for C₂₃H₃₁N₂S₂ [M + H] 399.1923, found 399.1916.

Synthesis of 10-(2-(1-benzylpiperidin-2-yl)ethyl)-2-(methylthio)-10H-phenothiazine (6b).



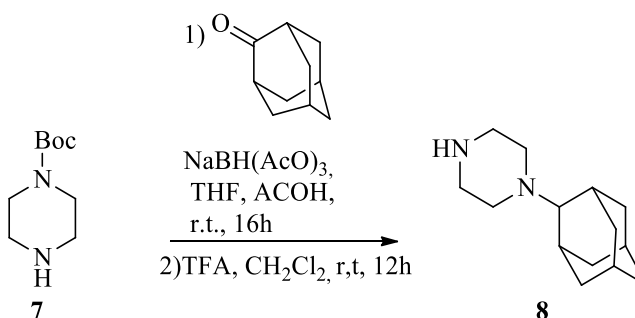
Yield: 67% (42.0 mg). **¹H NMR** (400 MHz CDCl₃) δ 7.28-7.17 (m, 5H) 7.14-7.10 (m, 2H), 7.03 (d, *J* = 4.0 Hz, 1H), 6.92-6.84 (m, 2H), 6.81 (d, *J* = 4.0 Hz, 2H), 3.97-3.83 (m, 3H), 3.32 (d, *J* = 8.0 Hz, 1H), 2.75-2.70 (m, 1H), 2.60-2.55 (m, 1H), 2.43 (s, 3H), 2.14 (s, 2H), 2.00-1.94 (m, 1H), 1.77-1.41 (m, 6H) ppm. **¹³C NMR** (100 MHz CDCl₃) δ 146.0, 145.1, 139.7, 137.6, 129.1, 128.8, 128.6, 128.3, 127.6, 127.6, 127.3, 126.8, 125.4, 122.6, 122.3, 120.9, 115.8, 114.7, 58.4, 57.7, 55.7, 50.6, 44.2, 29.6, 24.4, 23.1, 16.6 ppm. **LRMS** (ESI⁺): *m/z* = 447 [M + H]⁺. **HRMS** (ESI) *m/z* calcd. For C₂₇H₃₁N₂S₂ [M + H] 447.1923, found 447.1913.

Synthesis of 10-(2-(1-isopropylpiperidin-2-yl)ethyl)-2-(methylthio)-10H-phenothiazine (6c).



Yield: 68% (38.0 mg). **¹H NMR** (400 MHz CDCl₃) δ 7.15-7.11 (m, 2H), 7.03 (d, *J* = 4.0 Hz, 1H), 6.92-6.88 (m, 2H), 6.80 (d, *J* = 4.0 Hz, 2H), 3.96-3.98 (m, 1H), 3.83-3.79 (m, 1H), 3.15 (t, *J* = 8.0 Hz, 1H), 2.81-2.75 (m, 1H), 2.62-2.59 (m, 1H), 2.44 (s, 3H), 2.20-2.03 (m, 2H), 1.85-1.24 (m, 7H), 1.05 (d, *J* = 8.0 Hz, 3H), 0.77 (d, *J* = 8.0 Hz, 3H) ppm. **¹³C NMR** (100 MHz CDCl₃) δ 145.8, 127.6, 127.5, 127.3, 122.6, 122.3, 120.9, 115.7, 114.7, 56.1, 44.1, 43.9, 31.0, 28.5, 26.0, 24.0, 21.8, 16.6, 13.9 ppm. **LRMS** (ESI⁺): *m/z* = 399 [M + H]⁺. **HRMS** (ESI) *m/z* calcd. for C₂₃H₃₁N₂S₂ [M + H] 399.1923, found 399.1916.

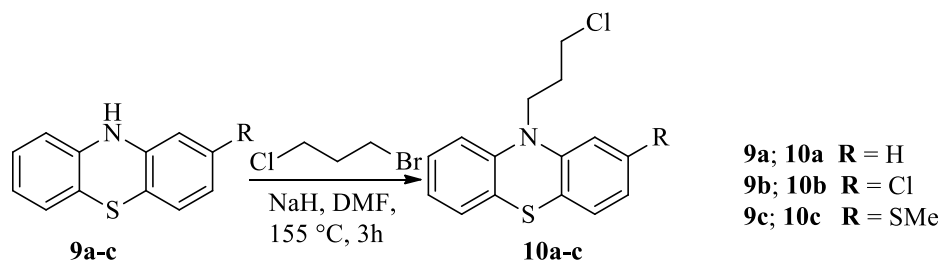
Synthesis of 1-(Adamantan-2-yl)piperazine (8)



The Boc-piperazine **7** (372.2 mg, 2.0 mmol, 1 eq.) and adamantan-2-one (300.0 mg, 2.0 mmol, 1 eq.) were dissolved in THF (8 mL), and the resulting mixture was stirred for 5 min.

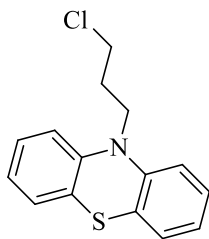
The reaction was cooled at 0 °C, and then NaBH(AcO)₃ (508.6 mg, 2.4 mmol, 1.2 eq.) and AcOH (0.115 mL, 2 mmol, 1 eq.) were carefully added. The resulting mixture was stirred at r.t. for 16 h. The reaction was quenched with NaOH (1 N, 20 mL) and the product was extracted with EtOAc (3 × 25 mL). The EtOAc extract was dried (MgSO₄), and the solvent was evaporated to give the crude piperazine derivatives, which were filtered through a pad of silica gel (eluent EtOAc/petroleum ether 1:1). The filtered compounds were then dissolved in DCM (4 mL) and treated with 1 mL of TFA. The resulting mixture was stirred at r.t for 12 h. The solvents were removed, and the crude compound was dissolved in EtOAc (10 mL) and washed several times with 1 N NaOH (20 mL). The organic phase was dried (MgSO₄), and the solvent was evaporated to yield the crude piperazines **8** which was purified by column chromatography using petroleum ether/EtOAc 1:1 as eluent. The pure product **8** was obtained as a yellow-brown oil. **Yield:** 78% (343.1 mg). **¹H NMR** (400 MHz CDCl₃) δ 3.31 (m, 4H), 2.81 (m, 2H), 2.31 (br s, 2H), 2.01–1.94 (m, 4H), 1.76–1.68 (m, 5H), 1.60–1.53 (m, 4H), 1.42–1.39 (m, 1H), 1.30–1.27 (m, 1H) ppm; **LRMS** (ESI⁺): m/z = 221 [M + H]⁺.

General procedure for the synthesis of compound (10a-c).



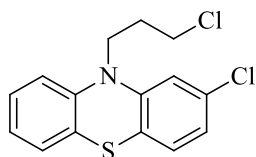
The appropriate 2-substituted phenothiazine **9a-c** (0.42 mmol, 1 eq.) was added to 5 mL of DMF in a double neck round bottom flask under N₂ atmosphere. NaH (6.34 mg, 0.46 mmol, 1.1 eq.) was added to the stirred solution at 0°C, which then was allowed to reach r.t stirring for 20 minutes. Then, 1-bromo-3-chloropropane (72.5 mg, 0.46 mmol, 1.1 eq.) was added to the stirring solution. The reaction mixture was allowed to stir under N₂ atmosphere for 3 h at 155 °C. Then, the reaction mixture was quenched with 10 mL of water and extracted twice with EtOAc (20 mL). The combined organic layers were washed with brine (10 mL), dried over Na₂SO₄ and concentrated under reduced pressure giving a yellow-brown crude oil. Pure product 10a-c was obtained as yellow-brown oil after purification of the crude mixture by chromatography on silica gel, using hexane/EtOAc (4:1) as eluent.

Synthesis of 10-(3-chloropropyl)-10H-phenothiazine (10a).



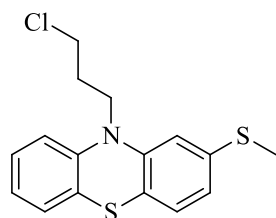
Yield: 82% (100.8 mg). **¹H NMR** (400 MHz CDCl₃) δ 7.19-7.15 (m, 4H), 6.96-6.89 (m, 4H), 4.07 (t, *J* = 8.0 Hz, 2H), 3.66 (t, *J* = 8.0 Hz, 2H), 2.23 (quint, *J* = 8.0 Hz, 2H) ppm. **¹³C NMR** (100 MHz CDCl₃) δ 145.2, 127.8, 127.4, 125.8, 122.9, 115.7, 44.0, 42.6, 29.7 ppm. **LRMS** (ESI⁺): *m/z* = 276 [M + H]⁺.

Synthesis of 2-chloro-10-(3-chloropropyl)-10H-phenothiazine (10b).



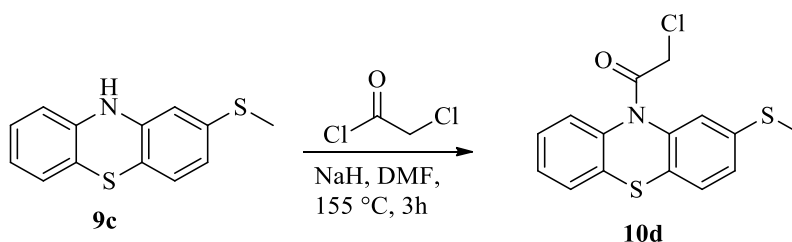
Yield: 84% (106.4 mg). **¹H NMR** (400 MHz CDCl₃) δ 7.19-7.14 (m, 2H) 7.04 (d, *J* = 8.0 Hz, 1H), 6.95 (t, *J* = 8.0 Hz, 1H), 6.91-6.88 (m, 2H), 6.86 (s, 1H), 4.04 (t, *J* = 8.0 Hz, 2H), 3.65 (t, *J* = 8.0 Hz, 2H), 2.25-2.18 (quint, *J* = 8.0 Hz, 2H) ppm. **¹³C NMR** (100 MHz CDCl₃) δ 146.5, 144.4, 133.4, 128.2, 127.8, 127.6, 125.5, 124.2, 123.3, 122.7, 116.0, 115.9, 44.1, 42.3, 29.5 ppm. **LRMS** (ESI⁺): *m/z* = 332 [M+Na]⁺

Synthesis of 10-(3-chloropropyl)-2-(methylthio)-10H-phenothiazine (10c).



Yield: 93% (125.4 mg). **¹H NMR** (400 MHz CDCl₃) δ 7.18-7.14 (m, 2H), 7.06 (d, *J* = 8.0 Hz, 1H), 6.95-6.88 (m, 2H), 6.81 (s, 2H), 4.06 (t, *J* = 8.0 Hz, 2H), 3.65 (t, *J* = 8.0 Hz, 2H), 2.46 (s, 3H), 2.22 (quint, *J* = 8.0 Hz, 2H) ppm. **¹³C NMR** (100 MHz CDCl₃) δ 145.6, 145.9, 137.8, 127.8, 127.7, 127.5, 125.8, 123.0, 122.7, 121.1, 115.9, 114.6, 44.1, 42.5, 29.7, 16.5 ppm. **LRMS** (ESI⁺): *m/z* = 322 [M + H]⁺.

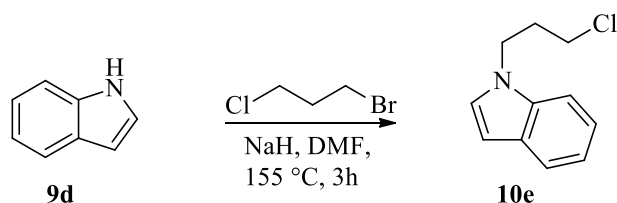
Synthesis of 2-chloro-1-(2-(methylthio)-10H-phenothiazin-10-yl)ethanone (10d).



2-SMe-phenothiazine **9c** (298.4 mg, 1.22 mmol, 1 eq.) was added to 15 mL of DMF in a double neck round bottom flask under N₂ atmosphere. NaH (25.2 mg, 1.83 mmol, 1.5 eq.)

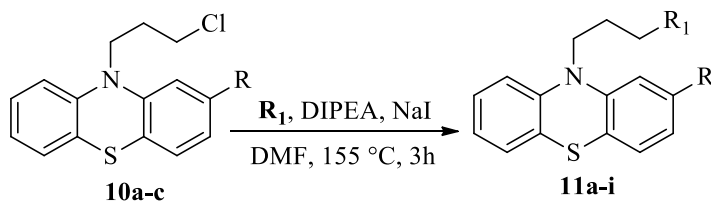
was added to the stirring solution at 0 °C which then was allowed to reach r.t stirring for 20 minutes. Then, 2-chloroacetyl chloride (0.288 mL, 3.66 mmol 3 eq.) was added to the stirring solution. The reaction mixture was allowed to stir under N₂ atmosphere for 3h at 155 °C. Then, the reaction mixture was quenched with water (10 mL) and extracted twice with EtOAc (20 mL). The combined organic layers were washed with brine, dried over Na₂SO₄ and concentrated under reduced pressure giving a yellow-brown crude oil. The obtained product was purified by chromatography on silica gel, using hexane/EtOAc (3:2) as eluent. **Yield:** 58% (227.2 mg). **¹H NMR** (400 MHz CDCl₃) δ 7.53 (d, *J* = 8.0 Hz, 1H), 7.47-7.43 (m, 2H), 7.36-7.31 (m, 2H), 7.27-7.23 (m, 1H), 7.14-7.11 (m, 1H), 4.16 (s, 2H), 2.49 (s, 3H) ppm. **¹³C NMR** (100 MHz CDCl₃) δ 166.3, 138.8, 138.3, 137.5, 128.3, 128.2, 127.7, 127.5, 126.5, 125.7, 124.1, 40.7, 15.9 ppm. **LRMS** (ESI⁺): *m/z* = 322 [M + H]⁺.

Synthesis of 1-(3-chloropropyl)-1H-indole (10e).



Indole **9d** (60.8 mg, 0.52 mmol, 1 eq.) was added to 10 mL of DMF in a double neck round bottom flask under N₂ atmosphere. NaH (7.8 mg, 0.57 mmol, 1.1 eq.) was added to the stirring solution at 0 °C which then was allowed to reach r.t stirring for 20 minutes. Then, 1-bromo-3-chloropropane (88.8 mg, 0.57 mmol 1.1 eq) was added to the stirring solution. The reaction mixture was allowed to stir under N₂ atmosphere for 3h at 155 °C. Then, the reaction mixture was quenched with water (10 mL) and extracted twice with EtOAc (20 mL). The combined organic layers were washed with brine (10 mL), dried over Na₂SO₄ and concentrated under reduced pressure giving a yellow-brown crude oil. The product **9e** was purified by chromatography on silica gel, using hexane/EtOAc (4:1) as eluent, affording **9e** as a light-yellow oil. **Yield:** 82% (82.3 mg). **¹H NMR** (400 MHz CDCl₃) δ 7.69 (d, *J* = 8.0 Hz, 1H), 7.41 (d, *J* = 8.0 Hz, 1H), 7.27 (t, *J* = 8.0 Hz, 1H), 7.19-7.15 (m, 2H), 6.56 (d, *J* = 4.0 Hz, 1H), 4.37-4.33 (m, 2H), 3.46 (t, *J* = 8.0 Hz, 1H), 3.32 (t, *J* = 8.0 Hz, 1H), 2.37-2.26 (quint, *J* = 8.0 Hz, 2H) ppm. **¹³C NMR** (100 MHz CDCl₃) δ 135.9, 128.8, 128.1, 121.8, 121.2, 119.6, 109.4, 101.6, 42.9, 42.0, 32.7 ppm. **LRMS** (ESI⁺): *m/z* = 194 [M + H]⁺.

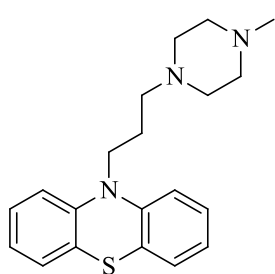
General procedure for the synthesis of thioridazine derivatives (11a-i).



Cmpd	R	R ₁	Yields
11a	H	1-methyl-piperazine	99%
11b	H	1-phenyl-piperazine	62%
11c	SMe	1-methyl-piperazine	99%
11d	SMe	1-phenyl-piperazine	77%
11e	SMe	thiomorpholine	99%
11f	SMe	1-adamantantyl-piperazine	71%
11g	SMe	2-adamantantyl-piperazine	72%
11h	Cl	1-phenyl-piperazine	57%
11i	Cl	thiomorpholine	90%

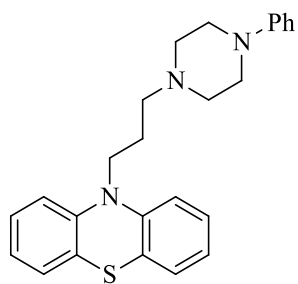
The appropriate N substituted piperazine or thiomorpholine (0.72 mmol, 4 eq.) was dissolved in a round bottom flask containing dry DMF (10 mL) and DIPEA (0.033 mL, 0.19 mmol, 1.1 eq.) under N₂ atmosphere. The mixture was stirred at r.t for 20 minutes, then, the appropriate compound **10a-c**, (0.18 mmol, 1 eq.) was added to the solution followed by NaI (5.7 mg, 0.04 mmol, 0.2 eq.). Then, the mixture was left under N₂ atmosphere at 155 °C for 3 h. Then, the reaction mixture was quenched with water (10 mL) and extracted twice with EtOAc (10 mL). The combined organic layers were washed with brine, dried over Na₂SO₄ and concentrated under reduced pressure. The pure product was obtained as a yellow oil after purification of the crude mixture by chromatography on silica gel, using EtOAc/MeOH/TEA (3.9:1:0.1) as eluent.

Synthesis of 10-(3-(4-methylpiperazin-1-yl)propyl)-10H-phenothiazine (**11a**).²¹³



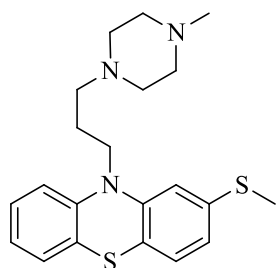
Yield: 99% (61.1 mg). **¹H NMR** (400 MHz CDCl₃) δ 7.12 (t, *J* = 8.0 Hz, 4H), 6.90 (t, *J* = 8.0 Hz, 4H), 3.90 (t, *J* = 8.0 Hz, 2H), 2.46 (t, *J* = 8.0 Hz, 2H), 2.42-2.34 (m, 8H), 2.26 (s, 3H), 1.94 (t, *J* = 8.0 Hz, 2H) ppm. **¹³C NMR** (100 MHz CDCl₃) δ 145.2, 127.5, 127.3, 125.1, 122.5, 115.6, 55.7, 55.1, 53.2, 46.0, 45.4, 24.5 ppm. **LRMS** (ESI⁺): *m/z* = 340 [M + H]⁺.

Synthesis of 10-(3-(4-phenylpiperazin-1-yl)propyl)-10H-phenothiazine (11b).



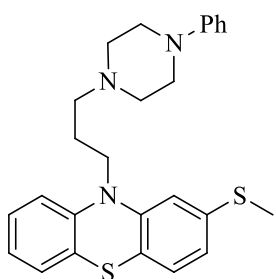
Yield: 62% (44.7 mg). **¹H NMR** (400 MHz CDCl₃) δ 7.25 (t, *J* = 8.0 Hz, 2H), 7.13 (d, *J* = 8.0 Hz, 4H), 6.92-6.88 (m, 6H), 6.84 (t, *J* = 8.0 Hz, 1H), 3.95 (t, *J* = 8.0 Hz, 2H), 3.14 (t, *J* = 8.0 Hz, 4H), 2.57 (t, *J* = 8.0 Hz, 4H), 2.53 (t, *J* = 8.0 Hz, 2H), 2.02-1.95 (m, 2H) ppm. **¹³C NMR** (100 MHz CDCl₃) δ 151.4, 145.3, 129.2, 127.5, 127.3, 125.2, 122.5, 119.7, 116.1, 115.6, 55.7, 53.4, 49.2, 45.3, 24.4 ppm. **LRMS** (ESI⁺): *m/z* = 402 [M + H]⁺. **HRMS** (ESI) *m/z* calcd. for C₂₅H₂₈N₃S [M + H] 402.1998, found 402.1995.

Synthesis of 10-(3-(4-methylpiperazin-1-yl)propyl)-2-(methylthio)-10H-phenothiazine (11c).



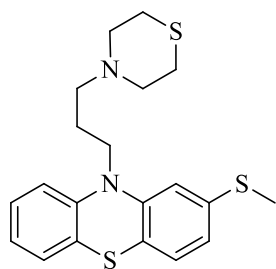
Yield: 99% (69.7 mg). **¹H NMR** (400 MHz CDCl₃) δ 7.11-7.09 (m, 2H), 7.01 (d, *J* = 8.0 Hz, 1H), 6.90-6.85 (m, 2H), 6.80-6.77 (m, 2H), 3.89 (t, *J* = 8.0 Hz, 2H), 2.50-2.33 (m, 8H), 2.46 (t, *J* = 8.0 Hz, 2H), 2.44 (s, 3H), 2.26 (s, 3H), 1.94-1.92 (m, 2H) ppm. **¹³C NMR** (100 MHz CDCl₃) δ 145.2, 144.9, 137.5, 127.6, 127.5, 127.3, 125.2, 122.6, 122.2, 120.8, 115.8, 114.7, 55.6, 55.1, 53.2, 46.0, 45.3, 24.4, 16.6 ppm. **LRMS** (ESI⁺): *m/z* = 386 [M + H]⁺. **HRMS** (ESI) *m/z* calcd. for C₂₁H₂₈N₃S₂ [M + H] 386.1719, found 386.1739.

Synthesis of 2-(methylthio)-10-(3-(4-phenylpiperazin-1-yl)propyl)-10H-phenothiazine (11d).



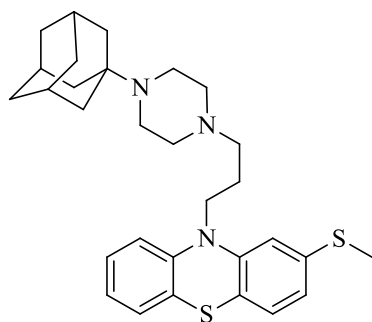
Yield: 77% (61.9 mg). **¹H NMR** (400 MHz CDCl₃) δ 7.24 (t, *J* = 8.0 Hz, 2H), 7.12 (d, *J* = 8.0 Hz, 2H), 7.03 (d, *J* = 8.0 Hz, 1H), 6.92-6.88 (m, 4H), 6.85-6.80 (m, 3H), 3.94 (t, *J* = 8.0 Hz, 2H), 3.14 (t, *J* = 8.0 Hz, 4H), 2.56 (t, *J* = 8.0 Hz, 4H), 2.51 (t, *J* = 8.0 Hz, 2H), 2.45 (s, 3H), 1.99-1.96 (m, 2H) ppm. **¹³C NMR** (100 MHz CDCl₃) δ 151.4, 145.7, 145.02, 137.6, 129.2, 127.6, 127.5, 127.3, 125.3, 122.7, 122.3, 120.9, 119.7, 116.1, 115.8, 114.8, 55.7, 53.4, 49.2, 45.3, 24.4, 16.6 ppm. **LRMS** (ESI⁺): *m/z* = 448 [M + H]⁺. **HRMS** (ESI) *m/z* calcd. for C₂₆H₃₀N₃S₂ [M + H] 448.1876, found 448.1866.

Synthesis of 2-(methylthio)-10-(3-thiomorpholinopropyl)-10H-phenothiazine (11e).



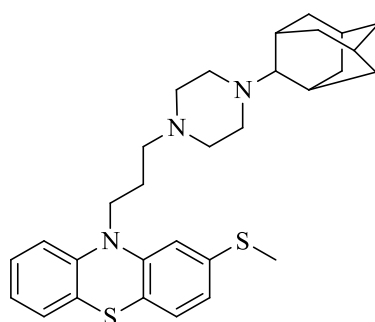
Yield: 99% (69.3 mg). **¹H NMR** (400 MHz CDCl₃) δ 7.14-7.03 (m, 2H), 7.01 (d, *J* = 8.0 Hz, 1H), 6.91-6.86 (m, 2H), 6.80-6.77 (m, 2H), 3.90 (t, *J* = 8.0 Hz, 2H), 2.63-2.57 (m, 8H), 2.45 (s, 3H), 1.89 (t, *J* = 8.0 Hz, 2H) 1.34-1.22 (m, 2H) ppm. **¹³C NMR** (100 MHz CDCl₃) δ 145.7, 144.9, 137.6, 127.6, 127.5, 127.3, 122.6, 122.2, 120.8, 115.9, 114.8, 56.1, 55.2, 45.1, 28.1, 24.1, 16.6 ppm. **LRMS** (ESI⁺): *m/z* = 389 [M + H]⁺. **HRMS** (ESI) *m/z* calcd. for C₂₀H₂₅N₂S₃ [M + H] 389.1174, found 389.1172.

Synthesis of 10-(3-(4-adamantan-1-yl)piperazin-1-yl)propyl)-2-(methylthio)-10H-phenothiazine (11f).



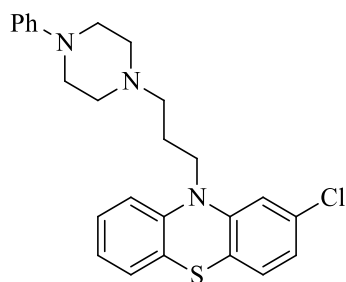
Yield: 71% (64.5 mg). **¹H NMR** (400 MHz CDCl₃) δ 7.17-7.07 (m, 2H), 7.02 (d, *J* = 7.5 Hz, 1H), 6.92-6.85 (m, 2H), 6.84-6.76 (m, 2H), 3.89 (t, *J* = 7.0 Hz, 2H), 2.56-2.26 (m, 10H), 2.44 (s, 3H), 2.07-1.88 (m, 8H), 1.88-1.74 (m, 4H), 1.71-1.53 (m, 4H), 1.36 (d, *J* = 12.0 Hz, 2H) ppm. **¹³C NMR** (100 MHz CDCl₃) δ 145.8, 144.9, 137.6, 127.6, 127.5, 127.3, 125.3, 122.7, 122.3, 120.8, 115.9, 114.7, 55.4, 54.3, 53.2, 46.7, 45.4, 45.2, 44.0, 43.9, 41.0, 38.7, 38.0, 36.8, 36.7, 29.7, 24.3, 16.6 ppm. **LRMS** (ESI⁺): *m/z* = 506 [M + H]⁺. **HRMS** (ESI) *m/z* calcd. for C₃₀H₄₀N₃S₂ [M + H] 506.2658, found 506.2644.

Synthesis of 10-(3-(4-(adamantan-2-yl)piperazin-1-yl)propyl)-2-(methylthio)-10H-phenothiazine (11g).



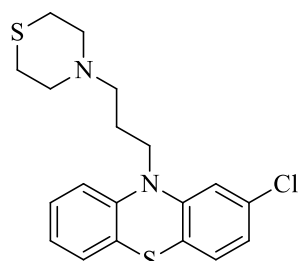
Yield: 72% (65.4 mg). **¹H NMR** (400 MHz CDCl₃) δ 7.15-7.04 (m, 2H), 7.01 (d, *J* = 7.5 Hz, 1H), 6.92-6.81 (m, 2H), 6.81 - 6.73 (m, 2H), 3.87 (t, *J* = 6.5 Hz, 2H), 3.50-3.49 (m, 1H), 3.33-3.32 (m, 1H), 2.81-2.65 (m, 3H), 2.64-2.59 (m, 4H), 2.59-2.44 (m, 5H), 2.43 (s, 3H), 2.07 (m, 5H), 1.97-1.87 (m, 2H), 1.73 (m, 5H), 1.64 (d, *J* = 2.0 Hz, 3H) ppm. **¹³C NMR** (100 MHz CDCl₃) δ 145.8, 144.9, 137.6, 127.6, 127.5, 127.3, 125.2, 122.6, 122.2, 120.8, 115.8, 114.7, 67.8, 56.0, 54.0, 49.6, 45.6, 40.6, 37.9, 37.3, 31.4, 29.1, 28.9, 27.6, 27.4, 24.4, 16.6 ppm. **LRMS** (ESI⁺): *m/z* = 506 [M + H]⁺. **HRMS** (ESI) *m/z* calcd. for C₃₀H₄₀N₃S₂ [M + H] 506.2658, found 506.2644.

Synthesis of 2-chloro-10-(3-(4-phenylpiperazin-1-yl)propyl)-10H-phenothiazine (11h).



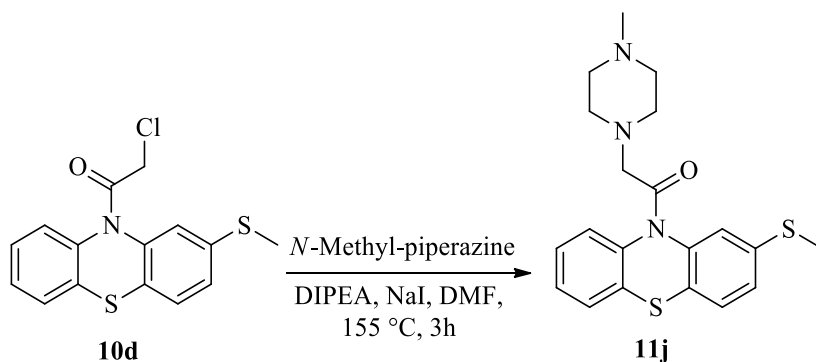
Yield: 57% (44.6 mg). **¹H NMR** (400 MHz CDCl₃) δ 7.24 (t, *J* = 8.0 Hz, 2H), 7.17-7.11 (m, 2H), 7.01 (d, *J* = 8.0 Hz, 1H), 6.94-6.63 (m, 7H), 3.92 (t, *J* = 8.0 Hz, 2H), 3.15 (t, *J* = 8.0 Hz, 4H), 2.57 (t, *J* = 8.0 Hz, 4H), 2.51 (t, *J* = 8.0 Hz, 2H), 2.00-1.96 (m, 2H) ppm. **¹³C NMR** (100 MHz CDCl₃) δ 151.4, 146.6, 144.6, 133.3, 129.2, 128.0, 127.6, 127.5, 124.8, 123.6, 123.0, 122.3, 119.8, 116.1, 115.9, 55.6, 53.5, 49.2, 45.4, 24.3 ppm. **LRMS** (ESI⁺): *m/z* = 436 [M + H]⁺. **HRMS** (ESI) *m/z* calcd. for C₂₅H₂₇ClN₃S [M + H] 436.1609, found 436.1618.

Synthesis of 2-chloro-10-(3-thiomorpholinopropyl)-10H-phenothiazine (11i).



Yield: 90% (60.9 mg). **¹H NMR** (400 MHz CDCl₃) δ 7.15-7.08 (m, 2H), 6.99 (d, *J* = 8.0 Hz, 1H), 6.93-6.81 (m, 4H), 3.88 (t, *J* = 8.0 Hz, 2H), 2.66-2.57 (m, 8H), 2.45 (t, *J* = 8.0 Hz, 2H), 1.91-1.85 (m, 2H) ppm. **¹³C NMR** (100 MHz CDCl₃) δ 146.5, 144.6, 133.2, 127.9, 127.6, 127.5, 124.8, 123.5, 122.9, 122.3, 115.9, 56.0, 55.8, 45.1, 28.1, 24.0 ppm. **LRMS** (ESI⁺): *m/z* = 377 [M + H]⁺. **HRMS** (ESI) *m/z* calcd. for C₁₉H₂₁ClN₂S₂ [M + H] 377.0834, found 377.0849.

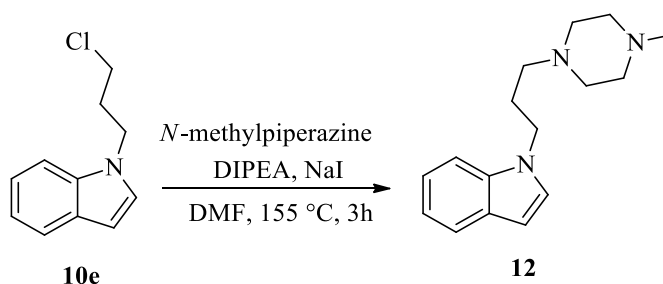
Synthesis of 2-(4-methylpiperazin-1-yl)-1-(2-(methylthio)-10H-phenothiazin-10-yl)ethanone (11j).



N-methylpiperazine (63.0 mg, 0.63 mmol, 4 eq.) was dissolved in a round bottom flask containing dry DMF (5 mL) and DIPEA (0.031 mL, 0.17 mmol, 1.1 eq.) under N₂ atmosphere. Then, 2-chloro-1-(2-(methylthio)-10H-phenothiazin-10-yl)ethanone (**10d**) (48.1 mg 0.15 mmol, 1 eq.) was added to the solution followed by NaI (4.5 mg, 0.03 mmol,

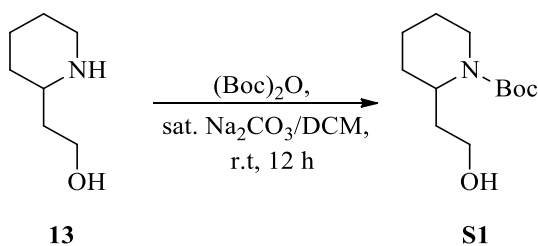
0.2 eq.). The mixture was left under N₂ atmosphere at 155 °C for 3 h. Then, the reaction mixture was quenched with water (10 mL) and extracted twice with EtOAc (20 mL). The combined organic layers were washed with brine (10 mL), dried over Na₂SO₄ and concentrated under reduced pressure giving a yellow-brown crude oil. The pure product **11j** was obtained as a brown solid after purification of the crude mixture by chromatography on silica gel, using EtOAc/MeOH/TEA (3.9:1:0.1) as eluent. **Yield:** 96% (55.4 mg). **¹H NMR** (400 MHz CDCl₃) δ 7.51-7.47 (m, 2H), 7.41 (d, *J* = 8.0 Hz, 1H), 7.32-7.26 (m, 2H), 7.22-7.18 (m, 1H), 7.10-7.08 (m, 1H), 3.30-3.31 (m, 2H), 2.47 (s, 3H), 2.44-2.27 (8H), 2.22 (s, 3H) ppm. **¹³C NMR** (100 MHz CDCl₃) δ 168.6, 139.3, 138.6, 137.9, 128.0, 127.9, 127.0, 126.9, 125.1, 124.9, 60.4, 54.9, 52.9, 45.9, 16.2 ppm. **LRMS** (ESI⁺): *m/z* = 386 [M + H]⁺. **HRMS** (ESI) *m/z* calcd. for C₂₀H₂₄N₃S₂O [M + H], 386.1355 found 386.1351.

Synthesis of 1-(3-(4-methylpiperazin-1-yl)propyl)-1H-indole (**12**).



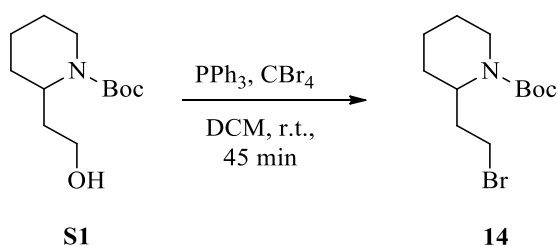
N-methylpiperazine (104.2 mg, 1.04 mmol, 4 eq.) was dissolved in a round bottom flask containing dry DMF (5 mL) and DIPEA (0.051 mL, 0.28 mmol, 1.1 eq.) under N₂ atmosphere. Then, 1-(3-chloropropyl)-1H-indole (50.2 mg, 0.26 mmol, 1 eq.) **10e** was added to the solution followed by NaI (10.5 mg, 0.07 mmol, 0.2 eq.). The mixture was left under N₂ atmosphere at 155 °C for 3 h. Then, the reaction mixture was quenched with water (10 mL) and extracted twice with EtOAc (20 mL). The combined organic layers were washed with brine (10 mL), dried over Na₂SO₄ and concentrated under reduced pressure giving a yellow-brown crude oil. The pure product **12** was obtained as a yellow oil after purification of the crude mixture by chromatography on silica gel, using hexane/EtOAc (4:1) as eluent. **Yield:** 63% (42.1 mg). **¹H NMR** (400 MHz CDCl₃) δ 7.61 (d, *J* = 8.0 Hz, 1H), 7.36 (d, *J* = 8.0 Hz, 1H), 7.18 (t, *J* = 8.0 Hz, 1H), 7.12 - 7.03 (m, 2H), 6.46 (d, *J* = 3.0 Hz, 1H), 4.19 (t, *J* = 6.0 Hz, 2H), 2.45 (m., 8H), 2.29 (s, 3H), 2.28-2.23 (m, 2H), 1.98 (m, 2H) ppm. **¹³C NMR** (100 MHz CDCl₃) δ 136.1, 128.6, 128.0, 121.4, 121.0, 119.3, 109.5, 101.0, 55.3, 54.9, 53.1, 46.1, 43.9, 27.4 ppm. **LRMS** (ESI⁺): *m/z* = 258 [M + H]⁺ **HRMS** (ESI) *m/z* calcd. for C₁₆H₂₄N₃ [M + H] 258.1965, found 258.1966.

***tert*-butyl 2-(2-hydroxyethyl)piperidine-1-carboxylate (S1).**



2-(piperidin-2-yl)ethanol **13** (200.2 mg, 1.55 mmol 1 eq.) was added to 10 mL mixture (1:1) of CH_2Cl_2 and Na_2CO_3 saturated solution in water (10 mL) in a round bottom flask. Di-*tert*-butyl dicarbonate (371.4 mg, 1.70 mmol, 1.1 eq.) was added to the stirring solution. The reaction mixture was allowed to stir under N_2 atmosphere for 12h at room temperature. Then, the reaction mixture was diluted with 10 mL of water and extracted twice with 20 mL of EtOAc. The combined organic layers were washed with brine, dried over Na_2SO_4 and concentrated under reduced pressure giving a yellow crude oil. The pure product **S1** was obtained as a yellow oil after purification of the crude mixture by chromatography on silica gel, using hexane/EtOAc (3:2) as eluent. **Yield:** 98% (314.4 mg). **^1H NMR** (400 MHz CDCl_3) δ 4.35-4.19 (m, 1H) 3.85-3.80 (m, 2H), 3.48-3.42 (m, 1H), 3.27 (br s, 1H), 2.59-2.52 (m, 1H), 1.81 (t, $J = 12.0$ Hz, 1H), 1.64-1.54 (m, 1H), 1.51-1.37 (m, 5H), 1.37 (s, 9H), 1.29-1.25 (m, 1H) ppm. **^{13}C NMR** (100 MHz CDCl_3) δ 155.0, 80.2, 58.7, 46.1, 39.4, 32.5, 28.5, 28.4, 25.6, 19.0 ppm. **LRMS** (ESI^+): $m/z = 230$ [$\text{M}+\text{Na}$] $^+$

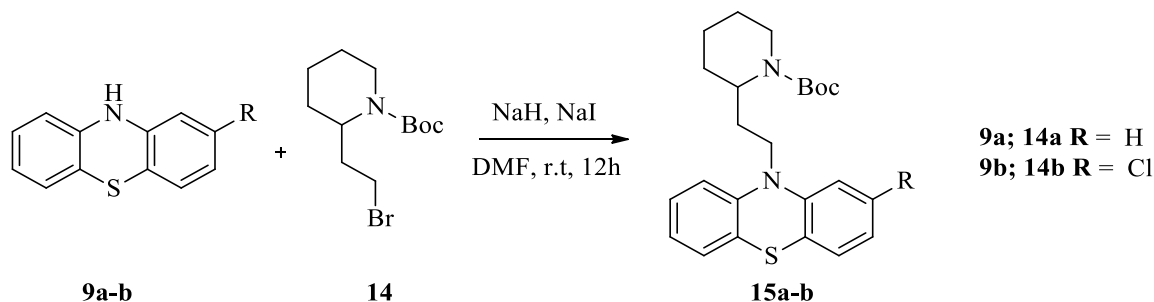
Synthesis of *tert*-butyl 2-(2-bromoethyl)piperidine-1-carboxylate (14).



To a solution of *tert*-butyl 2-(2-hydroxyethyl)piperidine-1-carboxylate (**S1**) (89.1 mg, 0.43 mmol, 1 eq.) in CH_2Cl_2 (10 mL) was added PPh_3 (123.3 mg, 0.47 mmol, 1.1 eq.) followed by a solution of CBr_4 (155.8 mg, 0.47 mmol, 1.1 eq.) in 20 mL of CH_2Cl_2 at r.t., and the mixture was allowed to stir for 45 min. Then, the reaction mixture was concentrated under reduced pressure giving a yellow crude oil. The obtained product was then immediately

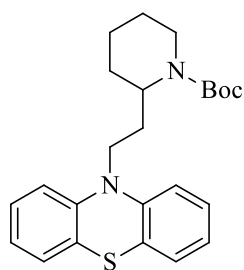
purified by chromatography on silica gel, using hexane/EtOAc (9:1) as eluent. The pure product **14** was obtained as a yellow oil. **Yield:** 79% (99.5 mg). **¹H NMR** (400 MHz CDCl₃) δ 4.35-4.31 (m, 1H) 4.02-3.84 (m, 1H), 3.33-3.19 (m, 2H), 2.70-2.64 (t, *J* = 12.0 Hz, 1H), 2.33-2.23 (m, 1H), 1.90-1.64 (m, 1H), 1.63-1.43 (m, 5H), 1.40 (s, 9H), 1.38-1.31 (m, 1H) ppm. **¹³C NMR** (100 MHz CDCl₃) δ 155.2, 79.6, 49.5, 38.7, 33.6, 30.3, 28.7, 28.5, 25.5, 19.2 ppm. **LRMS** (ESI⁺): *m/z* = 292 [M + H]⁺ 294 [M + H]⁺

General procedure for the synthesis of Boc-protected thioridazine derivatives (15a-b).



The appropriate 2-substituted phenothiazine (**9a-b**) (0.42 mmol, 1 eq.) was added to 10 mL of DMF in a double neck round bottom flask. NaH (19.3 mg, 0.52 mmol, 1.2 eq.) was added to the stirred solution at 0°C that then was allowed to reach r.t stirring for 20 minutes. Then, *t*-butyl 2-(2-bromoethyl)piperidine-1-carboxylate (**14**) (113.2 mg, 0.52 mmol 1.2 eq.) and NaI (2.98 mg, 0.02 mmol, 0.1 eq.) were added to the stirring solution. The reaction mixture was allowed to stir under N₂ atmosphere for 12h at r.t. Then, the reaction mixture was quenched with 20 mL of water and extracted twice with 20 mL of EtOAc. The combined organic layers were washed with brine, dried over Na₂SO₄ and concentrated under reduced pressure giving a yellow-brown crude oil. The obtained product was purified by chromatography on silica gel, using hexane/EtOAc (4:1) as eluent. The pure products **15a-b** were isolated as yellow-brown oil.

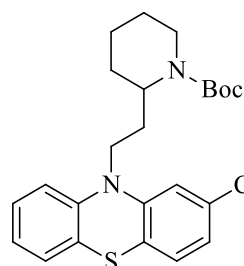
Synthesis of *tert*-butyl 2-(2-(10H-phenothiazin-10-yl)ethyl)piperidine-1-carboxylate (15a).



Yield: 45% (77.4 mg). **¹H NMR** (400 MHz CDCl₃) δ 7.16-7.12 (m, 4H), 6.93-6.89 (m, 2H), 6.84 (d, *J* = 8.0 Hz, 2H), 4.45-4.35 (m, 1H), 4.08-3.96 (m, 1H), 3.92-3.74 (m, 2H), 3.38-3.28 (m, 1H), 2.83-2.69 (m, 1H), 2.37-2.18 (m, 1H), 1.91-1.85 (m, 1H), 1.67-1.49 (m, 5H), 1.40 (s, 9H) ppm. **¹³C NMR** (100 MHz CDCl₃) δ 155.1, 145.3, 127.6, 127.3, 125.1, 122.5, 115.3, 79.4, 49.5, 38.7, 33.6, 30.3, 28.7, 28.5, 25.5, 19.2

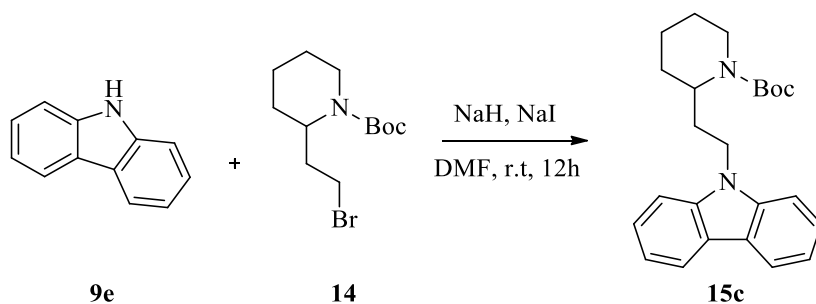
ppm. **LRMS** (ESI⁺): *m/z* = 411 [M + H]⁺.

Synthesis of *t*-butyl 2-(2-(2-chloro-10H-phenothiazin-10-yl)ethyl)piperidine-1-carboxylate (15b**).**



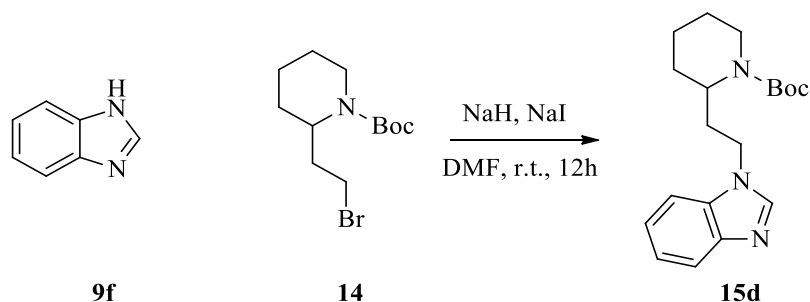
Yield: 61% (114.1 mg). **¹H NMR** (400 MHz CDCl₃) δ 7.17-7.11 (m, 2H) 7.02 (d, *J* = 8.0 Hz, 1H), 6.95-6.83 (m, 3H), 6.78 (d, *J* = 4.0 Hz, 1H), 4.44-4.39 (m, 1H), 4.38-4.35 (m, 1H), 4.05-4.00 (m, 1H), 3.88-3.79 (m, 2H), 2.78 (t, *J* = 12.0 Hz, 1H), 2.22-2.16 (m, 1H), 1.90-1.81 (m, 1H), 1.68-1.45 (m, 5H), 1.42 (s, 9H) ppm. **¹³C NMR** (100 MHz CDCl₃) δ 155.2, 146.7, 144.6, 133.4, 128.1, 127.5, 124.9, 123.0, 122.4, 115.7, 79.6, 48.8, 44.8, 39.1, 29.3, 28.5, 27.7, 25.6, 19.3 ppm. **LRMS** (ESI⁺): *m/z* = 468 [M+Na]⁺.

Synthesis of *t*-butyl 2-(2-(9H-carbazol-9-yl)ethyl)piperidine-1-carboxylate (15c**).**



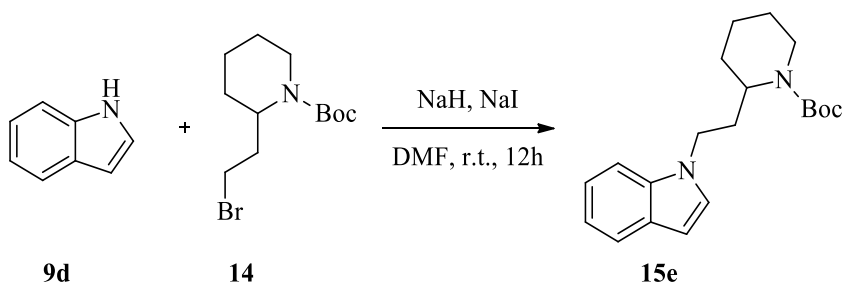
Carbazole (93.5 mg, 0.56 mmol, 1 eq.) **9e** was added to 5 mL of DMF in a double neck round bottom flask under N₂ atmosphere. NaH (26.2 mg, 0.68 mmol, 1.2 eq.) was added to the stirring solution at 0 °C which then was allowed to reach r.t stirring for 20 minutes. Then, *t*-butyl 2-(2-bromoethyl)piperidine-1-carboxylate **14** (199.1 mg, 0.68 mmol, 1 eq.) was added to the stirring solution. The reaction mixture was allowed to stir under N₂ atmosphere for 12 h at r.t. Then, the reaction mixture was quenched with 10 mL of water and extracted twice with 20 mL of EtOAc. The combined organic layers were washed with brine, dried over Na₂SO₄ and concentrated under reduced pressure giving a yellow-brown crude oil. The obtained product was purified by chromatography on silica gel, using hexane/EtOAc (4:1) as eluent. The pure product **15c** was obtained as a yellow oil. **Yield:** 61% (127.1 mg). **¹H NMR** (400 MHz CD₃OD) δ 8.37 (d, *J* = 7.5 Hz, 2H), 7.87-7.64 (m, 4H), 7.60-7.35 (m, 2H), 4.74 (m, 1H), 4.69-4.59 (m, 1H), 4.36-4.18 (m, 1H), 3.69-3.60 (m, 2H), 3.10-3.07 (m, 1H), 2.73-2.53 (m, 1H), 2.22 (m, 1H), 2.00-1.86 (m, 5H), 1.85-1.76 (m, 9H) ppm. **¹³C NMR** (100 MHz CD₃OD) δ 155.8, 140.6, 140.5, 125.9, 125.6, 123.4, 123.3, 120.4, 120.0, 119.1, 118.7, 110.8, 108.7, 80.1, 78.6, 40.2, 33.2, 28.5, 27.9, 27.8, 25.7, 19.1, 19.0 ppm. **LRMS** (ESI⁺): *m/z* = 401 [M+Na]⁺.

Synthesis of *t*-butyl 2-(2-(1H-benzo[d]imidazol-1-yl)ethyl)piperidine-1-carboxylate (15d).



benzo[d]imidazole **9f** (79.1 mg, 0.67 mmol, 1 eq.) was added to 5 mL of DMF in a double neck round bottom flask. NaH (11.5 mg, 0.80 mmol, 1.2 eq.) was added to the stirring solution at 0°C under N₂ atmosphere that then was allowed to reach r.t. stirring for 20 minutes. Then, *t*-butyl 2-(2-bromoethyl)piperidine-1-carboxylate **14** (233.2 mg, 0.80 mmol 1.2 eq.) and NaI (14.9 mg, 0.1 mmol, 0.1eq.) were added to the stirring solution. The reaction mixture was allowed to stir under N₂ atmosphere for 12 h at r.t. Then, the reaction mixture was quenched with 10 mL of water and extracted twice with 20 mL of EtOAc. The combined organic layers were washed with brine, dried over Na₂SO₄ and concentrated under reduced pressure giving a yellow-brown crude oil. The obtained product was purified by chromatography on silica gel, using hexane/EtOAc (4:1) as eluent. The pure product **15d** was obtained as a yellow oil. **Yield:** 63% (138.9 mg). **¹H NMR** (400 MHz CDCl₃) δ 7.91 (s, 1H), 7.84-7.67 (m, 1H), 7.39-7.31 (m, 1H), 7.31-7.09 (m, 2H), 4.49-4.19 (m, 1H), 4.10-3.90 (m, 2H), 2.81-2.65 (m, 1H), 2.38-2.18 (m, 1H), 1.96-1.77 (m, 1H), 1.72-1.44 (m, 7H), 1.44-1.29 (m, 9H) ppm. **¹³C NMR** (100 MHz CDCl₃) δ 155.2, 144.0, 143.2, 133.7, 122.9, 122.1, 120.6, 109.5, 79.9, 60.4, 42.4, 30.1, 28.9, 28.5, 25.5, 19.2, 14.2 ppm. **LRMS** (ESI⁺): *m/z* = 330 [M + H]⁺.

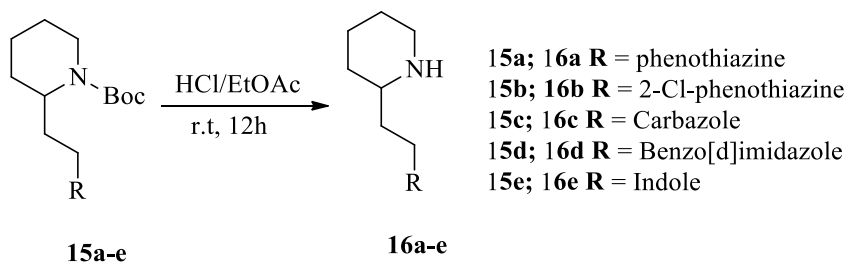
Synthesis of *tert*-butyl 2-(2-(1H-indol-1-yl)ethyl)piperidine-1-carboxylate (15e).



1H-indole **9d** (49.2 mg, 0.42 mmol, 1 eq.) was added to 5 mL of DMF in a double neck round bottom flask. NaH (20.0 mg, 0.50 mmol, 1.2 eq.) was added to the stirring solution at

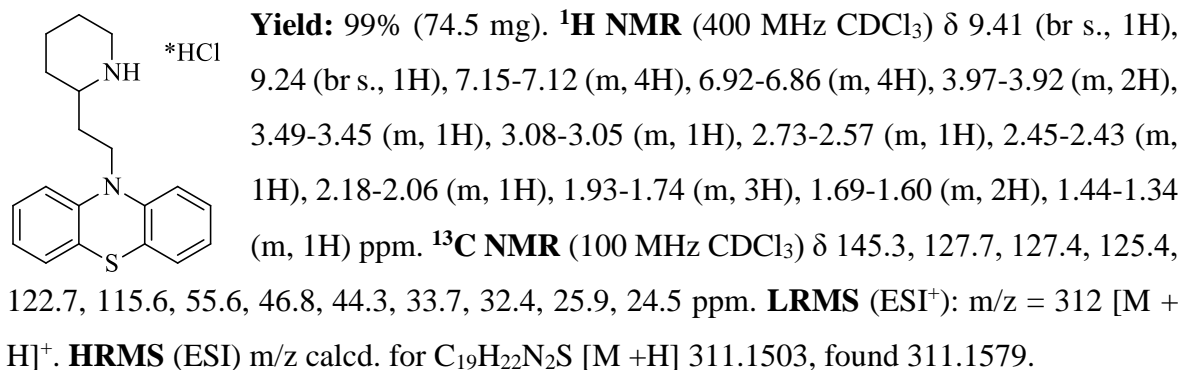
0°C under N₂ atmosphere that then was allowed to reach r.t stirring for 20 minutes. Then, *t*-butyl 2-(2-bromoethyl)piperidine-1-carboxylate **14** (145.0 mg, 0.50 mmol 1.2 eq.) and NaI (2.98 mg, 0.02 mmol, 0.1 eq.) were added to the stirring solution. The reaction mixture was allowed to stir under N₂ atmosphere for 12 h at r.t. Then, the reaction mixture was quenched with 10 mL of water and extracted twice with 20 mL of EtOAc. The combined organic layers were washed with brine, dried over Na₂SO₄ and concentrated under reduced pressure giving a yellow-brown crude oil. The obtained product was purified by chromatography on silica gel, using hexane/EtOAc (4:1) as eluent. The pure product **15e** was obtained as a yellow-brown oil. **Yield:** 42% (59.6 mg). **¹H NMR** (400 MHz CDCl₃) δ 7.62 (d, *J* = 8.0 Hz, 1H), 7.31 (d, *J* = 8.0 Hz, 1H), 7.22-7.18 (m, 1H), 7.12-7.07 (m, 2H), 6.48 (d, *J* = 4.0 Hz, 1H), 4.38-4.33 (m, 1H), 4.15-4.03 (m, 3H), 2.81 (t, *J* = 8.0 Hz, 1H), 2.31-2.21 (m, 1H), 1.93-1.86 (m, 1H), 1.68-1.58 (m, 6H), 1.45 (s, 9H) ppm **¹³C NMR** (100 MHz CDCl₃) δ 155.2, 135.8, 128.8, 127.9, 121.5, 121.1, 119.4, 109.2, 101.2, 79.7, 43.8, 30.7, 29.0, 28.6, 25.6, 19.2 ppm. **LRMS** (ESI⁺): *m/z* = 351 [M+Na]⁺.

General procedure for the synthesis of Thioridazine derivatives (16a-e).

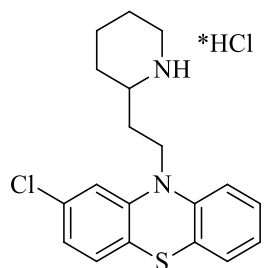


The appropriate Boc-protected compound **16a-e** (0.243 mmol 1 eq.) was added to a round bottom flask containing 10 mL saturated solution of HCl in EtOAc. Then, the reaction mixture was allowed to stir at room temperature for 12 h. The solvent was concentrated under reduced pressure giving a white solid as product of the reaction.

Synthesis of 10-(2-(piperidin-2-yl)ethyl)-10H-phenothiazine (16a).

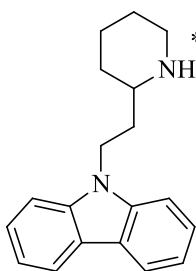


Synthesis of 2-chloro-10-(2-(piperidin-2-yl)ethyl)-10H-phenothiazine (16b).



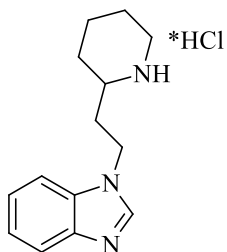
Yield: 94% (79.2 mg). **¹H NMR** (400 MHz CDCl₃) δ 9.54 (br s, 1H), 9.34 (br s, 1H), 7.19 (t, *J* = 8.0 Hz, 1H), 7.13 (d, *J* = 8.0 Hz, 1H), 7.04 (d, *J* = 8.0 Hz, 1H), 6.95-6.89 (m, 4H), 4.07-3.96 (m, 2H), 3.31 (d, *J* = 8.0 Hz, 1H), 3.12-3.04 (m, 1H), 2.77-2.68 (m, 1H), 2.50-2.42 (m, 1H), 2.13-2.09 (m, 1H), 1.85-1.69 (m, 6H) ppm. **¹³C NMR** (100 MHz CDCl₃) δ 146.6, 144.5, 133.3, 128.0, 127.6, 127.5, 125.1, 123.9, 123.1, 122.5, 115.9, 55.4, 46.7, 44.4, 33.5, 29.7, 25.8, 24.4 ppm. **LRMS** (ESI⁺): *m/z* = 367 [M+Na]⁺. **HRMS** (ESI) *m/z* calcd. for C₁₉H₂₁ClN₂S [M + H] 345.1113, found 345.1194.

Synthesis of 9-(2-(piperidin-2-yl)ethyl)-9H-carbazole (16c).



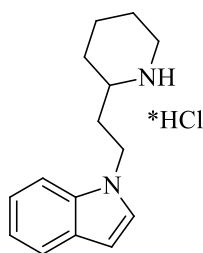
Yield: 95% (64.17 mg). **¹H NMR** (400 MHz CDCl₃) δ 9.66 (br s, 1H), 9.41 (br s, 1H), 8.02 (d, *J* = 8.0, 2H), 7.46-7.37 (m, 4H), 7.17 (t, *J* = 8.0, 2H), 4.51-4.43 (m, 1H), 4.31-4.25 (m, 1H), 3.38-3.36 (m, 1H), 3.02-2.90 (m, 1H), 2.70-2.67 (m, 1H), 2.49-2.48 (m, 1H), 2.18-2.12 (m, 1H), 1.88-1.61 (m, 6H) ppm. **¹³C NMR** (100 MHz CDCl₃) δ 140.0, 126.1, 122.9, 120.4, 119.3, 108.8, 55.5, 44.9, 39.5, 32.7, 30.0, 22.3, 22.0 ppm. **LRMS** (ESI⁺): *m/z* = 279 [M + H]⁺. **HRMS** (ESI) *m/z* calcd. for C₁₉H₂₂N₂ [M + H] 279.1782, found 279.1855.

Synthesis of 1-(2-(piperidin-2-yl)ethyl)-1H-benzo[d]imidazole (16d).



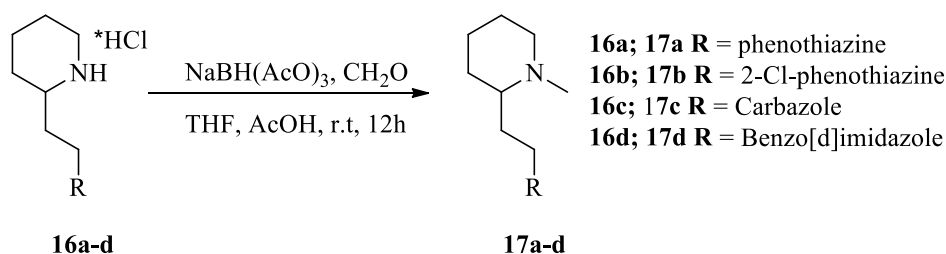
Yield: 90% (50.4 mg). **¹H NMR** (400 MHz CDCl₃) δ 10.17 (s 1H), 9.68 (br s, 2H), 7.82 (t, *J* = 8.0 Hz, 2H), 7.44-7.36 (m, 2H), 5.01-4.79 (m, 2H), 3.46-3.43 (m, 1H), 3.36-3.25 (m, 1H), 2.98-2.94 (m, 1H), 2.85-2.71 (m, 1H), 2.50-2.36 (m, 1H), 1.90-1.75 (m, 6H) ppm. **¹³C NMR** (100 MHz CDCl₃) δ 140.9, 130.7, 126.9, 126.7, 115.6, 112.7, 54.1, 45.0, 43.7, 33.4, 28.7, 22.3, 20.9 ppm. **LRMS** (ESI⁺): *m/z* = 230 [M + H]⁺. **HRMS** (ESI) *m/z* calcd. for C₁₄H₁₉N₃ [M + H] 230.1578, found 230.1652.

Synthesis of 1-(2-(piperidin-2-yl)ethyl)-1H-indole (16e).



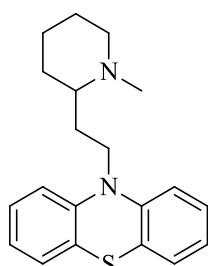
Yield: 94% (52.2 mg). **¹H NMR** (400 MHz CD₃OD) δ 7.42-7.34 (m, 1H), 7.24-7.19 (m, 1H), 7.10-7.01 (m, 2H), 6.90-6.80 (m, 2H), 4.12-4.01 (m, 2H), 3.39-3.24 (m, 1H), 2.95-2.89 (m, 2H), 2.82-2.73 (m, 1H), 2.75-2.59 (m, 1H), 2.49-2.40 (m, 1H), 2.38-2.29 (m, 2H), 1.84-1.67 (m, 3H) ppm. **¹³C NMR** (100 MHz (CD₃)₂SO) δ 135.8, 127.9, 121.8, 121.1, 119.6, 119.1, 109.7, 54.2, 45.2, 43.6, 33.3, 28.8, 22.1, 20.8 ppm. **LRMS** (ESI⁺): m/z = 229 [M + H]⁺. **HRMS** (ESI) m/z calcd. for C₁₅H₂₀N₂ [M + H] 229.1626, found 229.1701.

General procedure for the synthesis of thioridazine derivatives (17a-d).



The appropriate compounds **16a-d** (0.14 mmol, 1 eq.) was added to a round bottom flask containing THF (5 mL) and formaldehyde aqueous solution 37% w/v (0.75mL, 0.28 mmol, 2 eq.). The solution was then allowed to stir at room temperature for 30 minutes. Then, NaBH(AcO)₃ (59.2 mg, 0.28 mmol, 2.0 eq.) was added. The reaction was allowed to stir for 12h at r.t. Then the solution was quenched with (20 mL) NaOH 1N solution. The mixture was allowed to stir for 20 minutes then the organic solvent was removed through reduced pressure evaporation. The residue was diluted with EtOAc, extracted with EtOAc (3 x 10 mL) and dried over anhydrous MgSO₄. The product was purified by chromatography on silica gel, using EtOAc/MeOH/TEA (3.9:1:0.1) as eluent affording the product as a yellow-brown oil.

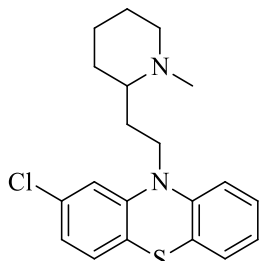
Synthesis of 10-(2-(1-methylpiperidin-2-yl)ethyl)-10H-phenothiazine (17a).



Yield: 47% (21.3 mg). **¹H NMR** (400 MHz CDCl₃) δ 7.19-7.07 (m, 4H), 6.95-6.85 (m, 4H), 3.95 (ddd, *J* = 13.9, 8.6, 5.5 Hz, 1H), 3.89-3.77 (m, 1H), 2.89-2.72 (m, 1H), 2.22-2.16 (m, 3H), 2.16-1.99 (m, 3H), 1.93-1.80 (m, 1H), 1.71 (d, *J* = 10.0 Hz, 1H), 1.64-1.50 (m, 2H), 1.34-1.18 (m, 3H) ppm. **¹³C NMR** (100 MHz CDCl₃) δ 145.4, 127.6, 127.3, 125.4, 122.5, 115.6, 62.2, 57.0, 43.9, 43.1, 30.8, 30.0, 25.7, 24.2 ppm. **LRMS** (ESI⁺):

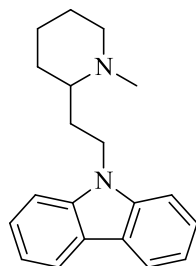
$m/z = 325$ $[M + H]^+$. **HRMS** (ESI) m/z calcd. for $C_{20}H_{25}N_2S$ $[M + H]$ 325.1733, found 325.1735.

Synthesis of 2-chloro-10-(2-(1-methylpiperidin-2-yl)ethyl)-10H-phenothiazine (17b).



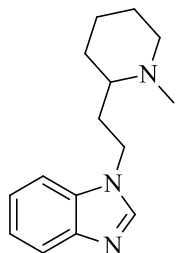
Yield: 38% (19.1 mg). **1H NMR** (400 MHz $CDCl_3$) δ 7.11-7.02 (m, 2H), 6.94 (d, $J = 8.0$ Hz, 1H), 6.85 (t, $J = 7.0$ Hz, 1H), 6.82-6.73 (m, 3H), 3.91-3.78 (m, 1H), 3.78-3.63 (m, 1H), 2.85-2.68 (m, 1H), 2.14 (s, 3H), 2.07-1.95 (m, 3H), 1.85-1.72 (m, 1H), 1.69-1.58 (m, 2H), 1.56-1.46 (m, 2H), 1.28-1.11 (m, 2H) ppm. **^{13}C NMR** (100 MHz $CDCl_3$) δ 147.5, 145.2, 133.8, 128.4, 128.1, 127.8, 126.0, 125.1, 123.6, 122.8, 116.8, 116.5, 62.5, 57.1, 44.4, 42.3, 30.9, 29.7, 25.6, 24.1 ppm. **LRMS** (ESI $^+$): $m/z = 359$ $[M + H]^+$. **HRMS** (ESI) m/z calcd. for $C_{20}H_{24}ClN_2S$ $[M + H]$ 359.1343, found 359.1347.

Synthesis of 9-(2-(1-methylpiperidin-2-yl)ethyl)-9H-carbazole (17c).



Yield: 67% (27.4 mg). **1H NMR** (400 MHz $CDCl_3$) δ 8.10 (d, $J = 7.0$ Hz, 2H), 7.52-7.32 (m, 4H), 7.29-7.06 (m, 2H), 4.52-4.38 (m, 1H), 4.38-4.22 (m, 1H), 2.97-2.82 (m, 1H), 2.33 (s, 3H), 2.17-2.06 (m, 2H), 2.06-1.94 (m, 2H), 1.79 (d, $J = 12.0$ Hz, 2H), 1.67-1.60 (m, 2H), 1.40-1.27 (m, 2H) ppm. **^{13}C NMR** (100 MHz $CDCl_3$) δ 140.2, 125.7, 123.0, 120.5, 118.8, 108.6, 61.7, 57.0, 43.0, 39.2, 31.5, 30.7, 25.6, 24.4 ppm. **LRMS** (ESI $^+$): $m/z = 293$ $[M + H]^+$. **HRMS** (ESI) m/z calcd. for $C_{20}H_{24}N_2$ $[M + H]$, 293.19 found 293.2014.

Synthesis of 1-(2-(1-methylpiperidin-2-yl)ethyl)-1H-benzo[d]imidazole (17d).



Yield: 70% (23.8 mg). **1H NMR** (400 MHz CD_3OD) δ 8.86 (s, 1H), 8.33-8.22 (m, 2H), 7.99-7.90 (m, 2H), 5.03-4.95 (m, 2H), 3.55-3.50 (m, 1H), 2.90 (s, 3H), 2.70-2.42 (m, 4H), 2.28-2.24 (m, 2H), 2.00-1.80 (m, 4H) ppm. **^{13}C NMR** (100 MHz CD_3OD) δ 144.0, 143.3, 134.0, 123.7, 122.9, 119.6, 110.7, 62.2, 57.1, 42.1, 32.8, 30.6, 30.1, 25.4, 24.1 ppm. **LRMS** (ESI $^+$): $m/z = 244$ $[M + H]^+$. **HRMS** (ESI) m/z calcd. for $C_{15}H_{22}N_3$ $[M + H]$ 244.1808, found 244.1811.

5.2.2. Virtual molecular hybridization approach for the synthesis of novel antitubercular agents effective against Multidrug-Resistant Mycobacteria.

5.2.2.1. Biology.

Bacterial Strains and Growth Conditions: The bacterial species used in this study were *Mycobacterium smegmatis* mc²155 (ATCC 700084), *Mycobacterium aurum* (ATCC23366), *Mycobacterium bovis* BCG Pasteur (ATCC 35734), *Mycobacterium tuberculosis* mc²7000,^{214–216} *Mycobacterium tuberculosis* H₃₇Rv (ATTC27294), and two MDR-TB clinical isolates (MDR1 and MDR2) obtained from Royal Free Hospital NHS Trust, London, UK. The bacterial growth was carried out by Dr. Bhakta group at Birbeck College London. The cell lines utilized for cytotoxicity studies were the murine macrophage cell line RAW264.7 (ATCC TIB-71) and the human peripheral blood monocyte-derived cell line THP-1. Mycobacterial species were cultured in either Middlebrook 7H9 broth or Middlebrook 7H10 agar media supplemented with albumin–dextrose–catalase (ADC) or oleic acid–albumin–dextrose–catalase (OADC) enrichments, respectively, purchased from BD Biosciences. All reagents were purchased from Sigma-Aldrich unless stated otherwise.

Bacterial Growth Inhibition Assays. Antimycobacterial Activity: This assay was conducted by Dr. Bhakta group at Birbeck College London. HT-SPOTi was performed based on previously published protocols^{217,218} to assess the minimum inhibitory concentrations of the compounds on *M. aurum*,²¹⁹ *M. tuberculosis* H₃₇Rv, and the MDR strains of the pathogen. Briefly, the assay was conducted in a semiautomated 96-well plate format. The compounds were dissolved in a suitable solvent to a concentration of 50 mg/mL and serially diluted (2-fold dilutions). Two microliters of each dilution was dispensed into a well of a 96-well plate to which 200 µL of Middlebrook 7H10 agar medium kept at 55 °C supplemented with 0.05% (v/v) glycerol and 10% (v/v) OADC was added. The concentration range of the compounds used was 500 – 0.5 µg/mL. Wells with no compounds (DMSO only) and with isoniazid were used as experimental controls. To all the plates, a drop (2 µL) of early-to mid-log bacterial culture containing 2 × 10³ colony forming units (CFUs) was spotted in the middle of each well, and the plates were incubated at 35 or 37°C, depending on the bacterial species, until distinct spots were observed in the control wells (this took 4 days in the case of *Mycobacterium aurum*, 7 days in the case of *Mycobacterium tuberculosis* H₃₇Rv, and 9 days for the drug-resistant clinical isolates). The MICs were determined as the lowest concentration of the compound where mycobacterial growth was completely inhibited. The MIC of the compounds against *Mycobacterium smegmatis* mc²155, *Mycobacterium bovis* BCG, and *Mycobacterium tuberculosis* mc²7000 were calculated by standard MABA as

previously described.²¹⁴ Briefly, 200 μ L of sterile deionized water was added to all outer-perimeter wells of a sterile 96-well plate (Corning Inc., Corning, NY) to minimize evaporation of the medium in the test wells during incubation. The wells in rows B–G in columns 3–11 received 100 μ L of 7H9 medium containing 0.2% casamino acids, 24 μ g/mL pantothenate, and 10% OADC (Beckton Dickinson, Sparks, MD). Compounds were added to rows B–G followed by 1:2 serial dilutions across the plate to column 10, and 100 μ L of excess medium was discarded from the wells in column 10. The bacterial culture at 0.5 McFarland standard diluted 1:25 (100 μ L) was added to the wells in rows B–G in columns 2–11, where the wells in column 11 served as drug-free controls. The plates were sealed with parafilm and were incubated at 37°C. A freshly prepared 1:1 mixture of Alamar Blue (Celltiter-Blue, Promega Corp, Madison, WI) reagent and 10% Tween 80 (50 μ L) was added, and the plates reincubated at 37°C for 24 h.

Eukaryotic Cell Toxicity and Selectivity Indices: The eukaryotic cell toxicity test was carried out by Dr. Bhakta group at Birbeck College London. The cell lines were grown and maintained in RPMI-1640 supplemented with 10% FBS incubated at 37°C with 5% CO₂ in a humidified incubator. For the experiment, 2 μ L of the 50 mg/mL stock solution of each compound was diluted in 200 μ L of RPMI-1640 medium in the first row of a 96-well microplate and 2-fold dilutions were performed along the rows, leaving the last one (row H) as a solvent control. Then 100 μ L containing 105 cells/mL of confluent murine macrophage cells (RAW 264.7) or THP-1 cells in logarithmic growth phase were added to each well. The plates were incubated at 37°C in a humidified CO₂ incubator (5% CO₂) for 48 h. Each well was washed twice with 1 \times PBS, and 170 μ L of fresh RPMI-1640 was added to each well, followed by 30 μ L of 0.01% Trypan Blue. As THP-1 cells are suspension cultures, the plates were centrifuged between the washing steps. After overnight incubation, the change in colour was observed and the fluorescence intensity was measured at 560/590 nm ($\lambda_{ex}/\lambda_{em}$).

Assaying Whole-Cell Drug Efflux Pump Inhibition: The assay was modified from a previously published protocol.²²⁰ The experiments were carried out by Dr. Bhakta group at Birbeck College London. Early log phase cells of *M. aurum* (OD₆₀₀ ~ 0.8) were taken and the OD₆₀₀ was adjusted to 0.4 by diluting the cells with culture medium. The cells were collected by centrifugation and resuspended in an equivalent volume of 1 \times PBS. The test samples contained (4–6) \times 10⁷ bacteria/mL in PBS, 0.4% glucose (as a source of energy for efflux pumps activity), 0.5 mg/L ethidium bromide (as a substrate for efflux pumps), and the compounds being tested at 1/4 \times MIC concentrations. Blank samples contained all of the

components mentioned above, except the bacterial suspension, which was replaced with 1× PBS. Verapamil, a known efflux pump inhibitor, was used as the positive control at a concentration of 125 µg/mL. Compounds **I** and **II** were also included in the experiment to obtain a comparison between them and the newly synthesized compounds with regard to their efflux inhibitory properties. The experiment was performed in a 96-well plate that was placed in a fluorimeter (FLUOstar OPTIMA, BMG Labtech), and the instrument was programmed with the following parameters: wavelengths of 544 and 590 nm for excitation and detection of fluorescence, gain 2200, a temperature of 37 °C, and a cycle of measurement every minute for a total period of 60 min. The accumulation or efflux of ethidium bromide was monitored for the mentioned period on a real-time basis.

5.2.2.2. Computational details.

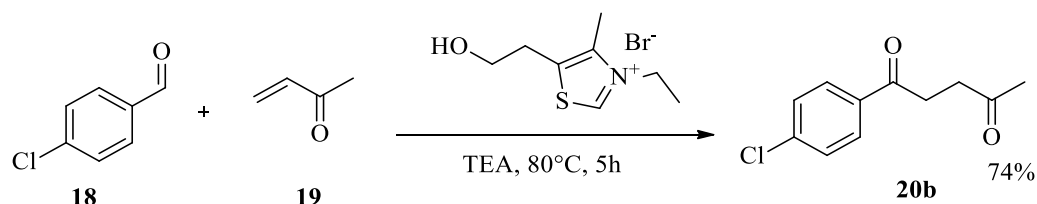
All the computational analysis have been performed by by Prof. Fabrizio Manetti at the University of Siena. The structures of all the molecules were sketched using Maestro (Maestro, version 9.2; Schrodinger LLC, New York, 2011) and then subjected to the program LigPrep to generate high-quality, all-atom 3D structures to be used as the input for the next calculations. The OPLS_2005 force field was applied, and possible ionization states were generated for the structures at pH 7 ± 2 using Epik. Conformers were generated by MacroModel (MacroModel, version 9.9; Schrodinger LLC, New York, 2011) with the Systematic Pseudo Monte Carlo (a systematic torsional sampling protocol) search algorithm and OPLS-2005 force field with implicit GB/SA distance-dependent dielectric solvent model (water as the solvent) at a cut-off root-mean-square deviation of 0.5 with 1000 steps. All the conformers were subsequently minimized using Polak–Ribiere conjugate gradient minimization with 5000 iterations. For each molecule, a conformer set with a maximum energy difference of 25 kcal/mol relative to the global energy minimum conformer was stored.

Both **I** and **II** were used to build three-dimensional common feature models comprised of chemical features common to the two compounds. Considering the reduced number of compounds and the fact that their antimycobacterial activity was assayed by different research groups with different tests, we chose to apply a common feature hypothesis generation routine, instead of building a quantitative model. Phase software (Phase, version 3.3, Schrodinger LLC, New York, 2011.) has been applied to generate the models. Minimum and maximum number of sites for all the features were set to 4 and 5, respectively. Only the positively ionisable group (P) and the hydrophobic region (H) features were used to build a

series of hypotheses, while the aromatic ring (R) feature was not further considered by the software because it was not present in the structure of **II**. The resulting four-feature hypotheses were constituted by two H and two P features.

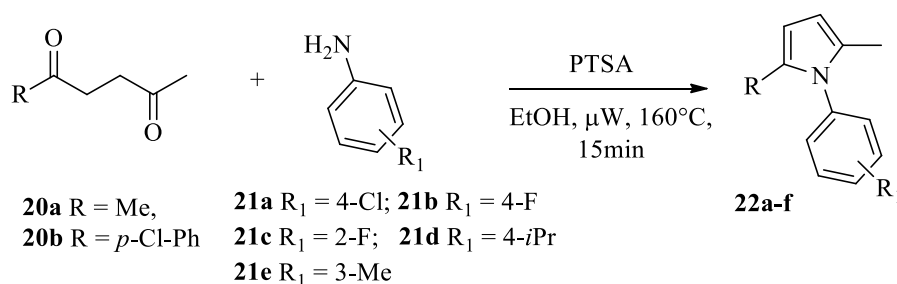
5.2.2.3. Chemistry.

Synthesis of 1-(4-chlorophenyl)pentane-1,4-dione (**20b**).



4-chlorobenzaldehyde (799.4 mg, 5.69 mmol, 1.2 eq.) **18** was dissolved in a dry round bottom flask containing a solution of but-3-en-2-one (0.395 mL, 4.74 mmol, 1 eq.) **19** and 3-ethyl-5-(2-hydroxyethyl)-4-methylthiazol-3-ium bromide (597.2 mg, 2.37 mmol, 0.2 eq) in TEA (2.113 mL 14.22 mmol, 3 eq.). The reaction mixture was allowed to stir at 80 °C for 5 h under N₂ atmosphere. Then, the reaction mixture was quenched with HCl 2N (20 mL) and the product was extracted twice with DCM (20 mL). The organic layer were collected and washed with NaHCO₃ (20 mL) and brine (20 mL), dried over Na₂SO₄ and concentrated under reduced pressure giving a yellow-brown crude oil. The obtained product **20b** was purified by chromatography on silica gel, using hexane/EtOAc (7:3) as eluent. The pure product **20b** was obtained as a pale yellow oil. **Yield:** 74% (884.2 mg). **¹H NMR** (400 MHz CDCl₃) δ 7.91-7.78 (d, *J* = 8.0 Hz, 2H), 7.45-7.31 (d, *J* = 8.0 Hz, 2H), 3.16 (t, *J* = 8.0, Hz, 2H), 2.82 (t, *J* = 8.0 Hz, 2H), 2.19 (s, 3H) ppm. **¹³C NMR** (100 MHz CDCl₃) δ 207.1, 197.3, 139.6, 135.0, 129.5, 128.9, 37.0, 32.3, 30.1 ppm. **LRMS** (ESI⁺): *m/z* = 211 [M + H]⁺.

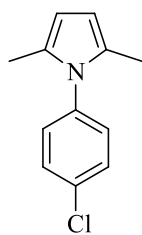
General procedure for the synthesis of pyrroles **22a-f**.



The appropriate aniline **21** (1 mmol 1 eq.) was dissolved in a round bottom flask containing a solution of EtOH (15 mL), and the appropriate methyl keton **20a,b** (1 mmol 1 eq.) PTSA

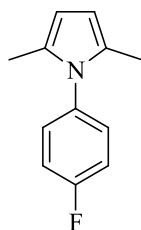
(172.2 mg, 1 mmol 1 eq.). The reaction was allowed to stir at 160°C under microwave irradiation for 15 min. Then the reaction was quenched with NaHCO₃ saturated aqueous solution (20 mL) and the solvent was concentrated through reduced pressure evaporation. The crude product was diluted in EtOAc (20 mL). The combined organic layers were washed with brine (20 mL), dried over Na₂SO₄ and concentrated under reduced pressure giving a yellow-brown crude oil. The obtained product (**22a-f**) was purified by chromatography on silica gel, using hexane/EtOAc (4:1) as eluent affording a yellow-brown oil.

Synthesis of 1-(4-chlorophenyl)-2,5-dimethyl-1H-pyrrole (22a**).**²²¹



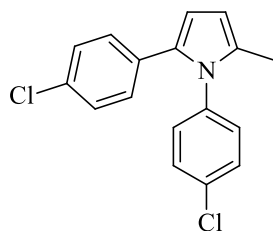
Yield: 93% (190.6 mg) **¹H NMR** (400 MHz CDCl₃) δ 7.36 (d, *J* = 8.5 Hz, 2H), 7.08 (d, *J* = 8.5 Hz, 2H), 5.81 (s, 2H), 1.93 (s, 6H) ppm. **¹³C NMR** (100 MHz CDCl₃) δ 137.9, 133.9, 129.9, 129.7, 129.1, 106.4, 13.3 ppm. **GC-MS** *m/z* (ES+) *m/z*: 205 [M]⁺

Synthesis of 1-(4-fluorophenyl)-2,5-dimethyl-1H-pyrrole (22b**).**²²¹



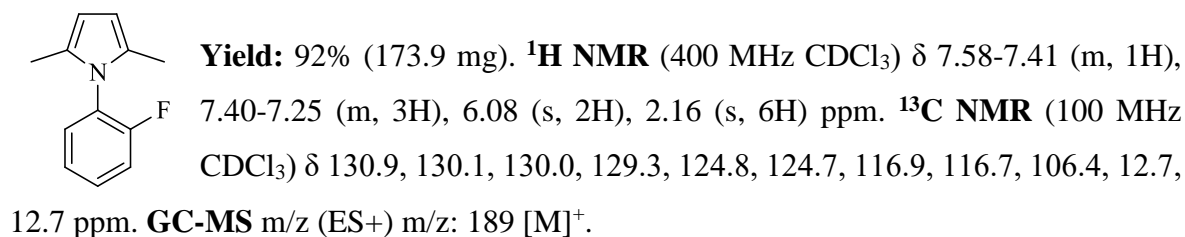
Yield: 98% (186.2 mg). **¹H NMR** (400 MHz CDCl₃) δ 7.25-7.10 (d, *J* = 8.0 Hz, 2H), 7.20 (d, *J* = 8.0 Hz, 2H), 6.04-5.80 (s, 2H), 2.22-1.92 (s, 6H) ppm. **¹³C NMR** (100 MHz CDCl₃) 135.2, 130.1, 130.0, 128.9, 116.2, 116.0, 106.1, 13.0 ppm. **GC-MS** *m/z* (ES+) *m/z* 190 [M]⁺.

Synthesis of 1,2-bis(4-chlorophenyl)-5-methyl-1H-pyrrole (22c**).**

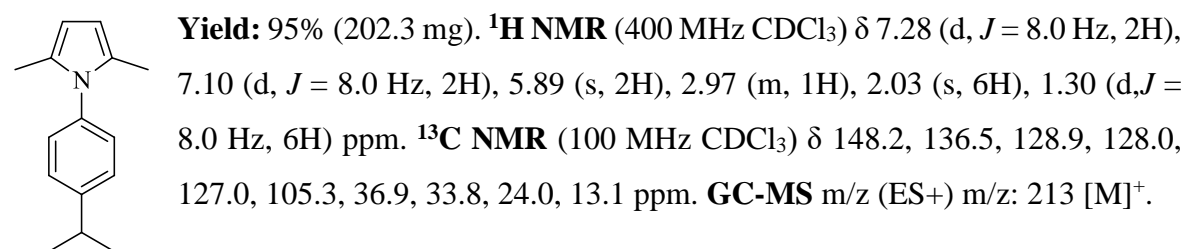


Yield: 90% (270.2 mg). **¹H NMR** (400 MHz CDCl₃) δ 7.33 (d, *J* = 8.0 Hz, 2H), 7.11 (d, *J* = 8.0 Hz, 2H), 7.06 (d, *J* = 8.0 Hz, 2H), 6.94 (d, *J* = 8.0 Hz, 2H), 6.41-6.17 (d, *J* = 4.0 Hz, 1H), 6.07 (d, *J* = 4.0 Hz, 1H), 2.11 (s, 3H) ppm. **¹³C NMR** (100 MHz CDCl₃) δ 163.2, 160.8, 137.7, 135.1, 129.7, 129.3, 129.0, 128.8, 128.3, 117.3, 117.0, 105.8, 13.3 ppm. **GC-MS** *m/z* (ES+) *m/z* 301 [M]⁺.

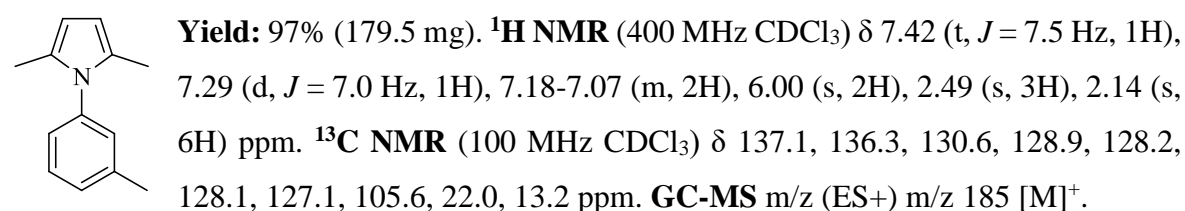
Synthesis of 1-(2-fluorophenyl)-2,5-dimethyl-1H-pyrrole (22d).²²¹



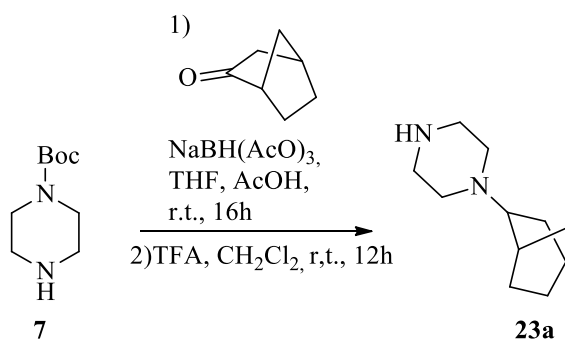
Synthesis of 1-(4-isopropylphenyl)-2,5-dimethyl-1H-pyrrole (22e).²²¹



Synthesis of 2,5-dimethyl-1-(m-tolyl)-1H-pyrrole (22f).²²¹



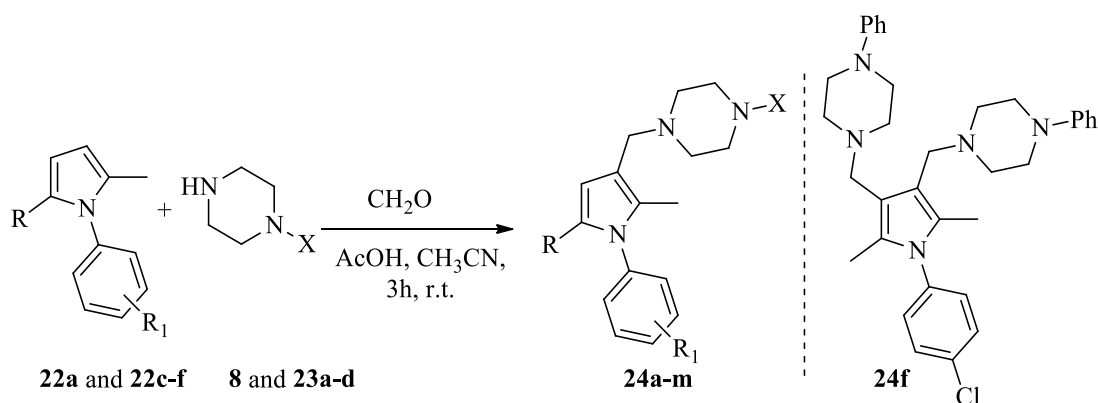
Synthesis of 1-(Bicyclo[2.2.1]heptan-2-yl)piperazine 23a.



The Boc-piperazine **7** (372.5 mg, 2 mmol, 1eq.) and bicyclo[2.2.1]heptan-2-one (220.3 mg, 2 mmol, 1 eq.) were dissolved in THF (8 mL), and the resulting mixture was stirred for 5

min. The reaction was cooled at 0 °C, and then NaBH(AcO)₃ (507.3 mg, 2.4 mmol, 1.2 eq.) and AcOH (0.116 mL, 2 mmol, 1 eq.) were carefully added. The resulting mixture was stirred at r.t. for 16 h. The reaction was quenched with NaOH (1 N, 20 mL) and the product was extracted with EtOAc (3 × 25 mL). The organic layers were gathered, dried over MgSO₄, and the solvent was evaporated to give the crude piperazine derivative, which were filtered through a pad of silica gel (eluent EtOAc/petroleum ether 1:1). The filtered compounds were then dissolved in DCM (4 mL) and treated with 1 mL of TFA. The resulting mixture was stirred at r.t. for 12 h. The solvents were removed, and the crude compound was dissolved in EtOAc (10 mL) and washed several times with 1 N NaOH (20 mL). The organic phase was dried over MgSO₄ and the solvent was evaporated to yield the crude piperazine **23a** which was purified by column chromatography using petroleum ether/EtOAc 1:1 as eluent. The pure piperazine **23a** was obtained as a pale yellow solid. **Yield:** 95% (343.4 mg). **¹H NMR** (400 MHz CDCl₃) δ 2.88–2.82 (m, 5H), 2.28 (br s, 3H), 2.20–2.09 (m, 3H), 1.67–1.60 (m, 2H), 1.41–1.39 (m, 1H), 1.28–1.19 (m, 4H), 0.82–0.79 (m, 1H) ppm. **LRMS** (ESI⁺): m/z = 181 [M + H]⁺.

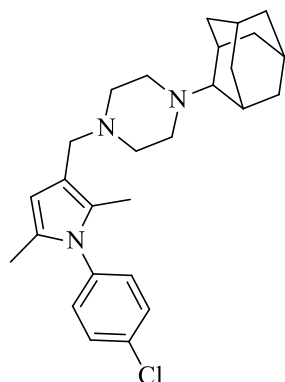
General procedure for the synthesis of pyrrole derivatives 24a–m.



Following the Mannich reaction, to a stirred solution of an appropriate pyrrole **22a**, **22c-f** (1.5 mmol, 1 eq.) in acetonitrile (5 mL) were added a mixture of the appropriate piperazine **8**, **23a-d** (1.5 mmol, 1 eq.), formaldehyde (40% in water) (1.5 mmol 1 eq.), and acetic acid (0.087 mL, 1.5 mmol, 1 eq.) which was added dropwise. After the addition was complete, the mixture was stirred at r.t. for 3 h. The mixture was then treated with a solution of sodium hydroxide (20%, w/v) (20 mL) and extracted with EtOAc (10 mL). The organic extracts

were combined, washed with water, and then dried over MgSO₄. After removal of solvent, the residue was purified by column chromatography, using silica gel and petroleum ether/ethyl acetate (4:1 v/v) as eluent affording the desired product as a yellow-brown oil.

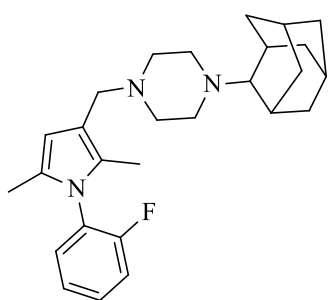
Synthesis of 1-(Adamantan-2-yl)-4-((1-(4-chlorophenyl)-2,5-dimethyl-1H-pyrrol-3-yl)methyl)piperazine (24a).



Yield: 56% (367.1 mg). **¹H NMR** (400 MHz CDCl₃) δ 7.41 (d, *J* = 8.5 Hz, 2H), 7.12 (d, *J* = 8.5 Hz, 2H), 5.92 (s, 1H), 3.36 (s, 2H), 2.50 (br s, 4H), 2.05–2.02 (m, 6H), 1.98 (s, 3H), 1.95 (s, 3H), 1.85–1.72 (m, 5H), 1.68–1.62 (m, 5H), 1.37–1.34 (m, 3H) ppm. **¹³C NMR** (100 MHz CDCl₃) δ 137.7, 133.4, 129.7, 129.3, 127.6, 126.8, 115.2, 108.7, 67.9, 54.4, 53.5, 49.6, 37.9, 37.3, 31.6, 31.4, 29.0, 27.6, 27.4, 22.7, 14.2, 12.9, 11.0 ppm. **LRMS** (ESI⁺): *m/z* = 438 [M + H]⁺. **HRMS** (ESI) calcd for C₂₇H₃₇ClN₃ (M + H⁺) 438.2671, found

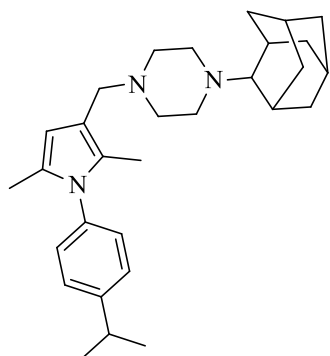
438.2664.

Synthesis of 1-(Adamantan-2-yl)-4-((1-(2-fluorophenyl)-2,5-dimethyl-1H-pyrrol-3-yl)methyl)piperazine (24b).



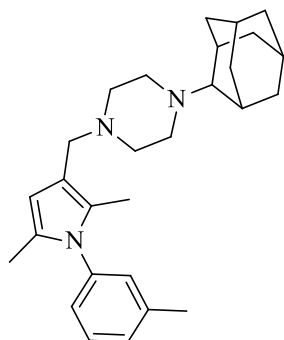
Yield: 45% (284.8 mg). **¹H NMR** (400 MHz CDCl₃) δ 7.37–7.36 (m, 1H), 7.22–7.17 (m, 3H), 5.95 (s, 1H), 3.36 (s, 2H), 2.59–2.29 (br s, 4H), 2.08–2.03 (m, 6H), 1.97 (s, 3H), 1.93 (s, 3H), 1.83–1.75 (m, 5H), 1.67–1.62 (m, 5H), 1.36–1.24 (m, 3H) ppm. **¹³C NMR** (100 MHz CDCl₃) δ 159.81, 157.31, 130.84, 129.6, 128.06, 127.2, 126.9, 124.5, 124.4, 116.7, 116.5, 115.3, 108.6, 67.9, 54.6, 53.6, 49.6, 39.3, 37.3, 31.9, 31.4, 29.0, 27.6, 27.5, 22.7, 14.2, 12.4, 10.5 ppm. **LRMS** (ESI⁺): *m/z* = 422 [M + H]⁺. **HRMS** (ESI) calcd for C₂₇H₃₇FN₃ (M + H⁺) 422.2966, found 422.2889.

Synthesis of 1-(Adamantan-2-yl)-4-((1-(4-isopropylphenyl)-2,5-dimethyl-1H-pyrrol-3-yl)methyl)piperazine (24c).



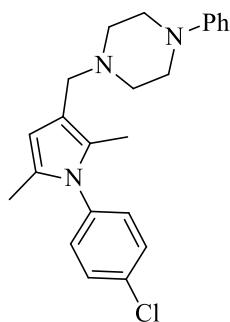
Yield: 51% (340.4 mg). **¹H NMR** (400 MHz CDCl₃) δ 7.27–7.24 (m, 2H), 7.10–7.04 (m, 2H), 5.91 (s, 1H), 3.46 (s, 2H), 2.97–2.92 (m, 1H), 2.52 (br s, 4H), 2.06–2.03 (m, 6H), 1.95 (s, 3H), 1.93 (s, 3H), 1.83–1.75 (m, 5H), 1.68–1.62 (m, 5H), 1.29 (s, 3H), 1.27 (s, 3H), 1.25 (m, 3H) ppm. **¹³C NMR** (100 MHz CDCl₃) δ 148.2, 136.6, 128.2, 128.1, 127.9, 127.1, 126.9, 108.0, 67.9, 54.5, 53.4, 50.8, 49.5, 37.9, 37.3, 33.8, 31.6, 31.4, 29.0, 27.6, 27.4, 24.0, 22.7, 14.2, 12.9, 11.2, 11.0 ppm. **LRMS** (ESI⁺): m/z = 446 [M + H]⁺. **HRMS** (ESI) calcd for C₃₀H₄₄N₃ (M + H⁺) 446.3530, found 446.3523.

Synthesis of 1-(Adamantan-2-yl)-4-((1-(3-methylphenyl)-2,5-dimethyl-1H-pyrrol-3-yl)methyl)piperazine (24d).



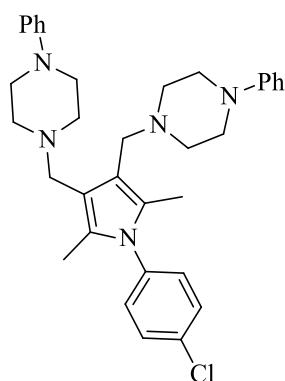
Yield: 48% (300.2 mg). **¹H NMR** (400 MHz CDCl₃) δ 7.32–7.29 (m, 1H), 7.18–7.16 (m, 1H), 6.99–6.95 (m, 2H), 5.91 (s, 1H), 3.39 (s, 2H), 2.53 (br s, 4H), 2.38 (s, 3H), 2.03 (m, 6H), 1.99 (s, 3H), 1.95 (s, 3H), 1.83–1.75 (m, 5H), 1.68–1.62 (m, 5H), 1.37–1.34 (m, 3H) ppm. **¹³C NMR** (100 MHz CDCl₃) δ 139.1, 138.9, 129.0, 128.7, 128.3, 127.7, 125.4, 108.2, 67.9, 54.5, 53.4, 49.5, 41.0, 37.9, 37.3, 31.4, 29.03, 28.5, 27.6, 27.4, 21.3, 12.9, 11.0 ppm. **LRMS** (ESI⁺): m/z = 418 [M + H]⁺. **HRMS** (ESI) calcd for C₂₈H₄₀N₃ (M + H⁺) 418.3217, found 418.3234.

Synthesis of 1-((1-(4-chlorophenyl)-2,5-dimethyl-1H-pyrrol-3-yl)methyl)-4-phenylpiperazine (24e).



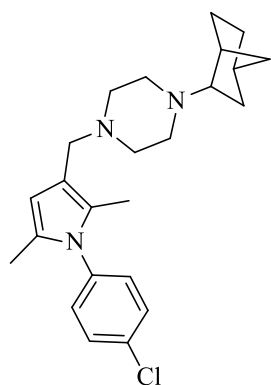
Yield: 65% (369.4 mg). **¹H NMR** (400 MHz CDCl₃) δ 7.44 (d, *J* = 8.0 Hz, 2H), 7.26 (dd, *J* = 8.0, 7.0 Hz, 2H), 7.15 (d, *J* = 7.0 Hz, 2H), 6.94 (d, *J* = 7.0 Hz, 2H), 6.85 (m, 1H), 5.96 (s, 1H), 3.45 (s, 2H), 3.23 (m, 4H), 2.66 (m, 4H), 2.02 (s, 3H), 2.00 (s, 3H) ppm. **¹³C NMR** (100 MHz CDCl₃) δ 151.5, 137.6, 133.5, 129.7, 129.3, 129.1, 127.8, 126.8, 119.5, 115.0, 108.6, 54.5, 52.9, 49.2, 12.9, 11.0 ppm; **LRMS** (ESI⁺): m/z = 380 [M + H]⁺. **HRMS** (ESI) calcd for C₂₃H₂₇ClN₃ (M + H⁺) 380.1888, found 380.1884.

Synthesis of 4,4'-((1-(4-chlorophenyl)-2,5-dimethyl-1H-pyrrole-3,4-diyl)bis(methylene))bis(1-phenylpiperazine) (24f).



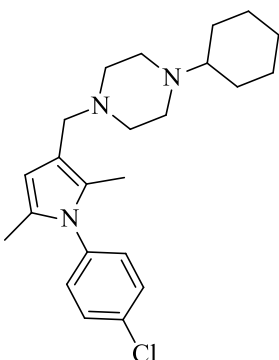
Yield: 35% (290.3 mg). **¹H NMR** (400 MHz CDCl₃) δ 7.29 (d, *J* = 8.0 Hz, 2H), 7.08 (dd, *J* = 8.0, 7.0 Hz, 4H), 7.01 (d, *J* = 8.0 Hz, 2H), 6.77 (d, *J* = 8.0 Hz, 4H), 6.66 (m, 2H), 3.34 (s, 4H), 3.03 (m, 8H), 2.47 (m, 8H), 1.85 (s, 6H) ppm. **¹³C NMR** (100 MHz CDCl₃) δ 151.5, 137.7, 133.4, 129.8, 129.3, 129.1, 126.5, 119.5, 116.0, 53.0, 52.8, 11.0 ppm. **LRMS** (ESI⁺): *m/z* = 555 [M + H]⁺. **HRMS** (ESI) calcd for C₃₄H₄₁ClN₅ (M + H⁺) 554.3045, found 554.3032.

Synthesis of 1-((1S,4R)-Bicyclo[2.2.1]heptan-2-yl)-4-((1-(4-chlorophenyl)-2,5-dimethyl-1H-pyrrol-3-yl)methyl)piperazine (24g).



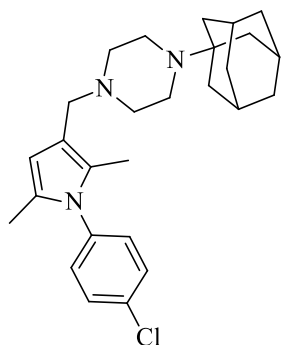
Yield: 55% (327.0 mg). **¹H NMR** (400 MHz CDCl₃) δ 7.40 (d, *J* = 8.0 Hz, 2H), 7.11 (d, *J* = 8.0 Hz, 2H), 5.90 (s, 1H), 3.37 (s, 2H), 2.48 (br m, 5H), 2.24–2.12 (m, 4H), 1.97 (s, 3H), 1.94 (s, 3H), 1.72–1.65 (m, 2H), 1.46 (m, 1H), 1.33–1.22 (m, 5H), 0.88–0.81 (m, 2H) ppm. **¹³C NMR** (100 MHz CDCl₃) δ 137.7, 133.4, 129.7, 129.3, 127.6, 126.8, 115.2, 108.7, 67.9, 54.4, 52.8, 52.7, 39.0, 38.1, 36.8, 35.8, 30.6, 21.1, 12.8, 11.0 ppm. **LRMS** (ESI⁺): *m/z* = 398 [M + H]⁺. **HRMS** (ESI) calcd for C₂₄H₃₃ClN₃ (M + H⁺) 398.2358, found 398.2352.

Synthesis of 1-((1-(4-chlorophenyl)-2,5-dimethyl-1H-pyrrol-3-yl)methyl)-4-cyclohexylpiperazine (24h).



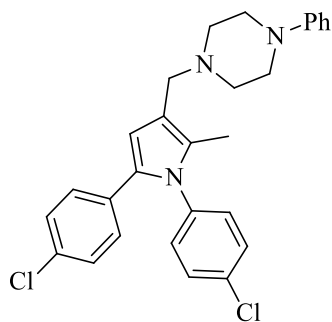
Yield: 52% (300.3 mg). **¹H NMR** (400 MHz CDCl₃) δ 7.40 (d, *J* = 8.0 Hz, 2H), 7.10 (d, *J* = 8.0 Hz, 2H), 5.89 (s, 1H), 3.37 (s, 2H), 2.60 (br s, 8H), 2.20 (m, 1H), 1.96 (s, 3H), 1.93 (s, 3H), 1.88–1.86 (m, 2H), 1.77–1.75 (m, 2H), 1.61–1.58 (m, 1H), 1.26–1.11 (m, 5H) ppm. **¹³C NMR** (100 MHz CDCl₃) δ 137.6, 133.5, 129.7, 129.6, 129.3, 127.7, 118.7, 108.7, 63.5, 56.2, 54.3, 53.0, 48.8, 29.0, 26.3, 25.9, 12.8, 11.0, 10.5 ppm. **LRMS** (ESI⁺): *m/z* = 386 [M + H]⁺. **HRMS** (ESI) calcd for C₂₃H₃₃ClN₃ (M + H⁺) 386.2358, found 386.2356.

Synthesis of 1-(Adamantan-1-yl)-4-((1-(4-chlorophenyl)-2,5-dimethyl-1H-pyrrol-3-yl)methyl)piperazine (24i).



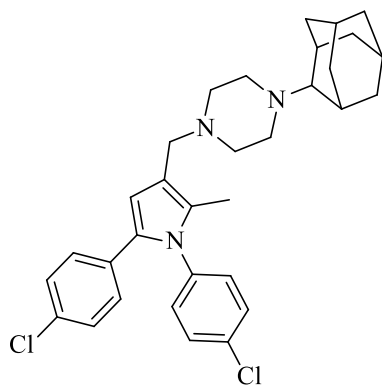
Yield: 54% (353.1 mg). **¹H NMR** (400 MHz CDCl₃) δ 7.41 (d, *J* = 8.5 Hz, 2H), 7.10 (d, *J* = 8.5 Hz, 2H), 5.89 (s, 1H), 3.38 (s, 2H), 2.67 (br s, 4H), 2.50 (br s, 4H), 2.05 (m, 4H), 1.96 (s, 3H), 1.93 (s, 3H), 1.69–1.59 (m, 11H) ppm. **¹³C NMR** (100 MHz CDCl₃) δ 137.7, 133.4, 129.7, 129.8, 129.3, 127.6, 126.8, 115.0, 108.8, 60.4, 56.1, 54.2, 53.5, 44.0, 38.5, 37.0, 31.6, 29.7, 25.3, 22.7, 20.7, 18.8, 14.1, 11.0 ppm. **LRMS** (ESI⁺): *m/z* = 439 [M + H]⁺. **HRMS** (ESI) calcd for C₂₇H₃₇ClN₃ (M + H⁺) 438.2671, found 438.2680.

Synthesis of 1-((1,5-Bis(4-chlorophenyl)-2-methyl-1H-pyrrol-3-yl)methyl)-4-phenylpiperazine (24j).



Yield: 64% (456 mg). **¹H NMR** (400 MHz CDCl₃) δ 7.33 (d, *J* = 8.0 Hz, 2H), 7.23 (m, 2H), 7.04 (d, *J* = 8.0 Hz, 2H), 6.97 (d, *J* = 8.0 Hz, 2H), 6.92 (m, 4H), 6.82 (m, 1H), 6.36 (s, 1H), 3.49 (s, 2H), 3.21 (m, 4H), 2.67 (m, 4H), 2.07 (s, 3H) ppm. **¹³C NMR** (100 MHz CDCl₃) δ 151.4, 137.8, 133.5, 132.0, 131.7, 131.5, 130.3, 129.8, 129.4, 129.1, 128.8, 128.4, 119.7, 116.9, 116.1, 111.7, 54.5, 52.9, 49.2, 11.3 ppm. **LRMS** (ESI⁺): *m/z* = 477 [M + H]⁺. **HRMS** (ESI) calcd for C₂₈H₂₈Cl₂N₃ (M + H⁺) 476.1655, found 476.1648.

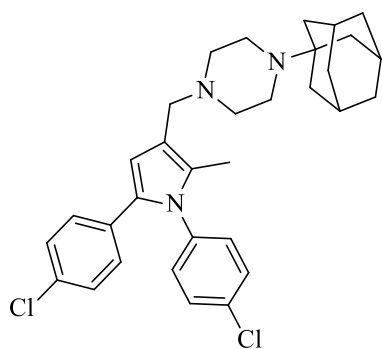
Synthesis of 1-(Adamantan-2-yl)-4-((1,5-bis(4-chlorophenyl)-2-methyl-1H-pyrrol-3-yl)methyl)piperazine (24k).



Yield: 65% (519.2 mg). **¹H NMR** (400 MHz CDCl₃) δ 7.33 (d, *J* = 8.0 Hz, 2H), 7.10–7.04 (m, 4H), 6.93 (d, *J* = 8.0 Hz, 2H), 6.36 (s, 1H), 3.44 (s, 2H), 2.54 (br s, 4H), 2.05 (s, 3H), 2.03 (m, 4H), 1.84–1.75 (m, 4H), 1.68–1.63 (m, 4H), 1.38–1.25 (m, 5H), 0.88–0.82 (m, 2H) ppm. **¹³C NMR** (100 MHz CDCl₃) δ 137.8, 133.4, 131.9, 131.5, 130.2, 129.8, 129.4, 128.8, 128.3, 117.1, 111.5, 67.9, 54.4, 53.5, 49.6, 37.9, 37.3, 31.6, 31.4, 29.0, 27.6, 27.4, 22.7, 14.2, 11.2 ppm.

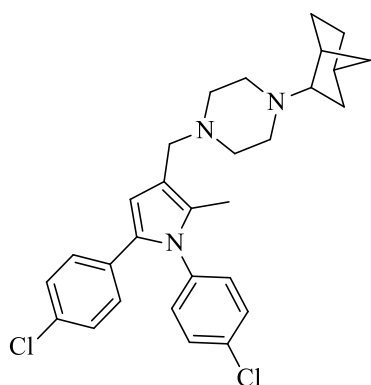
LRMS (ESI⁺): $m/z = 534$ [M + H]⁺. **HRMS** (ESI) calcd for C₃₂H₃₈Cl₂N₃ (M + H⁺) 534.2437, found 534.2425.

Synthesis of 1-(Adamantan-1-yl)-4-((1,5-bis(4-chlorophenyl)-2-methyl-1H-pyrrol-3-yl)methyl)piperazine (24l).



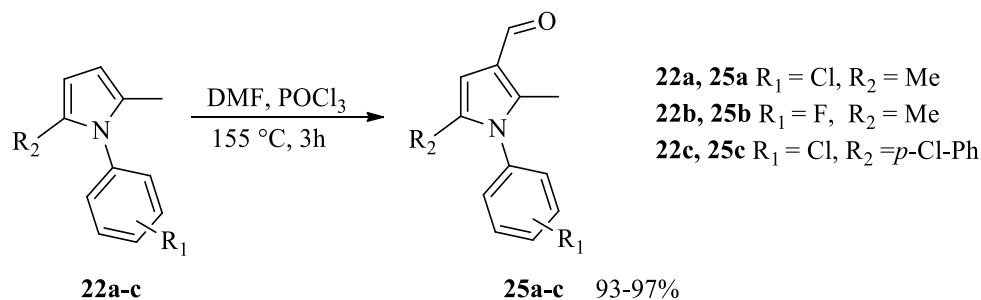
Yield: 60% (479.2 mg). **¹H NMR** (400 MHz CDCl₃) δ 7.34–7.32 (m, 2H), 7.10–7.03 (m, 4H), 6.91 (m, 2H), 6.33 (s, 1H), 5.92 (s, 1H), 3.48 (s, 2H), 2.72–2.70 (br s, 8H), 2.07–2.02 (m, 4H), 2.04 (s, 3H), 1.71–1.56 (m, 11H) ppm. **¹³C NMR** (100 MHz CDCl₃) δ 137.8, 133.4, 131.6, 131.5, 130.3, 129.7, 129.4, 128.8, 128.3, 125.1, 116.5, 111.9, 66.6, 54.1, 53.2, 44.0, 38.3, 36.9, 32.2, 29.7, 26.4, 23.5, 18.7, 13.2, 11.3 ppm. **LRMS** (ESI⁺): $m/z = 534$ [M + H]⁺. **HRMS** (ESI) calcd for C₃₂H₃₈Cl₂N₃ (M + H⁺) 534.2437, found 534.2424.

Synthesis of 1-(bicyclo[2.2.1]heptan-2-yl)-4-((1,5-bis(4-chlorophenyl)-2-methyl-1H-pyrrol-3-yl)methyl)piperazine (24m).



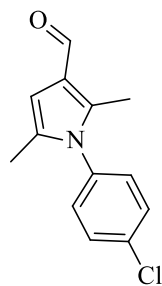
Yield: 56% (414.6 mg). **¹H NMR** (400 MHz CDCl₃) δ 7.26 (d, $J = 8.0$ Hz, 2H), 7.04 (d, $J = 8.0$ Hz, 2H), 6.99 (d, $J = 8.0$ Hz, 2H), 6.85 (d, $J = 8.0$ Hz, 2H), 6.30 (s, 1H), 3.44 (s, 2H), 2.51 (br s, 6H), 2.19–2.17 (m, 2H), 2.12–2.07 (m, 1H), 2.00 (s, 3H), 1.66–1.62 (m, 2H), 1.43–1.40 (m, 1H), 1.29–1.17 (m, 7H) ppm. **¹³C NMR** (100 MHz CDCl₃) δ 137.8, 133.4, 131.9, 131.5, 129.7, 128.7, 128.3, 111.8, 67.9, 65.9, 54.2, 52.6, 38.9, 38.0, 36.8, 36.8, 31.6, 30.6, 22.7, 21.0, 14.2, 11.2 ppm. **LRMS** (ESI⁺): $m/z = 494$ [M + H]⁺. **HRMS** (ESI) calcd for C₂₉H₃₄Cl₂N₃ (M + H⁺) 494.2124, found 494.2113.

General Procedure for the synthesis of Compounds **25a–c**.



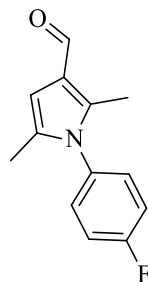
Phosphorus oxychloride (POCl_3) (0.571 mL, 6 mmol, 6 eq.) was added dropwise to a round-bottom flask containing ice cooled DMF (5 mL) under N_2 atmosphere. After 15 min, a solution of the appropriate pyrrole **22a–c** (1 mmol, 1eq.) was added to the stirring solution. Then the reaction mixture was allowed to stir at 155 °C for 3 h. The reaction was monitored through TLC. After completion, the reaction was quenched with 10% w/v NaOH solution (20 mL). The reaction mixture was then diluted with EtOAc (10 mL), extracted two times with EtOAc (10 mL) and then the organic extract was washed with brine (20 mL). The organic extracts were collected and dried over MgSO_4 , filtered, and concentrated under reduced pressure. The residue was then purified by flash chromatography (hexanes/EtOAc, 4:1 v/v), affording the desired compounds **25a–c** as a yellow-brown solid.

Synthesis of 1-(4-chlorophenyl)-2,5-dimethyl-1H-pyrrole-3-carbaldehyde (**25a**).¹²³



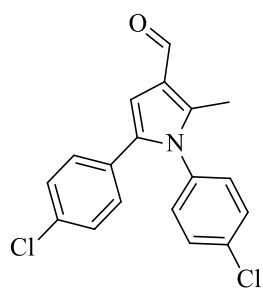
Yield: 93% (217.6 mg). **^1H NMR** (400 MHz CDCl_3) δ 9.71 (s, 1H), 7.40 (d, $J = 7.5$ Hz, 2H), 7.09 (d, $J = 7.5$ Hz, 2H), 6.25 (s, 1H), 2.17 (s, 3H), 1.88 (s, 3H) ppm. **^{13}C NMR** (100 MHz CDCl_3) δ 187.3, 129.8, 120.4, 117.2, 116.8, 116.6, 105.9, 12.7, 11.2 ppm. **LRMS** (ESI^+): $m/z = 234$ [$\text{M} + \text{H}$] $^+$.

Synthesis of 1-(4-fluorophenyl)-2,5-dimethyl-1H-pyrrole-3-carbaldehyde (**25b**).¹²³



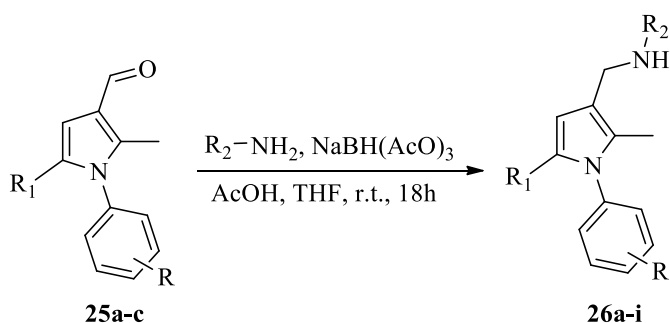
Yield: 97% (210.6 mg). **^1H NMR** (400 MHz CDCl_3) δ 9.86 (s, 1H), 7.20–7.17 (m, 4H), 6.36 (s, 1H), 2.26 (s, 3H), 1.96 (s, 3H) ppm. **^{13}C NMR** (100 MHz CDCl_3) δ 185.3, 162.6, 138.7, 135.5, 130.9, 129.6, 129.3, 122.1, 106.1, 12.7, 11.2 ppm. **LRMS** (ESI^+): $m/z = 218$ [$\text{M} + \text{H}$] $^+$.

Synthesis of 1,5-bis(4-chlorophenyl)-2-methyl-1H-pyrrole-3-carbaldehyde (**25c**).



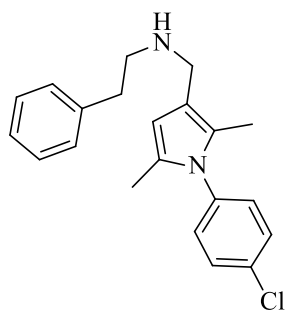
Yield: 96% (317.3 mg). **¹H NMR** (400 MHz CDCl₃) δ 9.89 (s, 1H), 7.33 (d, *J* = 12.0 Hz, 2H), 7.09 (d, *J* = 12.0 Hz, 2H), 7.01 (d, *J* = 12.0 Hz, 2H), 6.87 (d, *J* = 12.0 Hz, 2H), 6.70 (s, 1H), 2.32 (s, 3H) ppm. **¹³C NMR** (100 MHz CDCl₃) δ 185.6, 140.1, 135.6, 134.5, 133.2, 132.0, 130.0, 129.8, 129.5, 129.4, 128.6, 122.9, 108.9, 11.5 ppm. **LRMS** (ESI⁺): *m/z* = 331 [M + H]⁺.

General procedure for the synthesis of pyrrole derivatives **26a–i**.



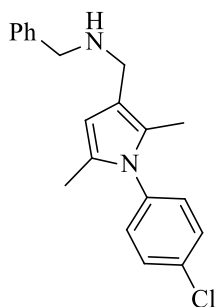
The appropriate aldehyde **25a–c** (1 mmol, 1 eq.) was dissolved in 5 mL of THF in a round-bottom flask. Then AcOH (0.058 mL, 1 mmol, 1 eq.) and the appropriate amine (1 mmol, 1 eq.) were added to the stirring solution at room temperature. The mixture was allowed to stir at room temperature for 20 min before NaBH(AcO)₃ (635.7 mg, 3 mmol, 3 eq.) was added. The mixture was allowed to stir at room temperature for 18 h. Then, after completion, the reaction was quenched with 1 M NaOH solution (25 mL). The mixture was then allowed to stir for 30 min. The reaction mixture was then diluted with EtOAc (10 mL), extracted two times with EtOAc (10 mL) and then the organic extracts were washed with brine (20 mL). The organic extracts were collected and then dried over MgSO₄, filtered, and concentrated under reduced pressure. The residue was then purified by flash chromatography (hexane/EtOAc, 6:4 v/v, affording the desired compounds **26a–i** as a yellow-brown solid.

Synthesis of *N*-((1-(4-chlorophenyl)-2,5-dimethyl-1H-pyrrol-3-yl)methyl)-2-phenylethan-1-amine (26a).



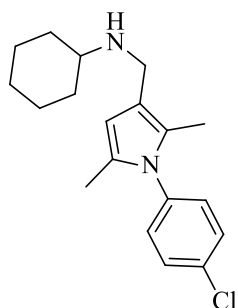
Yield: 75% (254.2 mg). **¹H NMR** (400 MHz CDCl₃) δ 7.41 (d, *J* = 8.0 Hz, 2H), 7.29–7.27 (m, 2H), 7.24–7.22 (m, 3H), 7.11 (d, *J* = 8.0 Hz, 2H), 5.90 (s, 1H), 3.63 (s, 2H), 2.95 (m, 2H), 2.86 (m, 2H), 1.99 (s, 3H), 1.94 (s, 3H) ppm. **¹³C NMR** (100 MHz CDCl₃) δ 140.3, 137.6, 133.5, 129.6, 129.3, 128.8, 128.5, 128.0, 126.1, 125.5, 118.1, 107.1, 51.0, 45.7, 36.4, 12.8, 10.7 ppm. **LRMS** (ESI⁺): *m/z* = 339 [M + H]⁺. **HRMS** (ESI) calcd for C₂₁H₂₄ClN₂ (M + H⁺) 339.1623, found 339.1603.

Synthesis of *N*-benzyl-1-(1-(4-chlorophenyl)-2,5-dimethyl-1H-pyrrol-3-yl)-methanamine (26b).



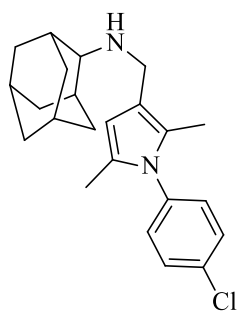
Yield: 79% (256 mg). **¹H NMR** (400 MHz CDCl₃) δ 7.39 (d, *J* = 8.5 Hz, 2H), 7.34–7.27 (m, 4H), 7.22–7.20 (m, 1H), 7.10 (d, *J* = 8.5 Hz, 2H), 5.92 (s, 1H), 3.83 (s, 2H), 3.60 (s, 2H), 1.97 (s, 3H), 1.91 (s, 3H) ppm. **¹³C NMR** (100 MHz CDCl₃) δ 140.7, 137.6, 133.5, 129.6, 129.3, 128.3, 128.1, 127.9, 126.8, 125.6, 118.1, 107.1, 53.5, 45.0, 12.8, 10.7 ppm. **LRMS** (ESI⁺): *m/z* = 325 [M + H]⁺. **HRMS** (ESI) calcd for C₂₀H₂₂ClN₂ (M + H⁺) 325.1466, found 325.1466.

Synthesis of *N*-((1-(4-chlorophenyl)-2,5-dimethyl-1H-pyrrol-3-yl)methyl)-cyclohexanamine (26c).



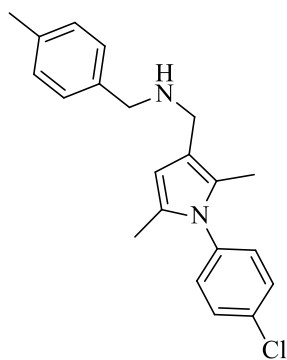
Yield: 77% (243.9 mg). **¹H NMR** (400 MHz CDCl₃) δ 7.40 (d, *J* = 8.0 Hz, 2H), 7.10 (d, *J* = 8.0 Hz, 2H), 5.91 (s, 1H), 3.59 (s, 2H), 2.53–2.48 (m, 1H), 1.98 (s, 3H), 1.95 (s, 3H), 1.94–1.90 (m, 2H), 1.74–1.70 (m, 2H), 1.16–1.06 (m, 3H), 0.85–0.81 (m, 3H) ppm. **¹³C NMR** (100 MHz CDCl₃) δ 137.6, 133.4, 129.6, 129.3, 128.0, 125.3, 118.6, 107.0, 56.7, 42.8, 33.6, 26.3, 25.1, 12.8, 10.7 ppm. **LRMS** (ESI⁺): *m/z* = 317 [M + H]⁺. **HRMS** (ESI) calcd for C₁₉H₂₆ClN₂ (M + H⁺) 317.1779, found 317.1779.

Synthesis of *N*-((1-(4-chlorophenyl)-2,5-dimethyl-1H-pyrrol-3-yl)methyl)-adamantan-2-amine (26d).



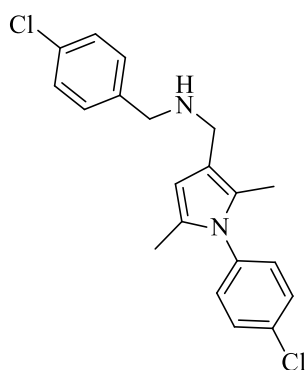
Yield: 60% (221.4 mg). **¹H NMR** (400 MHz CDCl₃) δ 7.41 (d, *J* = 8.0 Hz, 2H), 7.12 (d, *J* = 8.0 Hz, 2H), 5.94 (s, 1H), 3.57 (s, 2H), 2.81 (m, 1H), 2.04–2.00 (m, 2H), 1.99 (s, 3H), 1.97 (s, 3H), 1.93 (m, 2H), 1.86–1.83 (m, 3H), 1.76–1.70 (m, 5H), 1.50–1.47 (m, 2H) ppm. **¹³C NMR** (100 MHz CDCl₃) δ 137.6, 133.4, 129.6, 129.3, 127.9, 125.4, 118.8, 107.2, 61.7, 42.9, 38.1, 37.7, 32.1, 31.5, 28.0, 27.8, 12.9, 10.7 ppm. **LRMS** (ESI⁺): *m/z* = 369 [M + H]⁺. **HRMS** (ESI) calcd for C₂₃H₃₀ClN₂ (M + H⁺) 369.2092, found 369.2089.

Synthesis of 1-(1-(4-chlorophenyl)-2,5-dimethyl-1H-pyrrol-3-yl)-*N*-(4-methylbenzyl)methanamine (26e).



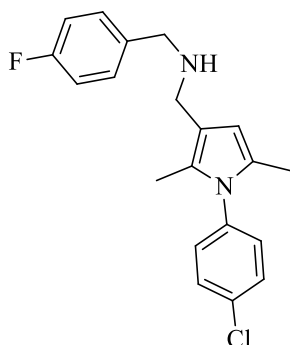
Yield: 82% (277.1 mg). **¹H NMR** (400 MHz CDCl₃) δ 7.41 (d, *J* = 8.5 Hz, 2H), 7.24 (d, *J* = 8.0 Hz, 2H), 7.13–7.10 (m, 4H), 5.94 (s, 1H), 3.61 (s, 2H), 3.18 (s, 2H), 2.32 (s, 3H), 1.99 (s, 3H), 1.93 (s, 3H), ppm. **¹³C NMR** (100 MHz CDCl₃) δ 137.6, 137.4, 136.4, 133.5, 129.6, 129.4, 129.1, 128.2, 128.0, 125.8, 117.9, 107.2, 53.1, 44.9, 21.2, 12.9, 10.8 ppm. **LRMS** (ESI⁺): *m/z* = 339 [M + H]⁺. **HRMS** (ESI) calcd for C₂₁H₂₄ClN₂ (M + H⁺) 339.1623, found 339.1624.

Synthesis of *N*-(4-chlorobenzyl)-1-(1-(4-chlorophenyl)-2,5-dimethyl-1H-pyrrol-3-yl)methanamine (26f).



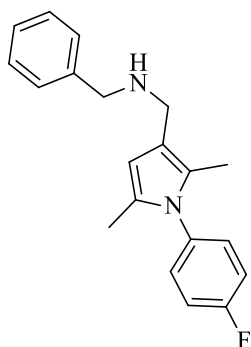
Yield: 78% (278.3 mg). **¹H NMR** (400 MHz CDCl₃) δ 7.41 (d, *J* = 8.5 Hz, 2H), 7.30–7.24 (m, 4H), 7.11 (d, *J* = 8.0 Hz, 2H), 5.91 (s, 1H), 3.81 (s, 2H), 3.59 (s, 2H), 1.99 (s, 3H), 1.92 (s, 3H) ppm. **¹³C NMR** (100 MHz CDCl₃) δ 139.3, 133.7, 129.6, 129.5, 129.4, 128.4, 128.1, 125.7, 117.9, 107.1, 52.7, 45.1, 12.8, 10.8 ppm. **LRMS** (ESI⁺): *m/z* = 359 [M + H]⁺. **HRMS** (ESI) calcd for C₂₀H₂₁Cl₂N₂ (M + H⁺) 359.1076, found 359.1076.

Synthesis of *N*-(4-fluorobenzyl)-1-(1-(4-chlorophenyl)-2,5-dimethyl-1H-pyrrol-3-yl)methanamine (26g).



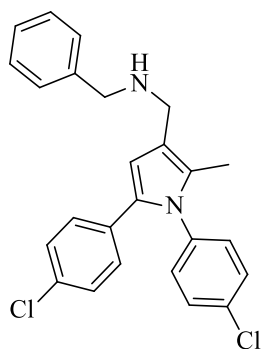
Yield: 80% (274.4 mg). **¹H NMR** (400 MHz CDCl₃) δ 7.41 (d, *J* = 8.5 Hz, 2H), 7.31 (dd, *J* = 8.5 Hz 2H), 7.11 (d, *J* = 8.0 Hz, 2H), 6.99 (t, *J* = 8.0 Hz, 2H), 5.91 (s, 1H), 3.81 (s, 2H), 3.59 (s, 2H), 1.99 (s, 3H), 1.92 (s, 3H) ppm. **¹³C NMR** (100 MHz CDCl₃) δ 163.1, 160.7, 137.6, 133.6, 129.7, 129.6, 129.4, 128.1, 125.7, 118.0, 115.2, 107.1, 52.8, 45.1, 12.8, 10.8 ppm. **LRMS** (ESI⁺): *m/z* = 343 [M + H]⁺. **HRMS** (ESI) calcd for C₂₀H₂₁ClFN₂ (M + H⁺) 343.1372, found 343.1374.

Synthesis of *N*-benzyl-1-(1-(4-fluorophenyl)-2,5-dimethyl-1H-pyrrol-3-yl)methanamine (26h).



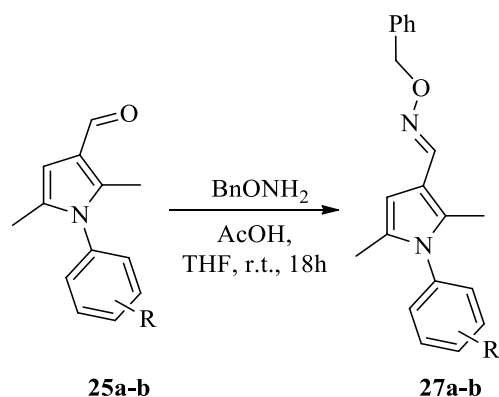
Yield: 82% (252.5 mg). **¹H NMR** (400 MHz CDCl₃) δ 7.36–7.29 (m, 4H), 7.23 (t, *J* = 8.0 Hz, 1H), 7.15–7.09 (m, 4H), 5.92 (s, 1H), 3.85 (s, 2H), 3.61 (s, 2H), 1.98 (s, 3H), 1.91 (s, 3H) ppm. **¹³C NMR** (100 MHz CDCl₃) δ 130.1, 129.9, 128.4, 128.2, 117.9, 116.2, 115.9, 106.8, 53.6, 45.2, 12.9, 10.8 ppm. **LRMS** (ESI⁺): *m/z* = 309 [M + H]⁺. **HRMS** (ESI) calcd for C₂₀H₂₂FN₂ (M + H⁺) 309.1762, found 309.1764.

Synthesis of *N*-benzyl-1-(1,5-bis(4-chlorophenyl)-2-methyl-1H-pyrrol-3-yl)methanamine (26i).



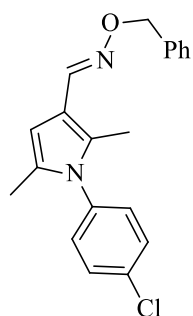
Yield: 78% (327.6 mg). **¹H NMR** (400 MHz CDCl₃) δ 7.31–7.25 (m, 7H), 7.04 (d, *J* = 12.0 Hz, 2H), 6.97 (d, *J* = 12.0 Hz, 2H), 6.86 (d, *J* = 12.0 Hz, 2H), 6.31 (s, 1H), 3.82 (s, 2H), 3.62 (s, 2H), 1.96 (s, 3H), 1.80 (br s, 1H) ppm. **¹³C NMR** (100 MHz CDCl₃) δ 137.3, 133.9, 132.7, 132.0, 130.0, 129.6, 129.5, 128.9, 128.3, 111.4, 110.5, 29.1, 24.6, 11.4 ppm. **LRMS** (ESI⁺): *m/z* = 421 [M + H]⁺. **HRMS** (ESI) calcd for C₂₅H₂₃Cl₂N₂ (M + H⁺) 421.1233, found 421.1228.

General procedure for the synthesis of oximes **27a** and **27b**.¹²³



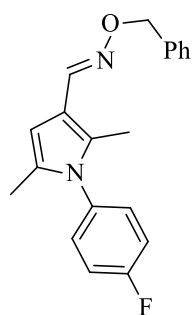
The appropriate aldehyde **25a-b** (1 mmol, 1eq.) was dissolved in 5 mL of THF in a round bottom flask. Then AcOH (0.058 mL, 1 mmol, 1eq.) and O-benzylhydroxylamine (123.1 mg, 1 mmol, 1eq.) were added to the stirring solution at room temperature. The mixture was allowed to stir at room temperature for 18 h. After completion, the reaction was quenched with 1 M NaOH solution (25 mL). The reaction mixture was then diluted with EtOAc (10 mL) and extracted two times with EtOAc (10 mL) and then the organic phases were washed with brine (20 mL). The organic extracts were collected and then dried over MgSO₄, filtered, and concentrated under reduced pressure. The residue was then purified by flash chromatography (hexanes-EtOAc, 6:4 v/v), affording the desired compounds **27a** and **27b** as yellow-brown solids.

Synthesis of 1-(4-chlorophenyl)-2,5-dimethyl-1H-pyrrole-3-carbaldehyde O-BenzylOxime (**27a**).



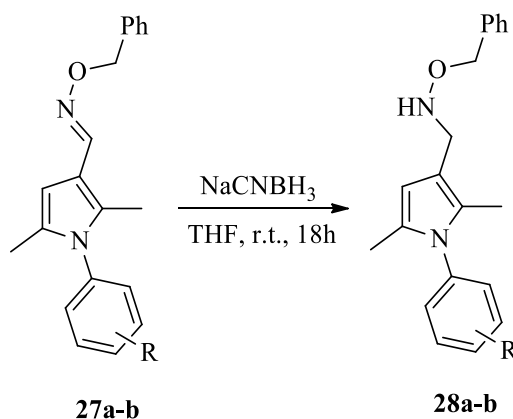
Yield: 75% (253.5 mg). **¹H NMR** (400 MHz CDCl₃) δ 8.15 (s, 1H), 7.45–7.41 (m, 4H), 7.37–7.33 (m, 2H), 7.30–7.29 (m, 1H), 7.11 (d, *J* = 8.5 Hz, 2H), 6.24 (s, 1H), 5.14 (s, 2H), 2.03 (s, 3H), 1.97 (s, 3H) ppm. **¹³C NMR** (100 MHz CDCl₃) δ 144.6, 138.0, 136.6, 134.3, 130.8, 130.1, 129.7, 129.6, 128.5, 128.4, 127.8, 112.9, 104.6, 75.9, 12.8, 11.5 ppm. **LRMS** (ESI⁺): *m/z* = 339 [M + H]⁺; **HRMS** (ESI) calcd for C₂₀H₁₉ClN₂O (M + H⁺) 339.1259, found 339.1260.

Synthesis of 1-(4-fluorophenyl)-2,5-dimethyl-1H-pyrrole-3-carbaldehyde O-BenzylOxime (27b).



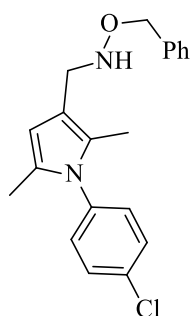
Yield: 78% (258.9 mg). **¹H NMR** (400 MHz CDCl₃) δ 8.15 (s, 1H), 7.42 (d, *J* = 8.0 Hz, 2H), 7.34 (t, *J* = 8.0 Hz, 2H), 7.28 (d, *J* = 8.0 Hz, 1H), 7.15 (d, *J* = 8.0 Hz, 2H), 6.23 (s, 1H), 5.13 (s, 2H), 2.01 (s, 3H), 1.96 (s, 3H) ppm. **¹³C NMR** (100 MHz CDCl₃) δ 144.6, 138.1, 134.1, 131.1, 130.3, 130.0, 129.9, 128.5, 128.4, 127.8, 127.7, 116.5, 116.3, 104.3, 12.8, 11.1 ppm. **LRMS** (ESI⁺): *m/z* = 333 [M + H]⁺

General procedure for the synthesis of compounds 28a and 28b.



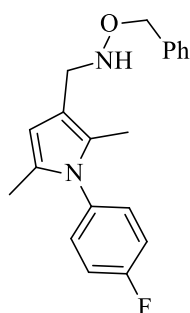
The appropriate oxime **27a,b** (1 mmol, 1eq.) was dissolved in 5 mL of THF in a round-bottom flask. Then, NaBH₃(CN) (635.7 mg, 3 mmol, 1eq.) was added to the solution and the mixture was allowed to stir at room temperature for 18 h. Then, the reaction was quenched with 1 M NaOH solution (25 mL). The reaction mixture was then diluted with EtOAc (10 mL) and extracted two times with EtOAc (10 mL) and then washed with brine (20 mL). The organic extracts were collected and then dried over MgSO₄, filtered, and concentrated under reduced pressure. The residue was then purified by flash chromatography (hexanes/EtOAc, 6:4 v/v), affording the desired compounds **28a** and **28b** as yellow-brown solids.

Synthesis of O-benzyl-N-((1-(4-chlorophenyl)-2,5-dimethyl-1H-pyrrol-3-yl)-methyl)hydroxylamine (28a).



Yield: 80% (270.4 mg). **¹H NMR** (400 MHz CDCl₃) δ 7.42–7.25 (m, 7H), 7.10 (d, *J* = 8.5 Hz, 2H), 5.90 (s, 1H), 5.48 (br s, 1H), 4.74 (s, 2H), 3.91 (s, 2H), 1.97 (s, 3H), 1.93 (s, 3H) ppm. **¹³C NMR** (100 MHz CDCl₃) δ 138.2, 137.5, 133.6, 129.6, 129.4, 128.6, 128.4, 128.2, 127.3, 126.9, 114.3, 107.6, 76.1, 48.5, 12.8, 10.7 ppm. **LRMS** (ESI): *m/z* = 339 [M–H⁺]. **HRMS** (ESI) calcd for C₂₀H₂₀ClN₂O (M – H⁺) 339.1264, found 339.1259.

Synthesis of O-benzyl-N-((1-(4-fluorophenyl)-2,5-dimethyl-1H-pyrrol-3-yl)-methyl)hydroxylamine (28b).

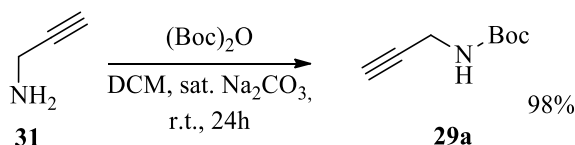


Yield: 82% (264.1 mg). **¹H NMR** (400 MHz CDCl₃) δ 7.39–7.28 (m, 5H), 7.12 (m, 4H), 5.90 (s, 1H), 4.75 (s, 2H), 3.92 (s, 2H), 1.96 (s, 3H), 1.92 (s, 3H) ppm. **¹³C NMR** (100 MHz CDCl₃) δ 138.2, 134.9, 130.0, 129.9, 128.6, 128.4, 128.3, 127.8, 127.1, 116.2, 115.9, 114.0, 107.3, 76.1, 48.5, 12.8, 10.7 ppm. **LRMS** (ESI): *m/z* = 323 [M–H⁺]. **HRMS** (ESI) calcd for C₂₀H₂₀FN₂O (M–H⁺) 323.1560, found 323.1554.

5.2.3. Synthesis of 1,2,3-substituted pyrroles from propargylamines via a one-pot tandem enyne cross metathesis – cyclization reaction.

5.2.3.1. Chemistry.

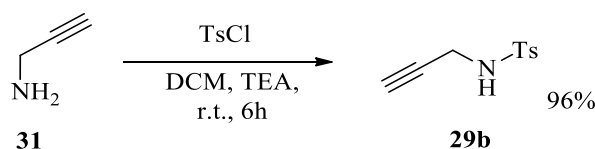
Synthesis of *t*-butyl-prop-2-ynylcarbamate (29a).²²²



Propargylamine **31** (0.086 mL, 1.81 mmol, 1 eq.) was added to 20 mL mixture (1:1) of CH₂Cl₂ and Na₂CO₃ saturated solution (ss) in water in a round bottom flask. Di-*tert*-butyl dicarbonate (436.5 mg, 2.00 mmol, 1.1 eq.) was added to the stirring solution. The reaction

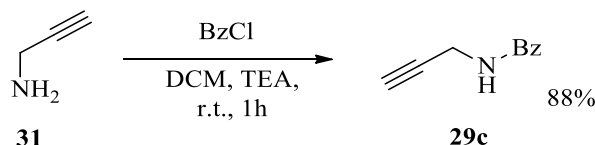
mixture was allowed to stir under N₂ atmosphere for 24 h at room temperature. Then, the reaction mixture was diluted with 10 mL of water and the product was extracted twice with 20 mL of EtOAc. The combined organic layers were collected, washed with brine, dried over Na₂SO₄ and concentrated under reduced pressure giving a yellow crude oil. The obtained product **29a** was purified by chromatography on silica gel, using hexane/EtOAc (9:1) as eluent. The pure product was obtained as a pale yellow solid. **Yield:** 98% (274.9 mg). **¹H NMR** (400 MHz CDCl₃) δ 4.78 (br s, 1H), 3.88 (s, 2H), 2.18 (t, *J* = 2.5 Hz, 1H), 1.42 (s, 9H) ppm. **¹³C NMR** (100 MHz CDCl₃) δ 155.2, 80.1, 80.0, 71.2, 30.4, 28.3 ppm. **LRMS** (ESI⁺): *m/z* = 156 [M + H]⁺.

Synthesis of 4-methyl-*N*-2-propyn-1-yl-benzenesulfonamide (**29b**).²²³



Propargylamine **31** (0.127 mL, 2.69 mmol, 1 eq.), and triethylamine (0.237 mL, 3.23 mmol, 1.2 eq.) were added to a solution of *p*-toluenesulfonyl chloride (564 mg, 2.96 mmol, 1.1 eq.) in anhydrous DCM at 0 °C, under N₂ atmosphere. The reaction mixture was allowed to stir at room temperature for 6 h, and then a saturated solution of NH₄Cl in water (20mL) was added to the reaction mixture. The aqueous layer was extracted with DCM. The combined organic layers were dried over Na₂SO₄ and concentrated under reduced pressure, giving the crude product which was then purified by chromatography on silica gel, using hexane/EtOAc (9:1) as eluent. The pure product **29b** was obtained as a yellow oil. **Yield:** 96% (200.6 mg). **¹H NMR** (400 MHz CDCl₃) δ 7.69 (d, *J* = 8.0 Hz, 2H), 7.19 (d, *J* = 8.0 Hz, 2H), 3.69 (d, *J* = 2.5 Hz, 2H), 2.31 (s, 3H), 2.03 (t, *J* = 2.0 Hz, 1H) ppm. **¹³C NMR** (100 MHz CDCl₃) δ 143.9, 136.3, 129.6, 127.3, 77.9, 72.8, 32.7, 21.5 ppm. **LRMS** (ESI⁺): *m/z* = 210 [M + H]⁺.

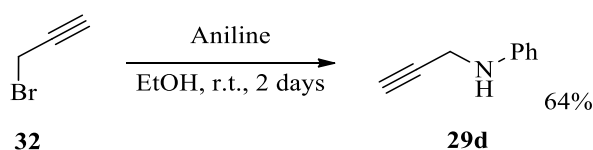
Synthesis of *N*-prop-2-ynylbenzamide (**29c**).²²⁴



Benzoyl chloride (0.210 mL 1.83 mmol, 1.01 eq.) and TEA (2.21 mmol, 1.2 eq.) were added to a solution of propargylamine **31** (1.82 mmol, 1 eq.) in DCM (20 mL) at 0 °C. The reaction

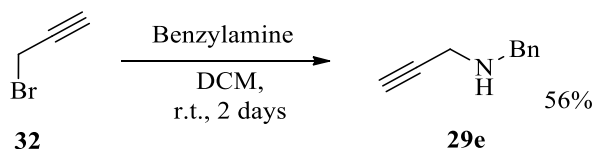
mixture was allowed to stir at room temperature for 1 h, then it was quenched with 1M HCl solution (20 mL), and extracted with DCM (20 mL). The combined organic layers were washed with brine (20 mL), dried over Na₂SO₄, and concentrated under reduced pressure. The crude mixture was purified by chromatography on silica gel, using hexane/EtOAc (4:1) as eluent, affording **29c** as a yellow oil. **Yield:** 88% (254.6 mg). **¹H NMR** (400 MHz CDCl₃) δ 7.77 (d, *J* = 7.5 Hz, 2H), 7.48-7.39 (m, 3H), 6.64 (br s, 1H), 4.22 (dd, *J* = 5.5, 3.0 Hz, 2H), 2.25 (t, *J* = 2.5 Hz, 1H) ppm. **¹³C NMR** (100 MHz CDCl₃) δ 167.2, 133.6, 131.9, 128.6, 127.0, 79.4, 71.9, 29.7 ppm. **LRMS** (ESI⁺): *m/z* = 160 [M + H]⁺.

Synthesis of *N*-2-propyn-1-yl-benzenamine (**29d**).¹⁶⁷



Aniline (0.46 mL, 5 mmol, 5 eq.) was added to a solution of propargyl bromide **32** (0.148 mL, 1 mmol, 1 eq.) in ethanol. The reaction mixture was stirred at room temperature for 2 days, and then concentrated under reduced pressure. The crude product was purified by chromatography on silica gel, using hexane/EtOAc (9:1) as eluent. The pure product **29d** was obtained as a yellow oil. **Yield:** 64% (83.8 mg). **¹H NMR** (400 MHz CDCl₃) δ 7.21 (t, *J* = 7.5 Hz, 2H), 6.78 (t, *J* = 7.0 Hz, 1H), 6.68 (d, *J* = 7.5 Hz, 2H), 3.93 (s, 2H), 3.96 (br s, 1H), 2.20 (t, *J* = 2.0 Hz, 1H) ppm. **¹³C NMR** (100 MHz CDCl₃) δ 146.9, 130.0, 118.7, 113.6, 81.1, 71.4, 33.4 ppm. **LRMS** (ESI⁺): *m/z* = 132 [M + H]⁺.

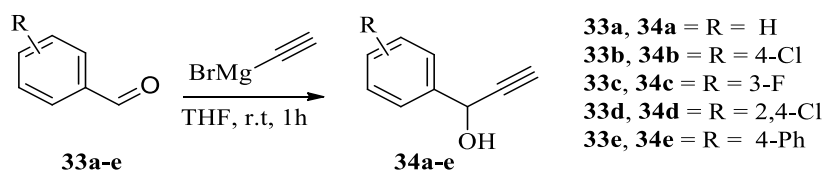
Synthesis of *N*-benzyl(prop-2-ynyl)amine (**29e**).



Benzylamine (1.101 mL, 10.08 mmol, 6 eq.) was added to a solution of propargyl bromide **32** (0.187 mL, 1.68 mmol, 1 eq.) in 1 mL of DCM. The reaction mixture was stirred at room temperature for 2 days, and then concentrated under reduced pressure. The crude product was purified by chromatography on silica gel, using hexane/EtOAc (9:1) as eluent. Compound **29e** was obtained as a tan oil. **Yield:** 56% (136.4 mg). **¹H NMR** (400 MHz CDCl₃) δ 7.35–7.25 (m, 5H), 3.85 (s, 2H), 3.40 (s, 2H), 2.25 (s, 1H) ppm. **¹³C NMR** (100

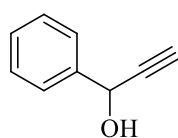
MHz CDCl₃) δ 141.4, 128.9, 128.4, 126.6, 81.2, 79.3, 52.4, 41.7 ppm. **LRMS** (ESI⁺): m/z = 146 [M + H]⁺.

General procedure for the synthesis of propargylalcohols **34a-e**.



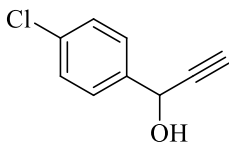
A solution of ethynyl magnesium bromide in THF (2.5 mL, 5 mmol, 2 eq.) was added dropwise at 0°C to a solution in anhydrous THF (10 mL) of the appropriate aldehyde **33a-e** (1 mmol, 1 eq.). The reaction was allowed to stir at r.t. for 1 h under N₂ atmosphere. Then the reaction mixture was quenched with a saturated NH₄Cl solution (20 mL). The aqueous layer was extracted with DCM (20 mL). The combined organic layers were dried over Na₂SO₄ and concentrated under reduced pressure, giving the crude product which was then used in the next reaction without further purifications.

Synthesis of 1-phenylprop-2-yn-1-ol (**34a**).²²⁵



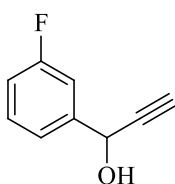
Yield: 98% (129.3 mg). **¹H NMR** (400 MHz CDCl₃) δ 7.55 (m, 2H), 7.42–7.31 (m, 3H), 5.49 (dd, J = 4.0 Hz, 1H), 2.65 (d, J = 2.0 Hz, 1H) 2.44 (br s, 1H) ppm. **¹³C NMR** (100 MHz CDCl₃) δ 140.2, 128.9, 128.8, 126.6, 83.5, 75.1, 64.6 ppm. **LRMS** (ESI⁺): m/z = 133 [M + H]⁺.

Synthesis of 1-(4-chlorophenyl)prop-2-yn-1-ol (**34b**).



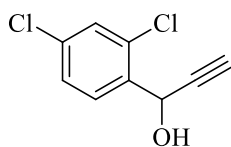
Yield: 94% (156.0 mg). **¹H NMR** (400 MHz CDCl₃) δ 7.50 (d, J = 8.0 Hz, 2H), 7.37 (d, J = 8.0 Hz, 2H), 5.43 (s, 1H), 2.69 (d, J = 4.0 Hz, 1H), 2.34 (br s, 1H) ppm. **¹³C NMR** (100 MHz CDCl₃) δ 138.5, 134.7, 129.1, 128.2, 83.3, 75.5, 63.9 ppm. **LRMS** (ESI⁺): m/z = 167 [M + H]⁺.

Synthesis of 1-(3-fluorophenyl)prop-2-yn-1-ol (**34c**).



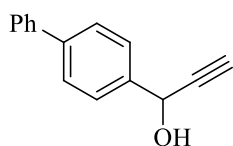
Yield: 96% (144.9 mg). **¹H NMR** (400 MHz CDCl₃) δ 7.39–7.27 (m, 3H), 7.05–7.02 (m, 1H), 5.47 (d, J = 4.0 Hz, 1H), 2.69 (d, J = 4.0 Hz, 1H), 2.33 (br s, 1H) ppm. **LRMS** (ESI⁺): m/z = 151 [M + H]⁺.

Synthesis of 1-(2,4-dichlorophenyl)prop-2-yn-1-ol (**34d**).²²⁶



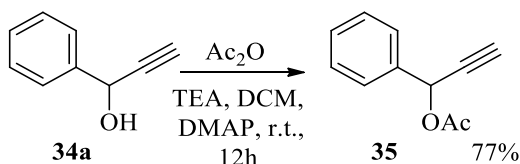
Yield: 97% (193.0 mg). **¹H NMR** (400 MHz CDCl₃) δ 7.68 (d, *J* = 8.0 Hz, 1H), 7.40 (br s, 1H), 7.29-7.30 (d, *J* = 8.0 Hz, 1H), 5.75 (s, 1H), 2.76 (d, *J* = 4.0 Hz 1H), 2.66 (br s, 1H) ppm. **¹³C NMR** (100 MHz CDCl₃) δ 135.8, 135.1, 133.2, 129.4, 129.2, 127.4, 81.7, 75.2, 61.1 ppm. **LRMS** (ESI⁺): *m/z* = 200 [M + H]⁺.

Synthesis of 1-([1,1'-biphenyl]-4-yl)prop-2-yn-1-ol (**34e**).



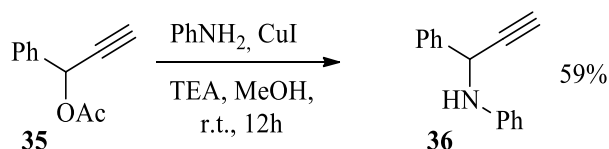
Yield: 98% (204.8 mg). **¹H NMR** (400 MHz CDCl₃) δ 7.55-7.59 (m, 6H), 7.34-7.45 (m, 3H), 5.48 (d, *J* = 4.0 Hz, 1H), 2.67 (d, *J* = 4.0 Hz, 1H), 2.54 (br s, 1H), **¹³C NMR** (100 MHz CDCl₃) δ 141.3 140.4, 138.8, 128.7, 127.3, 127.5, 127.2, 127.1, 83.5, 74.8, 64.2 ppm. **LRMS** (ESI⁺): *m/z* = 209 [M + H]⁺.

Synthesis of 1-phenylprop-2-yn-1-yl acetate (**35**).³²



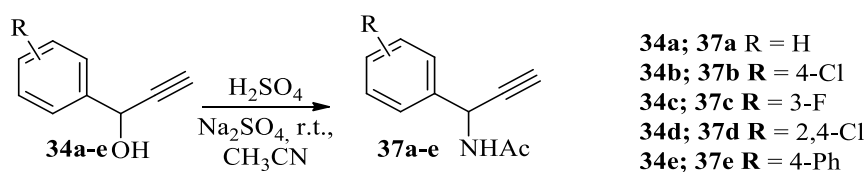
Acetic anhydride (0.19 mL, 1.96 mmol, 1.3 eq.), triethylamine (0.419 mL, 3.02 mmol, 2 eq.), and a catalytic amount of 4-dimethylaminopyridine (DMAP) were added to a solution of 1-phenyl- 2-propynol **34a** (199.3 mg, 1.51 mmol, 1 eq.) in DCM. The reaction mixture was stirred at room temperature for 12 h, and then the solvent was concentrated under reduced pressure. The crude product was purified by chromatography on silica gel, using hexane/EtOAc (9:1) as eluent. Compound **35** was obtained as a yellow-brown solid. **Yield:** 77% (201.1 mg). **¹H NMR** (400 MHz CDCl₃) δ 7.53 (d, *J* = 6.5 Hz, 2H), 7.39 (m, 3H), 6.45 (d, *J* = 2.0 Hz, 1H), 2.66 (d, *J* = 2.0 Hz, 1H), 2.10 (s, 3H) ppm. **¹³C NMR** (100 MHz CDCl₃) δ 169.8, 136.5, 129.2, 128.8, 127.8, 80.3, 75.5, 65.4, 21.1 ppm. **LRMS** (ESI⁺): *m/z* = 197 [M + Na]⁺.

Synthesis of *N*-(1-phenylprop-2-yn-1-yl)aniline (**36**).²²⁷



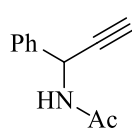
Copper iodide (24.7 mg, 0.13 mmol, 0.5 eq.) was added to a solution of propargylic acetate **35** (44.9 mg, 0.26 mmol, 1 eq.) in MeOH at 0 °C, under N_2 atmosphere. The reaction mixture was allowed to stir for 10 min before the addition of aniline (0.047 mL, 0.52 mmol, 2 eq.) and triethylamine (0.144 mL, 1.04 mmol, 4 eq.). The mixture was then stirred at 0 °C, for 10 minutes and then allowed to reach room temperature for 12 h. The reaction mixture was diluted with EtOAc (20 mL), and NH_4Cl (20 mL). The aqueous layer was extracted with EtOAc twice. The combined organic layers were dried over MgSO_4 and concentrated under reduced pressure. The crude product was purified by chromatography on silica gel, using hexane as eluent. Compound **36** was obtained as a yellow-brown solid. **Yield:** 59% (31.7 mg). **^1H NMR** (400 MHz CDCl_3) δ 7.61 (d, J = 8.0 Hz, 2H), 7.38 (m, 3H), 7.28 (m, 2H), 6.88-6.84 (m, 3H), 5.29 (s, 1H), 4.06 (br s, 1H), 2.50 (d, J = 2.0 Hz, 1H) ppm. **^{13}C NMR** (100 MHz CDCl_3) δ 146.1, 138.8, 129.1, 128.7, 128.2, 127.2, 118.7, 113.8, 82.9, 73.1, 49.7 ppm. **LRMS** (ESI^+): m/z = 230 $[\text{M} + \text{Na}]^+$.

General procedure for the synthesis of propargylamides **37a–e**.



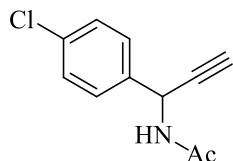
A solution of 96% H_2SO_4 (5 mmol, 5 eq.) in acetonitrile (2 mL) was added to a stirred mixture of the appropriate propargylalcohol **34a–e** (1 mmol 1 eq.) and anhydrous Na_2SO_4 (1 mmol 1eq.) in dry acetonitrile (3.1 mL) at r.t. The mixture was allowed to reach room temperature, and stirring was continued for the required time. The mixture was concentrated, poured on ice, and extracted with ether, (20 mL) and dichloromethane (20 mL). The combined organic layers were dried over Na_2SO_4 , filtered, and concentrated. Flash chromatography, using ethyl acetate/petroleum ether (1:1) as eluent, afforded pure propargylamides **37a–e** as yellow-brown solids.

Synthesis of *N*-(1-phenylprop-2-yn-1-yl)acetamide (37a).²²⁸



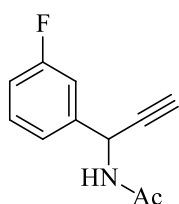
Yield: 78% (135.7 mg). **¹H NMR** (400 MHz CDCl₃) δ 7.58 (d, *J* = 8.0 Hz, 2H), 7.37–7.26 (m, 3H), 6.77 (d, *J* = 8.0 Hz, 1H), 5.98 (d, *J* = 8.0 Hz, 1H), 2.45 (s, 1H), 1.96 (s, 3H) ppm. **¹³C NMR** (100 MHz CDCl₃) δ 169.2, 138.3, 128.5, 128.0, 126.9, 81.7, 72.9, 44.1, 22.7 ppm. **LRMS** (ESI⁺): *m/z* = 174 [M + H]⁺.

Synthesis of *N*-(1-(4-chlorophenyl)prop-2-yn-1-yl)acetamide (37b).²²⁸



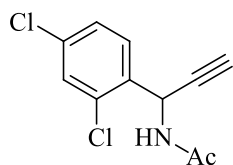
Yield: 77% (159.4 mg). **¹H NMR** (400 MHz CDCl₃) δ 7.43 (d, *J* = 8.5 Hz, 2H), 7.31 (d, *J* = 8.5 Hz, 2H), 6.00 (br s, 1H), 6.07 (s, 1H), 2.51 (s, 1H), 2.03 (s, 3H) ppm. **¹³C NMR** (100 MHz CDCl₃) δ 168.8, 136.7, 134.1, 128.8, 128.3, 81.3, 73.4, 43.9, 23.3 ppm. **LRMS** (ESI⁺): *m/z* = 208 [M + H]⁺.

Synthesis of *N*-(1-(3-fluorophenyl)prop-2-yn-1-yl)acetamide (37c).²²⁸



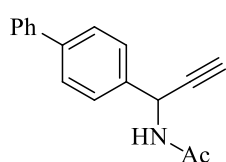
Yield: 73% (139.4 mg). **¹H NMR** (400 MHz CDCl₃) δ 7.29–7.15 (m, 3H), 6.99–6.95 (m, 1H), 6.15 (br d., *J* = 8.0 Hz, 1H), 5.96 (dd, *J* = 8.0, 2.0 Hz, 1H), 2.47 (d, *J* = 2.0 Hz, 1H) 2.00 (s, 3H) ppm. **¹³C NMR** (100 MHz CDCl₃) δ 169.0, 164.2, 140.8, 130.4, 122.8, 115.4, 114.3, 81.1, 73.5, 44.1, 23.2 ppm. **LRMS** (ESI⁺): *m/z* = 192 [M + H]⁺.

Synthesis of *N*-(1-(2,4-dichlorophenyl)prop-2-yn-1-yl)acetamide (37d).



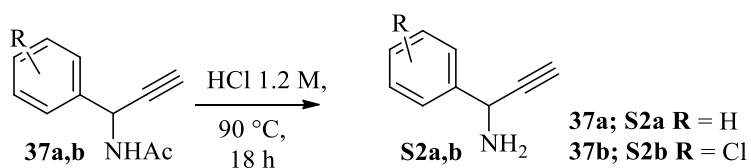
Yield: 76% (183.1 mg). **¹H NMR** (400 MHz CDCl₃) δ 7.56 (d, *J* = 8.0 Hz, 1H), 7.40 (s, 1H), 7.22–7.24 (m, 1H), 6.09 (br s, 1H), 6.08 (s, 1H), 2.46 (d, *J* = 1.5 Hz, 1H), 1.99 (s, 3H) ppm. **¹³C NMR** (100 MHz CDCl₃) δ 168.7, 135.0, 134.2, 134.1, 130.1, 127.5, 80.5, 73.3, 42.8, 23.0 ppm. **LRMS** (ESI⁺): *m/z* = 242 [M + H]⁺, 264 [M + Na]⁺. **HRMS** (ESI): calcd for C₁₁H₁₀Cl₂NO (M + H⁺) 242.0139, found 242.0137.

Synthesis of *N*-(1-([1,1-biphenyl]-4-yl)prop-2-yn-1-yl)acetamide (**37e**).



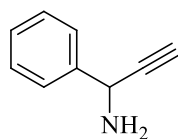
Yield: 75% (186.7 mg). **¹H NMR** (400 MHz CDCl₃) δ 7.57–7.55 (m, 6H), 7.45–7.41 (m, 2H), 7.36–7.33 (m, 1H), 6.05 (d, *J* = 8.0 Hz, 1H), 6.00 (br d, *J* = 8.0 Hz, 1H), 2.51 (s, 1H), 2.03 (s, 3H) ppm. **¹³C NMR** (100 MHz CDCl₃) δ 168.8, 141.4, 140.5, 137.3, 128.9, 127.6, 127.2, 81.7, 73.2, 44.3, 23.3 ppm. **LRMS** (ESI⁺): *m/z* = 250 [M + H]⁺, 272 [M + Na]⁺. **HRMS** (ESI): calcd for C₁₇H₁₆NO (M + H⁺) 250.1232, found 250.1227.

General procedure for the synthesis of propynylamines **S2a** and **S2b**.¹⁷³



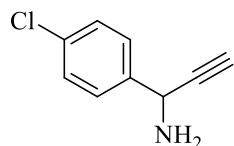
A suspension of **37a** or **37b** (0.76 mmol, 1 equiv) and an aqueous 1.2 M HCl solution (5 mL) was heated to 90°C for 18 h. The reaction mixture was then cooled at room temperature, quenched with saturated NaHCO₃ solution in water (20 mL), and diluted with Et₂O (10 mL). The aqueous layer was extracted twice with Et₂O (20 mL). The combined organic layers were washed with brine, dried over Na₂SO₄ and concentrated under reduced pressure. The crude product was purified by flash column chromatography (SiO₂) using 1:1 EtOAc/hexanes. Compound **S2a** and compound **S2b** were obtained as pale yellow oils.

Synthesis of 1-phenylprop-2-yn-1-amine (**S2a**).²²⁵



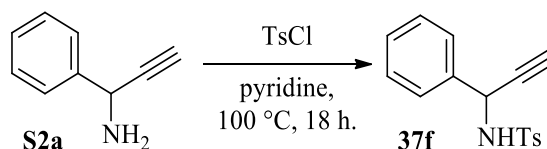
Yield: 72% (71.7 mg). **¹H NMR** (400 MHz CDCl₃) δ 7.57–7.50 (m, 2H), 7.39–7.29 (m, 3H), 5.06 (d, *J* = 2.5 Hz, 1H), 2.41 (d, *J* = 2.5 Hz, 1H), 1.91 (br s, 2H) ppm. **¹³C NMR** (100 MHz CDCl₃) δ 136.3, 129.4, 128.9, 127.7, 80.2, 75.4, 47.9 ppm. **LRMS** (ESI⁺): *m/z* = 132 [M + H]⁺.

Synthesis of 1-(4-chlorophenyl)prop-2-yn-1-amine (**S2b**).²²⁸



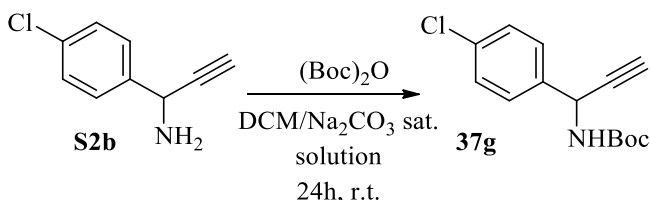
Yield: 74% (92.8 mg). **¹H NMR** (400 MHz CDCl₃) δ 7.49–7.30 (m, 4H), 4.71 (d, *J* = 4.2 Hz, 1H), 2.49 (d, *J* = 4.2 Hz, 1H), 1.75 (br s, 2H) ppm. **¹³C NMR** (100 MHz CDCl₃) δ 154.7, 137.4, 134.0, 128.8, 80.1, 75.5, 47.8 ppm. **LRMS** (ESI⁺): *m/z* = 166 [M + H]⁺.

Synthesis of 4-methyl-*N*-(1-phenylprop-2-yn-1-yl)benzenesulfonamide (**37f**).²²⁹



1-Phenyl-2-propynylamine **S2a** (45.8 mg, 0.35 mmol, 1 eq.) was added to a round-bottom flask containing pyridine (5 mL). Then *p*-toluenesulfonyl chloride (118.2 mg, 0.62 mmol, 1.77 eq.) was added at $0\text{ }^{\circ}\text{C}$ to the solution previously obtained. The solution was allowed to stir at $100\text{ }^{\circ}\text{C}$ for 18 h. The reaction mixture was then quenched with 1 M HCl solution (10 mL) and washed with (10 mL) DCM. Then, (20 mL) saturated NaHCO_3 solution were added to the aqueous layer and this was extracted twice with DCM (20 mL). The combined organic layers were washed with brine (20 mL), dried over Na_2SO_4 , and concentrated under reduced pressure. The crude compound was purified by flash column chromatography (SiO_2) using 1:4 EtOAc/hexanes as the eluent. Compound **37f** was obtained as a yellow-brown solid. **Yield:** 62% (61.9 mg). **^1H NMR** (400 MHz CDCl_3) δ 7.75 (d, $J = 8.0$ Hz, 2H), 7.50-7.35 (m, 2H), 7.35-7.06 (m, 5H), 5.30 (dd, $J = 8.0, 1.5$ Hz, 1H), 5.06 (d, $J = 8.0$ Hz, 1H), 2.41 (s, 3H), 2.30 (d, $J = 1.5$ Hz, 1H) ppm. **^{13}C NMR** (100 MHz CDCl_3) δ 143.7, 137.3, 137.0, 129.6, 128.8, 128.6, 127.5, 127.2, 80.5, 74.8, 49.0, 21.6 ppm. **LRMS** (ESI^+): $m/z = 308$ [$\text{M} + \text{Na}$] $^+$.

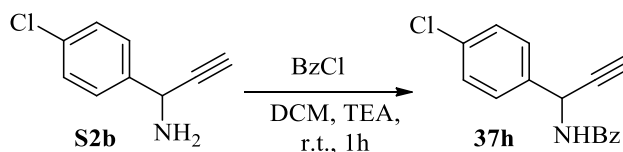
Synthesis of *tert*-butyl (1-(4-chlorophenyl)prop-2-yn-1-yl)carbamate (**37g**).



A solution of $(\text{Boc})_2\text{O}$ (183.1 mg, 0.84 mmol, 1 eq.) in DCM (5 mL) was added dropwise to a solution of propargylamine **S2b** (138.6 mg, 0.84 mmol, 1 eq.) in DCM (5 mL) and Na_2CO_3 saturated solution in water (5 mL), at $0\text{ }^{\circ}\text{C}$. The reaction mixture was then allowed to stir at room temperature for 24 h. The solution was diluted with DCM (10 mL). The aqueous layer was extracted with DCM (10 mL). The combined organic layers were dried over MgSO_4 and concentrated under reduced pressure. The obtained product was purified by silica gel chromatography, using hexane/EtOAc (4:1) as eluent. Compound **37g** was obtained as a tan oil. **Yield:** 60% (159 mg). **^1H NMR** (400 MHz CDCl_3) δ 7.45 (d, $J = 8.5$ Hz, 2H), 7.33 (d, $J = 8.5$ Hz, 2H), 5.64 (d, $J = 7.0$ Hz, 1H), 5.06 (br s, 1H), 2.51 (d, $J = 2.0$ Hz, 1H), 1.46 (s, 9H) ppm. **^{13}C NMR** (100 MHz CDCl_3) δ 154.7, 137.4, 134.0, 128.8, 128.3, 81.6, 80.6, 73.4,

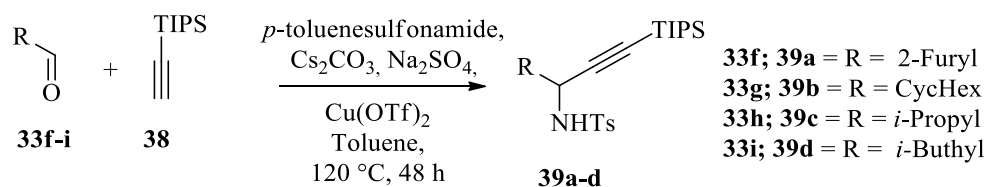
45.6, 28.3 ppm. **LRMS** (ESI⁺): $m/z = 288$ [M + Na]⁺. **HRMS** (ESI): calcd for C₁₄H₁₆ClNNaO₂ (M + Na⁺) 288.0767, found 288.0765.

Synthesis of *N*-[1-(4-chlorophenyl)-2-propyn-1-yl]-benzamide (**37h**).



Benzoyl chloride (0.062 mL, 0.57 mmol, 1.01 eq.) and triethylamine (0.087 mL, 0.67 mmol, 1.2 eq.) were added to a solution of propargylic amine **S2b** (92.4 mg, 0.56 mmol, 1 eq.) in DCM (20 mL) at 0 °C. The reaction mixture was allowed to stir at room temperature for 1 h, and then quenched with 1 M HCl solution (20 mL), and extracted with DCM (20 mL). The combined organic layers were washed with brine (20 mL), dried over Na₂SO₄, and concentrated under reduced pressure. The obtained product was purified by chromatography on silica gel, using hexane/EtOAc (4:1) as eluent. Compound **37h** was obtained as a yellow-brown oil. **Yield**: 65% (97.2 mg). **¹H NMR** (400 MHz CDCl₃) δ 7.79 (d, $J = 7.0$ Hz, 2H), 7.51 (d, $J = 6.0$ Hz, 3H), 7.43 (t, $J = 7.5$ Hz, 2H), 7.33 (d, $J = 8.0$ Hz, 2H), 6.72 (d, $J = 8.0$ Hz, 1H), 6.21 (dd, $J = 8.0, 2.0$ Hz, 1H), 2.55 (d, $J = 2.0$ Hz, 1H) ppm. **¹³C NMR** (100 MHz CDCl₃) δ 166.4, 136.9, 134.2, 133.4, 132.1, 128.9, 128.7, 128.6, 127.2, 81.2, 73.8, 44.4 ppm. **LRMS** (ESI⁺): $m/z = 270$ [M + H]⁺. **HRMS** (ESI): calcd for C₁₆H₁₃ClNO (M + H⁺) 270.0686, found 270.0683.

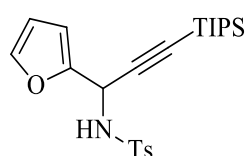
General procedure for the synthesis of silylpropargylamines **39a–d**.



The appropriate aldehyde **33f-i** (1.17 mmol, 1.1 eq.) and triisopropylsilyl acetylene **38** (319.2 mg, 1.75 mmol, 1.5 eq.) were added to a solution of *p*-toluenesulfonamide (200.3 mg, 1.17 mmol, 1 eq.), sodium sulfate (166.2 mg, 1.17 mmol, 1 eq.), cesium carbonate (381.2 mg, 1.17 mmol, 0.1 eq.), and copper triflate (42.3 mg, 0.117 mmol, 0.1 eq.) in anhydrous toluene under N₂ atmosphere. The reaction mixture was allowed to stir at 120 °C for 48 h. The

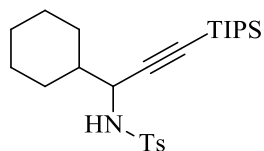
reaction mixture was then quenched with EtOAc (20 mL), and washed with a saturated NaHCO₃ solution (20 mL). The combined organic layers were dried over MgSO₄ and concentrated under reduced pressure. The crude product was purified by chromatography on silica gel, using hexane/EtOAc (4:1) as eluent affording the pure products as yellow-brown oils.

Synthesis of *N*-[1-(2-furanyl)-3-[tris(1-methylethyl)silyl]-2-propyn-1-yl]-4-methylbenzenesulfonamide (39a).



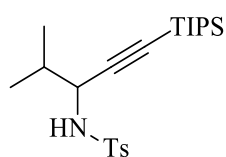
Yield: 48% (251.6 mg). **¹H NMR** (400 MHz CDCl₃) δ 7.75 (d, *J* = 8.0 Hz, 2H), 7.31 (s, 1H), 7.25 (d, *J* = 8.0 Hz, 2H), 6.35 (d, *J* = 3.0 Hz, 1H), 6.27 (t, *J* = 3.0 Hz, 1H), 5.41 (d, *J* = 8.0 Hz, 1H), 4.89 (d, *J* = 8.0 Hz, 1H), 2.39 (s, 3H), 0.96 (m, 18H), 0.93–0.82 (m, 3H) ppm. **¹³C NMR** (100 MHz CDCl₃) δ 150.1, 143.5, 143.2, 137.5, 129.7, 127.2, 110.4, 108.4, 101.4, 87.0, 44.1, 21.6, 18.5, 11.0 ppm. **LRMS** (ESI⁺): *m/z* = 432 [M + H]⁺. **HRMS** (ESI): calcd for C₂₃H₃₇SSiN₂O₃ (M + NH₄⁺) 449.2294, found 449.2284.

Synthesis of *N*-[1-cyclohexyl-3-[tris(1-methylethyl)silyl]-2-propyn-1-yl]-4-methylbenzenesulfonamide (39b).²³⁰



Yield: 45% (235.3 mg). **¹H NMR** (400 MHz CDCl₃) δ 7.74 (d, *J* = 8.0 Hz, 2H), 7.25 (d, *J* = 8.0 Hz, 2H), 4.55 (d, *J* = 9.5 Hz, 1H), 3.92 (dd, *J* = 9.5, 6.0 Hz, 1H), 2.38 (s, 3H), 1.84–1.68 (m, 5H), 1.68–1.50 (m, 4H), 1.30–0.97 (m, 2H), 0.91 (d, *J* = 5.0 Hz, 18H), 0.88–0.81 (m, 3H) ppm. **¹³C NMR** (100 MHz CDCl₃) δ 143.4, 138.4, 129.8, 127.1, 104.9, 85.1, 51.3, 43.8, 29.2, 28.2, 26.2, 25.8, 25.7, 20.7, 18.1, 11.1 ppm. **LRMS** (ESI⁺): *m/z* = 448 [M + H]⁺.

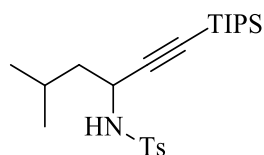
Synthesis of *N*-[1-methylethyl-3-[tris(1-methylethyl)silyl]-2-propyn-1-yl]-4-methylbenzenesulfonamide (39c).



Yield: 22% (104.7 mg). **¹H NMR** (400 MHz CDCl₃) δ 7.77 (d, *J* = 8.5 Hz, 2H), 7.28 (d, *J* = 8.5 Hz, 2H), 4.63 (d, *J* = 9.0 Hz, 1H), 3.95 (dd, *J* = 9.5, 6.0 Hz, 1H), 2.40 (s, 3H), 1.94–1.88 (m, 1H), 1.00 (d, *J* = 6.5 Hz, 6H), 0.92 (d, *J* = 5.0 Hz, 18H), 0.95–0.84 (m, 3H) ppm. **¹³C NMR** (100 MHz CDCl₃) δ 143.4, 137.5, 129.7, 127.2, 104.0, 86.0, 52.3, 34.3, 21.5, 18.7, 18.5, 17.4,

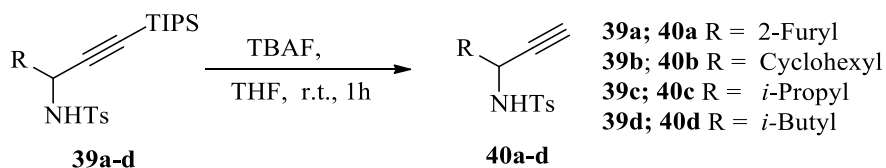
11.0 ppm. **LRMS** (ESI⁺): $m/z = 408$ [M + H]⁺. **HRMS** (ESI): calcd for C₂₂H₄₁SSiN₂O₂ (M + NH₄⁺) 425.2658, found 425.2645.

Synthesis of *N*-[1-(2-methylbutyl)-3-[tris(1-methylethyl)silyl]-2-propyn-1-yl]-4-methyl-benzenesulfonamide (39d).



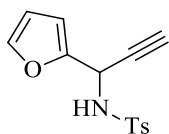
Yield: 56% (275.8 mg). **¹H NMR** (400 MHz CDCl₃) δ 7.77 (d, $J = 8.0$ Hz, 2H), 7.27 (d, $J = 8.0$ Hz, 2H), 4.49 (d, $J = 9.5$ Hz, 1H), 4.13 (q, $J = 7.5$ Hz, 1H), 2.40 (s, 3H), 1.96–1.83 (m, 1H), 1.60–1.44 (m, 2H), 0.92 (d, $J = 5.0$ Hz, 6H), 0.88 (d, $J = 5.0$ Hz, 18H), 0.87–0.86 (m, 3H) ppm. **¹³C NMR** (100 MHz CDCl₃) δ 143.4, 137.6, 129.7, 127.2, 85.0, 46.6, 45.0, 24.8, 22.3, 22.0, 21.5, 18.5, 11.0 ppm. **LRMS** (ESI⁺): $m/z = 422$ [M + H]⁺. **HRMS** (ESI): calcd for C₂₃H₄₃SSiN₂O₂ (M + NH₄⁺) 439.2815, found 439.2804.

General Procedure for the synthesis of propargylamides 40a–d.



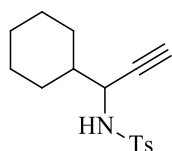
A 1 M TBAF solution in THF (0.54 mmol, 1.1 eq.) was added to a solution of compound **39** (0.27 mmol, 1 eq.) in THF (5 mL) at 0 °C. The reaction mixture was stirred at room temperature for 1h, then quenched with a saturated NaHCO₃ solution (20 mL), and extracted with EtOAc (20 mL). The combined organic layers were washed with brine, dried over MgSO₄, and concentrated under reduced pressure. The crude product was purified by chromatography on silica gel, using hexane/ EtOAc (4:1) as eluent affording the pure products as yellow-brown oils.

Synthesis of *N*-[1-(2-furanyl)-2-propyn-1-yl]-4-methyl-benzenesulfonamide (40a).²³¹



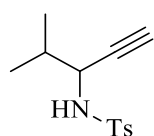
Yield: 82% (60.8 mg). **¹H NMR** (400 MHz CDCl₃) δ 7.75 (d, $J = 8.0$ Hz, 2H), 7.30 (d, $J = 1.0$ Hz, 1H), 7.28 (d, $J = 8.0$ Hz, 2H), 6.33 (d, $J = 3.0$ Hz, 1H), 6.27 (t, $J = 2.0$ Hz, 1H), 5.37 (d, $J = 2.0$ Hz, 1H), 2.42 (s, 3H), 2.30 (d, $J = 2.0$ Hz, 1H) ppm. **¹³C NMR** (100 MHz CDCl₃) δ 149.0, 143.6, 143.1, 137.1, 129.4, 127.3, 110.4, 108.4, 78.3, 73.6, 43.1, 21.5 ppm. **LRMS** (ESI⁺): $m/z = 298$ [M + Na]⁺.

Synthesis of *N*-(1-cyclohexyl-2-propyn-1-yl)-4-methyl-benzenesulfonamide (**40b**).²³¹



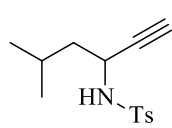
Yield: 99% (77.8 mg). **¹H NMR** (400 MHz CDCl₃) δ 7.75 (d, *J* = 6.5 Hz, 2H), 7.27 (d, *J* = 7.0 Hz, 2H), 4.69 (d, *J* = 7.0 Hz, 1H), 3.86 (m, 1H), 2.40 (s, 3H), 2.01 (s, 1H), 1.84–1.67 (m, 5H), 1.66–1.46 (m, 4H), 1.33–0.99 (m, 2H). **¹³C NMR** (100 MHz CDCl₃) δ 143.4, 132.2, 129.4, 127.3, 80.7, 73.1, 50.6, 42.8, 28.8, 25.7, 25.6, 21.5, 14.1 ppm. **LRMS** (ESI⁺): *m/z* = 314 [M + Na]⁺.

Synthesis of *N*-(1-isopropyl-2-propyn-1-yl)-4-methyl-benzenesulfonamide (**40c**).



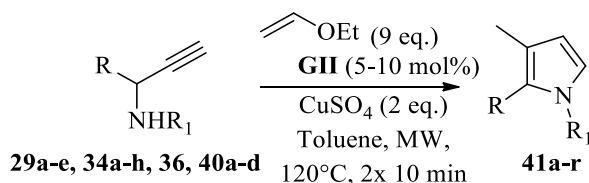
Yield: 95% (64.4 mg). **¹H NMR** (400 MHz CDCl₃) δ 7.78 (d, *J* = 8.0 Hz, 2H), 7.30 (d, *J* = 7.5 Hz, 2H), 4.71 (d, *J* = 9.5 Hz, 1H), 3.90 (ddd, *J* = 10.0, 5.5, 2.0 Hz, 1H), 2.43 (s, 3H), 2.04 (d, *J* = 2.5 Hz, 1H), 1.91 (m, 1H), 0.98 (d, *J* = 6.5 Hz, 6H) ppm. **¹³C NMR** (100 MHz CDCl₃) δ 143.5, 137.2, 129.5, 127.3, 80.4, 73.1, 51.3, 33.5, 21.5, 18.5, 17.3 ppm. **LRMS** (ESI⁺): *m/z* = 274 [M + Na]⁺.

Synthesis of *N*-(1-methylbutyl-2-propyn-1-yl)-4-methyl-benzenesulfonamide (**40d**).



Yield: 93% (66.5 mg). **¹H NMR** (400 MHz CDCl₃) δ 7.79 (d, *J* = 8.0 Hz, 2H), 7.30 (d, *J* = 8.5 Hz, 2H), 4.71 (d, *J* = 9.0 Hz, 1H), 4.15–4.04 (m, 1H), 2.43 (s, 3H), 2.03 (d, *J* = 2.0 Hz, 1H), 1.89–1.77 (m, 1H), 1.53 (td, *J* = 7.6, 3.0 Hz, 2H), 0.89 (dd, *J* = 6.0, 3.0 Hz, 6H) ppm. **¹³C NMR** (100 MHz CDCl₃) δ 143.6, 137.3, 129.5, 127.5, 82.2, 72.4, 45.6, 44.0, 24.6, 22.2, 22.0, 21.6 ppm. **LRMS** (ESI⁺): *m/z* = 288 [M + Na]⁺. **HRMS** (ESI): calcd for C₁₄H₁₉NNaO₂S (M + H⁺) 288.1034, found 288.1008.

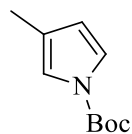
General Procedure for the synthesis of 3-methyl-pyrroles **41a-r**.



Ethyl vinyl ether (0.43 mL, 4.5 mmol, 9 eq.), CuSO₄ (159 mg, 1 mmol, 2 eq.) and Grubbs catalyst second generation (5–10 mol %) were added to a microwave vial containing a solution of the appropriate propargylamine derivative (0.5 mmol, 1 eq.) in 3 mL of degassed toluene. The reaction mixture was heated at 120 °C under microwave irradiation (300 W)

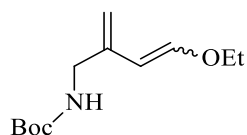
for 2×10 min. The maximum internal pressure observed during the reaction was 44 psi. The reaction mixture was then quenched with saturated aqueous NH_4Cl solution (10 mL), NH_4OH solution (0.5 mL), and Et_2O (10 mL). The aqueous layer was extracted twice with Et_2O (10 mL). The combined organic layers were washed with brine (10 mL), dried over Na_2SO_4 , and concentrated under reduced pressure. All the crude products were purified by flash column chromatography (SiO_2) using 1:4 Et_2O /hexanes as the eluent to yield the desired pyrroles **41** as tan oils.

Synthesis of *t*-butyl 3-Methyl-1H-pyrrole-1-carboxylate (**41a**).



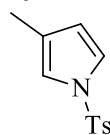
Yield: 56% (50.4 mg). **^1H NMR** (400 MHz CDCl_3) δ 7.12 (d, $J = 3.0$ Hz, 1H), 6.95 (s, 1H), 6.04 (d, $J = 3.0$ Hz, 1H), 2.04 (s, 3H), 1.56 (s, 9H) ppm. **^{13}C NMR** (100 MHz CDCl_3) δ 149.0, 122.6, 120.0, 117.2, 114.1, 83.2, 28.1, 12.0 ppm. **GC-MS** m/z (ES+) m/z : 181 $[\text{M}]^+$. **HRMS** (ESI): calcd for $\text{C}_{10}\text{H}_{16}\text{NO}_2$ ($\text{M} + \text{H}^+$) 182.1181, found 182.1173.

Synthesis of (E/Z)-*tert*-butyl-(4-ethoxy-2-methylenebut-3-en-1-yl)carbamate (**30**).



Yield: 41% (46.3 mg). obtained as a 2:1 mixture of E/Z isomers as revealed by **GC-MS**. This compound was isolated following the general procedure for the synthesis of 3-methyl-pyrroles **41a-r** without the presence of CuSO_4 . **^1H NMR** (400 MHz CDCl_3) major isomer E. δ 6.63 (d, $J = 12.0$ Hz, 1H), 5.53 (d, $J = 12.0$ Hz, 1H), 4.85 (s, 1H), 4.80 (s, 1H), 4.59 (br s, 1H), 3.84–3.76 (m, 4H), 1.43 (s, 9H), 1.27 (t, $J = 4.0$ Hz, 3H) ppm; peaks from minor isomer Z δ 5.96 (d, $J = 7.0$ Hz, 1H), 5.09 (s, 1H), 4.96 (s, 1H) ppm. **^{13}C NMR** (100 MHz CDCl_3) δ 155.8, 148.2, 140.9, 111.0, 106.2, 79.4, 65.8, 42.8, 28.4, 14.9 ppm; peaks from minor isomer δ 146.0, 113.6, 105.2, 69.0, 45.5, 27.4, 15.3 ppm. **GC-MS** m/z (ES+) m/z : 227 $[\text{M}]^+$, 171 $[\text{M} - t\text{-Bu}]^+$, 154 $[\text{M} - t\text{-BuOH}]^+$. **HRMS** (ESI): calcd for $\text{C}_{12}\text{H}_{21}\text{NO}_3$ $[\text{M}]^+$ 227.1516, found 227.1553.

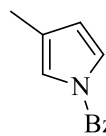
Synthesis of 3-methyl-1-[(4-methylphenyl)sulfonyl]-1H-pyrrole (**41b**).



Yield: 53% (62.0 mg). **^1H NMR** (400 MHz CDCl_3) δ 7.70 (d, $J = 7.5$ Hz, 2H), 7.25 (d, $J = 7.5$ Hz, 2H), 7.03 (d, $J = 3.0$ Hz, 1H), 6.86 (s, 1H), 6.10 (d, $J = 3.0$ Hz, 1H), 2.38 (s, 3H), 2.00 (s, 3H) ppm. **^{13}C NMR** (100 MHz CDCl_3) δ 144.6, 136.2, 129.8,

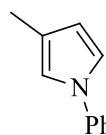
126.7, 124.5, 120.8, 117.7, 115.7, 21.6, 11.8 ppm. **GC-MS** m/z (ES+) m/z : 235 $[M]^+$. **HRMS** (ESI): calcd for $C_{12}H_{14}NO_2S$ ($M + H^+$) 236.0745, found 236.0738.

Synthesis of 3-methyl-1-benzoyl-1H-pyrrole (41c).



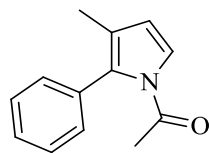
Yield: 39% (36.4 mg). **1H NMR** (400 MHz $CDCl_3$) δ 7.71 (d, $J = 7.0$ Hz, 2H), 7.57–7.55 (m, 1H), 7.50–7.46 (m, 2H), 7.16 (d, $J = 2.0$ Hz, 1H), 7.03 (d, $J = 2.0$ Hz, 1H), 6.18 (s, 1H), 2.08 (s, 3H) ppm. **^{13}C NMR** (100 MHz $CDCl_3$) δ 165.5, 132.0, 129.4, 128.4, 124.1, 121.4, 118.5, 115.6, 12.1 ppm. **GC-MS** m/z (ES+) m/z : 185 $[M]^+$. **HRMS** (ESI): calcd for $C_{12}H_{12}NO$ ($M + H^+$) 186.0919, found 186.0906.

Synthesis of 3-methyl-1-phenyl-1H-pyrrole (41d).²³²



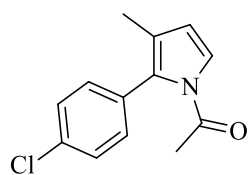
Yield: 54% (42.4 mg). **1H NMR** (400 MHz $CDCl_3$) δ 7.40–7.35 (m, 4H), 7.19–7.18 (m, 1H), 6.98 (d, $J = 2.5$ Hz, 1H), 6.86 (d, $J = 2.5$ Hz, 1H), 6.16 (s, 1H), 2.16 (s, 3H) ppm. **^{13}C NMR** (100 MHz $CDCl_3$) δ 140.8, 129.5, 125.1, 121.2, 120.0, 119.0, 117.2, 112.0, 12.0 ppm. **GC-MS** m/z (ES+) m/z : 157 $[M]^+$. **HRMS** (ESI): calcd for $C_{11}H_{12}N$ ($M + H^+$) 158.0970, found 158.0960.

Synthesis of 3-methyl-2-phenyl-1-acetyl-1H-pyrrole (41f).²³³



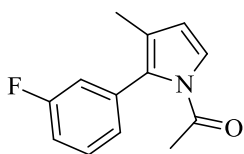
Yield: 70% (69.3 mg). **1H NMR** (400 MHz $CDCl_3$) δ 7.42–7.30 (m, 3H), 7.28 (d, $J = 3.5$ Hz, 1H), 7.27–7.23 (m, 2H), 6.16 (d, $J = 3.5$ Hz, 1H), 1.90 (s, 3H), 1.55 (s, 3H) ppm. **^{13}C NMR** (100 MHz $CDCl_3$) δ 169.1, 133.7, 130.5, 130.2, 128.1, 126.8, 124.5, 120.2, 113.9, 25.0, 11.4 ppm. **GC-MS** m/z (ES+) m/z : 199 $[M + H]^+$.

Synthesis of 3-methyl-2-(4-chlorophenyl)-1-acetyl-1H-pyrrole (41g).



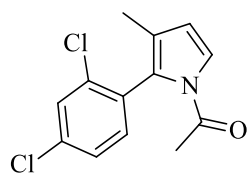
Yield: 72% (83.5 mg). **1H NMR** (400 MHz $CDCl_3$) δ 7.35 (d, $J = 8.0$ Hz, 2H), 7.21 (d, $J = 3.0$ Hz, 1H), 7.17 (d, $J = 8.0$ Hz, 2H), 6.16 (d, $J = 3.0$ Hz, 1H), 2.29 (s, 3H), 1.89 (s, 3H) ppm. **^{13}C NMR** (100 MHz $CDCl_3$) δ 168.4, 133.5, 132.1, 131.5, 129.4, 128.3, 123.9, 120.7, 114.3, 24.6, 11.4 ppm. **GC-MS** m/z (ES+) m/z : 233 $[M]^+$. **HRMS** (ESI): calcd for $C_{13}H_{13}ClNO$ ($M + H^+$) 234.0686, found 234.0677.

Synthesis of 3-methyl-2-(3-fluorophenyl)-1-acetyl-1H-pyrrole (41h).



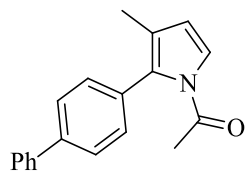
Yield: 76% (82.2 mg). **¹H NMR** (400 MHz CDCl₃) δ 7.36–7.29 (m, 1H), 7.21 (d, *J* = 3.0 Hz, 1H), 7.06–6.91 (m, 3H), 6.15 (d, *J* = 3.0 Hz, 1H), 2.27 (s, 3H), 1.90 (s, 3H) ppm. **¹³C NMR** (100 MHz CDCl₃) δ 168.4, 163.7, 135.8, 129.5, 126.0, 124.1, 120.7, 117.3, 114.6, 114.4, 114.2, 22.7, 14.2 ppm. **GC-MS** *m/z* (ES+) *m/z*: 217 [M]⁺. **HRMS** (ESI): calcd for C₁₃H₁₃FNO (*M* + H⁺) 218.0981, found 218.0975.

Synthesis of 3-methyl-2-(2,4-dichlorophenyl)-1-acetyl-1H-pyrrole (41i).



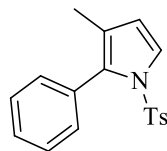
Yield: 38% (50.5 mg). **¹H NMR** (400 MHz CDCl₃) δ 7.47–7.40 (m, 1H), 7.30–7.25 (m, 1H), 7.20 (s, 1H), 7.19 (d, *J* = 3.5 Hz, 1H), 6.20 (d, *J* = 3.5 Hz, 1H), 2.35 (s, 3H) 1.85 (s, 3H) ppm. **¹³C NMR** (100 MHz CDCl₃) δ 168.6, 136.0, 134.4, 132.6, 131.9, 129.3, 127.0, 126.4, 124.3, 102.6, 114.3, 23.6, 11.1 ppm. **GC-MS** *m/z* (ES+) *m/z*: 267 [M]⁺. **HRMS** (ESI): calcd for C₁₃H₁₂Cl₂NO (*M* + H⁺) 268.0296, found 268.0285.

Synthesis of 3-methyl-2-(4-phenyl-phenyl)-1-acetyl-1H-pyrrole (41j).



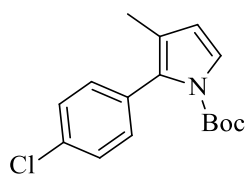
Yield: 59% (80.8 mg). **¹H NMR** (400 MHz CDCl₃) δ 7.67–7.59 (m, 4H), 7.48–7.40 (m, 2H), 7.37–7.30 (m, 3H), 7.28 (d, *J* = 3.0 Hz, 1H), 6.18 (d, *J* = 3.0 Hz, 1H), 2.26 (s, 3H), 1.96 (s, 3H) ppm. **¹³C NMR** (100 MHz CDCl₃) δ 168.9, 140.7, 140.2, 132.6, 130.6, 130.2, 128.8, 127.4, 127.1, 126.8, 123.8, 120.5, 114.2, 25.0, 11.6 ppm. **GC-MS** *m/z* (ES+) *m/z*: 275 [M]⁺. **HRMS** (ESI): calcd for C₁₉H₁₈NO (*M* + H⁺) 276.1388, found 276.1380.

Synthesis of 3-methyl-2-phenyl-1-[(4-methylphenyl)sulfonyl]-1H-pyrrole (41k).



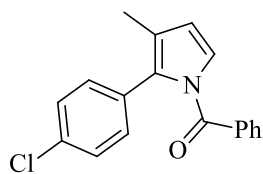
Yield: 38% (58.9 mg). **¹H NMR** (400 MHz CDCl₃) δ 7.38–7.18 (m, 7H), 7.08–7.05 (m, 3H), 6.18 (d, *J* = 3.0 Hz, 1H), 2.34 (s, 3H), 1.80 (s, 3H) ppm. **¹³C NMR** (100 MHz CDCl₃) δ 144.4, 135.9, 131.9, 131.2, 130.7, 129.3, 128.1, 127.4, 127.2, 123.8, 122.4, 114.2, 21.6, 11.6 ppm. **GC-MS** *m/z* (ES+) *m/z*: 311 [M]⁺. **HRMS** (ESI): calcd for C₁₈H₁₈NO₂S (*M* + H⁺) 312.1058, found 312.1047.

Synthesis of *tert*-butyl 2-(4-chlorophenyl)-3-methyl-1H-pyrrole-1-carboxylate (41l).



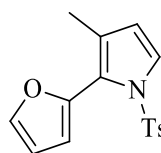
Yield: 50% (72.5 mg). **¹H NMR** (400 MHz CDCl₃) δ 7.39-7.29 (t, *J* = 8.2 Hz, 2H), 7.27 (d, *J* = 3.2 Hz, 1H), 7.19-7.12 (m, *J* = 8.2 Hz, 2H), 6.10 (d, *J* = 3.2 Hz, 1H), 1.89 (s, 3H), 1.30 (s, 9H) ppm. **¹³C NMR** (100 MHz CDCl₃/CDCl₃) δ 149.2, 133.0, 132.5, 131.6, 129.1, 127.2, 122.6, 121.3, 113.0, 83.3, 27.6, 11.6 ppm. **GC-MS** *m/z* (ES⁺) *m/z*: 291 [M]⁺. **HRMS** (ESI): calcd for C₁₆H₁₉ClNO₂ (M + H⁺) 292.1104, found 292.1098.

Synthesis of 3-methyl-2-(4-chlorophenyl)-1-benzoyl-1H-pyrrole (41m).



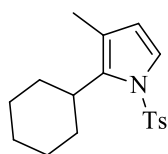
Yield: 64% (94.1 mg). **¹H NMR** (400 MHz CDCl₃) δ 7.74 (d, *J* = 7.0 Hz, 2H), 7.56 (t, *J* = 7.0 Hz, 1H), 7.43 (t, *J* = 7.0 Hz, 2H), 7.29 (d, *J* = 8.0 Hz, 2H), 7.18 (d, *J* = 8.0 Hz, 2H), 6.96 (d, *J* = 3.0 Hz, 1H), 6.18 (d, *J* = 3.0 Hz, 1H), 2.08 (s, 3H) ppm. **¹³C NMR** (100 MHz CDCl₃) δ 168.2, 133.6, 132.7, 131.4, 130.7, 130.2, 128.8, 128.4, 128.2, 128.0, 123.9, 123.7, 113.9, 11.6 ppm. **GC-MS** *m/z* (ES⁺) *m/z*: 295 [M]⁺. **HRMS** (ESI): calcd for C₁₈H₁₅ClNO (M + H⁺) 296.0842, found 296.0836.

Synthesis of 2-(furan-2-yl)-3-methyl-1-[(4-methylphenyl)sulfonyl]-1H-pyrrole (41o).



Yield: 76% (114.3 mg). **¹H NMR** (400 MHz CDCl₃) δ 7.49 (d, *J* = 8.0 Hz, 2H), 7.46 (dd, *J* = 2.0, 1.0 Hz, 1H), 7.39 (d, *J* = 3.0 Hz, 1H), 7.22 (d, *J* = 8.0 Hz, 2H), 6.47 (dd, *J* = 3.0, 1.5 Hz, 1H), 6.38 (d, *J* = 3.0 Hz, 1H), 6.19 (d, *J* = 3.0 Hz, 1H), 2.39 (s, 3H), 1.93 (s, 3H) ppm. **¹³C NMR** (100 MHz CDCl₃) δ 144.6, 143.1, 142.9, 136.0, 129.5, 127.7, 127.3, 123.5, 120.9, 113.9, 113.1, 110.7, 21.7, 11.8 ppm. **GC-MS** *m/z* (ES⁺) *m/z*: 301 [M]⁺. **HRMS** (ESI): calcd for C₁₆H₁₆NO₃S (M + H⁺) 302.0851, found 302.0846.

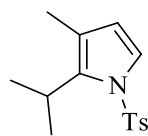
Synthesis of 2-cyclohexyl-3-methyl-1-[(4-methylphenyl)sulfonyl]-1H-pyrrole (41p).



Yield: 43% (67.9 mg). **¹H NMR** (400 MHz CDCl₃) δ 7.64 (d, *J* = 8.0 Hz, 2H), 7.29 (d, *J* = 8.0 Hz, 2H), 7.23 (d, *J* = 3.0 Hz, 1H), 6.03 (d, *J* = 3.0 Hz, 1H), 3.10 (dt, *J* = 12.0, 3.0 Hz, 1H), 2.42 (s, 3H), 2.06 (s, 3H), 1.69–1.58 (m, 4H), 1.51–1.44 (m, 4H), 1.34–1.27 (m, 2H) ppm. **¹³C NMR** (100 MHz CDCl₃) δ 144.5, 137.1, 134.4, 129.8, 126.8, 120.6, 120.3, 114.7, 36.0, 31.1, 29.7, 27.0, 26.0,

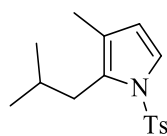
21.7, 13.2 ppm. **GC-MS** m/z (ES+) m/z: 317 [M]⁺. **HRMS** (ESI): calcd for C₁₈H₂₄NO₂S (M + H⁺) 318.1528, found 318.1516.

Synthesis of 3-methyl-1-[(4-methylphenyl)sulfonyl]-2-(propan-2-yl)-1H-pyrrole (41q).



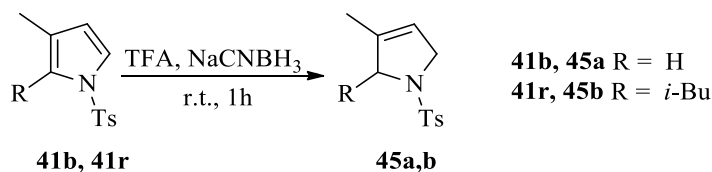
Yield: 71% (97.9 mg). **¹H NMR** (400 MHz CDCl₃) δ 7.60 (d, *J* = 8.0 Hz, 2H), 7.28 (d, *J* = 8.0 Hz, 2H), 7.21 (d, *J* = 3.0 Hz, 1H), 6.03 (d, *J* = 3.0 Hz, 1H), 3.51-3.44 (m, 1H), 2.41 (s, 3H), 2.04 (s, 3H), 1.04 (d, *J* = 6.5 Hz, 6H) ppm. **¹³C NMR** (100 MHz CDCl₃) δ 144.5, 137.1, 135.3, 129.9, 126.7, 120.6, 120.5, 114.9, 29.7, 25.4, 21.6, 21.2, 12.9 ppm. **GC-MS** m/z (ES+) m/z: 277 [M]⁺. **HRMS** (ESI): calcd for C₁₅H₂₀NO₂S (M + H⁺) 278.1215, found 278.1207.

Synthesis of 3-methyl-1-[(4-methylphenyl)sulfonyl]-2-(2-methylpropyl)-1H-pyrrole (41r).



Yield: 69% (100.3 mg). **¹H NMR** (400 MHz CDCl₃) δ 7.58 (d, *J* = 8.0 Hz, 2H), 7.26 (d, *J* = 8.0 Hz, 2H), 7.20 (d, *J* = 3.0 Hz, 1H), 6.09 (d, *J* = 3.0 Hz, 1H), 2.46 (d, *J* = 7.0 Hz, 2H), 2.40 (s, 3H), 2.03-1.93 (m, 1H), 1.92 (s, 3H), 0.86 (d, *J* = 6.0 Hz, 6H) ppm. **¹³C NMR** (100 MHz CDCl₃) δ 144.4, 137.0, 130.9, 129.8, 126.4, 122.5, 121.8, 114.5, 34.1, 29.9, 22.7, 22.3, 21.6, 12.0 ppm. **GC-MS** m/z (ES+) m/z: 291 [M]⁺. **HRMS** (ESI): calcd for C₁₆H₂₂NO₂S (M + H⁺) 292.1371, found 292.1364.

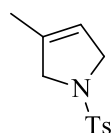
General procedure for the synthesis of pyrrolines (45a,b).



Sodium cyanoborohydride (23.8 mg, 0.38 mmol, 3 eq.) was added to a round-bottom flask containing trifluoroacetic acid (2 mL). The solution was allowed to stir for 20 min at room temperature. Then the appropriate pyrrole **41b** or **41r** (0.127 mmol, 1 eq.) was added to the solution previously obtained. The solution was allowed to stir at room temperature for 1 h.

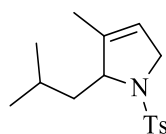
The reaction mixture was then quenched with water (10 mL) and DCM (10 mL). The aqueous layer was extracted twice with DCM (20 mL). The combined organic layers were washed with a NaHCO₃ saturated solution (10 mL), brine (10 mL), dried over Na₂SO₄, and concentrated under reduced pressure. The crude pyrrolines **45a,b** proved to be pure enough to be used in the next synthetic step without any further purification.

Synthesis of 3-methyl-1-[(4-methylphenyl)sulfonyl]-2,5-dihydro-1H-pyrrole (**45a**).



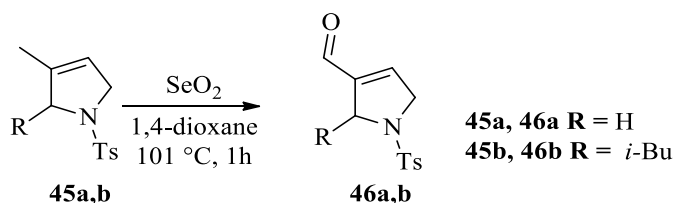
Yield: 65% (19.6 mg). **¹H NMR** (400 MHz CDCl₃) δ 7.69 (d, *J* = 8.0 Hz, 2H), 7.30 (d, *J* = 8.0 Hz, 2H), 5.22 (t, *J* = 4.0 Hz, 1H), 4.04 (d, *J* = 4.0 Hz, 2H), 3.94 (s, 2H), 2.40 (s, 3H), 1.63 (s, 3H) ppm. **¹³C NMR** (100 MHz CDCl₃) δ 143.4, 135.1, 134.2, 129.8, 127.5, 119.1, 57.7, 55.2, 21.5, 14.1 ppm. **LRMS** (ESI⁺): *m/z* = 238.

Synthesis of 2-isobutyl-3-methyl-1-[(4-methylphenyl)sulfonyl]-2,5-dihydro-1H-pyrrole (**45b**).



Yield: 56% (20.9 mg). **¹H NMR** (400 MHz CDCl₃) δ 7.65 (d, *J* = 8.0 Hz, 2H), 7.25 (d, *J* = 8.0 Hz, 2H), 5.02 (t, *J* = 1.5 Hz, 1H), 4.25 (s, 1H), 4.01 (d, *J* = 1.5 Hz, 2H), 2.38 (s, 3H), 1.92–1.85 (m, 1H), 1.56 (s, 3H), 1.48 (t, *J* = 1.5 Hz, 2H), 1.01 (d, *J* = 6.5 Hz, 3H), 0.88 (d, *J* = 6.5 Hz, 3H) ppm. **¹³C NMR** (100 MHz CDCl₃) δ 149.4, 138.6, 137.5, 129.6, 127.5, 118.9, 68.4, 42.4, 33.9, 24.3, 23.8, 23.2, 14.1 ppm. **LRMS** (ESI⁺): *m/z* = 294.

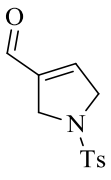
General procedure for the synthesis of aldehydes **46a,b**.



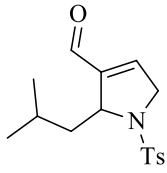
The appropriate pyrroline **45a,b** (0.076 mmol, 1 equiv) was added to a round-bottom flask containing anhydrous 1,4-dioxane (2 mL). Then SeO₂ (8.4 mg, 0.076 mmol, 1 eq.) was added to the solution previously obtained. The solution was allowed to stir at reflux for 1 h under N₂ atmosphere. The reaction mixture was then cooled at room temperature, quenched with 10 mL of water, and DCM (10 mL) was added. The aqueous layer was extracted twice with

DCM (20 mL). The combined organic layers were washed with a NaHCO₃ saturated solution (10 mL) and brine (10 mL), dried over Na₂SO₄, and concentrated under reduced pressure. The crude aldehydes were purified by flash column chromatography (SiO₂) using 2:3 EtOAc/hexanes as the eluent.

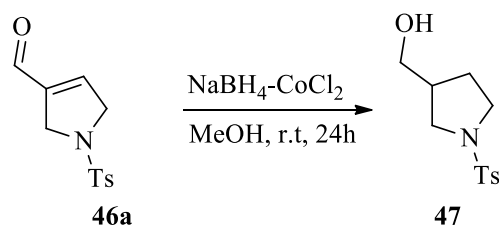
Synthesis of 1-[(4-methylphenyl)sulfonyl]-2,5-dihydro-1H-pyrrole-3-carbaldehyde (46a).

 **Yield:** 56% (10.6 mg). **¹H NMR** (400 MHz CDCl₃) δ 9.53 (s, 1H), 7.73 (d, *J* = 8.0 Hz, 2H), 7.33 (d, *J* = 8.0 Hz, 2H), 6.02 (t, *J* = 2.0 Hz, 1H), 4.38 (s, 2H), 4.26 (d, *J* = 2.0 Hz, 2H), 2.41 (s, 3H) ppm. **¹³C NMR** (100 MHz CDCl₃) δ 186.6, 144.1, 142.5, 141.7, 130.1, 127.6, 55.6, 51.9, 21.6 ppm. **LRMS** (ESI⁺): *m/z* = 252 [M + H]⁺, **HRMS** (ESI): calcd for C₁₂H₁₄NO₃S (M + H⁺) 252.0694, found 252.0686.

Synthesis of 2-isobutyl-1-[(4-methylphenyl)sulfonyl]-2,5-dihydro-1H-pyrrole-3-carbaldehyde (46b).

 **Yield:** 65% (15.1 mg). **¹H NMR** (400 MHz CDCl₃) δ 9.53 (s, 1H), 7.65 (d, *J* = 8.0 Hz, 2H), 7.25 (d, *J* = 8.0 Hz, 2H), 6.53 (s, 1H), 4.78 (d, *J* = 1.0 Hz, 1H), 4.34–4.32 (m, 2H), 2.41 (s, 3H), 1.92–1.85 (m, 1H), 1.48 (d, *J* = 2.0 Hz, 2H), 1.01 (d, *J* = 6.5 Hz, 3H), 0.88 (d, *J* = 6.5 Hz, 3H) ppm. **¹³C NMR** (100 MHz CDCl₃) δ 186.5, 146.1, 143.9, 143.4, 134.3, 129.5, 127.5, 63.7, 54.9, 43.1, 28.3, 28.1, 24.4, 23.8, 22.4, 21.6 ppm. **LRMS** (ESI⁺): *m/z* = 308 [M + H]⁺, **HRMS** (ESI): calcd for C₁₆H₂₂NO₃S (M + H⁺) 308.1320, found 308.1308.

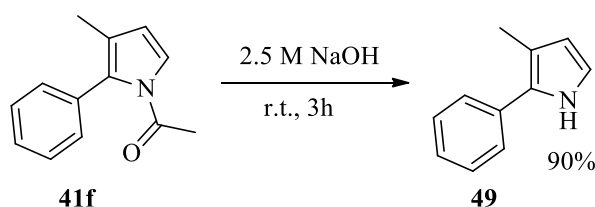
Synthesis of (1-tosylpyrrolidin-3-yl)methanol (47).¹⁸³



The aldehyde **46a** (10 mg, 0.04 mmol 1 eq.) was dissolved in MeOH (2 mL). The solution was treated with a mixture of NaBH₄ (4.53 mg, 0.12 mmol, 3 eq.) and CoCl₂·6H₂O (9.5 mg, 0.04 mmol, 1eq.) at room temperature. The reaction was stirred for 15 min and then further

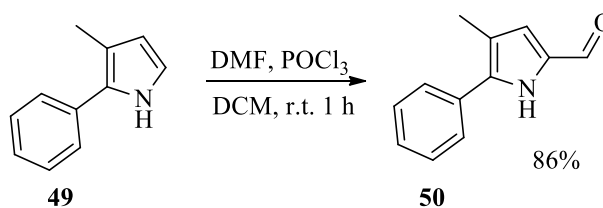
NaBH₄ was added until the reaction went to completion (24 h). The crude reaction was quenched with water (10 mL) and extracted twice with EtOAc (5 mL). The combined organic layers were washed with brine (10 mL), dried over Na₂SO₄ and concentrated under reduced pressure affording [1-(toluene-4-sulfonyl)-pyrrolidin-3-yl]-methanol **47**. **Yield:** 56% (5.7 mg). **¹H NMR** (400 MHz CDCl₃) δ 7.68 (d, *J* = 8.0 Hz, 2H), 7.32 (d, *J* = 8.0 Hz, 2H), 3.41 (m, 2H), 3.30 (m, 2H), 3.13 (m, 1H), 3.04 (dd, *J* = 10.0, 6.0 Hz, 1H), 2.66 (br s, 1H), 2.41 (s, 3H), 2.27 (m, 1H), 1.85 (m, 1H), 1.54 (m, 1H) ppm. **¹³C NMR** (100 MHz CDCl₃) δ 143.5, 133.1, 129.6, 127.7, 63.5, 50.3, 47.4, 40.6, 27.4, 21.4 ppm. **LRMS** (ESI⁺): *m/z* = 256 [M + H]⁺.

Synthesis of 3-methyl-2-phenyl-1H-pyrrole (49).



The pyrrole **41f** (89.4 mg, 0.452 mmol 1 eq.) was added to a round-bottom flask containing 2.5 M NaOH solution (2 mL). The reaction mixture was allowed to stir at r.t. for 3 h. The reaction mixture was then diluted with water (10 mL), and DCM (10 mL) was added. The aqueous layer was extracted twice with DCM (10 mL). The combined organic layers were washed with brine (10 mL), dried over Na₂SO₄, and concentrated under reduced pressure. The crude pyrrole **49** was purified by flash column chromatography (SiO₂) using 2:3 EtOAc/hexanes as the eluent. **Yield:** 90% (63.4 mg). **¹H NMR** (400 MHz CDCl₃) δ 8.13 (br s, 1H), 7.45–7.37 (m, 4H), 7.25–7.21 (m, 1H), 6.76 (d, *J* = 2.5 Hz, 1H), 6.14 (d, *J* = 2.5 Hz, 1H), 2.27 (s, 3H) ppm. **¹³C NMR** (100 MHz CDCl₃) δ 133.7, 128.7, 128.3, 128.0, 126.0, 117.3, 116.1, 112.2, 14.2 ppm. **GC-MS** *m/z* (ES⁺) *m/z*: 157 [M]⁺.

Synthesis of 4-methyl-5-phenyl-1H-pyrrole-2-carbaldehyde 50.



A solution of DMF (0.11 mmol, 1.1 eq.) and phosphorus oxychloride (0.01 mL, 0.10 mmol, 1 eq.) were added to a round-bottom flask containing DCM (2 mL). The solution was

allowed to stir for 15 min at room temperature. Then the solution was cooled down at 0 °C and 3-methyl-2-phenyl-1H-pyrrole **49** (15.6 mg, 0.10 mmol, 1 eq.) in 1 mL of DCM was added to the solution previously obtained. The solution was allowed to stir at room temperature for 1 h. The reaction mixture was then quenched with 1 M Na₂CO₃ aqueous saturated solution (10 mL). The aqueous layer was extracted twice with DCM (20 mL). The combined organic layers were washed with a NaHCO₃ saturated solution (10 mL), brine (10 mL), and dried over Na₂SO₄ and concentrated under reduced pressure. The crude pyrrole was purified by flash column chromatography (SiO₂) using 1:4 EtOAc/hexanes as the eluent. **Yield:** 86% (15.9 mg). **¹H NMR** (400 MHz CDCl₃) δ 9.44 (s, 1H), 9.22 (br s, 1H), 7.51–7.43 (m, 4H), 7.38–7.34 (m, 1H), 6.84 (s, 1H), 2.27 (s, 3H) ppm. **¹³C NMR** (100 MHz CDCl₃) δ 178.6, 136.9, 131.6, 131.4, 129.0, 128.3, 127.2, 123.7, 119.5, 12.5 ppm. **GC-MS** m/z (ES+) m/z: 185 [M]⁺. **HRMS** (ESI): calcd for C₁₂H₁₂NO (M + H⁺) 186.0919, found 186.0912.

5.2.4. Applications of MAO catalysed oxidation/aromatization reaction toward the synthesis of antitubercular pyrrole derivatives.

5.2.4.1. Preparation of biocatalysts. The preparation of the biocatalysts was performed by Prof. Gary Black at Northumbria University. MAO-N (monoamine oxidase from *Aspergillus niger*) was transformed into *E. coli* according to previously reported procedures.^{234,235} MAO-D5 was produced in *E. coli* BL21(DE3). MAO-D9 was produced in *E. coli* BL21(DE3). 6-HDNO E350L/E352D was produced in *E. coli* BL21(DE3). In all cases an overnight 10 mL starter culture of each clone was grown in LB (Luria-Bertani) broth + Ap (Ampicillin) (100 µg/mL) at 37°C, 200 rpm. The starter culture was then inoculated into 1 L of Auto Induction Media Super Broth Base including trace elements (Formedium Ltd, UK) + Ap (100 µg/mL), in a 2 L baffled flask, and grown at 30°C, 180 rpm for 2 days. Cells were then harvested by centrifugation at 4000 x g for 10 min at 4°C. The supernatant was discarded and the cell pellet was resuspended in 10 mL of 18.2 MΩ/cm H₂O. The resuspended cells were then frozen and freeze-dried. Typically 4 g of lyophilized *E. coli* cells were obtained from a 600 mL culture.

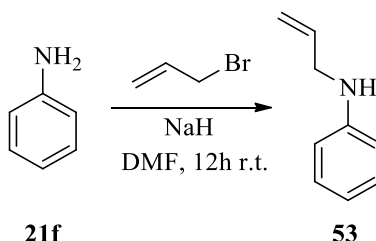
5.2.4.2. Computational details.

The computational analysis was carried out by by collaborators at King's College London. The substrates were docked into MAO-D5 (PDB: 2VVM)²³⁶ with the PLANTS 1.2 software²³⁷ using the ChemPLP scoring function. Chain A was chosen for the simulation.

The structures were prepared with the protein preparation tool which has been implemented in MOE 2014: Hydrogens were added, the missing loops (2VVM: E32-D37, 3ZDN: E32-P39) were modelled, the C-termini were capped and the protonation states were corrected to pH 7.8 with the Protonate3D tool. Search spaces were set as spheres with a radius of 15 Å. The centre of the search space was positioned, in MAO-D5, on the centre of mass of the proline molecule co-crystallised in the active site.

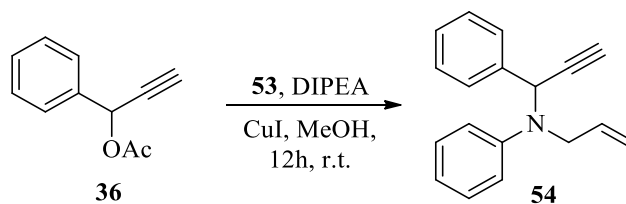
5.2.4.3. Chemistry.

Synthesis of *N*-allylaniline (**53**).²³⁸



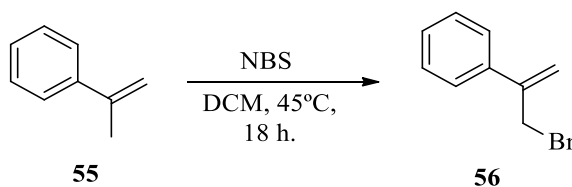
Aniline **21f** (0.466 mL, 5.15 mmol, 1 eq.) was dissolved in a round bottom flask containing dry DMF (10 mL) under nitrogen atmosphere, and NaH (123.6 mg, 5.15 mmol, 1 eq.) was added at 0°C. The reaction mixture was allowed to stir for 30 minutes at room temperature. Then allylbromide (0.445 mL, 5.15 mmol, 1 eq.) was added to the stirring solution. The reaction was allowed to stir at room temperature for 12 h. The reaction mixture was then quenched with saturated NaHCO₃ aqueous solution (20 mL) and extracted twice with 20 mL of Et₂O. The combined organic layers were collected, washed with brine, dried over Na₂SO₄ and concentrated under reduced pressure giving a yellow crude oil. The crude product was purified by chromatography on silica gel, using hexane/EtOAc (30:1) as eluent. The pure product **53** was obtained as a pale yellow oil. **Yield:** 80% (552.1 mg). **¹H NMR** (400 MHz, CDCl₃): δ 7.19-7.13 (m, 2H), 6.72-6.67 (m, 1H), 6.64-6.60 (m, 2H), 6.01-5.89 (tdd, *J* = 18.0, 10.0, 1.5 Hz, 1H), 5.27 (dd, *J* = 18.0, 1.5 Hz, 1H), 5.15 (dd, *J* = 10.0, 1.5 Hz, 1H), 3.78-3.75 (m, 2H) ppm. **LRMS** (ESI⁺): *m/z* = 134 [M + H]⁺.

Synthesis of *N*-allyl-*N*-(1-phenylprop-2-yn-1-yl)aniline (**54**).



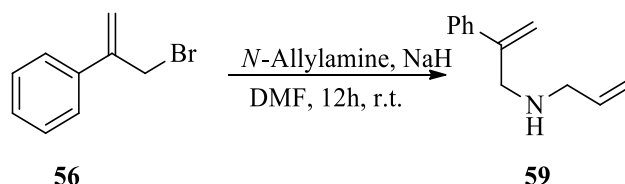
1-phenylpropargyl-acetate **36** (48.7 mg, 0.28 mmol, 1 eq.) was dissolved in a round bottom flask containing MeOH (10 mL) and DIPEA (0.059 mL, 0.34 mmol 1.2 eq.). *N*-allylaniline **53** (45.2 mg, 0.34 mmol 1.2 eq.) and CuI (5.3 mg, 0.028 mmol 0.1 eq.) were added at 0°C and the resulting solution was left stirring for 12 h at room temperature. After completion of the reaction, the solvent was evaporated and the resulting crude product was purified by column chromatography (hexane/ethyl acetate 4:1) to give aniline **54** as a colourless oil. **Yield:** 85% (209.9 mg). **¹H NMR** (400 MHz, CDCl₃): δ 7.58 (d, *J* = 7.0 Hz, 2H), 7.38-7.21 (m, 5H), 6.94 (d, *J* = 7.0 Hz, 2H), 6.83 (t, *J* = 7.0 Hz, 1H), 5.75-5.69 (m, 1H), 5.67 (d, *J* = 2.0 Hz, 1H), 5.18 (d, *J* = 16.0 Hz, 1H), 5.06 (d, *J* = 16.0 Hz, 1H), 3.90 (dd, *J* = 16.0, 5.0 Hz, 1H), 3.82 (dd, *J* = 16.0, 5.0 Hz, 1H), 2.53 (d, *J* = 2.0 Hz, 1H) ppm. **¹³C NMR** (100 MHz, CDCl₃): δ 148.4, 137.9, 135.6, 128.7, 128.4, 128.4, 127.8, 127.6, 118.9, 116.4, 116.1, 80.8, 74.6, 55.8, 51.3 ppm. **LRMS** (ESI⁺): *m/z* = 248 [M + H]⁺.

Synthesis of (3-bromoprop-1-en-2-yl)benzene (**56**).



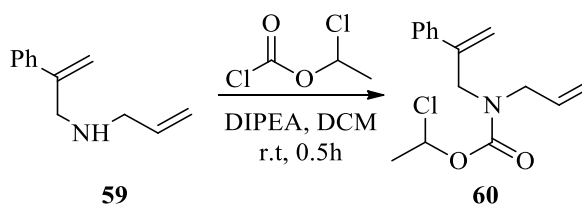
Prop-1-en-2-ylbenzene **55** (3 mmol, 1 eq.) was dissolved in a round bottom flask containing DCM (10 mL). NBS (6 mmol, 2 eq.) was added to the solution which was then allowed to stir at 45°C for 18 h. After completion of reaction, the resulting solution was quenched with aqueous NaHCO₃ solution (30 mL). The reaction mixture was extracted with Et₂O (30 mL × 3) and dried over anhydrous MgSO₄. After the solvent was evaporated, the crude product was purified by column chromatography (hexane 100%) to give (3-bromoprop-1-en-2-yl)benzene **56** as a colourless oil. **Yield:** 90% (198 mg). **¹H NMR** (400 MHz, CDCl₃): δ 7.55–7.23 (m, 5H), 5.58 (d, *J* = 0.8 Hz, 1H), 5.51 (d, *J* = 0.8 Hz, 1H), 4.41 (d, *J* = 0.8 Hz, 2H) ppm. **¹³C NMR** (100 MHz, CDCl₃): δ 144.4, 137.5, 128.6, 128.3, 126.2, 117.3, 34.4 ppm. **LRMS** (ESI⁺): *m/z* = 197 [M + H]⁺, 199 [M + H]⁺.

Synthesis of *N*-allyl-2-phenylprop-2-en-1-amine (**59**).



Commercial *N*-allylamine (0.148 mL, 2.4 mmol, 3 eq.) was dissolved in a round bottom flask containing DMF (10 mL). NaH (55.2 mg, 2.4 mmol, 3 eq.) was added at 0 °C under N₂ atmosphere. The mixture was allowed to stir for 20 minutes at 0°C. Then compound **56** (158.4 mg, 0.8 mmol, 1 eq.) was added. The reaction mixture was allowed to stir for 4h at room temperature. After completion of reaction, the resulting solution was quenched with aqueous NaHCO₃ solution (30 mL). The reaction mixture was extracted with Et₂O (30 mL ×3) and dried over anhydrous MgSO₄. After the solvent was evaporated, the crude product was purified by column chromatography (hexane/Et₂O 9:1) to give **59** as a colourless oil. **Yield:** 55% (76.5 mg). **¹H NMR** (400 MHz, CDCl₃): δ 7.54-7.42 (m, 2H), 7.41-7.22 (m, 3H), 6.09-5.83 (m, 1H), 5.44 (s, 1H), 5.28 (d, *J* = 1.3 Hz, 1H), 5.25-5.06 (m, 2H), 3.75-3.63 (m, 2H), 3.30 (td, *J* = 1.4, 6.0 Hz, 2H) ppm. **¹³C NMR** (100 MHz, CDCl₃): δ 145.5, 140.4, 135.7, 128.0, 127.3, 126.3, 117.3, 115.0, 57.5, 56.4 ppm. **LRMS** (ESI⁺): *m/z* = 174 [*M* + H]⁺

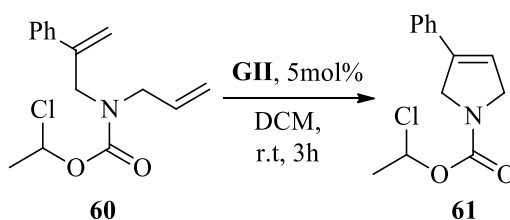
Synthesis of 1-chloroethyl-allyl-(2-phenylallyl)-carbamate (**60**).



Amine **59** (69.2 mg, 0.4 mmol, 1 eq.) was dissolved in a round bottom flask containing DCM (10 mL) and DIPEA (0.209 mL, 1.2 mmol, 3 eq.). 1-Chloroethyl chloroformate (0.064 mL, 0.6 mmol, 1.5 eq.) was added to the stirring solution which was left stirring for 30 minutes. After completion of reaction, the solvent was evaporated and the crude product was directly used for the next synthetic step without further purification. **Yield:** 92% (103.1 mg). **¹H NMR** (400 MHz, CDCl₃): δ 7.36 (d, *J* = 8.0 Hz, 2H), 7.32-7.19 (m, 3H), 6.56 (q, *J* = 8.0, 4.0 Hz, 1H), 5.75-5.59 (m, 1H), 5.39 (d, *J* = 14.0 Hz, 1H), 5.11-5.02 (m, 3H), 4.35-4.33 (m, 2H), 3.83-3.70 (m, 2H), 1.74 (d, *J* = 4.0 Hz, 3H) ppm. **LRMS** (ESI⁺): *m/z* = 280 [*M* + H]⁺

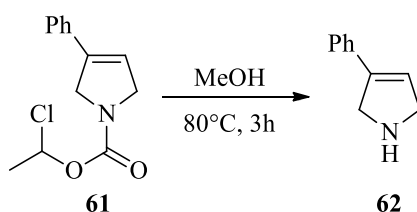
Synthesis of 1-chloroethyl-3-phenyl-2,5-dihydro-1H-pyrrole-1-carboxylate (**61**).

Mixture of rotamers.



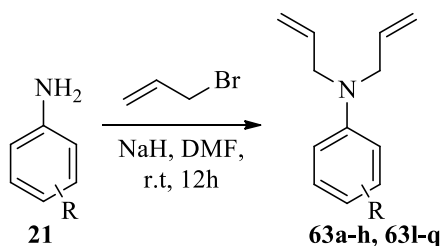
Compound **60** (139.5 mg, 0.5 mmol, 1 eq.) was dissolved in a round bottom flask containing DCM (10 mL) and **GII** (21.2 mg, 0.025 mmol, 0.05 eq.). The solution was left stirring at room temperature for 3h. After completion of the reaction, the solvent was evaporated and the crude product was purified by column chromatography (hexane/ethyl acetate 9:1) to give **61** as a pale yellow oil. **Yield:** 72% (90.4 mg). **¹H NMR** (400 MHz, CDCl₃): δ 7.33-7.23 (m, 5H), 6.62-6.56 (q, *J* = 8.0, 4.0 Hz, 1H), 6.08 (d, *J* = 12.0 Hz, 1H), 4.58-4.43 (d, *J* = 12.0 Hz, 2H), 4.39-4.25 (m, 2H), 1.78 (d, *J* = , 4.0 Hz, 3H) ppm. **¹³C NMR** (100 MHz, CDCl₃): δ 151.8, 137.4, 132.8, 128.7, 125.4, 119.1, 118.8, 83.0, 54.4, 53.9, 53.6, 53.2, 25.6 ppm. **LRMS** (ESI⁺): *m/z* = 252 [M + H]⁺

Synthesis of 3-phenyl-2,5-dihydro-1H-pyrrole (**62**).²³⁹



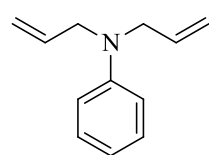
Compound **61** (378 mg, 1.5 mmol, 1 eq.) was dissolved in a round bottom flask containing MeOH (10 mL). The solution was left stirring at 80 °C for 3h. After completion of the reaction, the solvent was evaporated and the crude product was purified by column chromatography (ethyl acetate/ methanol 4:1) to give **62** as a white solid. **Yield:** 99% (216.8 mg). **¹H NMR** (400 MHz, CDCl₃): δ 10.39 (br s, 1H), 7.33-7.26 (m, 5H), 6.04 (s, 1H), 4.48-4.42 (m, 2H) 4.33-4.27 (m, 2H) ppm. **¹³C NMR** (100 MHz, CDCl₃): δ 137.2, 131.1, 129.2, 128.9, 125.9, 117.5, 52.9, 52.0 ppm. **LRMS** (ESI⁺): *m/z* = 146 [M + H]⁺.

General procedure for the synthesis of diallylanilines **63a-h** and **63n-q**.



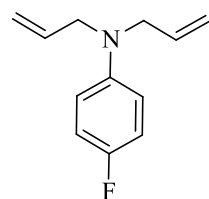
The opportunely substituted aniline **21** (5.00 mmol, 1 eq.) was dissolved in a round bottom flask containing dry DMF (10 mL) and NaH (230 mg, 10.0 mmol, 2 eq.) at 0 °C under nitrogen atmosphere. The reaction mixture was stirred for 30 minutes at room temperature. Then, allylbromide (0.864 mL, 10.0 mmol, 2 eq.) was added to the stirring solution. The reaction was allowed to stir at room temperature for 12h. The reaction mixture was quenched with saturated NaHCO₃ aqueous solution (20 mL) and extracted twice with 20 mL of Et₂O. The combined organic layers were collected, washed with brine, dried over Na₂SO₄ and concentrated under reduced pressure giving a yellow crude oil. The crude product was purified by chromatography on silica gel, using hexane/EtOAc (9:1) as eluent.

Synthesis of *N,N*-diallylaniline (**63a**).²³⁸



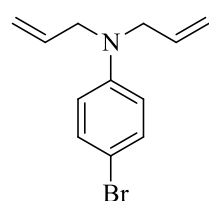
Yield: 73% (631.4 mg). **¹H NMR** (400 MHz CDCl₃): δ 7.38 (t, *J* = 8.0 Hz, 2H), 6.90-6.95 (m, 3H), 6.08-5.98 (m, 2H), 5.38-5.32 (m, 4H), 4.08 (d, *J* = 4.0 Hz, 4H) ppm. **¹³C NMR** (100 MHz CDCl₃): δ 147.6, 132.9, 128.0, 115.2, 114.9, 111.2, 51.6 ppm. **LRMS** (ESI⁺): *m/z* = 174 [M + H]⁺.

Synthesis of *N,N*-diallyl-4-fluoroaniline (**63b**).²⁴⁰



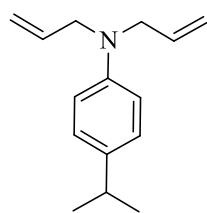
Yield: 93% (888.1 mg). **¹H NMR** (400 MHz, CDCl₃): δ 6.88 (t, *J* = 8.0, 8.0 Hz, 2H), 6.62-6.58 (m, 2H), 5.87-5.78 (m, 2H), 5.18-5.13 (m, 4H), 3.87-3.86 (m, 4H) ppm. **¹³C NMR** (100 MHz, CDCl₃): δ 134.0, 116.2, 115.5, 115.3, 113.6, 113.5, 53.4 ppm. **LRMS** (ESI⁺): *m/z* = 192 [M + H]⁺.

Synthesis of *N,N*-diallyl-4-bromoaniline (**63c**).²⁴¹



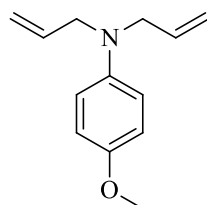
Yield: 86% (1079 mg). **¹H NMR** (400 MHz, CDCl₃): δ 7.20 (d, *J* = 9.0 Hz, 2H), 6.51 (d, *J* = 7.5 Hz, 2H), 5.77 (m, 2H), 5.11 (m, 4H), 3.85 (m, 4H) ppm. **¹³C NMR** (100 MHz, CDCl₃): δ 147.6, 133.5, 131.7, 116.2, 114.0, 108.1, 52.9 ppm. **LRMS** (ESI⁺): *m/z* = 252 [M + H]⁺, 254 [M + H]⁺.

Synthesis of *N,N*-diallyl-4-isopropylaniline (63d).²³²



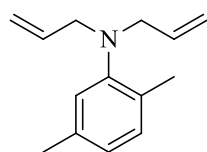
Yield: 94% (1010.5 mg). **¹H NMR** (400 MHz, CDCl₃): δ 7.10 (d, *J* = 8.5 Hz, 2H), 6.69 (d, *J* = 8.5 Hz, 2H), 5.94-5.85 (m, 2H), 5.24-5.16 (m, 4H), 3.92 (d, *J* = 4.5 Hz, 4H), 2.89-2.79 (m, 1H), 1.24 (d, *J* = 7.0 Hz, 6H) ppm. **¹³C NMR** (100 MHz, CDCl₃): δ 147.0, 136.8, 134.5, 127.0, 116.0, 112.5, 53.0, 33.1, 24.4 ppm. **LRMS** (ESI⁺): *m/z* = 216 [M + H]⁺.

Synthesis of *N,N*-diallyl-4-methoxyaniline (63e).²⁴²



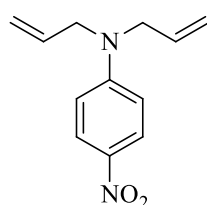
Yield: 79% (801.8 mg). **¹H NMR** (400 MHz, CDCl₃): δ 6.78 (d, *J* = 9.0 Hz, 2H), 6.66 (d, *J* = 9.2, 2H), 5.82 (ddt, *J* = 17.0, 10.0, 5.0 Hz, 2H), 5.16 (ddd, *J* = 17.0, 1.5, 1.0 Hz, 2H), 5.12 (ddd, *J* = 10.0, 1.6, 1.0 Hz, 2H), 3.82 (dt, *J* = 5.0, 1.5 Hz, 4H) 3.68 (s, 3H) ppm. **¹³C NMR** (100 MHz, CDCl₃): δ 151.7, 143.4, 134.6, 115.9, 114.8, 114.7, 55.5, 53.6 ppm. **LRMS** (ESI⁺): *m/z* = 204 [M + H]⁺.

Synthesis of *N,N*-diallyl-2,5-dimethylaniline (63f).²⁴³



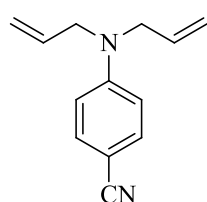
Yield: 79% (793.9 mg). **¹H NMR** (400 MHz, CDCl₃): δ 7.01 (dd, *J* = 7.0, 3.5 Hz, 1H), 6.88-6.65 (m, 2H), 5.88-5.67 (m, 2H), 5.12-5.00 (m, 4H), 3.71-3.42 (m, 4H), 2.21 (s, 3H), 2.20 (s, 3H) ppm. **¹³C NMR** (100 MHz, CDCl₃): δ 135.5, 130.8, 123.8, 122.6, 116.9, 55.6, 21.2, 18.0 ppm. **LRMS** (ESI⁺): *m/z* = 202 [M + H]⁺.

Synthesis of *N,N*-diallyl-4-nitroaniline (63g).²⁴⁴



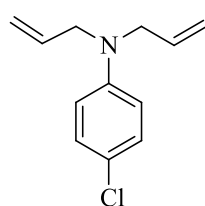
Yield: 92% (1002.5 mg). **¹H NMR** (400 MHz, CDCl₃): δ 8.11-8.08 (m, 2H), 6.64-6.61 (m, 2H), 5.89-5.80 (m, 2H), 5.25-5.14 (m, 4H), 4.02 (d, *J* = 2.0 Hz, 4H) ppm. **¹³C NMR** (100 MHz, CDCl₃): δ 153.3, 137.3, 131.8, 126.2, 117.0, 111.4, 45.8 ppm. **LRMS** (ESI⁺): *m/z* = 219 [M + H]⁺.

Synthesis of 4-(diallylamino)benzonitrile (63h).²⁴⁵



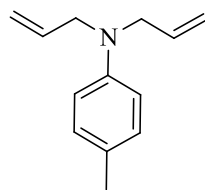
Yield: 92% (910.8 mg). **¹H NMR** (400 MHz, CDCl₃): δ 7.37-7.23 (m, 2H), 6.60-6.46 (m, 2H), 5.78-5.58 (m, 2H), 5.16-4.90 (m, 4H), 3.92-3.76 (m, 4H) ppm. **¹³C NMR** (100 MHz, CDCl₃): δ 149.3, 133.7, 133.6, 133.5, 126.0, 121.0, 111.2, 97.6, 54.3 ppm. **LRMS** (ESI⁺): *m/z* = 199 [M + H]⁺.

Synthesis of *N,N*-diallyl-4-chloroaniline (**63n**).²⁴²



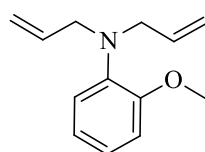
Yield: 74%. **¹H NMR** (400 MHz, CDCl₃): δ 7.11 (dd, *J* = 9.0, 0.5 Hz, 2H), 6.59 (d, *J* = 8.5 Hz, 2H), 5.89–5.74 (m, 2H), 5.19–5.15 (m, 2H), 5.15–5.09 (m, 2H), 3.91–3.85 (m, 4H) ppm. **¹³C NMR** (100 MHz, CDCl₃): δ 147.3, 133.6, 128.8, 121.2, 116.2, 113.6, 53.0 ppm. **LRMS** (ESI⁺): *m/z* = 208 [M + H]⁺.

Synthesis of *N,N*-diallyl-4-methylaniline (**63o**).



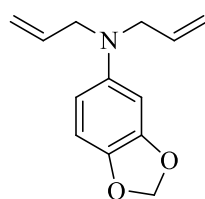
Yield: 88%. **¹H NMR** (400 MHz, CDCl₃): δ 7.13 (d, *J* = 12.0 Hz, 2H), 6.75 (d, *J* = 12.0 Hz, 2H), 6.00–5.92 (m, 2H), 5.32–5.25 (m, 4H), 4.01 (s, 2H), 4.00 (s, 2H), 2.37 (s, 3H) ppm. **¹³C NMR** (100 MHz, CDCl₃): δ 146.8, 134.5, 129.8, 125.8, 116.1, 112.8, 53.1, 20.4 ppm. **LRMS** (ESI⁺): *m/z* = 188 [M + H]⁺.

Synthesis of *N,N*-diallyl-2-methoxyaniline (**63p**).



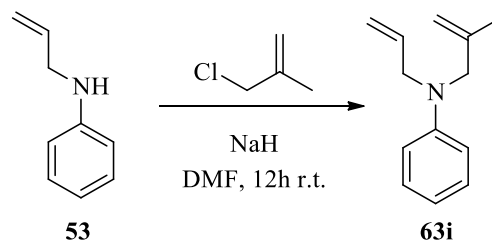
Yield: 88%. **¹H NMR** (400 MHz, CDCl₃): δ 6.98–6.85 (m, 4H), 5.87–5.77 (m, 2H), 5.18–5.10 (m, 4H), 3.86 (s, 3H), 3.76 (s, 2H), 3.74 (s, 2H) ppm. **¹³C NMR** (100 MHz, CDCl₃): δ 152.9, 139.5, 135.3, 122.6, 121.2, 120.5, 117.9, 111.5, 55.5, 54.6 ppm. **LRMS** (ESI⁺): *m/z* = 204 [M + H]⁺.

Synthesis of *N,N*-diallylbenzo[d][1,3]dioxol-5-amine (**63q**).



Yield: 92%. **¹H NMR** (400 MHz, CDCl₃): δ 6.60 (d, *J* = 8.5 Hz, 1H), 6.29 (d, *J* = 2.5 Hz, 1H), 6.06 (dd, *J* = 8.5, 2.0 Hz, 1H), 5.84–5.67 (m, 2H), 5.78 (s, 2H), 5.17–5.01 (m, 4H), 3.77 (dt, *J* = 4.0, 1.5 Hz, 4H) ppm. **¹³C NMR** (100 MHz, CDCl₃): δ 148.3, 145.1, 138.9, 134.2, 116.2, 108.4, 104.9, 100.6, 96.2, 53.8 ppm. **LRMS** (ESI⁺): *m/z* = 218 [M + H]⁺.

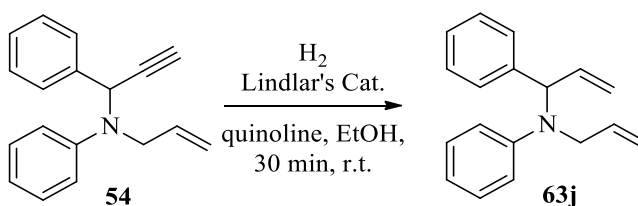
Synthesis of *N*-allyl-*N*-(2-methylallyl)aniline (**63i**).²³²



N-Allylaniline **53** (665 mg, 5.0 mmol, 1 eq.) was dissolved in a round bottom flask containing dry DMF (10 mL) under nitrogen atmosphere and NaH (115 mg, 5.0 mmol, 1

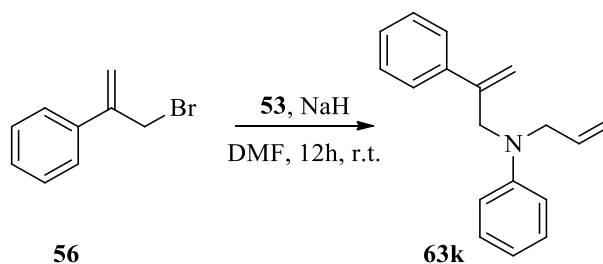
eq.) was then added at 0°C. The reaction mixture was allowed to stir for 30 minutes at room temperature. Then 3-chloro-2-methylprop-1-ene (0.418 mL, 5.0 mmol, 1 eq.) was added to the stirring solution. The reaction was allowed to stir at room temperature for 12 h. The reaction mixture was quenched with saturated NaHCO₃ aqueous solution (20 mL) and extracted twice with 20 mL of Et₂O. The combined organic layers were collected, washed with brine, dried over Na₂SO₄ and concentrated under reduced pressure giving a yellow crude oil. The crude product was purified by chromatography on silica gel, using hexane/EtOAc (9:1) as eluent. Compound **63i** was obtained as a pale yellow oil. **Yield:** 94% (878.9 mg). **¹H NMR** (400 MHz, CDCl₃): δ 7.11 (t, *J* = 8.0 Hz, 2H), 6.59 (d, *J* = 8.5 Hz, 3H), 5.84-5.74 (m, 1H), 5.11-5.06 (m, 2H), 4.78-4.74 (d, *J* = 10.5 Hz, 2H), 3.86 (d, *J* = 4.0 Hz, 2H), 3.71 (s, 2H), 1.66 (s, 3H) ppm. **LRMS** (ESI⁺): *m/z* = 188 [M + H]⁺.

Synthesis of *N*-allyl-*N*-(1-phenylallyl)aniline (**63j**).



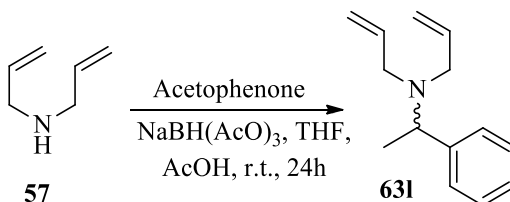
The aniline **54** (0.135 mL, 1.5 mmol, 1 eq.) was dissolved in a two neck round bottom flask containing EtOH (20 mL). Lindlar's catalyst (31.5 mg, 0.15 mmol 0.1 eq.) and quinoline (0.177 mL, 1.5 mmol 1 eq.) were added to the reaction mixture. The reaction mixture was allowed to stir under H₂ atmosphere for 30 minutes. After completion of reaction, the mixture was filtered through celite pad and washed three times with EtOAc (30 mL). The EtOH was removed under reduced pressure. The reaction mixture was then washed twice with aqueous NaHCO₃ solution (30 mL) and dried over anhydrous MgSO₄. After the solvent was evaporated, the crude product was purified by column chromatography (hexane/ethyl acetate 4:1) to give aniline **63j** as a colourless oil. **Yield:** 87% (162.7 mg). **¹H NMR** (400 MHz, CDCl₃): δ 7.26-7.16 (m, 5H), 7.09 (t, *J* = 8.0 Hz, 2H), 6.71 (d, *J* = 8.0 Hz, 2H), 6.63 (t, *J* = 8.0 Hz, 1H), 6.13-6.04 (m, 1H), 5.72-5.63 (m, 1H), 5.40 (d, *J* = 8.0 Hz, 1H), 5.23 (t, *J* = 12.0 Hz, 1H), 5.10 (d, *J* = 8.0 Hz, 1H), 5.05 (d, *J* = 8.0 Hz, 1H), 4.99 (d, *J* = 8.0 Hz, 1H), 3.86-3.84 (m, 2H). **¹³C NMR** (100 MHz, CDCl₃): δ 149.0, 140.3, 136.5, 136.4, 136.0, 129.0, 128.5, 128.1, 127.3, 118.2, 117.2, 116.0, 114.2, 65.3, 50.6. **LRMS** (ESI⁺): *m/z* = 250 [M + H]⁺.

Synthesis of *N*-allyl-*N*-(2-phenylallyl)aniline (**63k**).



Allylaniline **53** (0.135 mL, 1 mmol 1 eq.) was dissolved in a round bottom flask containing DMF (10 mL). NaH (23 mg, 1 mmol 1 eq.) was added at 0 °C under N₂ atmosphere. The mixture was allowed to stir for 20 minutes and then compound **56** (292.2 mg, 1.5 mmol 1.5 eq.), dissolved in 1 mL of DCM, was added. The reaction mixture was allowed to stir for 12 h at room temperature. After completion of the reaction, the resulting solution was quenched with aqueous NaHCO₃ solution (30 mL). The reaction mixture was extracted with Et₂O (30 mL × 3) and dried over anhydrous MgSO₄. After the solvent was evaporated, the crude product was purified by column chromatography (hexane/Et₂O 9:1) to give *N*-allyl-*N*-(2-phenylallyl)aniline **63k** as a colourless oil. **Yield:** 87% (216.6 mg). **¹H NMR** (400 MHz, CDCl₃): δ 7.40-7.33 (m, 2H), 7.32-7.17 (m, 3H), 7.17-7.02 (m, 2H), 6.68-6.52 (m, 3H), 5.86-5.73 (m, 1H), 5.40-5.30 (m, 1H), 5.15-5.07 (m, 2H), 5.07-5.04 (m, 1H), 4.20 (m, 2H), 3.97-3.87 (m, 2H) ppm. **¹³C NMR** (100 MHz, CDCl₃): δ 148.7, 142.3, 139.7, 133.7, 129.1, 128.5, 127.8, 126.1, 116.4, 116.2, 112.2, 112.1, 54.0, 52.8 ppm. **LRMS** (ESI⁺): *m/z* = 250 [M + H]⁺.

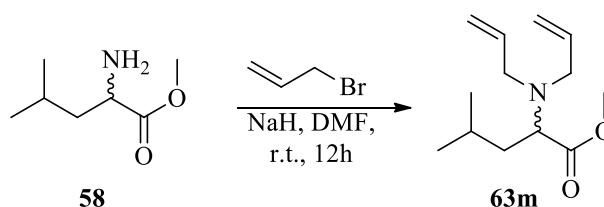
Synthesis of *N*-allyl-*N*-(1-phenylethyl)prop-2-en-1-amine (**63l**).²⁴⁶



N,N-Diallylamine **57** (247 mg, 2.0 mmol, 1 eq.) was dissolved in a round bottom flask containing dry THF (10 mL) under nitrogen atmosphere. AcOH (0.117 mL, 2.0 mmol, 1 eq.) and acetophenone (0.467 mL, 4.0 mmol, 2 eq.) were then added at room temperature. The reaction mixture was allowed to stir for 20 minutes after which time NaBH(AcO)₃ (1695

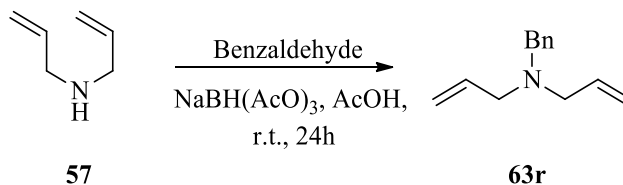
mg, 8.0 mmol, 4 eq.) was added. The reaction mixture was stirred at room temperature for 24 h, then quenched with 1M NaOH aqueous solution (20 mL) and extracted twice with 20 mL of Et₂O. The combined organic layers were collected, washed with brine, dried over Na₂SO₄ and concentrated under reduced pressure giving a yellow crude oil. The crude compound was purified by chromatography on silica gel, using hexane/EtOAc 1:1 as eluent to give *N*-allyl-*N*-(1-phenylethyl)prop-2-en-1-amine **63l** as a colourless oil. **Yield:** 93% (373.9 mg). **¹H NMR** (400 MHz, CDCl₃): δ 7.41-7.32 (m, 4H), 7.26-7.21 (m, 1H), 5.89 (m, 2H), 5.29-5.08 (m, 4H), 3.94 (q, *J* = 6.5 Hz, 1H), 3.18 (dd, *J* = 14.0, 6.0 Hz, 2H), 3.07 (dd, *J* = 14.0, 6.0 Hz, 2H), 1.44-1.33 (d, 6.5 Hz, 3H) ppm. **¹³C NMR** (100 MHz, CDCl₃): δ 144.1, 136.7, 128.2, 127.8, 126.8, 116.9, 58.4, 52.6, 17.2 ppm. **LRMS** (ESI⁺): *m/z* = 202 [M + H]⁺.

Synthesis of methyl-2-(diallylamino)-4-methylpentanoate (**63m**).



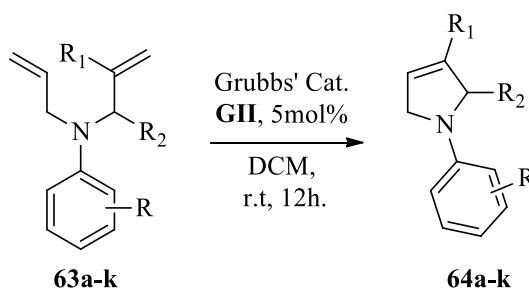
Leucine (655.8 mg, 5.00 mmol, 1 eq.) was dissolved in a round bottom flask containing dry DMF (10 mL) and NaH (230 mg, 10.0 mmol, 2 eq.) at 0 °C under nitrogen atmosphere. The reaction mixture was stirred for 30 minutes at room temperature. Then, allylbromide (0.766 mL, 10.0 mmol, 2 eq.) was added to the stirred solution. The reaction was allowed to stir at room temperature for 12 h. The reaction mixture was quenched with saturated NaHCO₃ aqueous solution (20 mL) and extracted twice with 20 mL of Et₂O. The combined organic layers were collected, washed with brine, dried over Na₂SO₄ and concentrated under reduced pressure giving a yellow crude oil. The crude was purified by chromatography on silica gel, using hexane/EtOAc (9:1) as eluent to give methyl-2-(diallylamino)-4-methylpentanoate **63m** as a colourless oil. **Yield:** 95% (1068.9 mg). **¹H NMR** (400 MHz, CDCl₃): δ 5.70 (m, 2H), 5.24-4.97 (m, 4H), 3.61 (s, 3H), 3.44 (t, *J* = 7.0 Hz, 1H), 3.28 (d, *J* = 7.0 Hz, 2H), 2.96 (d, *J* = 7.0 Hz, 2H), 1.70-1.55 (m, 1H), 1.51-1.36 (m, 2H), 0.82 (d, *J* = 7.0 Hz, 6H) ppm. **¹³C NMR** (100 MHz, CDCl₃): δ 174.2, 136.7, 116.9, 59.9, 53.4, 51.0, 38.6, 24.6, 23.0, 22.0 ppm. **LRMS** (ESI⁺): *m/z* = 226 [M + H]⁺

Synthesis of *N*-Allyl-*N*-benzylprop-2-en-1-amine (**63r**).²⁴⁷



N,N-Diallylamine **57** (0.246 mL, 2.0 mmol, 1 eq.) was dissolved in a round bottom flask containing dry THF (10 mL) under nitrogen atmosphere. AcOH (0.114 mL, 2.0 mmol, 1 eq.) and benzaldehyde (0.408 mL, 4.0 mmol, 2 eq.) were then added at room temperature. The reaction mixture was allowed to stir for 20 minutes after which time NaBH(AcO)₃ (1695 mg, 8.0 mmol, 4 eq.) was added. The reaction mixture was stirred at room temperature for 24 h, then quenched with 1M NaOH aqueous solution (20 mL) and extracted twice with 20 mL of Et₂O. The combined organic layers were collected, washed with brine, dried over Na₂SO₄ and concentrated under reduced pressure giving a yellow crude oil. The crude compound was purified by chromatography on silica gel, using hexane/EtOAc 1:1 as eluent to give **63r** as a colourless oil. **Yield:** 97% (364.7 mg). **¹H NMR** (400 MHz, CDCl₃): δ 7.35-7.32 (m, 3H), 7.30-7.21 (m, 2H), 5.88 (ddt, *J* = 17.0, 10.3, 6.0 Hz, 2H), 5.19 (ddt, *J* = 17.0, 2.0, 1.5 Hz, 2H), 5.14 (ddt, *J* = 10.0, 2.0, 1.0 Hz, 2H), 3.57 (s, 2H), 3.08 (ddd, *J* = 6.5, 1.5, 1.0 Hz, 4H) ppm. **¹³C NMR** (100 MHz, CDCl₃): δ 139.6, 136.0, 129.0, 128.3, 126.9, 117.4, 57.7, 56.6 ppm. **LRMS** (ESI⁺): *m/z* = 188 [M + H]⁺.

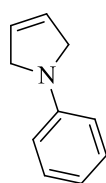
General procedure for the synthesis of *N*-aryl-3-pyrroline (**64a-k**).



Cmpd	R	R1	R2	Pyrroline
63a	H	H	H	64a
63b	4-F	H	H	64b
63c	4-Br	H	H	64c
63d	4- <i>i</i> Pr	H	H	64d
63e	4-OMe	H	H	64e
63f	2-5-Me	H	H	64f
63g	4-NO ₂	H	H	64g
63h	4-CN	H	H	64h
63i	H	Me	H	64i
63j	H	H	Ph	64j
63k	H	Ph	H	64k

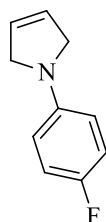
The appropriate diallylaniline **63a-k** (1.5 mmol, 1 eq.) was dissolved in a round bottom flask containing degassed DCM (10 mL) and **GII** (63.67 mg, 0.075 mmol 0.05 eq.). The solution was left stirring at room temperature. After completion of reaction (monitored by TLC), the resulting solution was quenched with a saturated aqueous NaHCO₃ solution (30 mL). The reaction mixture was extracted with Et₂O (30 mL × 3) and dried over anhydrous MgSO₄. After the solvent was evaporated, the crude product was purified by column chromatography (hexane/ethyl acetate 9:1) to give **64** as a yellow-white solid.

Synthesis of 1-phenyl-2,5-dihydro-1H-pyrrole (**64a**).²⁴⁸



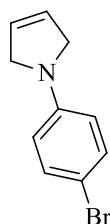
Yield: 79% (171.2 mg). **¹H NMR** (400 MHz, CDCl₃): δ 7.24 (m, 2H), 6.67 (m, 1H), 6.54 (m, 2H), 5.95 (s, 2H), 4.11 (s, 4H) ppm. **¹³C NMR** (100 MHz, CDCl₃): δ 147.1, 129.4, 126.5, 115.6, 111.2, 54.5 ppm. **LRMS** (ESI⁺): m/z = 146 [M + H]⁺.

Synthesis of 1-(4-fluorophenyl)-2,5-dihydro-1H-pyrrole (**64b**).²⁴⁹



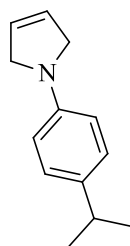
Yield: 75% (183.4 mg). **¹H NMR** (400 MHz, CDCl₃): δ 6.95 (t, *J* = 8.0 Hz, 2H), 6.42 (d, *J* = 8.0 Hz, 2H), 5.93 (s, 2H), 4.06 (s, 4H) ppm. **¹³C NMR** (100 MHz, CDCl₃): δ 142.8, 126.1, 115.9, 115.8, 111.5, 54.2 ppm. **LRMS** (ESI⁺): m/z = 164 [M + H]⁺.

Synthesis of 1-(4-bromophenyl)-2,5-dihydro-1H-pyrrole (**64c**).²⁵⁰



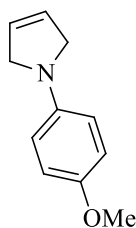
Yield: 75% (253.2 mg). **¹H NMR** (400 MHz, CDCl₃): δ 7.23 (d, *J* = 8.0 Hz, 2H), 6.32 (d, *J* = 8.5 Hz, 2H), 5.87 (s, 2H), 3.99 (s, 4H) ppm. **¹³C NMR** (100 MHz, CDCl₃): δ 145.9, 131.9, 126.3, 112.7, 107.4, 54.5 ppm. **LRMS** (ESI⁺): m/z = 224 [M + H]⁺ 226 [M + H]⁺.

Synthesis of 1-(4-isopropylphenyl)-2,5-dihydro-1H-pyrrole (**64d**).



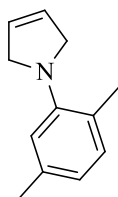
Yield: 79% (221.5 mg). **¹H NMR** (400 MHz, CDCl₃): δ 7.07-7.01 (m, *J* = 8.5 Hz, 2H), 6.45-6.33 (m, *J* = 8.5 Hz, 2H), 5.86 (s, 2H), 4.02 (s, 4H), 2.78-2.70 (m, 1H), 1.15-1.12 (d, *J* = 3.0 Hz, 6H) ppm. **¹³C NMR** (100 MHz, CDCl₃): δ 145.4, 135.9, 127.2, 126.5, 111.1, 54.6, 24.3, 14.1 ppm. **LRMS** (ESI⁺): m/z = 188 [M + H]⁺.

Synthesis of 1-(4-methoxyphenyl)-2,5-dihydro-1H-pyrrole (64e).²⁴²



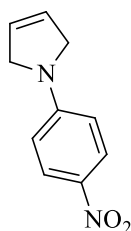
Yield: 79% (207.4 mg). **¹H NMR** (400 MHz, CDCl₃): δ 6.80 (d, *J* = 8.5 Hz, 2H), 6.42 (d, *J* = 8.5 Hz, 2H), 5.87 (s, 2H), 4.00 (s, 4H), 3.69 (s, 3H) ppm. **¹³C NMR** (100 MHz, CDCl₃): δ 152.2, 141.1, 127.8, 126.9, 114.6, 59.2, 55.6 ppm. **LRMS** (ESI⁺): *m/z* = 176 [M + H]⁺.

Synthesis of 1-(2,5-dimethylphenyl)-2,5-dihydro-1H-pyrrole (64f).



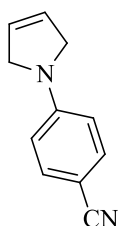
Yield: 79% (205.1 mg). **¹H NMR** (400 MHz, CDCl₃): δ 6.92 (d, *J* = 7.5 Hz, 1H), 6.61 (s, 1H), 6.55 (d, *J* = 7.5 Hz, 1H), 5.83 (s, 2H), 4.11 (s, 4H), 2.28 (s, 3H), 2.22 (s, 3H) ppm. **¹³C NMR** (100 MHz, CDCl₃): δ 148.2, 136.2, 132.2, 126.7, 124.3, 120.4, 116.7, 57.3, 21.3, 21.2 ppm. **LRMS** (ESI⁺): *m/z* = 174 [M + H]⁺.

Synthesis of 1-(4-nitrophenyl)-2,5-dihydro-1H-pyrrole (64g).



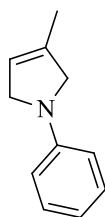
Yield: 80% (228.0 mg). **¹H NMR** (400 MHz, CDCl₃): δ 8.14 (d, *J* = 12.0 Hz, 2H), 6.45 (d, *J* = 12.0 Hz, 2H), 5.89 (s, 2H), 4.21 (s, 4H) ppm. **¹³C NMR** (100 MHz, CDCl₃): δ = 150.6, 137.3, 126.5, 125.9, 110.2, 54.7 ppm. **LRMS** (ESI⁺): *m/z* = 191 [M + H]⁺.

Synthesis of 4-(2,5-dihydro-1H-pyrrol-1-yl)benzonitrile (64h).



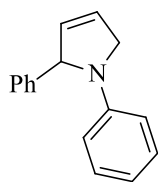
Yield: 79% (201.4 mg). **¹H NMR** (400 MHz, CDCl₃): δ 7.50-7.36 (d, *J* = 8.5 Hz, 2H), 6.51-6.37 (m, *J* = 8.5 Hz, 2H), 5.90 (s, 2H), 4.08 (s, 4H) ppm. **¹³C NMR** (100 MHz, CDCl₃): δ 149.4, 133.7, 126.0, 120.9, 111.2, 97.2, 54.3 ppm. **LRMS** (ESI⁺): *m/z* = 171 [M + H]⁺.

Synthesis of 3-Methyl-1-phenyl-2,5-dihydro-1H-pyrrole (64i).²⁴⁹



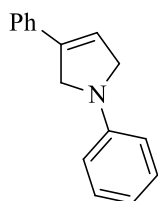
Yield: 79% (188.4 mg). **¹H NMR** (400 MHz, CDCl₃): δ 7.20-7.07 (m, 2H), 6.60 (t, *J* = 7.0 Hz, 1H), 6.44 (d, *J* = 7.0 Hz, 2H), 5.47 (s, 1H), 3.99 (m, 2H), 3.91 (m, 2H), 1.77 (s, 3H) ppm. **¹³C NMR** (100 MHz, CDCl₃): δ 147.2, 135.9, 129.5, 129.3, 120.0, 111.0, 57.8, 54.8, 14.5 ppm. **LRMS** (ESI⁺): *m/z* = 160 [M + H]⁺.

Synthesis of 1,2-diphenyl-2,5-dihydro-1H-pyrrole (64j).



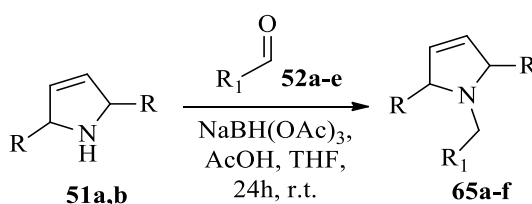
Yield: 65% (215.5 mg). **¹H NMR** (400 MHz, CDCl₃): δ 7.37–7.09 (m, 7H), 6.57 (t, *J* = 8.0 Hz, 1H), 6.44 (d, *J* = 4.0 Hz, 2H), 5.89 (m, 1H), 5.80 (m, 1H), 5.35 (m, 1H), 4.44 (m, 1H), 4.22 (m, 1H) ppm. **¹³C NMR** (100 MHz, CDCl₃): δ 146.4, 142.6, 132.5, 129.1, 128.8, 127.2, 126.2, 124.3, 116.1, 112.2, 69.8, 55.2 ppm. **LRMS** (ESI⁺): *m/z* = 222 [M + H]⁺.

Synthesis of 1,3-diphenyl-2,5-dihydro-1H-pyrrole (64k).²⁵¹



Yield: 70% (103.1 mg). **¹H NMR** (400 MHz, CDCl₃): δ 7.59 (d, *J* = 7.0 Hz, 2H), 7.50–7.19 (m, 5H), 6.74 (t, *J* = 7.0 Hz, 1H), 6.68–6.63 (m, 2H), 6.25 (m, 1H), 4.52–4.40 (m, 2H), 4.32–4.30 (m, 2H) ppm. **¹³C NMR** (100 MHz, CDCl₃): δ 146.9, 138.1, 135.3, 133.6, 129.6, 129.4, 128.6, 128.1, 125.8, 125.5, 125.2, 120.4, 115.8, 108.7, 55.7, 54.8 ppm. **LRMS** (ESI⁺): *m/z* = 222 [M + H]⁺.

General procedure for the synthesis of *N*-alkyl-3-pyrroline 65a-f.

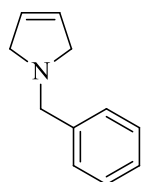


Cmpd	R	R ₁	Pyrroline
51a	H	Ph	65a
51a	H	<i>iso</i> -Butyl	65b
51a	H	Cyclohexyl	65c
51a	H	4-Cl-Ph	65d
51b	Me	Cyclohexyl	65e
51b	Me	4-Cl-Ph	65f

The appropriate 3-pyrroline **51a-b** (2.0 mmol, 1 eq.) was dissolved under nitrogen atmosphere in a round bottom flask containing dry THF (10 mL). Then, AcOH (114.4 mL, 2.0 mmol, 1 eq.) and the appropriate aldehyde (4.0 mmol, 2 eq.) were added at r.t. and the reaction mixture was allowed to stir for 20 minutes. NaBH(OAc)₃ (887.8 mg, 8.0 mmol, 4 eq.) was then added and the reaction mixture was allowed to stir at room temperature for 24 h. The mixture was quenched with 1M NaOH aqueous solution (20 mL) and extracted twice with 20 mL of Et₂O. The combined organic layers were collected, washed with brine, dried

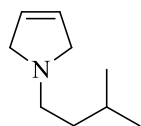
over Na₂SO₄ and concentrated under reduced pressure giving a yellow crude oil. The obtained product was purified by chromatography on silica gel, using hexane/EtOAc (1:1) as eluent to give **51** as yellow-brown oils.

Synthesis of 1-benzyl-2,5-dihydro-1H-pyrrole (65a).²⁵²



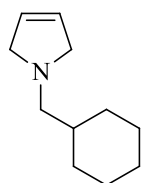
Yield: 81% (128.8 mg). **¹H NMR** (400 MHz, CDCl₃): δ 7.34-7.09 (m, 5H), 5.69 (s, 2H), 3.72 (s, 2H), 3.40 (s, 4H) ppm. **¹³C NMR** (100 MHz, CDCl₃): δ 139.6, 128.7, 128.4, 127.8, 127.0, 60.4, 59.7 ppm. **LRMS** (ESI⁺): m/z = 160 [M + H]⁺.

Synthesis of 1-isopentyl-2,5-dihydro-1H-pyrrole (65b).



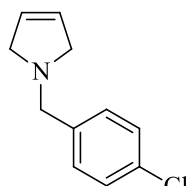
Yield: 84% (116.8 mg). **¹H NMR** (400 MHz, CDCl₃): δ 5.70 (s, 2H), 3.39 (s, 4H), 2.65-2.46 (m, 2H), 1.56 (dt, *J* = 13.0, 6.5 Hz, 1H), 1.39-1.27 (m, 2H), 0.90-0.75 (m, 6H) ppm. **¹³C NMR** (100 MHz, CDCl₃): δ = 127.6, 59.7, 54.5, 38.3, 31.6, 26.3, 22.8 ppm. **LRMS** (ESI⁺): m/z = 140 [M + H]⁺.

Synthesis of 1-(cyclohexylmethyl)-2,5-dihydro-1H-pyrrole (65c).



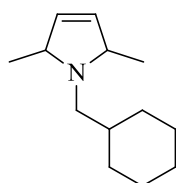
Yield: 75% (124.5 mg). **¹H NMR** (400 MHz, CDCl₃): δ 5.70 (s, 2H), 3.37 (s, 4H), 2.37 (d, *J* = 7.0 Hz, 2H), 1.74 (d, *J* = 12.5 Hz, 2H), 1.70-1.53 (m, 3H), 1.35 (ddd, *J* = 10.0, 7.0, 4.0 Hz, 1H), 1.27-0.99 (m, 3H), 0.93-0.72 (m, 2H) ppm. **¹³C NMR** (100 MHz, CDCl₃): δ 127.7, 63.7, 60.2, 37.5, 31.7, 26.8, 26.2 ppm. **LRMS** (ESI⁺): m/z = 166 [M + H]⁺.

Synthesis of 1-(4-chlorobenzyl)-2,5-dihydro-1H-pyrrole (65d).



Yield: 76% (146.7 mg). **¹H NMR** (400 MHz, CDCl₃): δ 7.22 (s, 4H), 5.72 (s, 2H), 3.71 (s, 2H), 3.40 (s, 4H) ppm. **¹³C NMR** (100 MHz, CDCl₃): δ 138.1, 132.6, 130.0, 128.5, 127.7, 59.6, 59.6 ppm. **LRMS** (ESI⁺): m/z = 194 [M + H]⁺.

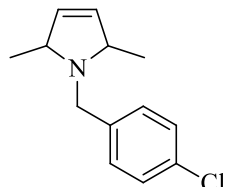
Synthesis of 1-(cyclohexylmethyl)-2,5-dimethyl-2,5-dihydro-1H-pyrrole (65e). Mixture of cis-trans.



Yield: 52% (98.4 mg). **¹H NMR** (400 MHz, CDCl₃): δ **¹H NMR** (400 MHz, CDCl₃): δ 5.63 (s, 2H), 3.72-3.61 (m, 2H), 2.49 (dd, *J* = 13.0, 4.0 Hz, 1H), 2.26-2.08 (m, 1H), 1.92 (d, *J* = 13.0 Hz, 1H), 1.67-1.56 (m, 4H), 0.97-0.88 (m, 6H), 0.85-0.76 (m, 6H) ppm. **¹³C NMR** (100 MHz, CDCl₃): δ 132.9, 183

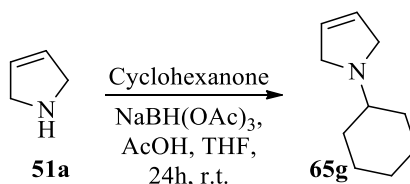
104.9, 61.8, 53.2, 36.8, 32.1, 32.0, 27.0, 26.4, 26.1, 26.0, 17.3 ppm. **LRMS** (ESI⁺): $m/z = 194$ [M + H]⁺.

Synthesis of 1-(4-chlorobenzyl)-2,5-dimethyl-2,5-dihydro-1H-pyrrole (65f). Mixture of cis-trans.



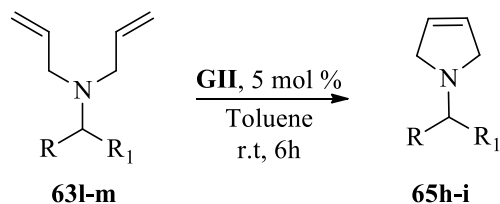
Yield: 46% (101.7 mg). **¹H NMR** (400 MHz, CDCl₃): δ 7.44-7.17 (m, 4H), 5.74 (s, 1H), 5.57 (s, 1H), 3.99-3.72 (m, 4H), 3.69 (d, $J = 4.0$ Hz, 1H), 1.11-0.96 (m, 6H) ppm. **¹³C NMR** (100 MHz, CDCl₃): δ 139.4, 132.8, 132.3, 132.1, 131.9, 130.3, 129.5, 128.3, 128.1, 67.2, 61.7, 57.2, 50.1, 22.4, 17.5 ppm. **LRMS** (ESI⁺): $m/z = 222$ [M + H]⁺.

Synthesis of 1-cyclohexyl-2,5-dihydro-1H-pyrrole (65g).



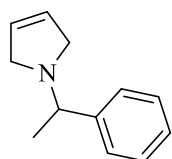
The appropriate 3-pyrroline **51a** (0.152 mL, 2.0 mmol, 1 eq.) was dissolved in a round bottom flask containing dry THF (10 mL). Then, AcOH (0.126 mL, 2.0 mmol, 1 eq.) and cyclohexanone (0.414 mL, 4.0 mmol, 2 eq.) were added at r.t. and the reaction mixture was allowed to stir for 20 minutes. NaBH(OAc)₃ (1775 mg, 8.0 mmol, 4 eq.) was then added and the reaction mixture was allowed to stir at room temperature for 24 h. The mixture was quenched with 1M NaOH aqueous solution (20 mL) and extracted twice with 20 mL of Et₂O. The combined organic layers were collected, washed with brine, dried over Na₂SO₄ and concentrated under reduced pressure giving a yellow crude oil. The obtained product was purified by chromatography on silica gel, using hexane/EtOAc (1:1) as eluent to give **65g** as a colourless oil. **Yield:** 82% (247.6 mg). **¹H NMR** (400 MHz, CDCl₃): δ 5.72 (s, 2H), 3.58 (s, 4H), 2.29-2.09 (m, 1H), 1.91-1.73 (m, 2H), 1.73-1.59 (m, 2H), 1.59-1.46 (m, 1H), 1.28-0.99 (m, 5H) ppm. **¹³C NMR** (100 MHz, CDCl₃): δ 127.5, 62.4, 57.0, 32.0, 26.0, 24.8 ppm. **LRMS** (ESI⁺): $m/z = 152$ [M + H]⁺.

General procedure for the synthesis of *N*-alkyl-3-pyrroline **65h** and **65i**.



The appropriate diallylamine **63l,m** (1.5 mmol, 1 eq.) was dissolved in a round bottom flask containing toluene (10 mL) and Grubbs catalyst II generation **GII** (63.67 mg, 0.075 mmol, 0.05 eq.). The solution was left stirring at room temperature. After completion of reaction (6h, monitored by TLC), the resulting solution was quenched with aqueous NaHCO₃ solution (30 mL). The reaction mixture was extracted with Et₂O (30 mL × 3) and dried over anhydrous MgSO₄. After the solvent was evaporated, the crude product **65h-i** was purified by column chromatography (hexane/ethyl acetate 9:1) to give **65** as white solids.

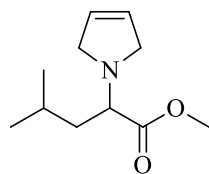
Synthesis of 1-(1-phenylethyl)-2,5-dihydro-1H-pyrrole (**65h**).²⁵³



Yield: 75% (194.6 mg). ¹H NMR (400 MHz, CDCl₃): δ 7.31–7.14 (m, 5H), 5.71 (s, 2H), 3.50–3.24 (m, 5H), 1.32 (d, *J* = 6.5 Hz, 3H) ppm. ¹³C NMR (100 MHz, CDCl₃): δ 145.6, 128.4, 127.8, 127.3, 126.9, 65.2, 58.6, 23.6 ppm.

LRMS (ESI⁺): *m/z* = 174 [M + H]⁺.

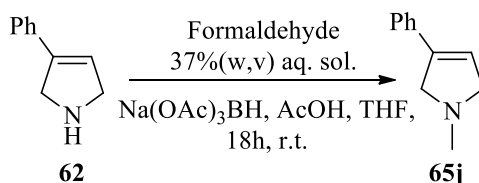
Synthesis of methyl-2-(2,5-dihydro-1H-pyrrol-1-yl)-4-methylpentanoate (**65i**).



Yield: 76% (224.6 mg). ¹H NMR (400 MHz, CDCl₃): δ 5.75–5.63 (m, 2H), 3.71–3.64 (m, 2H), 3.63 (s, 3H), 3.55–3.47 (m, 2H), 3.43 (t, *J* = 7.0 Hz, 1H), 1.66–1.43 (m, 3H), 0.85 (d, *J* = 6.0 Hz, 3H), 0.88 (d, *J* = 6.0 Hz, 3H) ppm. ¹³C NMR (100 MHz, CDCl₃): δ 174.3, 127.2, 62.3, 56.0, 51.2, 40.4, 29.7, 25.1, 22.6, 22.6 ppm.

LRMS (ESI⁺): *m/z* = 198 [M + H]⁺

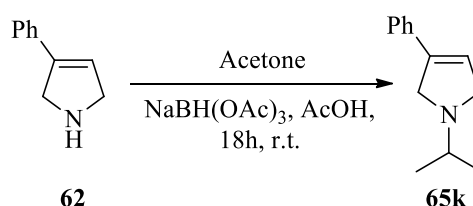
Synthesis of 1-methyl-3-phenyl-2,5-dihydro-1H-pyrrole (**65j**).¹⁵⁸



Pyrroline **62** (72.5 mg, 0.5 mmol, 1 eq.) was dissolved in a round bottom flask containing THF (10 mL). Formaldehyde aqueous solution 37% w/v (1 mmol, 2 eq.) was added to the

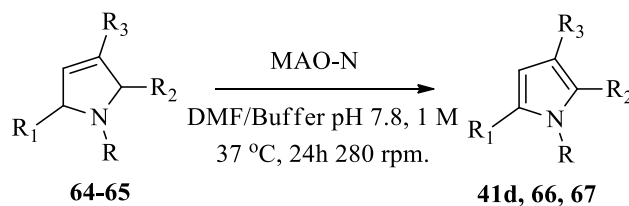
solution followed by AcOH (0.028 mL, 0.5 mmol, 1 eq.). The reaction mixture was allowed to stir at room temperature for 20 minutes. Then, NaBH(AcO)₃ (443.8 mg, 2 mmol, 4 eq.) was added and the solution was left stirring at room temperature for 18 h. After completion of the reaction, the solution was quenched with aqueous NaOH 1M solution (30 mL). The reaction mixture was extracted with EtOAc (30 mL × 3) and dried over anhydrous MgSO₄. After the solvent was evaporated, the crude product was purified by column chromatography (ethyl acetate/MeOH 4:1) to give **65j** as a white solid. **Yield:** 99% (78.7 mg). **¹H NMR** (400 MHz, CDCl₃): δ 7.49–7.35 (m, 5H), 6.28 (s, 1H), 4.56 (s, 2H), 4.34 (s, 2H), 3.09 (s, 3H) ppm. **¹³C NMR** (100 MHz, CDCl₃): δ 137.6, 132.1, 126.2, 125.3, 123.2, 119.8, 60.3, 59.8, 40.5 ppm. **LRMS** (ESI⁺): m/z = 160 [M + H]⁺.

Synthesis of 1-isopropyl-3-phenyl-2,5-dihydro-1H-pyrrole (**65k**).



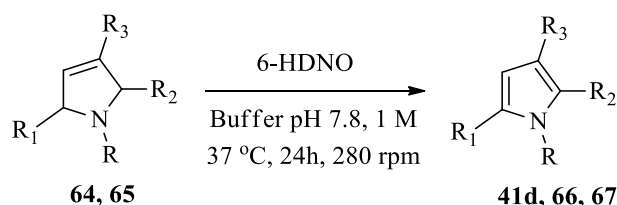
Pyrroline **62** (72.6 mg, 0.5 mmol, 1 eq.) was dissolved in a round bottom flask containing acetone (10 mL) and AcOH (0.028 mL, 0.5 mmol, 1 eq.). The reaction mixture was allowed to stir at room temperature for 20 minutes. Then, NaBH(AcO)₃ (443.8 mg, 2 mmol, 4 eq.) was added and the solution was left stirring at room temperature for 18 h. After completion of the reaction, the solution was quenched with aqueous NaOH 1M solution (30 mL). The reaction mixture was extracted with EtOAc (30 mL × 3) and dried over anhydrous MgSO₄. After the solvent was evaporated, the crude product was purified by column chromatography (ethyl acetate/MeOH = 4/1) to **65k** as a white solid. **Yield:** 99% (185.1 mg). **¹H NMR** (400 MHz, CDCl₃): δ 7.31–7.24 (m, 4H), 7.20–7.17 (m, 1H), 6.07 (s, 1H), 3.88 (s, 2H), 3.69 (s, 2H), 2.81–2.75 (m, 1H), 1.13 (d, *J* = 8.0 Hz, 6H) ppm. **¹³C NMR** (100 MHz, CDCl₃): δ 139.3, 134.0, 128.5, 127.7, 125.5, 121.3, 58.1, 57.6, 54.6, 21.1 ppm. **LRMS** (ESI⁺): m/z = 188 [M + H]⁺.

General procedure for the MAO-N catalysed biotransformation of 3-pyrrolines into pyrroles **66 and **67**.**



In a Falcon tube (15 mL), freeze dried whole cells of *E.coli* expressing recombinant monoamine oxidase MAO-N (variants D5, D9) (140 mg) were suspended in 800 μ L of potassium phosphate buffer (1M pH = 7.8). Then, the appropriate pyrroline **64** or **65** (0.1 mmol) dissolved in DMF (12.9 μ L) was added leading to a solution with a final concentration of 0.02 g/mL. The reaction mixture was incubated at 37 °C and shaken at 280 rpm for 24 h. The reaction mixture was added EtOAc (5 mL) and then centrifuged at 4000 rpm for 10 minutes. The organic layer was then separated and dried over anhydrous $MgSO_4$. After the solvent was evaporated, the crude product was analysed through 1H -NMR spectroscopy and the conversion values were determined by integration. The crude product was finally purified by column chromatography affording the pure pyrroles **41d, 66** or **67** as yellow-brown oils.

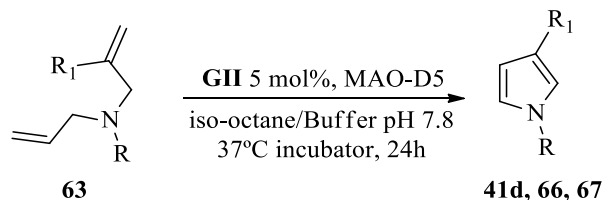
General procedure for the 6-HDNO catalysed biotransformation of 3-pyrrolines into pyrroles **66 and **67**.**



In a Falcon tube (15 mL), freeze dried whole cells of *E.coli* expressing recombinant monoamine oxidase 6-HDNO (140 mg) were suspended in 1 mL of potassium phosphate buffer (1M pH = 7.8). Then, the appropriate pyrroline **64** or **65** (0.1 mmol) was added and the reaction mixture was incubated at 37 °C and shaken at 280 rpm for 24 h. The reaction mixture was added EtOAc (5 mL) and then centrifuged at 4000 rpm for 10 minutes. The organic layer was then separated and dried over anhydrous $MgSO_4$. After the solvent was evaporated, the crude product was analysed through 1H -NMR spectroscopy and the

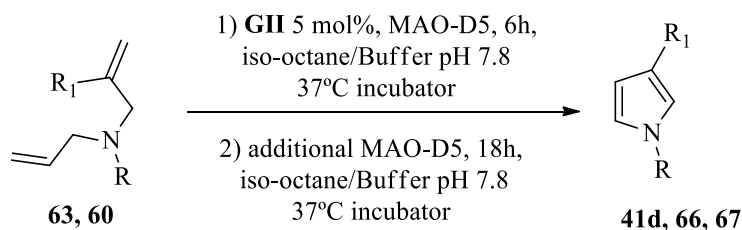
conversion values were determined by integration. The crude product was finally purified by column chromatography affording the pure pyrrole **41d**, **66** or **67** as yellow-brown oils.

General procedure for the chemoenzymatic cascade biotransformation (Method A).



In a Falcon tube (15 mL), freeze dried whole cells of *E.coli* expressing recombinant monoamine oxidase MAO-D5 (140 mg) were suspended in 800 μ L of potassium phosphate buffer (1M pH = 7.8). Then, the appropriate *N,N*-diallylaniline/amine **63** (0.1 mmol, 1 eq.) dissolved in isooctane (200 μ L) was added to the reaction mixture leading to a final concentration of 0.02 g/mL. Grubbs cat. II gen. **GII** (0.005 mmol, 0.05 eq.) was then added to the reaction mixture. The mixture was incubated at 37 °C and shaken at 280 rpm for 24h. EtOAc (5 mL) was added and the mixture was centrifuged at 4000 rpm for 10 minutes. The organic layer was then separated and dried over anhydrous MgSO_4 . After the solvent was evaporated, the crude product was analysed through ^1H -NMR spectroscopy and the conversion value was determined. The crude product was finally purified by column chromatography affording the desired pyrrole **41d**, **66** or **67** as yellow-brown oils.

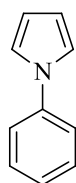
General procedure for the chemoenzymatic cascade biotransformation (Method B).



In a Falcon tube (15 mL), freeze dried whole cells of *E.coli* expressing recombinant monoamine oxidase MAO-D5 (140 mg) were suspended in 800 μ L of potassium phosphate buffer (1M pH = 7.8). Then, the appropriate diallylaniline/amine **63** and **60** (0.1 mmol, 1 eq.) dissolved in isooctane (200 μ L) was added to the reaction mixture leading to a final concentration of 0.02 g/mL. Grubbs cat. II gen. **GII** (0.005 mmol, 0.05 eq.) was then added

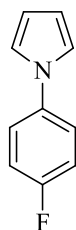
to the reaction mixture. The mixture was incubated at 37 °C and shaken at 280 rpm for 6h. Additional lyophilized cells (140 mg) were added and the suspension was incubated at 37 °C and shaken at 280 rpm for further 18h. EtOAc (5 mL) was added and the mixture was centrifuged at 4000 rpm for 10 minutes. The organic layer was then separated and dried over anhydrous MgSO₄. After the solvent was evaporated, the crude product was analysed through ¹H-NMR spectroscopy and the conversion value was determined. The crude product was finally purified by column chromatography affording the desired pyrrole **41d**, **66** or **67** as yellow-brown oils.

Synthesis of 1-phenyl-1H-pyrrole (**66a**).²⁵⁴



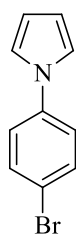
Yield: 78% (11.1 mg). **¹H NMR** (400 MHz, CDCl₃): δ 7.34-7.28 (m, 4H), 7.14 (t, *J* = 7.0 Hz, 1H), 6.99 (d, *J* = 2.0 Hz, 2H), 6.26 (dd, *J* = 2.5, 2.0 Hz, 2H) ppm. **¹³C NMR** (100 MHz, CDCl₃): δ 140.82, 129.60, 125.66, 120.57, 119.37, 110.46. **LRMS** (ESI⁺): *m/z* = 144 [M + H]⁺.

Synthesis of 1-(4-fluorophenyl)-1H-pyrrole (**66b**).²⁴⁹



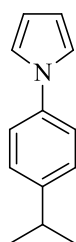
Yield: 59% (9.4 mg). **¹H NMR** (400 MHz, CDCl₃): δ 7.37-7.34 (m, 2H), 7.15-7.11 (m, 2H), 7.03 (d, *J* = 2.0 Hz, 2H), 6.36 (dd, *J* = 2.5, 2.0 Hz, 2H). **¹³C NMR** (100 MHz, CDCl₃): δ 159.4, 137.1, 122.3, 122.2, 119.6, 116.4, 116.1, 110.4 ppm. **LRMS** (ESI⁺): *m/z* = 162 [M + H]⁺.

Synthesis of 1-(4-bromophenyl)-1H-pyrrole (**66c**).²⁵⁵



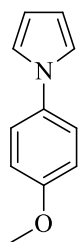
Yield: 23% (5.1 mg). **¹H NMR** (400 MHz, CDCl₃): δ 7.48-7.46 (m, 2H), 7.21-7.18 (m, 2H), 7.00 (d, *J* = 2.0 Hz, 2H), 6.32 (dd, *J* = 2.5, 2.0 Hz, 2H). **¹³C NMR** (100 MHz, CDCl₃): δ 139.6, 132.5, 121.7, 119.1, 118.6, 110.8. **LRMS** (ESI⁺): *m/z* = 221-223 [M + H]⁺.

Synthesis of 1-(4-isopropylphenyl)-1H-pyrrole (**66d**).²⁵⁶



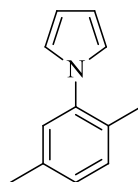
Yield: 70% (12.9 mg). **¹H NMR** (400 MHz, CDCl₃): δ 7.34-7.28 (m, 4H), 7.08 (d, *J* = 2.0 Hz, 2H), 6.35 (dd, *J* = 2.5, 2.0 Hz, 2H), 2.96 (m, 1H), 1.29 (d, *J* = 7.0 Hz, 6H) ppm. **¹³C NMR** (100 MHz, CDCl₃): δ 146.8, 139.1, 127.8, 121.0, 119.8, 110.4, 34.0, 24.4. **LRMS** (ESI⁺): *m/z* = 186 [M + H]⁺.

Synthesis of 1-(4-methoxyphenyl)-1H-pyrrole (66e).²⁴⁹



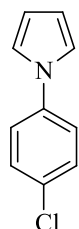
Yield: 42% (7.3 mg). **¹H NMR** (400 MHz, CDCl₃): δ 7.33 (d, *J* = 9.0 Hz, 2H), 7.02 (d, *J* = 2.0 Hz, 2H), 6.96 (d, *J* = 9.0 Hz, 2H), 6.34 (dd, 2.5, *J* = 2.5, 2.0 Hz, 2H), 3.85 (s, 3H) ppm. **¹³C NMR** (100 MHz, CDCl₃): δ 157.6, 134.5, 122.2, 119.7, 114.6, 109.8, 55.5 ppm. **LRMS** (ESI⁺): *m/z* = 174 [M + H]⁺.

Synthesis of 1-(2,5-Dimethylphenyl)-1H-pyrrole (66f).²⁵⁷



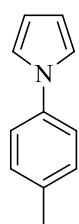
Yield: 20% (3.4 mg). **¹H NMR** (400 MHz, CDCl₃): δ 7.09 (d, *J* = 9.0 Hz, 2H), 7.00 (s, 1H), 6.71 (d, *J* = 2.0 Hz, 2H), 6.22 (dd, *J* = 2.5, 2.0 Hz, 2H), 2.27 (s, 3H), 2.09 (s, 3H) ppm. **¹³C NMR** (100 MHz, CDCl₃): δ 136.3, 130.9, 130.3, 128.2, 127.3, 122.0, 108.5, 20.8, 17.4 ppm. **LRMS** (ESI⁺): *m/z* = 172 [M + H]⁺.

Synthesis of 1-(4-chlorophenyl)-1H-pyrrole (66l).²³²



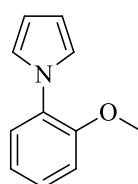
Yield: 56% (9.9 mg). **¹H NMR** (400 MHz, CDCl₃): δ 7.56 (d, *J* = 8.5 Hz, 2H), 7.29 (d, *J* = 8.5 Hz, 2H), 7.07 (d, *J* = 2.0 Hz, 2H), 6.38 (dd, *J* = 2.5, 2.0 Hz, 2H). **¹³C NMR** (100 MHz, CDCl₃): δ 139.8, 132.6, 121.9, 119.2, 118.7, 110.9 ppm. **LRMS** (ESI⁺): *m/z* = 178 [M + H]⁺.

Synthesis of 1-(*p*-tolyl)-1H-pyrrole (66m).²⁵⁸



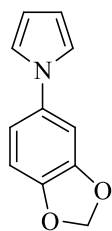
Yield: 50% (7.9 mg). **¹H NMR** (400 MHz, CDCl₃): δ 7.31-7.30 (d, *J* = 8.0 Hz, 2H), 7.24 (d, *J* = 8.0 Hz, 2H), 7.08 (d, *J* = 2.0 Hz, 2H), 6.35 (dd, *J* = 2.5, 2.0 Hz, 2H), 2.40 (s, 3H) ppm. **¹³C NMR** (100 MHz, CDCl₃): δ 138.6, 135.5, 130.2, 120.7, 119.5, 110.2, 21.0 ppm. **LRMS** (ESI⁺): *m/z* = 158 [M + H]⁺.

Synthesis of 1-(2-methoxyphenyl)-1H-pyrrole (66n).²⁵⁹



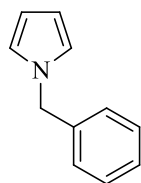
Yield: 84% (14.5 mg). **¹H NMR** (400 MHz, CDCl₃): δ 7.27-7.16 (m, 2H), 7.01-6.94 (m, 2H), 6.90 (d, *J* = 2.0 Hz, 2H), 6.25 (dd, *J* = 2.5, 2.0 Hz, 2H), 3.83 (s, 3H) ppm. **¹³C NMR** (100 MHz, CDCl₃): δ 152.7, 130.2, 127.3, 125.7, 122.0, 120.8, 112.2, 108.7, 55.7 ppm. **LRMS** (ESI⁺): *m/z* = 174 [M + H]⁺.

Synthesis of 1-(benzo[d][1,3]dioxol-5-yl)-1H-pyrrole (66o).



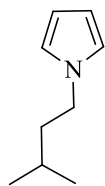
Yield: 57% (10.6 mg). **¹H NMR** (400 MHz, CDCl₃): δ 6.92-6.88 (m, 2H), 6.82 (dd, *J* = 2.0, 0.5 Hz, 1H), 6.77-6.74 (m, 2H), 6.26-6.22 (m, 2H), 5.94 (s, 2H) ppm. **¹³C NMR** (100 MHz, CDCl₃): δ 148.3, 135.7, 119.9, 114.1, 110.0, 108.5, 103.1, 101.6 ppm. **LRMS** (ESI⁺): *m/z* = 188 [M + H]⁺. **HRMS** (ESI) *m/z* calcd. For C₁₁H₉NO₂ [M + H] 188.0712, found 188.0711.

Synthesis of 1-benzyl-1H-pyrrole (67a).²⁶⁰



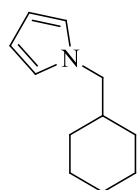
Yield: 75% (11.8 mg). **¹H NMR** (400 MHz, CDCl₃): δ 7.39-7.27 (m, 3H), 7.18-7.11 (m, 2H), 6.72 (d, *J* = 1.5 Hz, 2H), 6.22 (dd, *J* = 2.0, 1.5 Hz, 2H), 5.09 (s, 2H) ppm. **¹³C NMR** (100 MHz, CDCl₃): δ 138.3, 128.8, 127.8, 127.1, 121.3, 108.6, 53.5 ppm. **LRMS** (ESI⁺): *m/z* = 158 [M + H]⁺.

Synthesis of 1-isopentyl-1H-pyrrole (67b).²⁶¹



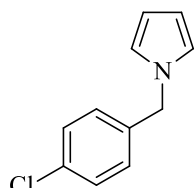
Yield: 52% (7.1 mg). **¹H NMR** (400 MHz, CDCl₃): δ 6.58 (d, *J* = 2.0 Hz, 2H), 6.06 (dd, *J* = 2.5, 2.0 Hz, 2H), 3.84-3.76 (m, 2H), 1.63-1.56 (m, 2H), 1.51 (d, *J* = 6.5 Hz, 1H), 0.87 (s, 3H), 0.85 (s, 3H) ppm. **¹³C NMR** (100 MHz, CDCl₃): δ 120.4, 107.8, 57.6, 40.4, 25.5, 22.4 ppm. **LRMS** (ESI⁺): *m/z* = 138 [M + H]⁺.

Synthesis of 1-(cyclohexylmethyl)-1H-pyrrole (67c).²⁶²



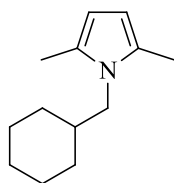
Yield: 63% (10.2 mg). **¹H NMR** (400 MHz, CDCl₃): δ 6.59 (d, *J* = 2.0 Hz, 2H), 6.18 (dd, *J* = 2.5, 2.0 Hz, 2H), 3.73 (d, *J* = 7.0 Hz, 2H), 1.80-1.63 (m, 6H), 1.32-1.15 (m, 3H), 1.02-0.93 (m, 2H) ppm. **¹³C NMR** (100 MHz, CDCl₃): δ 121.0, 107.5, 56.3, 39.9, 30.8, 26.3, 25.7 ppm. **LRMS** (ESI⁺): *m/z* = 164 [M + H]⁺.

Synthesis of 1-(4-chlorobenzyl)-1H-pyrrole (67d).²⁶³



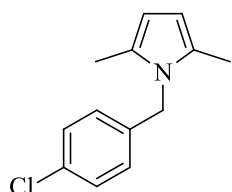
Yield: 61% (11.6 mg). **¹H NMR** (400 MHz, CDCl₃): δ 7.37 (d, *J* = 8.0 Hz, 2H), 7.12 (d, *J* = 8.0 Hz, 2H), 6.66 (d, *J* = 2.0 Hz, 2H), 6.12 (dd, *J* = 2.5, 2.0 Hz, 2H), 5.02 (s, 2H) ppm. **¹³C NMR** (100 MHz, CDCl₃): δ 136.6, 133.3, 128.7, 128.2, 120.9, 108.7, 52.4 ppm. **LRMS** (ESI⁺): *m/z* = 192 [M + H]⁺.

Synthesis of 1-(cyclohexylmethyl)-2,5-dimethyl-1H-pyrrole (67e).



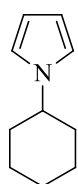
Yield: 40% (7.6 mg). **¹H NMR** (400 MHz, CDCl₃): δ = 5.69 (s, 2H), 3.46 (d, *J* = 7.0 Hz, 2H), 2.13 (s, 6H), 1.65 (s, 2H), 1.56 (d, *J* = 12.5 Hz, 2H), 1.12-1.07 (m, 2H), 0.81 (t, *J* = 6.5 Hz, 5H) ppm. **¹³C NMR** (100 MHz, CDCl₃): δ = 127.9, 104.9, 50.0, 39.5, 31.6, 31.1, 26.4, 26.0, 22.7, 14.2, 12.9 ppm. **LRMS** (ESI⁺): *m/z* = 192 [M + H]⁺ **HRMS** (ESI) *m/z* calcd. For C₁₃H₂₂N [M + H] 192.1752, found 192.1753.

Synthesis of 1-(4-chlorobenzyl)-2,5-dimethyl-1H-pyrrole (67f).²⁶⁴



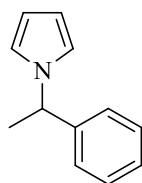
Yield: 42% (9.2 mg). **¹H NMR** (400 MHz, CDCl₃): δ 7.30 (d, *J* = 8.5 Hz, 2H), 6.85 (d, *J* = 8.5 Hz, 2H), 5.92 (s, 2H), 5.01 (s, 2H), 2.17 (s, 6H) ppm. **¹³C NMR** (100 MHz, CDCl₃): δ 137.0, 128.8, 127.8, 127.0, 125.6, 46.1, 12.7, 11.2 ppm. **LRMS** (ESI⁺): *m/z* = 220 [M + H]⁺.

Synthesis of 1-cyclohexyl-1H-pyrrole (67g).²⁶⁵



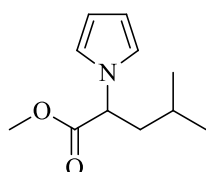
Yield: 70% (10.4 mg). **¹H NMR** (400 MHz, CDCl₃): δ 6.66 (d, *J* = 2.0 Hz, 2H), 6.07 (dd, *J* = 2.5, 2.0 Hz, 2H), 3.74 (tt, *J* = 12.0, 4.0 Hz, 1H), 2.09-1.99 (m, 2H), 1.81 (dt, *J* = 13.5, 3.0 Hz, 2H), 1.71-1.59 (m, 2H), 1.57 (d, *J* = 3.5 Hz, 1H), 1.54 (d, *J* = 3.5 Hz, 1H), 1.35-1.29 (m, 2H) ppm. **¹³C NMR** (100 MHz, CDCl₃): δ = 118.4, 107.3, 34.7, 31.6, 25.7, 25.5, 22.7, 14.1 ppm. **LRMS** (ESI⁺): *m/z* = 150 [M + H]⁺.

Synthesis of 1-(1-Phenylethyl)-1H-pyrrole (67h).²⁶⁶



Yield: 41% (7.0 mg). **¹H NMR** (400 MHz, CDCl₃): δ 7.14 (m, 3H), 7.01 (d, *J* = 7.5 Hz, 2H), 6.68 (d, *J* = 2.0 Hz, 2H), 6.11 (dd, *J* = 2.5, 2.0 Hz, 2H), 5.20 (q, *J* = 7.0 Hz, 1H), 1.75 (d, *J* = 7.0 Hz, 3H) ppm. **¹³C NMR** (100 MHz, CDCl₃): δ = 142.5, 127.5, 126.3, 124.7, 118.4, 106.9, 57.0, 21.0 ppm. **LRMS** (ESI⁺): *m/z* = 172 [M + H]⁺.

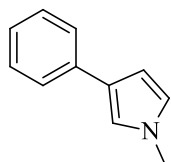
Synthesis of methyl-4-methyl-2-(1H-pyrrol-1-yl)pentanoate (67i).^{263,266}



Yield: 21% (4.1 mg). **¹H NMR** (400 MHz, CDCl₃): δ 6.75 (d, *J* = 2.0 Hz, 2H), 6.17 (dd, *J* = 2.5, 2.0 Hz, 2H), 4.65 (t, *J* = 7.5 Hz, 1H), 3.70 (s, 3H), 1.95 (m, 2H), 1.40 (m, 1H), 0.95 (d, *J* = 7.5 Hz, 3H), 0.83 (d, *J* = 7.5 Hz,

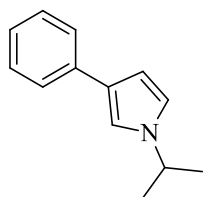
3H) ppm. **¹³C NMR** (100 MHz, CDCl₃): δ 171.0, 120.1, 108.5, 68.8, 51.9, 32.0, 19.4, 18.7 ppm. **LRMS** (ESI⁺): m/z = 196 [M + H]⁺.

Synthesis of 1-methyl-3-phenyl-1H-pyrrole (67j).¹⁹⁹



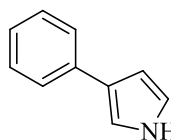
Yield 70% (11.0 mg). **¹H NMR** (400 MHz, CDCl₃): δ 7.42 (dd, *J* = 8.0, 4.0 Hz, 2H), 7.25 (t, *J* = 8.0 Hz, 2H), 7.08 (t, *J* = 8.0 Hz, 1H), 6.84 (d, *J* = 2.0 Hz, 1H), 6.56 (s, 1H), 6.37 (d, *J* = 2.0 Hz, 1H), 3.62 (m, 3H) ppm. **¹³C NMR** (100 MHz, CDCl₃): δ 136.3, 131.0, 129.0, 125.7, 125.4, 123.1, 119.0, 106.7, 36.8 ppm. **LRMS** (ESI⁺): m/z = 158 [M + H]⁺. **HRMS** (ESI) m/z calcd. For C₁₁H₁₂N [M + H] 158.0970, found 158.0966.

Synthesis of 1-isopropyl-3-phenyl-1H-pyrrole (67k).



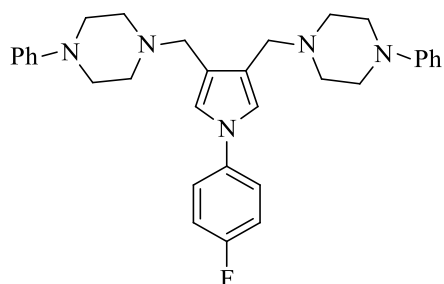
Yield 30% (5.6 mg). **¹H NMR** (400 MHz, CDCl₃): δ 7.46-7.34 (m, 2H), 7.30-7.20 (m, 2H), 7.06 (tt, *J* = 7.4, 1.0 Hz, 1H), 6.96 (d, *J* = 1.5 Hz, 1H), 6.67 (s, 1H), 6.38 (d, *J* = 1.5 Hz, 1H), 4.18 (dt, *J* = 6.5 Hz, 1H), 1.42 (d, *J* = 6.5 Hz, 6H) ppm. **¹³C NMR** (100 MHz, CDCl₃): δ 136.1, 128.5, 125.1, 124.9, 124.3, 119.2, 115.1, 105.7, 51.0, 23.9 ppm. **LRMS** (ESI⁺): m/z = 186 [M + H]⁺. **HRMS** (ESI) m/z calcd. For C₁₃H₁₅N [M + H] 186.1283, found 186.1282.

Synthesis of 3-phenyl-1H-pyrrole (67l).



Yield: 34% (4.8 mg). **¹H NMR** (400 MHz, CDCl₃): δ 7.47 (dd, *J* = 8.0, 4.0 Hz, 2H), 7.27 (t, *J* = 8.0 Hz, 2H), 7.13-7.09 (m, 1H), 7.03 (d, *J* = 1.5 Hz, 1H), 6.78 (d, *J* = 1.5 Hz, 1H), 6.49-6.48 (m, 1H) ppm. **¹³C NMR** (100 MHz, CDCl₃): δ 135.8, 128.6, 125.3, 125.2, 118.9, 114.6, 106.6 ppm. **LRMS** (ESI⁺): m/z = 144 [M + H]⁺.

Synthesis of 4,4'-((1-(4-fluorophenyl)-1H-pyrrole-3,4-diyl)bis(methylene))bis(1-phenylpiperazine) (68**) via MAO-D5 - Mannich reaction cascade.**



In a Falcon tube (15 mL), whole cells of *E.coli* expressing recombinant MAO-D5 (140 mg), were suspended in potassium phosphate buffer 1M pH = 7.8 (800 μ L). Then, the pyrroline **64b** (0.1 mmol, 1 eq.) dissolved in isooctane (200 μ L) was added to the reaction mixture in order to have a final concentration of 0.02 g/mL. The reaction mixture was incubated at 37 °C and shaken at 280 rpm for 24 h. The reaction mixture was then diluted with CH₃CN (2 mL) and centrifuged. The supernatant was removed and added to a stirring solution of *N*-phenyl piperazine (8.1 mg, 0.05 mmol, 0.5 eq.), formaldehyde 37% w/v (0.05 mmol, 0.5 eq.) and glacial acetic acid (0.003 mL, 0.05 mmol, 0.5 eq.) in CH₃CN (2 mL). The mixture was stirred at room temperature for 12 h. Then, the reaction was quenched with saturated NaHCO₃ aqueous solution (20 mL) and extracted twice with 20 mL of Et₂O. The combined organic layers were collected, washed with brine, dried over Na₂SO₄ and concentrated under reduced pressure. The crude product **68** was purified by chromatography on silica gel, using hexane/EtOAc (4:1) as eluent. **Yield** 25% (12.7 mg). **¹H NMR** (400 MHz, CDCl₃): δ 7.45-7.27 (m, 2H), 7.24-7.13 (m, 5H), 7.05-6.93 (m, 2H), 6.86-6.79 (m, 4H), 6.77 (tt, J = 7.3, 1.0 Hz, 2H), 6.06 (s, 2H), 3.19 (s, 4H), 3.08-2.87 (m, 8H), 2.47-2.25 (m, 8H) ppm. **¹³C NMR** (100 MHz, CDCl₃): δ 160.7, 151.4, 130.9, 130.8, 129.1, 119.6, 116.0, 114.9, 114.7, 108.8, 53.9, 52.4, 49.2 ppm. **LRMS** (ESI⁺): m/z = 509 [M + H]⁺. **HRMS** (ESI) m/z calcd. For C₃₄H₃₈FN₃ [M + H] 509.2946, found 509.2947.

6. References.

- (1) Koch, R. *Klin. Wochenschr.* **1932**, *11* (12), 490–492.
- (2) World Health Organization, (WHO). *WHO/ Global tuberculosis report 2015*; **2015**.
- (3) Corbett, E. L.; Bandason, T.; Yin, B. C.; Munyati, S.; Godfrey-Faussett, P.; Hayes, R.; Churchyard, G.; Butterworth, A.; Mason, P. *PLoS Med.* **2007**, *4* (1), 0164–0172.
- (4) Dooley, K. E.; Chaisson, R. E. *Lancet. Infect. Dis.* **2009**, *9* (12), 737–746.
- (5) Rastogi, N.; Legrand, E.; Sola, C. *Rev. Sci. Tech.* **2001**, *20* (1), 21–54.
- (6) Parish, T.; Stoker, N. G. *Mol. Biotechnol.* **1999**, *13* (3), 191–200.
- (7) Brennan, P. J.; Nikaido, H. *Annu. Rev. Biochem.* **1995**, *64* (1), 29–63.
- (8) Kleinnijenhuis, J.; Oosting, M.; Joosten, L. A. B.; Netea, M. G.; Van Crevel, R. *Clin. Dev. Immunol.* **2011**, *2011*, 1–12.
- (9) Pieters, J. *Cell Host Microbe* **2008**, *3* (6), 399–407.
- (10) Aderem, A.; Underhill, D. M. *Annu. Rev. Immunol.* **1999**, *17*, 593–623.
- (11) Schmid, S. L. *Annu. Rev. Biochem.* **1997**, *66*, 511–548.
- (12) Vergne, I.; Chua, J.; Deretic, V. *J. Exp. Med.* **2003**, *198* (4), 653–659.
- (13) Knutson, K. L.; Hmama, Z.; Herrera-Velit, P.; Rochford, R.; Reiner, N. E. *J. Biol. Chem.* **1998**, *273* (1), 645–652.
- (14) Chan, J.; Fan, X.; Hunter, S. W.; Brennan, P. J.; Bloom, B. R. *Infect. Immun.* **1991**, *59* (5), 1755–1761.
- (15) Gatfield, J.; Albrecht, I.; Zanolari, B.; Steinmetz, M. O.; Pieters, J. *Mol. Biol. Cell* **2005**, *16* (6), 2786–2798.
- (16) Vergne, I.; Chua, J.; Lee, H.-H.; Lucas, M.; Belisle, J.; Deretic, V. *Proc. Natl. Acad. Sci. U. S. A.* **2005**, *102* (11), 4033–4038.
- (17) Walburger, A.; Koul, A.; Ferrari, G.; Nguyen, L.; Prescianotto-Baschong, C.; Huygen, K.; Klebl, B.; Thompson, C.; Bacher, G.; Pieters, J. *Science* **2004**, *304* (5678), 1800–1804.
- (18) Gordon, S.; Keshav, S.; Stein, M. *Immunobiology* **1994**, *191* (4–5), 369–377.
- (19) Wolf, P. R.; Ploegh, H. L. *Annu. Rev. Cell Dev. Biol.* **1995**, *11*, 267–306.
- (20) Pieters, J. *Curr. Opin. Immunol.* **1997**, *9* (1), 89–96.
- (21) Poizat, M.; Arends, I. W. C. E.; Hollmann, F. *J. Mol. Catal. B Enzym.* **2010**, *63* (3–4), 149–156.
- (22) Young, D.; Hussell, T.; Dougan, G. *Nat. Immunol.* **2002**, *3* (11), 1026–1032.
- (23) Saunders, B. M.; Britton, W. J. *Immunol. Cell Biol.* **2007**, *85* (2), 103–111.
- (24) Bartlett, J. G. J. *Infect. Dis.* **2007**, *196* (Suppl 1), S124–S125.

- (25) Kawai, V.; Soto, G.; Gilman, R. H.; Bautista, C. T.; Caviades, L.; Huaroto, L.; Ticona, E.; Ortiz, J.; Tovar, M.; Chavez, V.; Rodriguez, R.; Escombe, A. R.; Evans, C. A. *Am. J. Trop. Med. Hyg.* **2006**, 75 (6), 1027–1033.
- (26) Corbett, E. L.; Watt, C. J.; Walker, N.; Maher, D.; Williams, B. G.; Raviglione, M. C.; Dye, C. *Arch. Intern. Med.* **2003**, 163 (9), 1009–1021.
- (27) Connors, M.; Kovacs, J. A.; Krevat, S.; Gea-Banacloche, J. C.; Sneller, M. C.; Flanigan, M.; Metcalf, J. A.; Walker, R. E.; Falloon, J.; Baseler, M.; Stevens, R.; Feuerstein, I.; Masur, H.; Lane, H. C. *Nat. Med.* **1997**, 3 (5), 533–540.
- (28) Geldmacher, C.; Zumla, A.; Hoelscher, M. *Curr. Opin. HIV AIDS* **2012**, 7 (3), 268–274.
- (29) Metcalfe, C.; Macdonald, I. K.; Murphy, E. J.; Brown, K. A.; Raven, E. L.; Moody, P. C. E. *J. Biol. Chem.* **2008**, 283 (10), 6193–6200.
- (30) Singh, A. K.; Kumar, R. P.; Pandey, N.; Sinha, N.; Sinha, M.; Bhushan, A.; Kaur, P.; Sharma, S.; Singh, T. P. *J. Biol. Chem.* **2010**, 285 (2), 1569–1576.
- (31) Timmins, G. S.; Deretic, V. *Mol. Microbiol.* **2006**, 62 (5), 1220–1227.
- (32) American Thoracic Society/Centers for Disease Control/Infectious Diseases Society of America. *MMWR. Recomm. reports Morb. Mortal. Wkly. report. Recomm. reports*, **2003**, 52 (11), 1–77.
- (33) Viveiros, M.; Bettencourt, R.; Victor, T. C.; Jordaan, A. M.; Leandro, C.; Ordway, D.; Amaral, L. *Antimicrob. Agents Chemother.* **2002**, 46 (9), 2804–2810.
- (34) Seifert, M.; Catanzaro, D.; Catanzaro, A.; Rodwell, T. C. *PLoS One* **2015**, 10 (3).
- (35) CDC. CDC **2014**. <https://www.cdc.gov/tb/statistics/reports/2014/pdfs/tb-surveillance-2014-report.pdf>
- (36) Traore, H.; Fissette, K.; Bastian, I.; Devleeschouwer, M.; Portaels, F. *Int. J. Tuberc. Lung Dis.* **2000**, 4 (5), 481–484.
- (37) Lee, H.; Myoung, H. J.; Bang, H. E.; Bai, G. H.; Kim, S. J.; Kim, J. D.; Cho, S. N. *Yonsei Med. J.* **2002**, 43 (1), 59–64.
- (38) Shi, W.; Zhang, X.; Jiang, X.; Yuan, H.; Lee, J. S.; Barry, C. E.; Wang, H.; Zhang, W.; Zhang, Y. *Science* **2011**, 333 (6049), 1630–1632.
- (39) Zhang, Y.; Shi, W.; Zhang, W.; Mitchison, D. *Microbiol. Spectr.* **2013**, 2 (4), 1–12.
- (40) Shi, W.; Chen, J.; Feng, J.; Cui, P.; Zhang, S.; Weng, X.; Zhang, W.; Zhang, Y. *Emerg. Microbes Infect.* **2014**, 3 (8), 58.
- (41) Zhu, M.; Burman, W. J.; Jaresko, G. S.; Berning, S. E.; Jelliffe, R. W.; Peloquin, C. A. *Pharmacotherapy* **2001**, 21 (9), 1037–1045.
- (42) Streptomycin in Tuberculosis Trials Committee. *Bmj* **1948**, 2, 769–782.
- (43) Steyn, L. M.; Douglass, J. *J. Infect. Dis.* **1993**, 167 (6), 1505–1506.
- (44) Zhanel, G. G.; Ennis, K.; Vercaigne, L.; Walkty, A.; Gin, A. S.; Embil, J.; Smith, H.; Hoban, D. J. *Drugs* **2002**, 62 (1), 13–59.

- (45) Ginsburg, A. S.; Grosset, J. H.; Bishai, W. R. *Lancet Infect. Dis.* **2003**, 3 (7), 432–442.
- (46) Wang, J. Y.; Hsueh, P. R.; Jan, I. S.; Lee, L. N.; Liaw, Y. S.; Yang, P. C.; Luh, K. T. *Thorax* **2006**, 61 (10), 903–908.
- (47) Alangaden, G. J.; Kreiswirth, B. N.; Aouad, A.; Khetarpal, M.; Igno, F. R.; Moghazeh, S. L.; Manavathu, E. K.; Lerner, S. A. *Antimicrob. Agents Chemother.* **1998**, 42 (5), 1295–1297.
- (48) Maus, C. E.; Plikaytis, B. B.; Shinnick, T. M. *Antimicrob. Agents Chemother.* **2005**, 49 (8), 3192–3197.
- (49) Banerjee, A.; Dubnau, E.; Quemard, A.; Balasubramanian, V.; Um, K. S.; Wilson, T.; Collins, D.; Lisle, G. De; Jr, W. R. J. *Science* **1993**, 263, 227–230.
- (50) DeBarber, A. E.; Mdluli, K.; Bosman, M.; Bekker, L. G.; Barry, C. E. *Proc. Natl. Acad. Sci. U. S. A.* **2000**, 97 (17), 9677–9682.
- (51) Schaaf, H. S.; Victor, T. C.; Venter, A.; Brittle, W.; Jordaan, A. M.; Hesselning, A. C.; Marais, B. J.; Van Helden, P. D.; Donald, P. R. *Int. J. Tuberc. Lung Dis.* **2009**, 13 (11), 1355–1359.
- (52) Nikolov, D., Hu, S., Lin, J., Gasch, A., Hoffmann, A., Horikoshi, M., Chua, N., Roeder, G., Burley, S. *Nature* **1992**, 360, 40–46.
- (53) Ori, R.; Amos, T.; Bergman, H.; Soares-Weiser, K.; Ipser, J. C.; Stein, D. J. *Cochrane database Syst. Rev.* **2015**, 5, 7803.
- (54) Saraf, G.; Akshata, J. S.; Kuruthukulangara, S.; Thippeswamy, H.; Reddy, S. K.; Buggi, S.; Chaturvedi, S. K. Egypt. J. *Chest Dis. Tuberc.* **2015**, 64 (2), 449–451.
- (55) Amaral, L.; Molnar, J. In Vivo (Brooklyn). **2012**, 26 (2), 231–236.
- (56) Fenton, M.; Rathbone, J.; Reilly, J.; Sultana, A. *Cochrane Database Syst. Rev.* **2000**, 3, CD001944.
- (57) Amaral, L.; Kristiansen, J. E.; Viveiros, M.; Atouguia, J. J. *Antimicrob. Chemother.* **2001**, 47 (5), 505–511.
- (58) Amaral, L.; Viveiros, M. *Int. J. Antimicrob. Agents* **2012**, 39 (5), 376–380.
- (59) Tenover, F. C.; McGowan, J. E. *Int. Encycl. Public Heal.* **2008**, 211–219.
- (60) Machado, D.; Couto, I.; Perdigão, J.; Rodrigues, L.; Portugal, I.; Baptista, P.; Veigas, B.; Amaral, L.; Viveiros, M. *PLoS One* **2012**, 7 (4), e34538.
- (61) Bellamy, W. T. *Annu. Rev. Pharmacol. Toxicol.* **1996**, 36, 161–183.
- (62) Amaral, L.; Martins, M.; Viveiros, M.; Molnar, J.; Kristiansen, J. E. *Curr. Drug Targets* **2008**, 9 (9), 816–819.
- (63) McShane, H. *Philos. Trans. R. Soc. Lond. B. Biol. Sci.* **2011**, 366 (1579), 2782–2789.
- (64) Hesselning, A. C.; Marais, B. J.; Gie, R. P.; Schaaf, H. S.; Fine, P. E. M.; Godfrey-Faussett, P.; Beyers, N. *Vaccine* **2007**, 25 (1), 14–18.

- (65) Qie, Y. Q.; Wang, J. L.; Liu, W.; Shen, H.; Chen, J. Z.; Zhu, B. D.; Xu, Y.; Zhang, X. L.; Wang, H. H. *Scand. J. Immunol.* **2009**, 69 (4), 342–350.
- (66) Vordermeier, H. M.; Villarreal-Ramos, B.; Cockle, P. J.; McAulay, M.; Rhodes, S. G.; Thacker, T.; Gilbert, S. C.; McShane, H.; Hill, A. V. S.; Xing, Z.; Hewinson, R. G. *Infect. Immun.* **2009**, 77 (8), 3364–3373.
- (67) Levy, S. B.; Marshall, B. *Nat. Med.* **2004**, 10 (12s), S122–S129.
- (68) Gillespie, S. H. *Curr. Respir. Med. Rev.* **2013**, 9 (3), 211–216.
- (69) Who. *World Heal. Organ.* **2011**, 258.
- (70) Akbar Velayati, A.; Farnia, P.; Reza Masjedi, M. *Int. J. Clin. Exp. Med.* **2013**, 6 (4), 307–309.
- (71) Protopopova, M.; Hanrahan, C.; Nikonenko, B.; Samala, R.; Chen, P.; Gearhart, J.; Einck, L.; Nacy, C. A. *J. Antimicrob. Chemother.* **2005**, 56 (5), 968–974.
- (72) Ruan, Q.; Liu, Q.; Sun, F.; Shao, L.; Jin, J.; Yu, S.; Ai, J.; Zhang, B.; Zhang, W. *Emerg. Microbes Infect.* **2016**, 5 (2), e12.
- (73) Lee, M.; Lee, J.; Carroll, M. W.; Choi, H.; Min, S.; Song, T.; Via, L. E.; Goldfeder, L. C.; Kang, E.; Jin, B.; Park, H.; Kwak, H.; Kim, H.; Jeon, H.-S.; Jeong, I.; Joh, J. S.; Chen, R. Y.; Olivier, K. N.; Shaw, P. a; Follmann, D.; Song, S. D.; Lee, J.-K.; Lee, D.; Kim, C. T.; Dartois, V.; Park, S.-K.; Cho, S.-N.; Barry, C. E. *Nejm* **2012**, 367 (16), 1508–1518.
- (74) Upton, A. M.; Cho, S.; Yang, T. J.; Kim, A. Y.; Wang, Y.; Lu, Y.; Wang, B.; Xu, J.; Mdluli, K.; Ma, Z.; Franzblaub, S. G. *Antimicrob. Agents Chemother.* **2015**, 59 (1), 136–144.
- (75) Tasneen, R.; Williams, K.; Amoabeng, O.; Minkowski, A.; Mdluli, K. E.; Upton, A. M.; Nuermbergera, E. L. *Antimicrob. Agents Chemother.* **2015**, 59 (1), 129–135.
- (76) Kakkar, A. K.; Dahiya, N. *Tuberculosis* **2014**, 94 (4), 357–362.
- (77) Gler, M. T.; Skripconoka, V.; Sanchez-Garavito, E.; Xiao, H.; Cabrera-Rivero, J. L.; Vargas-Vasquez, D. E.; Gao, M.; Awad, M.; Park, S.; Shim, T. S.; Suh, G. Y.; Danilovits, M.; Ogata, H.; Kurve, A.; Chang, J.; Suzuki, K.; Tupasi, T.; Koh, W.-J.; Seaworth, B.; Geiter, L. J.; Wells, C. D. N. *Engl. J. Med.* **2012**, 366 (23), 2151–2160.
- (78) Amaral, L.; Viveiros, M.; Kristiansen, J. E. *Curr. Drug Targets* **2006**, 7 (7), 887–891.
- (79) Schneider, N.; Lowe, D. M.; Sayle, R. A.; Tarselli, M. A.; Landrum, G. A. *J. Med. Chem.* **2016**, 59 (9), 4385–4402.
- (80) Brown, D. G.; Boström, J. *J. Med. Chem.* **2016**, 59 (10), 4443–4458.
- (81) Zhang, T. Y. *Adv. Heterocycl. Chem.* **2017**, 121, 1–12.
- (82) Taylor, A. P.; Robinson, R. P.; Fobian, Y. M.; Blakemore, D. C.; Jones, L. H.; Fadeyi, O. *Org. Biomol. Chem.* **2016**, 14 (28), 6611–6637.
- (83) Amaral, L.; Molnar, J. *Recent Pat. Antiinfect. Drug Discov.* **2010**, 5 (2), 109–114.

- (84) Chachignon, H.; Scalacci, N.; Petricci, E.; Castagnolo, D. *J. Org. Chem.* **2015**, *80* (10), 5287–5295.
- (85) Scalacci, N.; Black, G. W.; Mattedi, G.; Brown, N. L.; Turner, N. J.; Castagnolo, D. *ACS Catal.* **2017**, *7*, 1295.
- (86) Hughes, J. P.; Rees, S. S.; Kalindjian, S. B.; Philpott, K. L. *Br. J. Pharmacol.* **2011**, *162* (6), 1239–1249.
- (87) Zheng, W.; Thorne, N.; McKew, J. C. *Drug Discov. Today.* **2013**, 1067–1073.
- (88) Liu, K.; Li, F.; Lu, J.; Liu, S.; Dorko, K.; Xie, W.; Ma, X. *Drug Metab. Dispos.* **2014**, *42* (5), 863–866.
- (89) Hards, K.; Robson, J. R.; Berney, M.; Shaw, L.; Bald, D.; Koul, A.; Andries, K.; Cook, G. M. *J. Antimicrob. Chemother.* **2014**, *70* (7), 2028–2037.
- (90) Amaral, L.; Viveiros, M.; Kristiansen, J. E. *Curr. Drug Targets* **2006**, *7* (7), 887–891.
- (91) NHS. Tuberculosis (TB) - Causes - NHS Choices
<http://www.nhs.uk/Conditions/Tuberculosis/Pages/Causes.aspx>.
- (92) Cohen, K.; Meintjes, G. *Curr. Opin. HIV AIDS* **2010**, *5* (1), 61–69.
- (93) Munro, S.; Lewin, S.; Swart, T.; Volmink, J. *BMC Public Health* **2007**, *7*, 104.
- (94) Ignatyeva, O.; Balabanova, Y.; Nikolayevskyy, V.; Koshkarova, E.; Radiulyte, B.; Davidaviciene, E.; Riekstina, V.; Jaama, K.; Danilovits, M.; Popa, C. M.; Drobniewski, F. A. *Tuberculosis* **2015**, *95* (5), 581–588.
- (95) De Keijzer, J.; Mulder, A.; De Haas, P. E. W.; De Ru, A. H.; Heerkens, E. M.; Amaral, L.; Van Soolingen, D.; Van Veelen, P. A. *J. Proteome Res.* **2016**, *15* (6), 1776–1786.
- (96) Rodrigues, L.; Ramos, J.; Couto, I.; Amaral, L.; Viveiros, M. *BMC Microbiol* **2011**, *11*, 35.
- (97) Rodrigues, L.; Machado, D.; Couto, I.; Amaral, L.; Viveiros, M. *Infect. Genet. Evol.* **2012**, *12* (4), 695–700.
- (98) Amaral, L.; Molnar, J. *Pharmaceuticals* **2012**, *5* (9), 1021–1031.
- (99) Wainwright, M. *Open J. Pharmacol.* **2012**, 2–1.
- (100) Dutta, N. K.; Mehra, S.; Kaushal, D. *PLoS One* **2010**, *5* (4).
- (101) Amaral, L.; Martins, A.; Gabriella, S.; Attila, H.; Molnar, J. *Recent Pat. Antiinfect. Drug Discov.* **2013**, *8* (3), 206–212.
- (102) Weinstein, E. a; Yano, T.; Li, L.-S.; Avarbock, D.; Avarbock, A.; Helm, D.; McColm, A. a; Duncan, K.; Lonsdale, J. T.; Rubin, H. *Proc. Natl. Acad. Sci. U. S. A.* **2005**, *102* (12), 4548–4553.
- (103) Sohaskey, C. *Recent Pat. Antiinfect. Drug Discov.* **2011**, *6* (2), 139–146.
- (104) Sohaskey, C. D. *J. Bacteriol.* **2008**, *190* (8), 2981–2986.

- (105) Martins, M.; Schelz, Z.; Martins, A.; Molnar, J.; Hajos, G.; Riedl, Z.; Viveiros, M.; Yalcin, I.; Aki-Sener, E.; Amaral, L. *Int. J. Antimicrob. Agents* **2007**, 29 (3), 338–340.
- (106) Martins, M.; Viveiros, M.; Couto, I.; Amaral, L. *Int. J. Tuberc. Lung Dis.* **2009**, 13 (5), 569–573.
- (107) Martins, M.; Viveiros, M.; Amaral, L. *In Vivo (Brooklyn)*. **2008**, 22 (1), 69–76.
- (108) Martins, M.; Viveiros, M.; Amaral, L. *Future Microbiol.* **2008**, 3 (2), 135–144.
- (109) Amaral, L.; Martins, M.; Viveiros, M. *J. Antimicrob. Chemother.* **2007**, 59 (6), 1237–1246.
- (110) Madrid, P. B.; Polgar, W. E.; Toll, L.; Tanga, M. *J. Bioorg. Med. Chem. Lett.* **2007**, 17 (11), 3014–3017.
- (111) Addla, D.; Jallapally, A.; Gurram, D.; Yogeewari, P.; Sriram, D.; Kantevari, S. *Bioorg. Med. Chem. Lett.* **2013**, 1–6.
- (112) Pieroni, M.; Machado, D.; Azzali, E.; Santos Costa, S.; Couto, I.; Costantino, G.; Viveiros, M. *J. Med. Chem.* **2015**, 58 (15), 5842–5853.
- (113) Scalacci, N.; Brown, A. K.; Pavan, F. R.; Ribeiro, C. M.; Manetti, F.; Bhakta, S.; Maitra, A.; Smith, D. L.; Petricci, E.; Castagnolo, D. *Eur. J. Med. Chem.* **2017**, 127, 147–158.
- (114) Schlauderer, F.; Lammens, K.; Nagel, D.; Vincendeau, M.; Eitelhuber, A. C.; Verhelst, S. H. L.; Kling, D.; Chrusciel, A.; Ruland, J.; Krappmann, D.; Hopfner, K. *P. Angew. Chem. - Int. Ed.* **2013**, 52 (39), 10384–10387.
- (115) Phelan, J.; Maitra, A.; McNerney, R.; Nair, M.; Gupta, A.; Coll, F.; Pain, A.; Bhakta, S.; Clark, T. G. *Int. J. Mycobacteriology* **2015**, 4 (3), 207–216.
- (116) Bhakta, S.; Scalacci, N.; Maitra, A.; Brown, A. K.; Dasugari, S.; Evangelopoulos, D.; McHugh, T. D.; Mortazavi, P. N.; Twist, A.; Petricci, E.; Manetti, F.; Castagnolo, D. *J. Med. Chem.* **2016**, 59 (6), 2780–2793.
- (117) Raschke, W.C.; Baird, S.; Ralph, P.; Nakoinz, I. *Cell.* **1978** 15-(1), 261–267.
- (118) Biava, M.; Porretta, G.; Manetti, F. *Mini-Reviews Med. Chem.* **2007**, 7 (1), 65–78.
- (119) Poce, G.; Bates, R. H.; Alfonso, S.; Coccozza, M.; Porretta, G. C.; Ballell, L.; Rullas, J.; Ortega, F.; De Logu, A.; Agus, E.; La Rosa, V.; Pasca, M. R.; De Rossi, E.; Wae, B.; Franzblau, S. G.; Manetti, F.; Botta, M.; Biava, M. *PLoS One* **2013**, 8 (2), 1–8.
- (120) Boshoff, H.; Tahlan, K. *Drugs Future* **2013**, 38 (7), 467–474.
- (121) Li, W.; Upadhyay, A.; Fontes, F. L.; North, E. J.; Wang, Y.; Crans, D. C.; Grzegorzewicz, A. E.; Jones, V.; Franzblau, S. G.; Lee, R. E.; Crick, D. C.; Jackson, M. *Antimicrob. Agents Chemother.* **2014**, 58 (11), 6413–6423.
- (122) La Rosa, V.; Poce, G.; Canseco, J. O.; Buroni, S.; Pasca, M. R.; Biava, M.; Raju, R. M.; Porretta, G. C.; Alfonso, S.; Battilocchio, C.; Javid, B.; Sorrentino, F.; Ioerger, T. R.; Sacchettini, J. C.; Manetti, F.; Botta, M.; De Logu, A.; Rubin, E. J.; De Rossi, E. *Antimicrob. Agents Chemother.* **2012**, 56 (1), 324–331.

- (123) Manetti, F.; Magnani, M.; Castagnolo, D.; Passalacqua, L.; Botta, M.; Corelli, F.; Saddi, M.; Deidda, D.; De Logu, A. *ChemMedChem* **2006**, *1* (9), 973–989.
- (124) Ritchie, T. J.; MacDonald, S. J. F.; Young, R. J.; Pickett, S. D. *Drug Discov. Today* **2011**, *16* (3–4), 164–171.
- (125) Castagnolo, D.; Manetti, F.; Radi, M.; Bechi, B.; Pagano, M.; De Logu, A.; Meleddu, R.; Saddi, M.; Botta, M. *Bioorg. Med. Chem.* **2009**, *17* (15), 5716–5721.
- (126) Stetter, H. *Angew. Chem. Int. Ed. English* **1976**, *15* (11), 639–647.
- (127) Biava, M.; Porretta, G. C.; Poce, G.; Deidda, D.; Pompei, R.; Tafi, A.; Manetti, F. *Bioorg. Med. Chem.* **2005**, *13* (4), 1221–1230.
- (128) Gupta, A.; Bhakta, S. *J. Antimicrob. Chemother.* **2012**, *67* (6), 1380–1391.
- (129) Gomtsyan, A. *Chem. Heterocycl. Compd.* **2012**, *48* (1), 7–10.
- (130) Meanwell, N. A. *J. Med. Chem.* **2011**, *54* (8), 2529–2591.
- (131) Khaghaninejad, S.; Heravi, M. M. *Chapter Three – Paal–Knorr Reaction in the Synthesis of Heterocyclic Compounds*; **2014**; Vol. 111.
- (132) Miles, K. C.; Mays, S. M.; Southerland, B. K.; Auvil, T. J.; Ketcha, D. M. *Arkivoc* **2009**, *2009* (14), 181–190.
- (133) Freifeld, I.; Shojaei, H.; Langer, P. *J. Org. Chem.* **2006**, *71* (13), 4965–4968.
- (134) Arcadi, A.; Rossi, E. *Tetrahedron* **1998**, *54* (50), 15253–15272.
- (135) Ziegler, K.; Holzkamp, E.; Breil, H.; Martin, H. *Angew. Chem.* **1955**, *67* (16), 426.
- (136) Hérissou, J.-L.; Chauvin, Y. *Die Makromol. Chemie* **1970**, *141* (3487), 161–176.
- (137) Schrock, R. R.; DePue, R. T.; Feldman, J.; Schaverien, C. J.; Dewan, J. C.; Liu, A. H. *J. Am. Chem. Soc.* **1988**, *110* (5), 1423–1435.
- (138) Trnka, T. M.; Grubbs, R. H. *Acc. Chem. Res.* **2001**, *34* (1), 18–29.
- (139) Garber, S. B.; Kingsbury, J. S.; Gray, B. L.; Hoveyda, A. H. *J. Am. Chem. Soc.* **2000**, *122* (34), 8168–8179.
- (140) Michrowska, A.; Bujok, R.; Harutyunyan, S.; Sashuk, V.; Dolgonos, G.; Grela, K. *J. Am. Chem. Soc.* **2004**, *126* (30), 9318–9325.
- (141) Michrowska, A.; Mennecke, K.; Kunz, U.; Kirschning, A.; Grela, K. *J. Am. Chem. Soc.* **2006**, *128* (40), 13261–13267.
- (142) Wakamatsu, H.; Blechert, S. *Angew. Chem. - Int. Ed.* **2002**, *41* (13), 2403–2405.
- (143) Zaja, M.; Connon, S. J.; Dunne, A. M.; Rivard, M.; Buschmann, N.; Jiricek, J.; Blechert, S. *Tetrahedron* **2003**, *59* (34), 6545–6558.
- (144) Diver, S. T.; Giessert, A. J. *Chem. Rev.* **2004**, *104* (3), 1317–1382.
- (145) Donohoe, T. J.; Kershaw, N. M.; Orr, A. J.; Wheelhouse, K. M. P.; Fishlock, L.; Lacy, A. R.; Bingham, M.; Procopiou, P. A. *Tetrahedron* **2008**, *64* (5), 809–820.
- (146) Donohoe, T. J.; Orr, A. J.; Gosby, K.; Bingham, M. *Eur. J. Org. Chem.* **2005**, *2005* (10), 1969–1971.

- (147) De Matteis, V.; Dufay, O.; Waalboer, D. C. J.; Van Delft, F. L.; Tiebes, J.; Rutjes, F. P. J. T. *Eur. J. Org. Chem.* **2007**, 2007 (16), 2667–2675.
- (148) Dieltiens, N.; Stevens, C. V.; Vos, D. De; Allaert, B.; Drozdak, R.; Verpoort, F. *Tetrahedron Lett.* **2004**, 45 (49), 8995–8998.
- (149) Chen, W.; Wang, J. *Organometallics* **2013**, 32 (6), 1958–1963.
- (150) Schmidt, B.; Krehl, S.; Jablowski, E. *Org. Biomol. Chem.* **2012**, 10 (26), 5119.
- (151) Sanchez., I. *Synth.* **2006**, 11, 1898.
- (152) Donohoe, T. J.; Race, N. J.; Bower, J. F.; Callens, C. K. A. *Org. Lett.* **2010**, 12 (18), 4094–4097.
- (153) Shafi, S.; Kędziołek, M.; Grela, K. *Synlett* **2011**, 1 (1), 124–128.
- (154) Villar, H.; Frings, M.; Bolm, C. *Chem. Soc. Rev.* **2007**, 36 (1), 55–66.
- (155) Kotha, S.; Meshram, M.; Tiwari, A. *Chem. Soc. Rev.* **2009**, 38 (7), 2065.
- (156) Dieltiens, N.; Moonen, K.; Stevens, C. V. *Chem. Eur. J.* **2007**, 13 (1), 203–214.
- (157) Fagan, R. L.; Palfey, B. A. *Compr. Nat. Prod. II* **2010**, 7, 37–113.
- (158) Ogunrombi, M. O.; Malan, S. F.; Terre'Blanche, G.; Castagnoli, K.; Castagnoli, N.; Bergh, J. J.; Petzer, J. P. *Life Sci.* **2007**, 81 (6), 458–467.
- (159) Fitzpatrick, P. F. *Arch. Biochem. Biophys.* **2010**, 493 (1), 13–25.
- (160) Köhler, V.; Wilson, Y. M.; Dürrenberger, M.; Ghislieri, D.; Churakova, E.; Quinto, T.; Knörr, L.; Häussinger, D.; Hollmann, F.; Turner, N. J.; Ward, T. R. *Nat. Chem.* **2013**, 5, 93–99.
- (161) Ghislieri, D.; Turner, N. J. *Top. Catal.* **2014**, 57 (5), 284–300.
- (162) Heath, R. S.; Pontini, M.; Bechi, B.; Turner, N. J. *ChemCatChem* **2014**, 6 (4), 996–1002.
- (163) Chandrasekhar, S.; Patro, V.; Chavan, L. N.; Chegondi, R.; Grée, R. *Tetrahedron Lett.* **2014**, 55 (43), 5932–5935.
- (164) Taguchi, K.; Sakaguchi, S.; Ishii, Y. *Tetrahedron Lett.* **2005**, 46 (27), 4539–4542.
- (165) Castagnolo, D.; Botta, L.; Botta, M. *J. Org. Chem.* **2009**, 74 (8), 3172–3174.
- (166) Campolo, D.; Arif, T.; Borie, C.; Mouysset, D.; Vanthuyne, N.; Naubron, J. V.; Bertrand, M. P.; Nechab, M. *Angew. Chem. - Int. Ed.* **2014**, 53 (12), 3227–3231.
- (167) Dinges, J.; Albert, D. H.; Arnold, L. D.; Ashworth, K. L.; Akritopoulou-Zanze, I.; Bousquet, P. F.; Bouska, J. J.; Cunha, G. A.; Davidsen, S. K.; Diaz, G. J.; Djuric, S. W.; Gasięcki, A. F.; Gintant, G. A.; Gracias, V. J.; Harris, C. M.; Houseman, K. A.; Hutchins, C. W.; Johnson, E. F.; Li, H.; Marcotte, P. A.; Martin, R. L.; Michaelides, M. R.; Nyein, M.; Sowin, T. J.; Su, Z.; Tapang, P. H.; Xia, Z.; Zhang, H. Q. *J. Med. Chem.* **2007**, 50 (9), 2011–2029.
- (168) Wipf, P.; Aoyama, Y.; Benedum, T. E. *Org. Lett.* **2004**, 6 (20), 3593–3595.

- (169) Iafe, R. G.; Kuo, J. L.; Hochstatter, D. G.; Saga, T.; Turner, J. W.; Merlic, C. A. *Org. Lett.* **2013**, *15* (3), 582–585.
- (170) Slugovc, C.; Demel, S.; Riegler, S.; Hobisch, J.; Stelzer, F. *J. Mol. Catal. A Chem.* **2004**, *213* (1), 107–113.
- (171) Compain, P. *Adv. Synth. Catal.* **2007**, *349* (11–12), 1829–1846.
- (172) Woodward, C. P.; Spiccia, N. D.; Jackson, W. R.; Robinson, A. J. *Chem. Commun. (Camb)*. **2011**, *47* (2), 779–781.
- (173) Castagnolo, D.; Armaroli, S.; Corelli, F.; Botta, M. *Tetrahedron Asymmetry* **2004**, *15* (6), 941–949.
- (174) Castagnolo, D.; Renzulli, M. L.; Galletti, E.; Corelli, F.; Botta, M. *Tetrahedron Asymmetry* **2005**, *16* (17), 2893–2896.
- (175) Castagnolo, D.; Dessì, F.; Radi, M.; Botta, M. *Tetrahedron Asymmetry* **2007**, *18* (11), 1345–1350.
- (176) Detz, R. J.; Abiri, Z.; Le Griel, R.; Hiemstra, H.; Van Maarseveen, J. H. *Chem. - Eur. J.* **2011**, *17* (21), 5921–5930.
- (177) Meyet, C. E.; Pierce, C. J.; Larsen, C. H. *Org. Lett.* **2012**, *14* (4), 964–967.
- (178) Lee, S. H.; Seo, H. J.; Kim, M. J.; Kang, S. Y.; Lee, S. H.; Ahn, K.; Lee, M.; Han, H. K.; Kim, J.; Lee, J. *Bioorg. Med. Chem. Lett.* **2009**, *19* (23), 6632–6636.
- (179) Wang, J.-G.; Yang, Y.; Huang, Z.-H.; Kang, F. *J. Mater. Chem.* **2012**, *22* (33), 16943.
- (180) Ketcha, D. M.; Carpenter, K. P.; Zhou, Q. *J. Org. Chem.* **1991**, *56* (3), 1318–1320.
- (181) Reder, E.; Veith, H. J.; Buschinger, A. *Helv. Chim. Acta* **1995**, *78* (1), 73–79.
- (182) Carballo, R. M.; Purino, M.; Ramírez, M. A.; Martín, V. S.; Padrón, J. I. *Org. Lett.* **2010**, *12* (22), 5334–5337.
- (183) Aramini, A.; Brinchi, L.; Germani, R.; Savelli, G. *Eur. J. Org. Chem.* **2000**, *9* (9), 1793–1797.
- (184) Gurung, N.; Ray, S.; Bose, S.; Rai, V. *Biomed Res. Int.* **2013**, *2013*, 329121.
- (185) Wang, M.; Si, T.; Zhao, H. *Bioresour. Technol.* **2012**, *115*, 117–125.
- (186) Bornscheuer, U. T.; Huisman, G. W.; Kazlauskas, R. J.; Lutz, S.; Moore, J. C.; Robins, K. *Nature* **2012**, *485* (7397), 185–194.
- (187) Khersonsky, O.; Roodveldt, C.; Tawfik, D. S. *Curr. Opin. Chem. Biol.* **2006**, *10* (5), 498–508.
- (188) Wallace, S.; Balskus, E. P. *Curr. Opin. Biotechnol.* **2014**, *30*, 1–8.
- (189) Gaweska, H.; Fitzpatrick, P. F. *Biomol. Concepts* **2011**, *2* (5), 365–377.
- (190) Carr, R.; Alexeeva, M.; Enright, A.; Eve, T. S. C.; Dawson, M. J.; Turner, N. J. *Angew. Chem. - Int. Ed.* **2003**, *42* (39), 4807–4810.

- (191) Alexeeva, M.; Enright, A.; Dawson, M. J.; Mahmoudian, M.; Turner, N. J. *Angew. Chem. - Int. Ed.* **2002**, *41* (17), 3177–3180.
- (192) Carr, R.; Alexeeva, M.; Dawson, M. J.; Gotor-Fernández, V.; Humphrey, C. E.; Turner, N. J. *ChemBioChem* **2005**, *6* (4), 637–639.
- (193) Ghislieri, D.; Green, A. P.; Pontini, M.; Willies, S. C.; Rowles, I.; Frank, A.; Grogan, G.; Turner, N. J. *J. Am. Chem. Soc.* **2013**, *135* (29), 10863–10869.
- (194) Ghislieri, D.; Houghton, D.; Green, A. P.; Willies, S. C.; Turner, N. J. *ACS Catal.* **2013**, *3* (12), 2869–2872.
- (195) Wen, Y.; Zhao, B.; Shi, Y. *Org. Lett.* **2009**, *11* (11), 2365–2368.
- (196) Fu, G. C.; Grubbs, R. H. *J. Am. Chem. Soc.* **1992**, *114* (d), 7324–7325.
- (197) Kim, J.-M.; Bogdan, M. A.; Mariano, P. S. *J. Am. Chem. Soc.* **1993**, *115* (23), 10591–10595.
- (198) Miller, J. R.; Edmondson, D. E. *Biochemistry* **1999**, *38* (41), 13670–13683.
- (199) Atkin, K. E.; Reiss, R.; Koehler, V.; Bailey, K. R.; Hart, S.; Turkenburg, J. P.; Turner, N. J.; Brzozowski, A. M.; Grogan, G. *J. Mol. Biol.* **2008**, *384* (5), 1218–1231.
- (200) Korb, O.; Stützle, T.; Exner, T. E. *J. Chem. Inf. Model.* **2009**, *49* (1), 84–96.
- (201) Wang, X.; Lane, B. S.; Sames, D. *J. Am. Chem. Soc.* **2005**, *127* (14), 4996–4997.
- (202) Fu, G. C.; Grubbs, R. H. *J. Am. Chem. Soc.* **1992**, *114* (18), 7324–7325.
- (203) Denard, C. A.; Bartlett, M. J.; Wang, Y.; Lu, L.; Hartwig, J. F.; Zhao, H. *ACS Catal.* **2015**, *5* (6), 3817–3822.
- (204) Denard, C. A.; Huang, H.; Bartlett, M. J.; Lu, L.; Tan, Y.; Zhao, H.; Hartwig, J. F. *Angew. Chem. Int. Ed.* **2014**, *53* (2), 465–469.
- (205) Denard, C. A.; Hartwig, J. F.; Zhao, H. *ACS Catal.* **2013**, *3* (12), 2856–2864.
- (206) Woodward, C. P.; Spiccia, N. D.; Jackson, W. R.; Robinson, A. J. *Chem. Commun.* **2011**, *47* (2), 779–781.
- (207) Mingotaud, A. F.; Mingotaud, C.; Moussa, W. *J. Polym. Sci. Part A Polym. Chem.* **2008**, *46* (8), 2833–2844.
- (208) Binder, J. B.; Blank, J. J.; Raines, R. T. *Org. Lett.* **2007**, *9* (23), 4885–4888.
- (209) Schena, E.; Nedialkova, L.; Borroni, E.; Battaglia, S.; Cabibbe, A. M.; Niemann, S.; Utpatel, C.; Merker, M.; Trovato, A.; Hofmann-Thiel, S.; Hoffmann, H.; Cirillo, D. *M. J. Antimicrob. Chemother.* **2016**, *71* (6), 1532–1539.
- (210) Palomino, J.-C.; Martin, A.; Camacho, M.; Guerra, H.; Swings, J.; Portaels, F. *Antimicrob. Agents Chemother.* **2002**, *46* (8), 2720–2722.
- (211) O’Brien, J.; Wilson, I.; Orton, T.; Pognan, F. *Eur. J. Biochem.* **2000**, *267* (17), 5421–5426.
- (212) Pavan, F. R.; Maia, P. I. da S.; Leite, S. R. A.; Deflon, V. M.; Batista, A. A.; Sato, D. N.; Franzblau, S. G.; Leite, C. Q. F. *Eur. J. Med. Chem.* **2010**, *45* (5), 1898–1905.

- (213) Pelizzetti, E.; Mentasti, E. *Inorg. Chem.* **1979**, *18* (3), 583–588.
- (214) Sambandamurthy, V. K.; Derrick, S. C.; Hsu, T.; Chen, B.; Larsen, M. H.; Jalapathy, K. V.; Chen, M.; Kim, J.; Porcelli, S. A.; Chan, J.; Morris, S. L.; Jacobs, W. R. *Vaccine* **2006**, *24* (37–39), 6309–6320.
- (215) Larsen, M. H.; Biermann, K.; Chen, B.; Hsu, T.; Sambandamurthy, V. K.; Lackner, A. A.; Aye, P. P.; Didier, P.; Huang, D.; Shao, L.; Wei, H.; Letvin, N. L.; Frothingham, R.; Haynes, B. F.; Chen, Z. W.; Jacobs, W. R. *Vaccine* **2009**, *27* (34), 4709–4717.
- (216) Sambandamurthy, V. K.; Wang, X.; Chen, B.; Russell, R. G.; Derrick, S.; Collins, F. M.; Morris, S. L.; Jacobs, W. R. *Nat. Med.* **2002**, *8* (10), 1171–1174.
- (217) Guzman, J. D.; Evangelopoulos, D.; Gupta, A.; Birchall, K.; Mwaigwisya, S.; Saxty, B.; McHugh, T. D.; Gibbons, S.; Malkinson, J.; Bhakta, S. *BMJ Open* **2013**, *3*, e002672.
- (218) Trache, A.; Meininger, G. a. *Curr. Protoc. Microbiol.* **2008**, February (9), 1–17.
- (219) Gupta, A.; Bhakta, S. *J. Antimicrob. Chemother.* **2012**, *67* (6), 1380–1391.
- (220) Rodrigues, L.; Wagner, D.; Viveiros, M.; Sampaio, D.; Couto, I.; Vavra, M.; Kern, W. V.; Amaral, L. *J. Antimicrob. Chemother.* **2008**, *61* (5), 1076–1082.
- (221) Lee, H.; Kim, B. H. *Tetrahedron* **2013**, *69* (32), 6698–6708.
- (222) Molander, G. A.; Cadoret, F. *Tetrahedron Lett.* **2011**, *52* (17), 2199–2202.
- (223) Campolo, D.; Arif, T.; Borie, C.; Mouysset, D.; Vanthuynne, N.; Naubron, J. V.; Bertrand, M. P.; Nechab, M. *Angew. Chem. - Int. Ed.* **2014**, *53* (12), 3227–3231.
- (224) Wipf, P.; Aoyama, Y.; Benedum, T. E. *Org. Lett.* **2004**, *6* (20), 3593–3595.
- (225) Brittain, W. D. G.; Chapin, B. M.; Zhai, W.; Lynch, V. M.; Buckley, B. R.; Anslyn, E. V.; Fossey, J. S. *Org. Biomol. Chem.* **2016**, *14* (46), 10778–10782.
- (226) Kolarovič, A.; Fáberová, Z. *J. Org. Chem.* **2009**, *74* (18), 7199–7202.
- (227) Sakai, N.; Hori, H.; Ogiwara, Y. *Eur. J. Org. Chem.* **2015**, 2015 (9), 1905–1909.
- (228) Messina, F.; Botta, M.; Corelli, F.; Schneider, M. P.; Fazio, F. *J. Org. Chem.* **1999**, *64* (10), 3767–3769.
- (229) Nishibayashi, Y.; Milton, M. D.; Inada, Y.; Yoshikawa, M.; Wakiji, I.; Hidai, M.; Uemura, S. *Chem. - Eur. J.* **2005**, *11* (5), 1433–1451.
- (230) Meyet, C. E.; Pierce, C. J.; Larsen, C. H. *Org. Lett.* **2012**, *14* (4), 964–967.
- (231) Labonne, A.; Zani, L.; Hintermann, L.; Bolm, C. *J. Org. Chem.* **2007**, *72* (15), 5704–5708.
- (232) Chen, W.; Wang, J. *Organometallics* **2013**, *32* (6), 1958–1963.
- (233) Castagnolo, D.; Giorgi, G.; Spinosa, R.; Corelli, F.; Botta, M. *Eur. J. Org. Chem.* **2007**, 2007 (22), 3676–3686.
- (234) Ghislieri, D.; Green, A. P.; Pontini, M.; Willies, S. C.; Rowles, I.; Frank, A.; Grogan, G.; Turner, N. J. *J. Am. Chem. Soc.* **2013**, *135* (29), 10863–10869.

- (235) Ghislieri, D.; Houghton, D.; Green, A. P.; Willies, S. C.; Turner, N. J. *ACS Catal.* **2013**, *3* (12), 2869–2872.
- (236) Atkin, K. E.; Reiss, R.; Koehler, V.; Bailey, K. R.; Hart, S.; Turkenburg, J. P.; Turner, N. J.; Brzozowski, A. M.; Grogan, G. *J. Mol. Biol.* **2008**, *384* (5), 1218–1231.
- (237) Korb, O.; Stütze, T.; Exner, T. E. *J. Chem. Inf. Model.* **2009**, *49* (1), 84–96.
- (238) Ohshima, T.; Miyamoto, Y.; Ipposhi, J.; Nakahara, Y.; Utsunomiya, M.; Mashima, K. *J. Am. Chem. Soc.* **2009**, *131* (40), 14317–14328.
- (239) Du, H.-J.; Zhen, L.; Wen, X.; Xu, Q.-L.; Sun, H. *Org. Biomol. Chem.* **2014**, *12* (47), 9716–9719.
- (240) Ramachary, D. B.; Narayana, V. V. *Eur. J. Org. Chem.* **2011**, *2011* (19), 3514–3522.
- (241) Singh, C. B.; Kavala, V.; Samal, A. K.; Patel, B. K. *Eur. J. Org. Chem.* **2007**, *2007* (8), 1369–1377.
- (242) Schmidt, B.; Krehl, S.; Jablowski, E. *Org. Biomol. Chem.* **2012**, *10* (26), 5119.
- (243) Li, N.; Jones, W. D. *J. Am. Chem. Soc.* **2007**, *129* (35), 10707–10713.
- (244) Shetty, M. R.; Kshirsagar, S. W.; Lanka, S. V.; Samant, S. D. *Green Chem. Lett. Rev.* **2012**, *5* (3), 291–301.
- (245) Zhang, Y.; Yang, X.; Yao, Q.; Ma, D. *Org. Lett.* **2012**, *14* (12), 3056–3059.
- (246) Terada, Y.; Arisawa, M.; Nishida, A. *Angew. Chem. - Int. Ed.* **2004**, *43* (31), 4063–4067.
- (247) Rahman, O.; Kihlberg, T.; Långström, B. *Org. Biomol. Chem.* **2004**, *2* (11), 1612–1616.
- (248) Martinez, V.; Blais, J. C.; Bravic, G.; Astruc, D. *Organometallics* **2004**, *23* (4), 861–874.
- (259) Sawadjoon, S.; Samec, J. S. M. *Org. Biomol. Chem.* **2011**, *9* (7), 2548–2554.
- (250) Roberts, J. J.; Ross, W. C. J. *J. Chem. Soc.* **1952**, 4288.
- (251) Bunrit, A.; Sawadjoon, S.; Tšupova, S.; Sjöberg, P. J. R.; Samec, J. S. M. *J. Org. Chem.* **2016**, *81* (4), 1450–1460.
- (252) Majumdar, K. C.; Chakravorty, S.; Taher, A. *Synth. Commun.* **2008**, *38* (18), 3159–3169.
- (253) Durrat, F.; Sanchez, M. V.; Couty, F.; Evano, G.; Marrot, J. *Eur. J. Org. Chem.* **2008**, *2008* (19), 3286–3297.
- (254) Taillefer, M.; Xia, N.; Ouali, A. *Angew. Chem. - Int. Ed.* **2007**, *46* (6), 934–936.
- (255) Jiang, D.; Fu, H.; Jiang, Y.; Zhao, Y. *J. Org. Chem.* **2007**, *72* (2), 672–674.
- (256) Azizi, N.; Khajeh-Amiri, A.; Ghafari, H.; Bolourtchian, M.; Saidi, M. R. *Synlett* **2009**, *2009* (14), 2245–2248.

- (257) Dumoulin, H.; Boulouard, M.; Daoust, M.; Rault, S. *Eur. J. Med. Chem.* **1998**, *33* (3), 201–207.
- (258) Dreher, S. D.; Lim, S. E.; Sandrock, D. L.; Molander, G. A. *J. Org. Chem.* **2009**, *74* (10), 3626–3631.
- (259) Reddy, V. P.; Kumar, A. V.; Rao, K. R. *Tetrahedron Lett.* **2011**, *52* (7), 777–780.
- (260) Taylor, J. E.; Jones, M. D.; Williams, J. M. J.; Bull, S. D. *Org. Lett.* **2010**, *12* (24), 5740–5743.
- (261) Goldman, I. M.; Seibl, J.; Flament, I.; Gautschi, F.; Winter, M.; Willhalm, B.; Stoll, M. *Helv. Chim. Acta* **1967**, *50* (2), 694–705.
- (262) Deb, I.; Coiro, D. J.; Seidel, D. *Chem. Commun. (Camb)*. **2011**, *47* (22), 6473–6475.
- (263) Lee, C. K.; Jun, J. H.; Yu, J. S. *J. Heterocycl. Chem.* **2000**, *37* (1), 15–24.
- (264) Joshi, S. D.; Kumar, D.; More, U. A.; Yang, K. S.; Aminabhavi, T. M. *Med. Chem. Res.* **2016**, *25* (4), 672–689.
- (265) Abid, M.; Landge, S. M.; Török, B. *Org. Prep. Proced. Int.* **2006**, *38* (5), 495–500.
- (266) Aydogan, F.; Basarir, M.; Yolacan, C.; Demir, A. S. *Tetrahedron* **2007**, *63* (39), 9746–9750.